Low-Energy Phenomenology of Neutrino Mass Mechanisms

André Morgado Patrício

Thesis to obtain the Master of Science Degree in

Engineering Physics

Supervisor(s): Prof. Filipe Rafael Joaquim

Examination Committee

Chairperson:	Prof.ª Doutora Maria Teresa Haderer de la Peña Stadler
Supervisor:	Prof. Doutor Filipe Rafael Joaquim
Member of the Committee:	Prof. Doutor Ricardo Jorge González Felipe

November 2014

" The worthwhile problems are the ones you can really solve or help solve, the ones you can really contribute something to. A problem is grand in science if it lies before us unsolved and we see some way for us to make some headway into it.

No problem is too small or too trivial if we can really do something about it. "

– Richard P. Feynman to Koichi Mano, February 3, 1966

Acknowledgments

First of all, I would like to express my gratitude to Professor Filipe Joaquim, for his guidance and continuous support throughout the development of this work. Thank you especially for having carefully read every detail of this thesis and for the never-ending suggestions, corrections or just comments.

I am additionally indebted to Fundação para a Ciência e Tecnologia (FCT) and to the whole team of *Centro de Física Teórica de Partículas* (CFTP). I thank in particular to Professor Gustavo Castelo Branco for his good advices and for having poviding me the opportunity to participate in the *Graduate School in Particle and Astroparticle physics of Annecy-le-Vieux*. A word of appreciation goes also to Professor Jorge Romão for his openness to help me whenever I had a more tricky question related to quantum field theory. Also not forgotten is all the help and kindness provided by Cláudia Romão in all bureaucratic matters.

I thank all my friends and colleagues for the great friendly environment during this hard challenge that MEFT is and that is finally coming to an end. Wherever you are reading this thesis, I wish you the best of luck and hope to see you again.

Finally, I would like to thank my family for their continuous support, encouragement and especially for helping me when I most needed.

Este trabalho foi financiado pela Fundação para a Ciência e a Tecnologia (FCT) sob o contrato BL73/2014 atribuída no âmbito do projeto de investigação "Sinergia entre a Física do sabor e do LHC" (EXPL/FIS-NUC/0460/2013).

This work has been financially supported by *Fundação para a Ciência e a Tecnologia* (FCT) under the grant BL73/2014 from the research project "Sinergia entre a Física do sabor e do LHC" (EXPL/FIS-NUC/0460/2013).

Resumo

Apesar dos repetidos sucessos, uma evidência clara de que o Modelo Padrão (MP) não é a teoria final provém da observação de oscilações de neutrinos, que implicam massas de neutrinos não nulas.

Na presente dissertação, analisamos extensões do MP baseadas no mecanismo *seesaw*, em que as pequenas massas dos neutrinos surgem naturalmente da troca a nível árvore de campos pesados, que podem ser singletos fermiónicos, tripletos fermiónicos ou tripletos escalares. De um ponto de vista efetivo a baixas energias, o operador de dimensão cinco responsável pelas massas dos neutrinos é comum a todas as teorias com neutrinos de Majorana. No entanto, existe uma grande variedade de operadores de dimensão seis. Nesta tese, obtemos então os operadores efetivos de dimensão seis para as três versões do mecanismo de *seesaw* e verificamos que poderão existir efeitos observáveis em experiências futuras se os coeficientes dos operadores de dimensão seis forem desacoplados dos do operador de dimensão cinco segundo um padrão comum aos vários modelos.

Exploramos também consequências fenomenológicas, incluindo uma análise detalhada de processos violadores do sabor leptónico (LFV). Em particular, obtemos constrangimentos a cada modelo *seesaw* e discutimos a possibilidade de observar tais processos em experiências atuais e futuras. As predições obtidas para tais processos poderão constituir uma ferramenta fundamental para discriminar entre os três modelos considerados. Para além disto, uma análise combinada incluindo outros decaimentos eletrofracos mostra que os desvios à unitariedade nos modelos de seesaw fermiónicos são menores que 2σ.

Palavras-chave:

Física de neutrinos; Extensões do MP; Mecanismos *seesaw*; Fenomenologia; Decaimentos raros; Violação do sabor leptónico.

Abstract

Despite all its successes, strong evidence that the Standard Model of particle physics is not the ultimate theory comes from neutrino oscillation experiments, which imply nonvanishing neutrino masses and mixing.

In the present thesis, we analyse seesaw extensions of the SM, which naturally accomodate tiny neutrino masses through tree-level exchange of heavy fields, which may be either fermionic singlets/triplets or scalar triplets. From a low-energy effective viewpoint, neutrino masses are generated by a dimension-five operator, characteristic of all theories with Majorana neutrinos. However, a plethora of dimension-six operators exists. In this thesis, we derive the low-energy dimension six operators for the basic seesaw scenarios, and verify that they may lead to observable effects in the near future if the coefficients of the dimension five and six operators are decoupled along a pattern common to all models.

The phenomenological consequences are explored as well, including a detailed analysis of charged lepton flavour violating (CLFV) processes. Our focus relies, mainly, on predictions and constraints set on each model from muon and tau decays and from muon to electron conversion in nuclei. The possibilities to observe these processes in present and future experiments are also considered. The analytic results for the rates of CLFV processes rates might be a decisive tool to discriminate between the three models of neutrino mass generation. Besides that, a combined analysis including other electroweak decays shows that departures from unitarity are not larger than 2σ in the fermionic seesaw models.

Keywords:

Neutrino Physics; SM extensions; Seesaw mechanisms; Phenomenology; Rare decays; Lepton flavour violation.

Contents

Page

Acknowledgments . . . v
Resumo . . . ix
Abstract . . . xi
List of Tables . . . xv
List of Figures . . . xviii
List of Abbreviations . . . xix

1 Introduction and motivation **1**
1.1 Historical introduction . . . 1
1.2 Motivation and thesis outline . . . 8

2 The Standard Model of particle physics **9**
2.1 Field content and Lagrangian . . . 9
2.2 Higgs mechanism . . . 13
2.3 Fermion masses . . . 17
2.4 Electroweak currents and fermion mixing . . . 18
2.5 Summary of the SM . . . 22

3 Neutrino masses and seesaw-type models **23**
3.1 The Dirac-Majorana mass term . . . 23
3.2 Lepton mixing and observables . . . 26
3.3 Seesaw mechanism(s) . . . 29
3.3.1 Type I seesaw mechanism . . . 31
3.3.2 Type II seesaw mechanism . . . 37
3.3.3 Type III seesaw mechanism . . . 41
3.4 Low scale seesaw, $M \sim \mathcal{O}(\mathrm{TeV})$ . . . 47
3.4.1 Electroweak hierarchy problem . . . 47
3.4.2 *Direct lepton violation* . . . 48

4 Phenomenology of seesaw models **50**
4.1 Type I seesaw model . . . 52
4.1.1 Charged-lepton flavour violating processes . . . 52
4.1.2 Unitarity of the lepton mixing matrix . . . 56

4.2 Type II seesaw model . . . 58
4.2.1 Charged lepton flavour violating processes . . . 58
4.2.2 M_W and the ρ parameter . . . 63
4.2.3 Experimental signatures of scalar triplets . . . 64
4.3 Type III seesaw model . . . 65
4.3.1 Charged lepton flavour violating processes . . . 65
4.3.2 Unitarity of the leptonic mixing matrix . . . 68

5 Summary and conclusions **70**

A One-loop calculations **77**
A.1 Beyond the unitary gauge: R_ξ gauges . . . 77
A.2 Regularisation procedure . . . 78

B Feynman rules with Majorana fermions **81**

C Type I seesaw form factors **83**
C.1 Photon-exchange diagrams . . . 84
C.2 Z-boson exchange diagrams . . . 87
C.3 Calculation of box diagrams . . . 90
C.3.1 d-type box diagrams . . . 90
C.3.2 u-type box diagrams . . . 92

D Type II seesaw form factor calculation **94**

E $\ell_\alpha \to \ell_\beta\,\gamma$ decays in the type III seesaw model **97**

List of Tables

2.1 Fermionic content of the SM, electric charges and masses. 10
2.2 SM fermionic fields and associated quantum numbers. 11
2.3 Generators of SU(3)$_c$, SU(2)$_L$ and U(1)$_Y$ transformations in the SM. 12
2.4 Number of parameters for the various types of matrices considered in this thesis. 20
2.5 Assignment of flavour lepton numbers to particles (left) and antiparticles (right). 21
2.6 Symmetries of the Standard Model. 22

3.1 Global fit results for neutrino oscillation parameters. 28
3.2 Number of parameters in the type I seesaw scenario. 36
3.3 Coefficients and low-energy effective operators obtained for the three seesaw scenarios. . 46

4.1 Present experimental bounds and future sensitivities to CLFV processes. 50
4.2 Low-energy gauge boson decays. 51
4.3 Low-energy decays of leptons, pions and kaons. 51
4.4 Bounds on non-unitarity resulting from $\ell_\alpha \to \ell_\beta \gamma$ decays in the type I seesaw scenario. . . 52
4.5 Nuclear parameters related to $\mu - e$ conversion in nuclei. 53
4.6 Constraints on non-unitarity from a selection of processes, in the type I seesaw model. . . 57
4.7 Bounds on combinations of Yukawa couplings resulting from $\ell_\alpha \to \ell_\beta \gamma$ in the type II seesaw. 60
4.8 Bounds resulting from $\mu - e$ conversion in the type II seesaw model 61
4.9 Bounds on $\mathbf{Y}_{\Delta ij} \left[\times \left(\frac{M_\Delta}{1\,\mathrm{TeV}}\right)^2\right]$ from tree level $\ell \to 3\ell$ decays in the type II seesaw scenario. 63
4.10 Bounds on non-unitarity resulting from CLFV decays in the type III seesaw scenario. . . . 65

List of Figures

1.1 Continuous β-decay spectrum from radium E. 2

2.1 Higgs potential for $\mu^2 > 0$ and for $\mu^2 < 0$. 14
2.2 Tree-level diagram for muon decay (left) and its low-energy approximation (right). . . . 19

3.1 Tree-level exchange interactions which generate the Weinberg operator. 31
3.2 Tree-level diagrams for muon decay in the effective description of the type III seesaw model. . 46

4.1 $\mu \to 3e$ and $\mu - e$ conversion loop factors as functions of the seesaw scale in the type I seesaw. 54
4.2 Ratios of the $\mu \to 3e$ decay rate factor $|C_{\mu 3e}|^2$ in the type I seesaw model. 55
4.3 Bounds on $|\sum_{N_j} U_{e\,j} U^\dagger_{j\,\mu}|$ and $|\sum_{N_j} \mathbf{Y}_{e\,j} \mathbf{Y}^\dagger_{j\,\mu}|$ in the type I seesaw scenario. 55
4.4 Plot of $f(r, S_\sigma)$ in Eq. (4.26), as a function of the type II seesaw mass scale M_Δ. 59
4.5 Ratios $f(r, S_e)/f(r, S_\sigma)$ as a function of the type II seesaw mass scale M_Δ. 59
4.6 $\ell \to 3\ell$ in the type II the effective theory. 62
4.7 $\ell \to 3\ell$ in the type II full theory. 62
4.8 Tree-level contributions to $\ell^-_\alpha \to \ell^+_\rho \ell^-_\beta \ell^-_\sigma$ decays in the type III seesaw scenario. 66

A.1 Propagators of gauge and Goldstone bosons in R_ξ gauges. 77

B.1 Feynman rules for Yukawa interactions between the heavy scalar triplet and leptons in the type II seesaw model. 81
B.2 Feynman rules for heavy scalar triplet gauge interactions in the type II seesaw model. . . 81
B.3 Relevant Feynman rules in the type I seesaw scenario. 82
B.4 Feynman rules for interactions between fermions and scalars in the type III seesaw. 82
B.5 Feynman rules for gauge interactions with SM fermions, in the type III seesaw model. . . 82

C.1 One-loop contributions to the effective vertex $\overline{\ell_\beta}\ell_\alpha\gamma$ in the Type I Seesaw scenario. 84
C.2 One-loop contributions to the effective vertex $\overline{\ell_\beta}\ell_\alpha Z$ in the type I seesaw scenario. 87
C.3 d-box type diagrams that contribute at one-loop order to μ-e conversion in nuclei and to the $\mu \to \ell^-_j \ell^-_j \ell^+_k$ decays, in the type I seesaw scenario. 90
C.4 u-box type diagrams that contribute at one-loop order to μ-e conversion in nuclei and to the $\mu \to \ell^-_j \ell^-_j \ell^+_k$ decays, in the type I seesaw scenario. 92

D.1 Diagrams that contribute at one-loop order to the type II seesaw form factor. 94

E.1 One-loop diagrams contributing to $\ell_\alpha \to \ell_\beta \gamma$ in the type III seesaw model. 97

List of Abbreviations

BR	**B**ranching **R**atio
CC	**C**harged **C**urrents
CKM	**C**abibbo-**K**obayashi-**M**askawa
CLFV	**C**harged **L**epton **F**lavor **V**iolation
CP	**C**harge Conjugation and **P**arity
CR	**C**onversion **R**ate
EW	**E**lectro**W**eak
EWSB	**E**lectroweak **S**ymmetry **B**reaking
FCNC	**F**lavor **C**hanging **N**eutral **C**urrents
LFV	**L**epton **F**lavor **V**iolation
LHC	**L**arge **H**adron **C**ollider
NC	**N**eutral **C**urrents
PMNS	**P**ontecorvo-**M**aki-**N**akagawa-**S**akata
QCD	**Q**uantum **C**romodynamics
QED	**Q**uantum **E**lectrodynamics
QFT	**Q**uantum **E**lectrodynamics
SM	**S**tandard **M**odel of **P**article **P**hysics
SSB	**S**pontaneous **S**ymmetry **B**reaking
VEV	**V**acuum **E**xpectation **V**alue

1 Introduction and motivation

1.1 Historical introduction

> *"... a way out for saving the law of conservation of energy. Namely, the possibility that there could exist in the nuclei electrically neutral particles, that I will call neutrons which have spin 1/2 and follow the exclusion principle. The continuous β-spectrum would then be understandable assuming that in β-decay together with the electron, in all cases, also a neutron is emitted... "*
>
> – Wolfgang Pauli, 1930

Neutrinos are very fascinating particles: they are the only elementary fermions with no electric charge and their masses are many orders of magnitude below the masses of their charged counterparts. As such, studying neutrino properties has been of utmost importance in particle physics for the last decades. From these studies, clear evidence has been gathered regarding an ultimate relation between the knowledge of neutrino properties and the understanding of fundamental properties of the Universe. In view of this, the History of neutrinos is very instructive and it is worth taking a glance at its highlights [1–3], from the proposal of the neutrino until the confirmation of neutrino oscillations.

The History of neutrinos begins with a famous Pauli letter [4] addressed to the participants of a nuclear physics conference in Tübingen, in December 1930. At that time, nuclei were considered to be bound states of protons and electrons. In that framework, there were two fundamental problems:

1. β-decay exhibited a continuous spectrum;
2. some nuclei had the 'wrong' spin (such as $^{14}_{7}N$, observed to satisfy the Bose-Einstein statistics but with a predicted half-integer spin, contradicting the *spin-statistics theorem*).

From the point of view of this electron-proton model, the β-decay of a nucleus (A, Z) consisted in an electron emitted in the nuclear transition $(A, Z) \to (A, Z + 1) + e^-$. Applying the law of energy-momentum conservation to this process, the electrons produced in β-decays should have a fixed kinetic energy approximately equal to the release energy Q_e for the reaction.

However, by 1911, L. Meitner and O. Hahn verified that β-spectra were continuous, with an end-point energy equal to Q_e (see Fig. 1.1). This result was subsequently confirmed in the calorimetric experiment performed by C. Ellis and W. Wooster in 1927 [5]. They found that the energy released per β-decay was equal to the average energy over the spectrum, proving that the energy detected was smaller than the total energy released. Later, Meitner and Orthmann [6] showed that γ-rays could not solve this problem, which led to the idea of explaining the missing energy with the existence of a new particle.

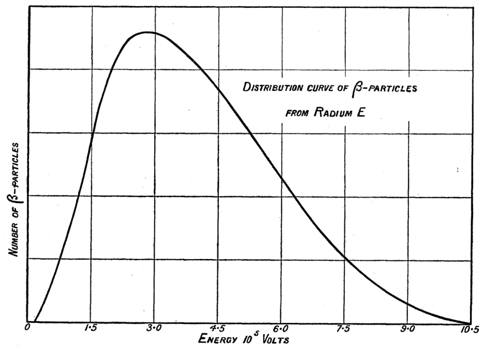

Figure 1.1: Continuous β-decay spectrum from radium E, from experiment [5].

As a desperate way out, in 1930, Pauli proposed to the “Radioactive Ladies and Gentlemen” that the existence of a new weakly interacting neutral particle emitted in β-decay could solve the existing problems [4]. He called this particle a "neutron", with a mass of "the same order of magnitude as the electron mass". Pauli further assumed that "neutrons" had spin $1/2$ and that, together with protons and electrons, were constituents of nuclei. This allowed him to solve the spin problem of some nuclei.

Two years later, J. Chadwick discovered the neutron [7] as we know it today (with a mass approximately equal to the mass of the proton and spin equal to $1/2$) and, soon after, Heisenberg [8], Majorana [9] and Ivanenko [10] suggested that nuclei were bound states of neutrons and protons. This assumption was the key to explain all nuclear data existing at the time as well as the spin of ${}^{14}_{7}\mathrm{N}$ and other nuclei. After the discovery of the neutron, E. Fermi renamed the Pauli particle to *neutrino*, with the first published reference to it in the *Proceedings of the Solvay Conference* of October 1933. In that same year, Fermi [11] and Perrin [12] independently concluded that neutrinos could be massless!

Later on, in 1934, E. Fermi formulated a theory of β-decay [13]. He assumed that nuclei are bound states of neutrons and protons and that the electron-(anti)neutrino pair was produced in the transition of a neutron into a proton: $n \to p + e^- + \overline{\nu}$. In analogy with Quantum ElectroDynamics (QED), Fermi assumed that the neutron decay is governed by the following *effective Lagrangian*

$$\mathcal{L}^{\beta}(x) = \frac{G_\beta}{\sqrt{2}} \left[\overline{\psi}_p(x)\gamma_\mu\psi_n(x)\right] \left[\overline{\psi}_e(x)\gamma^\mu\psi_\nu(x)\right] \;+\; \text{h.c.}\,, \tag{1.1}$$

with $G_\beta \approx 1.1 \times 10^{-5}\ \mathrm{GeV}^{-2}$ a coupling constant (slightly different from the now known *Fermi constant* G_F, determined from the muon decay) extracted from the neutron decay width.

The simple Fermi theory, however, could not describe all β-decay data. Indeed, the largest contributions to β-decay come from transitions in which the electron-(anti)neutrino pair is produced in a singlet state (total spin $S = 0$). Thus, the observation of β-decays with electron and (anti)neutrino produced in a triplet state ($S = 1$) led to the Gamov-Teller generalisation of the Fermi theory in 1936 [14], where the Lagrangian included also an axial vector current $\overline{\psi}\gamma_\mu\gamma_5\psi$, in such a way that parity was still conserved. The Fermi-Gamov-Teller interaction turned out to be valid in view of all β-decay data , which was an indirect evidence of the correctness of the Pauli neutrino hypothesis.

However, a fundamental complication of the Fermi theory arised when calculations beyond the lowest order in perturbation theory led to infinite results. An additional problem was the loss of unitarity, with cross sections growing with energy to arbitrarily large values. The solution to the first difficulty came a few years later by Bethe in 1947 [15] with the concept of renormalisation, i.e. physical quantities are not the bare parameters of the theory and infinites that arise are absorbed in physical quantities. This has led to modern QED, formulated by Feynman, Schwinger and Tomonaga in the 1950s [16–18], whose concepts of gauge symmetry and renormalisability prevailed until today.

The weakly-interacting particle content was then extended with the discovery of the muon (μ) in 1937, by E.C. Stevenson and J.C. Street [19] and C.D. Anderson and S.H. Neddermeyer [20]. Observations of muon decay led B. Pontecorvo to suggest in 1947 [21] the universality of electron and muon weak interactions with nucleons. Such hypothesis was further discussed by G. Puppi [22], O. Klein [23], J. Tiomno and J.A. Wheeler [24] and T.D. Lee, M. Rosenbluth and C.N. Yang [25]. This is probably the origin of the concept now known as *generation* or *family*.

The fact that the neutrino in β-decay is produced together with an electron suggested the introduction of some new conserved quantum number, the *lepton number* L. Its assignments are $L = 1$ for particles and $L = -1$ for the corresponding antiparticles. The existence of a conserved lepton number predicted that neutrino and antineutrino are different particles: the neutrino has $L = +1$ while the antineutrino has $L = -1$. This was confirmed in the reactor experiment of R. Davis in 1955 [26], in which it was verified that the lepton number violating reaction $\overline{\nu} + {}^{37}\mathrm{Cl} \rightarrow e^- + {}^{37}\mathrm{Ar}$ is forbidden. On the other hand, conservation of lepton number also predicted that in inverse β-decay there must exist an antineutrino in the initial state: $\overline{\nu} + p \rightarrow e^+ + n$. It was precisely in the search for a method to measure inverse β-decay that F. Reines and C.L. Cowan devised an experiment in 1953 "to detect the free (anti)neutrino" [27]. Their experiment was the first reactor-neutrino experiment, in which antineutrinos from a nuclear reactor (produced via β-decay) could be detected via the observation of inverse β-decay. The neutrino was finally discovered in 1956 [28] and, for this discovery, F. Reines was awarded the Nobel prize in 1995.

Contemporary to the Cowan-Reines experiment, and motivated by the $\theta - \tau$ puzzle [29], T. D. Lee and C. N. Yang [30] started to question the validity of parity conservation in **all** weak interactions and proposed a number of ways to test it. In the same year, W. S. Wu and collaborators [31] investigated the β-decay of polarised ^{60}Co nuclei and found a large asymmetry in the emission of the electrons with respect to the nuclei polarisation: electrons were predominantly emitted opposite to the direction of the nuclei polarisation. This proved that parity is not conserved in β-decays. Later, parity violation was also observed in other weak processes, such as $\pi^+ \rightarrow \mu^+ + \nu_\mu$ and $\mu^+ \rightarrow e^+ + \nu_e + \overline{\nu}_\mu$. In order to explain parity violation in interactions involving neutrinos, A. Salam in 1956 [32], and L. Landau [33], T. D. Lee and C. N. Yang [34] in 1957 proposed the two-component neutrino theory. Here, the neutrino is a massless spin-$\frac{1}{2}$ particle with only "one spin state", i.e. it has always the same helicity. One year later, Goldhaber, Grodzins and Sunyar [35] measured the polarisation of the neutrino in electron capture $e^- +^{152}\mathrm{Eu} \rightarrow^{152}\mathrm{Sm}^* + \nu_e$, followed by the decay ${}^{152}\mathrm{Sm}^* \rightarrow^{152}\mathrm{Sm} + \gamma$. By measuring the circular polarisation of the photon, they found that the neutrino is a particle with negative helicity, thus supporting the two-component theory. However, these results could not exclude the existence of extremely light neutrinos. In order to account for parity violation in weak interactions, parity-violating couplings had to be included in the weak Lagrangian. This was accomplished with the effective V-A theory formulated in 1958 by R.P. Feynman and M. Gell-Mann [36], E.C.G. Sudarshan and R.E. Marshak [37] and J.J. Sakurai [38], realised in the leptonic sector by the two-component neutrino theory.

In the late fifties, the concept of lepton number was firmly established. However, if muon and electron neutrinos were the same particle, muons would also decay through the $\mu \to e\gamma$ channel, for which experimental limits were many orders of magnitude below predictions. This suggested that ν_e and ν_μ were actually different particles. To test this hypothesis, B. Pontecorvo proposed an experiment in 1959 [39], later realised by L. Lederman et al. in Brookhaven (1962) [40]. This was the first accelerator neutrino experiment, where neutrinos were obtained from decays of pions (produced by the bombardment of a Be target by 15 GeV protons). In these decays, predominantly muon neutrinos are produced ($\pi^+ \to \mu^+ + \nu_\mu$) and if ν_e and ν_μ were the same particles the two processes

$$\nu_\mu + \text{nucleons} \to \mu^- + \text{hadrons}\ , \tag{1.2}$$

$$\nu_\mu + \text{nucleons} \to e^- + \text{hadrons}\ , \tag{1.3}$$

would have the same cross section and equal number of electrons and muons would be detected. The Brookhaven experiment detected 29 muons and only 6 background electrons, thus establishing the existence of a second neutrino. As a consequence, it was necessary to introduce two conserved quantities, the electron lepton number L_e and the muon lepton number L_μ, making $\mu \to e\gamma$ forbidden.

But the sixties were mostly marked by the formulation of the Glashow-Weinberg-Salam Standard Model (SM) of electroweak interactions in 1967-1968 [41, 42]. The SM is based on the SU(2)×U(1) gauge group proposed by S.L. Glashow in 1961 [43] which, in addition to the photon, predicted the existence of weak neutral currents mediated by the Z boson, as well as the $W^\pm$ charged bosons mediating weak charged currents. A key ingredient of the SM is the Higgs mechanism or, in a more conciliatory renaming by P. Higgs, the *ABEGHHK'tH mechanism* (for Anderson [44], Brout and Englert [45], Guralnik [46], Hagen, Higgs [47], Kibble [48] and 't Hooft). This mechanism allows the massless gauge bosons that appear in the gauge model to acquire longitudinal degrees of freedom, making them massive without explicitly breaking the symmetries of the model. The renormalisability of the theory was proved in 1971 by G.'t Hooft and M. Veltman [49, 50], showing the consistency of the model as it allows to calculate higher order corrections to physical quantitites (contrarily to what happened with the current-current and intermediate vector boson theories).

The first crucial confirmation of the success of the SM was the discovery of neutral current neutrino interactions in the bubble chamber "Gargamelle" (1973) [51, 52]. Anoter great triumph of the SM came one year later, with the discovery of the charm quark in the form of the J/Ψ particle ($c\bar{c}$) at BNL (J) [53] and at SLAC (ψ) [54], as predicted by the S. Glashow, J. Iliopoulos and L. Maiani (GIM) mechanism of quark mixing [55]. Finally, the subsequent dicovery of the $W^\pm$ [56, 57] and Z^0 [58, 59] gauge bosons at CERN firmly established the SM as the model for leptonic and hadronic electroweak interactions.

The remaining building blocks of the SM were then gradually discovered, first with the τ lepton discovery by M. Perl in 1975 [60] and with the b quark discovery at Fermilab in 1977 [61]. Through the analysis of invisible Z decay at LEP in 1989, the number of lepton generations was later fixed to three [62]. Finally, as predicted by M. Kobayashi and T. Maskawa in 1973 [63], in order to explain CP violation in K^0-decays, the t quark was discovered at Fermilab in 1995 [64, 65]. This confirmed the existence of three SM generations of leptons and quarks. The only missing piece at the time was the Higgs boson, the quanta of the Higgs field necessary to break the gauge symmetry spontaneously. Its detection took almost fifty years to come about but, as a result of an enormous experimental enterprise put up to find this elusive particle, the observation of a Higgs-like boson with a mass of 125.9 ± 0.4 GeV [66] was finally announced in 2012 by the ATLAS and CMS collaborations [67, 68].

From all existing data at the time of the SM formulation, it followed that neutrino interactions were well described by that theory. However, neutrino masses, magnetic moments and other properties were basically unknown. Measurements of the shape of the high-energy part of the β-decay spectrum of tritium (method proposed by Fermi [11] and Perrin [12]) indicated that neutrinos are much lighter than electrons, with an upper bound at about 100 eV when parity violation in β-decay was discovered [69]. Together with the success of both the SM and the two-component theory (both based on the assumption of massless neutrinos), this led to a general belief that neutrinos were actually massless particles.

It was B. Pontecorvo who, in 1957 (even before the formulation of the SM), considered the possibility of *small but nonzero* neutrino masses [70]. He noted that, contrary to what happens in QED where gauge invariance prevents the photon from acquiring a mass, there is no such principle for neutrinos. Motivated by $K^0 \leftrightarrows \bar{K}^0$ oscillations (M. Gell-Mann and A. Pais [71], 1955), in which the strangeness quantum number is oscillating, Pontecorvo suggested that lepton number is not conserved and that neutrino states produced in weak decays are superpositions of states with definite masses. As a result, *neutrino oscillations* would take place in neutrino beams propagating in vacuum. A seminal paper on neutrino oscillations was published by B. Pontecorvo in 1958 [72]. At that time, R. Davis was conducting an experiment with reactor antineutrinos [73] with the aim of testing lepton number conservation. Davis searched for the production of ^{37}Ar in the process $\bar{\nu}_e + ^{37}\text{Cl} \to e^- + ^{37}\text{Ar}$ with reactor antineutrinos, which is forbidden if L is conserved. A rumor that Davis had seen some events reached B. Pontecorvo, who interpreted that the successful observation could be due to $\bar{\nu} \to \nu$ transitions and a subsequent $\nu + ^{37}\text{Cl} \to e^- + ^{37}\text{Ar}$ reaction (at the time, only one type of neutrino was known and the possible oscillations that he could find were neutrino-antineutrino oscillations). Later, after the Davis experiment was finished and no production of ^{37}Ar was observed, B. Pontecorvo understood that, due to oscillations, the neutrino (antineutrino) could transform into $\overline{\nu_R}$ (ν_R), particles that do not participate in weak interactions. It was thus introduced the concept of *sterile neutrinos*.

A more realistic model of oscillations was discussed at the time of the discovey of the muon neutrino ν_μ in 1962, when Z. Maki, M. Nakagawa and S. Sakata [74] assumed that ν_e and ν_μ are linear orthogonal combinations of two neutrino mass eigenstates, and pointed out that in such case $\nu_e \leftrightarrows \nu_\mu$ transitions become possible. The same idea was published by Pontecorvo in 1967 [75], who considered the oscillations $\nu_{e\,L} \leftrightarrows \nu_{\mu L}$, $\nu_{eL} \leftrightarrows \overline{\nu_{eR}}$ (sterile), $\nu_{e\,L} \leftrightarrows \overline{\nu_{\mu R}}$ (sterile), etc. and applied this idea to solar neutrinos.

At that time, R. Davis and collaborators had started his famous experiment [76] to detect solar neutrinos through the reaction $\nu_e +^{37}\mathrm{Cl} \to e^- +^{37}\mathrm{Ar}$. The solar neutrino flux measured by Davis revealed a deficit of solar neutrinos when compared with the current solar model predictions. This led to the so-called "solar neutrino problem". It took many years of research to find that the neutrino oscillation hypothesis was the best candidate to explain the solar neutrino deficit. The development of the theory of neutrino oscillations was finally achieved in 1975-76 by S. Eliezer and A. Swift [77], H. Fritzsch and P. Minkowski [78], S. Bilenky and B. Pontecorvo [79].

Despite some plausible arguments given in the seventies for small but nonzero neutrino masses there was not much interest in neutrino masses and mixings at that time: the two-component theory for a massless neutrino was still the popular. The interest in massive neutrinos and neutrino oscillations increased significantly by the end of the seventies with the works by Pati and Salam in 1973 [80] and Georgi and Glashow in 1974 [81] on grand unified theories (GUTs). Such interest was driven by the fact that in these models leptons and quarks appear in the same multiplets, and the mass-generation mechanism naturally leads to nonzero neutrino masses. A major cornerstone for the theoretical research on neutrino physics was the formulation of the seesaw mechanism in 1979 [82], in the context of specific GUT models such as horizontal, left-right and SO(10) symmetric models. The seesaw model could explain the smallness of neutrino masses with respect to the masses of charged fermions in the SM. In that same year, a model-independent description of small neutrino masses was written down by S. Weinberg [83] and, as an application, a minimal nonsupersymmetric SO(10) model was constructed. From this early enthusiasm, it became clear that the seesaw mechanism would be a major tool in understanding neutrino masses and mixings if experimental evidence would ever appear. Indeed, this turned out to be the case and, as a consequence, neutrino masses and mixing started to be considered as a signature of physics beyond the SM, beginning a new era in neutrino physics.

In the 1980's, several short-baseline experiments with accelerator and reactor neutrinos were performed but no positive indication of oscillations was found using these artificially produced neutrinos [1]. On the other hand, the neutrino oscillation hypothesis to explain the solar neutrino deficit was strengthened by the Kamiokande experiment [84]. In this water Cherenkov experiment, high-energy solar neutrinos from the decay $^8\mathrm{B} \to ^8\mathrm{Be} + e + \nu_e$ were detected via the observation of recoil electrons from electron-neutrino scattering $\nu_e + e \to \nu_e + e$. The observed flux of solar neutrinos was about $1/2$ of the predictions, and was later confirmed by the results of GALLEX/GNO [85], SAGE [86], Super-Kamiokande [87] and SNO [88]. Particularly relevant, the results of the SNO experiment allowed to obtain model-independent evidence of solar ν_e disappearance. Observations showed that the flux of ν_e was three times smaller than the flux of ν_e, ν_μ and ν_τ, which was instrumental in solving the solar neutrino problem in 2002. The solar electron-neutrino deficit was finally found to be due to oscillations of ν_e into ν_μ and ν_τ inside the Sun through the Mikheev-Smirnov-Wolfenstein effect [89–91], and the model proposed by J. Bahcall and others [92] has become the Standard Solar Model.

Atmospheric neutrinos were first detected by underground experiments located in South Africa

[1] More recently, the recalculated fluxes of $\bar{\nu}_e' s$ from reactors were found to be (3-4)% higher than the old ones, which is nowadays interpreted as a positive indication of short-baseline neutrino oscillations.

[93] and India [94] and the first measurements of atmospheric neutrino fluxes were performed in the iron calorimeter experiments NUSEX [95] in 1989 and Fréjus [96] in 1995. The results of these experiments were apparently in agreement with the predicted ratio, but this turned out to be contradicted by the Kamiokande and IMB experiments, which found a significantly smaller number of ν_μ-induced events. This effect was called the *atmospheric neutrino anomaly* and could be explained by transitions of ν_μ into other neutrino states. But the breakthrough in (atmospheric) neutrino physics happened in 1998, when the Super-Kamiokande (SK) collaboration proved that the number of observed muon neutrinos depended on the distance travelled by neutrinos from the production point in the atmosphere to the detector. This was the *first model-independent evidence of neutrino oscillations*. One of the most important results obtained by SK is that the mixing angle θ_{23} involved in atmospheric neutrino oscillations is large (almost maximal), contrarily to what happens in the quark sector where all mixing angles are small. This was later confirmed by the independent results of the long-baseline K2K [97] and MINOS [98] accelerator experiments. Another very important experiment was the KamLAND reactor neutrino experiment in Japan [99]. In 2002-2004, KamLAND reported that the total number of $\bar{\nu}_e$ events was $\sim 60\,\%$ of the number of expected events, providing another model-independent evidence of reactor neutrino oscillations. Together, the data from SNO, SK and KamLAND experiments established the large mixing angle pattern as a solution to the solar neutrino problem, with a solar neutrino mass-squared difference $\Delta m^2_\odot \sim \mathcal{O}(10^{-5}\,\mathrm{eV}^2)$ and a mixing angle $\sin^2\theta_{12} \approx 0.3$. Subsequent experiments using reactor and accelarator neutrinos have gradually measured the solar and atmospheric neutrino parameters with a few to several percent accuracy.

In recent years, the T2K collaboration (in 2011) reported evidence for a non-zero reactor mixing angle θ_{13} [100]. This was subsequently supported by observations from the MINOS [101] and Double Chooz [102] collaborations, although with smaller statistical significance. Finally, in 2013, the Daya Bay reactor antineutrino [103] and the RENO experiments [104] both reported results consistent with a nonvanishing reactor mixing angle θ_{13} with rather high precisions of 5.2σ and 4.9σ, respectively.

1.2 Motivation and thesis outline

Despite the precise experimental determination of the parameters responsible for neutrino oscillations, the most fundamental questions regarding neutrinos are still to be answered. In first place, from neutrino oscillation experiments, neutrino mass-squared differences and mixing angles are very well known. However, absolute neutrino masses and their hierarchy are still unknown. Besides probing the neutrino mass scale and their mass hierarchy, we also need to make clear what is the nature of neutrinos: are they Dirac or Majorana particles? Secondly, in spite of irrefutable evidence for Lepton Flavor Violation (LFV) in neutrino oscillations, all searches for LFV in the charged lepton sector (CLFV) have obtained negative results so far. However, the expected improvement of experimental sensitivities on CLFV processes by several orders of magnitude justifies the theoretical study of CLFV processes in models for neutrino masses.

Concerning CLFV, it is well known that a minimal extension of the SM with massive (Dirac) neutrinos, in which total lepton number L is conserved, guarantees non-vanishing CLFV, but at a strongly suppressed level. The predictions of this model obviously satisfy the current experimental limits but do not give a natural explanation to the huge disparity between the magnitude of neutrino masses and the masses of charged fermions. This suggests that neutrino masses are related to a new, yet unknown, physics scale Λ, i.e. to physics beyond the SM. A natural explanation for tiny neutrino masses is provided by the seesaw models of neutrino mass generation. In these models, the scale Λ is set by the scale of masses of the new degrees of freedom, which can be either fermion singlets (triplets) in the minimal type I (type III) seesaw scenario or scalar triplets in the type II seesaw model.

The scale Λ at which the new physics manifests itself can, in principle, have an arbitrary large value, up to the GUT scale and even beyond. An interesting possibility, which may even be supported by hierarchy arguments, is to have Λ at the TeV scale, i.e. $\Lambda \sim \mathcal{O}(\text{TeV})$, in a way which naturally accomodates tiny neutrino masses while allowing for large Yukawa couplings. Such low-energy scenario requires a common and model-independent pattern, which we discuss [105]. In such scenario, predicted rates of CLFV processes, such as $\ell_\alpha \to \ell_\beta \gamma$, $\ell \to 3\ell$ and $\mu - e$ conversion in nuclei, can lie within the reach of future experimental sensitivities, even when direct detection of the new particles is not achievable at the LHC [106]. Moreover, an analysis of the behavior of CLFV rates in each type of seesaw could be used to determine (or exclude) the mechanism responsible for neutrino masses.

The present thesis is organised as follows. In Chapter 2, we review the main aspects of the SM, in particular of its electroweak sector. Then, in Chapter 3, we discuss how to describe massive neutrinos in the most general Dirac-Majorana case and review the main features of the three canonical seesaw scenarios, both their complete and effective description. In the end of the chapter, we also consider the possibility of a TeV-scale seesaw. In Chapter 4 we analyse phenomenological signals for each seesaw, such as those associated with non-unitarity. Limits on the parameters of each model are obtained from present bounds on CLFV processes as well as data on other electroweak decays, and sensitivities of future experiments are also discussed. Finally, we draw an overall conclusion in Chapter 5. Technical details, like one-loop calculations, are collected at the end of the thesis.

2 The Standard Model of particle physics

"The Standard Model is the ultimate result of a long period of progress in elementary particle physics. It is a consistent, finite and, within the limitations of our present technical hability, compuTable theory of fundamental microscopic interactions that sucessfully explains all known phenomena in elementary particle physics, describing strong, electromagnetic and weak interactions. "

– G. Altarelli, *Encyclopedia of Mathematical Physics*

Despite all its successes, the Standard Model (SM) of strong and electroweak interactions contains some flaws and unexplained phenomena. However, it still constitutes the foundations on which our quest for new physics must be built. As such, we start the present work by making a brief introduction to the SM, with particular emphasis to the problem of neutrino masses and mixings.

2.1 Field content and Lagrangian

The SM of particle physics consists in a mathematical description of strong, weak and electromagnetic interactions. It is a relativistic quantum field theory built by postulating an underlying symmetry group of *local* (continuous) transformations

$$G_{\text{SM}} = \underbrace{\text{SU}(3)_c}_{\text{QCD}} \otimes \underbrace{\text{SU}(2)_L \otimes \text{U}(1)_Y}_{\text{EW interactions}} \,, \tag{2.1}$$

being thus a so-called *gauge theory*. The subscripts label new degrees of freedom called colour (c), left-handed chirality (L) and weak hypercharge (y). The $\text{SU}(3)_c$ factor is the symmetry group responsible for strong interactions whereas $\text{SU}(2)_L \otimes \text{U}(1)_Y$ accounts for electroweak (EW) interactions.

As we will see, the symmetry group G_{SM} fixes the possible interactions of the theory, i.e. the number and properties of mediating vector gauge bosons. On the other hand, the number and properties of fermions and scalar bosons is unconstrained, except for the fact that they must transform under a definite representation of the symmetry group G_{SM}, and the fermion content must not lead to quantum anomalies[1] [107]. There exist $n_g = 3$ generations of spin 1/2 fermions with identical properties (apart from their masses), which are the fundamental constituents of visible matter. They are divided in quarks

[1]Quantum anomalies refer to quantum effects that break the symmetries associated with the classical equations of motion. In particular, they may occur when the divergences in a theory cannot be regularised consistently with the original symmetries.

and leptons, as shown in Table 2.1. Quarks are the elementary components of hadrons (but do not exist as free particles), and participate in all interactions, whereas leptons do not undergo strong interactions.

	Leptons				Quarks		
	Flavour		Electric charge (e)	Mass (GeV$/c^2$)	Flavour	Electric charge (e)	Mass (GeV$/c^2$)
Generations	ν_e	electron neutrino	0	$< 1 \times 10^{-5}$	u (up)	2/3	2.3×10^{-3}
	e	electron	-1	5.11×10^{-4}	d (down)	-1/3	4.8×10^{-3}
	ν_μ	muon neutrino	0	$< 1 \times 10^{-8}$	c (charm)	2/3	1.3
	μ	muon	-1	0.106	s (strange)	-1/3	9.5×10^{-2}
	ν_τ	tau neutrino	0	≈ 0	t (top)	2/3	173
	τ	tau	-1	1.78	b (bottom)	-1/3	4.2

Table 2.1: Fermionic content of the SM. Electric charges and masses were taken from Ref. [66].

The next step in the construction of the theory is to choose proper representations for the fermion fields. This choice has been guided by the wisdom of history, in particular by the $V - A$ theory of weak interactions and the two-component theory of the massless neutrinos. These theories are chiral theories, i.e. they treat differently right- and left-handed components of fermion fields

$$\psi_R = \frac{1+\gamma_5}{2}\psi \equiv P_R\psi \, , \qquad\qquad \psi_L = \frac{1-\gamma_5}{2}\psi \equiv P_L\psi \, . \tag{2.2}$$

where γ_5 is the chirality matrix and P_L (P_R) is the left (right)-handed chirality operator. The chiral fields $\psi_{R,L}$ can be described as two-component spinors and are the simplest nontrivial representations of the Lorentz group [3], i.e. the fields ψ_R and ψ_L transform independently under Lorentz transformations. In view of this, they must be considered as the fundamental ingredients for the construction of the SM Lagrangian, which must be a scalar under the Poincaré group. The SM is also a chiral theory with left-handed chiral components of the fermion fields grouped into weak isospin doublets (two-component column vectors under SU(2)$_L$) and with right-handed fields being singlets under SU(2)$_L$, thus leading to parity breaking in SU(2)$_L$. The fermionic field content of the SM is conveniently summarised in Table 2.2. It should be noticed that these fields are weak eigenstates, i.e. they have definite gauge transformation properties and only after spontaneous symmetry breaking (SSB) of the gauge symmetry will these states become admixtures of mass eigenfields. As can be seen from Table 2.2, there are $2n_g = 6$ quark flavours and each carries a colour index $m = 1, 2, 3$, $u^m_{\alpha L,R}$ or $d^m_{\alpha L,R}$ (each quark flavour is thus a three-component column vector under SU(3)$_c$). On the other hand, leptons are colour singlets, i.e. they are invariant under SU(3)$_c$. Leptons are divided into charged components (e, μ, τ) and corresponding neutrinos (ν_e, ν_μ, ν_τ), with electric charges -1 and 0, respectively. Particularly relevant for our later discussion is the fact that, in the SM, only left-handed neutrinos are introduced (inherited from the two-component neutrino theory). This property will be specially important because it leads to strictly massless neutrinos in the SM.

Quark fields	Quantum numbers $(\boldsymbol{n_3}, \boldsymbol{n_2}, y)$	Lepton fields	Quantum numbers $(\boldsymbol{n_3}, \boldsymbol{n_2}, y)$
$Q_{\alpha L} = \begin{pmatrix} u_{\alpha L} \\ d_{\alpha L} \end{pmatrix}$	(**3**, **2**, 1/3)	$L_{\alpha L} = \begin{pmatrix} \nu_{\alpha L} \\ \ell_{\alpha L} \end{pmatrix}$	(**1**, **2**, -1)
$u^m_{\alpha R}$	(**3**, **1**, 4/3)	$\ell_{\alpha R}$	(**1**, **1**, -2)
$d^m_{\alpha R}$	(**3**, **1**, -2/3)		

Table 2.2: SM fermionic fields, with the quantum numbers regarding (SU(3),SU(2),U(1)) representation assignments. The index α runs over three generations (or families) of fermions.

The quantum numbers $(\boldsymbol{n_3}, \boldsymbol{n_2}, y)$ in Table 2.2 are representation assignments for each fermion. They are thus related to the transformation properties of the fields under the group G_{SM} of local transformations. An element g of $G_{\text{SM}} = \text{SU(3)}_c \otimes \text{SU(2)}_L \otimes \text{U(1)}_Y$ can be parametrised by $8+3+1$ local parameters $(\underline{\Theta}(x), \underline{\theta}(x), \eta(x))$, with $\underline{\Theta}(x) = (\Theta_1(x), ..., \Theta_8(x))$ and $\underline{\theta}(x) = (\theta_1(x), \theta_2(x), \theta_3(x))$, which depend on space-time coordinates x. Thus, under $g \in G_{\text{SM}}$ a general field ψ transforms as

$$\psi(x) \to U_g(x)\psi(x) \equiv \exp\left[\, i\Theta^s(x)T^s \,\right] \exp\left[\, i\theta^k(x)I^k \,\right] \exp\left[\, i\eta(x)Y \,\right] \psi(x) \,. \tag{2.3}$$

The operators T_s, I_k and Y are the generators of SU(3)_c, SU(2)_L and U(1)_Y, respectively. For a general SU(N) group there are N^2-1 generators t^k obeying the relations

$$\left[t^a, t^b\right] = i f_{abc} t_c \quad \text{with} \quad \text{Tr}[t^a t^b] = \frac{1}{2}\delta_{ab} \,, \qquad a,b,c = 1, ..., N^2-1 \,, \tag{2.4}$$

where f_{abc} are the structure constants of the group, $f_{abc} = \varepsilon_{abc}$ for SU(2). Hence, there are eight generators T^s for SU(3)_c and three generators I^k for SU(2)_L, and the trace in Eq. (2.4) implies that for each representation of the gauge groups the scale of the generators is fixed. On the other hand, for U(1)_Y the only generator is the hypercharge operator Y, whose action on each representation is fixed after SSB. As can be seen from Table 2.2, SM fermions are either in a fundamental or in a singlet representation of SU(3)_c and SU(2)_L. The corresponding generators for each representation are organised in Table 2.3.

In order to implement local gauge invariance of the Lagrangian under G_{SM}, the usual partial derivative ∂_μ must be replaced by a covariant one D_μ in the kinetic terms of the Lagrangian:

$$\partial_\mu \to D_\mu = \partial_\mu - i g_s G^s_\mu T_s - i g A^k_\mu I_k - i g' B_\mu \frac{Y}{2} \,, \tag{2.5}$$

where g_s, g and g' are coupling constants associated with each invariant subgroup of G_{SM}. For each generator of the gauge, local gauge invariance requires the introduction of one vector gauge boson, which transforms in such a way that the kinetic terms are kept invariant under G_{SM}. These will give origin to the vector bosons that mediate strong and EW interactions: eight massless gluons for strong interactions, the massive Z and $W^\pm$ for weak interactions and the photon for electromagnetism.

	Quantum number	T_s	I_k	Y
Fundamental representation	$n_3 = 3$ / $n_2 = 2$ / $y \neq 0$	$\frac{1}{2}\lambda_s$	$\frac{1}{2}\tau_k$	y
Singlet representation	$n_3 = 1$ / $n_2 = 1$ / $y = 0$	0	0	0

Table 2.3: Generators of SU(3)$_c$, SU(2)$_L$ and U(1)$_Y$ transformations for the fundamental and singlet representations in the SM. λ_s are the Gell-Mann matrices in a certain basis and τ_k are the Pauli matrices.

At this point, the SM Lagrangian is then the most general renormalisable Lagrangian invariant under the local symmetry group G_{SM} and written in terms of fermion and gauge boson fields,

$$\mathcal{L} = \mathcal{L}_{\text{gauge}} + \mathcal{L}_{\text{f}} \, , \tag{2.6}$$

where the gauge Lagrangian $\mathcal{L}_{\text{gauge}}$ contains the kinetic terms and self-couplings of the gauge bosons:

$$\mathcal{L}_{\text{gauge}} = -\frac{1}{4} G^s_{\mu\nu} G^{\mu\nu s} - \frac{1}{4} A^k_{\mu\nu} A^{\mu\nu k} - \frac{1}{4} B_{\mu\nu} B^{\mu\nu} \, . \tag{2.7}$$

It corresponds to the Proca Lagrangian for massless vector (spin 1) fields with the following definitions of the field strength tensors for SU(3)$_c$, SU(2)$_L$ and U(1)$_Y$, respectively:

$$G^s_{\mu\nu} = \left(\partial_\mu G^s_\nu - \partial_\nu G^s_\mu\right) + g_s f_{sjl} G^j_\mu G^l_\nu \, , \qquad s, j, l = 1, ..., 8 \, , \tag{2.8}$$

$$A^k_{\mu\nu} = \left(\partial_\mu A^k_\nu - \partial_\nu A^k_\mu\right) + g \varepsilon_{kjl} A^j_\mu A^l_\nu \, , \qquad k, j, l = 1, \, 2 \, , 3 \, , \tag{2.9}$$

$$B_{\mu\nu} = \left(\partial_\mu B_\nu - \partial_\nu B_\mu\right) \, . \tag{2.10}$$

On the other hand, the SU(2)$_L$ and U(1)$_Y$ fermion representations are chiral and, therefore, no fermion (Dirac) mass terms of the type $m\overline{\psi}\psi$ are explicitly allowed because they would break the gauge symmetry. Therefore, the fermions Lagrangian $\mathcal{L}_{\text{f}}$ consists entirely of gauge invariant kinetic terms,

$$\mathcal{L}_{\text{f}} = \underbrace{\left(\overline{Q_{L\alpha}} i \not{D} Q_{L\alpha} + \overline{u_{R\alpha}} i \not{D} u_{R\alpha} + \overline{d_{R\alpha}} i \not{D} d_{R\alpha}\right)}_{\mathcal{L}_{\text{quarks}}} + \underbrace{\left(\overline{L_{R\alpha}} i \not{D} L_{R\alpha} + \overline{\ell_{R\alpha}} i \not{D} \ell_{R\alpha}\right)}_{\mathcal{L}_{\text{leptons}}} \, . \tag{2.11}$$

Expanding the first term,

$$\overline{Q_{\alpha L}} i \not{D} Q_{\alpha L} = i \begin{pmatrix} \overline{u_L} & \overline{d_L} \end{pmatrix}_{m\alpha} \gamma^\mu \left[\left(\partial_\mu I - \frac{ig}{2} \vec{\tau} \cdot \vec{A}_\mu - \frac{ig'}{6} I B_\mu \right) \delta_{mn} - \frac{ig_s}{2} \vec{\lambda}_{mn} \cdot \vec{G}_\mu I \right] \begin{pmatrix} \overline{u_L} \\ \overline{d_L} \end{pmatrix}_{n\alpha} \, , \tag{2.12}$$

it is clear that the SU(3)$_c$ and SU(2)$_L$ $\otimes$U(1)$_Y$ groups commute [108]. Added to the fact that the colour group SU(3)$_c$ will remain unbroken, this implies that EW interactions can be studied separately from strong itneractions. As such, in the following we will simplify the notation by suppressing colour indices on quark fields and omitting contributions from SU(3)$_c$ in the covariant derivatives.

2.2 Higgs mechanism

"If my view is correct, the universe may have a kind of domain structure. In one part of the universe you may have one preferred direction of the axis; in another part the direction may be different."

– Y. Nambu

The SM as described is not a realistic theory since bare mass terms for fermions or electroweak gauge bosons are not allowed in the Lagrangian, contrarily to the experimentally known existence of massive fermions and vector bosons. However, effective masses may be generated if we give up from an exact and unbroken gauge symmetry principle by breaking the SM gauge symmetry spontaneously [109, 110]:

$$G_{\text{SM}} = \text{SU}(3)_c \otimes \text{SU}(2)_L \otimes \text{U}(1)_Y \quad \xrightarrow{\text{SSB}} \quad \text{SU}(3)_c \otimes \text{U}(1)_Q \ . \tag{2.13}$$

The $\text{SU}(3)_c$ symmetry remains unaffected by SSB since it encodes an exact symmetry of nature whereas the electroweak $\text{SU}(2)_L \otimes \text{U}(1)_Y$ symmetry is spontaneously broken into an $\text{U}(1)_Q$ symmetry corresponding to electric charge conservation. The gauge symmetry must be spontaneously broken instead of explicitly to ensure renormalisability [49] and unitarity [111].

The SSB mechanism is implemented by introducing in the theory scalar fields whose vacuum state $|0\rangle$ is not $\text{SU}(2)_L \otimes \text{U}(1)_Y$ symmetric, i.e. $U_{G_{\text{SM}}} |0\rangle \neq |0\rangle$. Fermion and vector boson fields cannot be used for this purpose because their ground state must be zero in order to preserve Lorentz invariance. Also, charged scalar fields must vanish in the vacuum, to keep it electrically neutral[2]. Thus, only neutral scalar fields can have a nonzero value in vacuum, the so-called *vacuum expectation value* (VEV). Considering that masses for the Z and $W^{\pm}$ vector bosons must be generated while keeping the photon massless, we must introduce at least 3 degrees of freedom for the scalar fields, two of which are charged. The simplest/minimal choice is a complex $\text{SU}(2)_L$ doublet of scalar fields, the Higgs doublet:

$$\Phi(x) = \begin{pmatrix} \phi^+(x) \\ \phi^0(x) \end{pmatrix} = \frac{1}{\sqrt{2}} \begin{pmatrix} \varphi_1(x) + i\varphi_2(x) \\ \varphi_3(x) + i\varphi_4(x) \end{pmatrix} \ , \qquad \Phi \sim (\mathbf{1},\mathbf{2},1) \ , \tag{2.14}$$

where φ_i are real fields and the signs in superscript will soon be explained. To the SM Lagrangian (2.6) we then need to add the gauge invariant Lagrangian term for the scalar field:

$$\mathcal{L}_{\text{Higgs}} = (D_\mu \Phi)^\dagger (D^\mu \Phi) - V(\Phi) \ . \tag{2.15}$$

The term $V(\Phi^\dagger \Phi)$ corresponds to the most general renormalisable scalar potential[3],

$$V(\Phi) = \mu^2 \Phi^\dagger \Phi + \lambda \left(\Phi^\dagger \Phi\right)^2 = \mu^2 \left(\sum_{i=1}^{4} \varphi_i^2\right) + \lambda \left(\sum_{i=1}^{4} \varphi_i^2\right)^2 \ . \tag{2.16}$$

[2]This is a consequence of the CPT theorem, according to which any Lorentz-invariant gauge quantum field theory is invariant under a CPT transformation.

[3]Power counting of divergent diagrams dictates that Lagrangian terms containing products of fields with energy dimension larger than four are not renormalisable (see, for example, [112]).

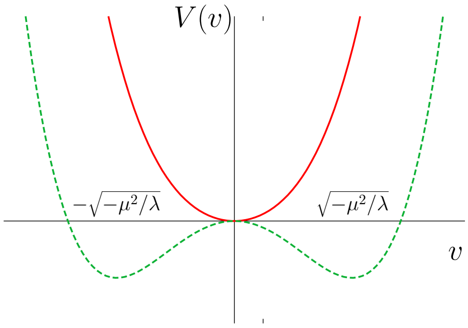

Figure 2.1: Potential $V(v)$ in Eq. (2.17) for $\mu^2 > 0$ (solid) and for $\mu^2 < 0$ (dashed).

and is obviously O(4) $\sim$ SU(2) $\otimes$ SU(2) invariant, which is a clear example of an *accidental symmetry*. However, the associated extra generators are explicitly broken by the gauge interactions in Eq. (2.15).

Since our interest lies on the mass spectrum, we must study the theory around the minimum energy state (lowest-energy classical solution), because particles are the result of oscillations around it. This state is the ground state value of Φ, $\langle 0|\Phi|0\rangle \equiv \langle\Phi\rangle$. From the Lagrangian (2.15), we see that the lowest-energy solution is for $\varphi_i(t,\vec{x})$ = 'constant' since any x-dependence of the ground state would violate translation invariance. Without loss of generality, we can perform an SU(2)$_L\otimes$ U(1)$_Y$ rotation so that

$$\langle\Phi\rangle = \frac{1}{\sqrt{2}}\begin{pmatrix}0\\ v\end{pmatrix} \qquad \text{and} \qquad \langle V(\Phi)\rangle \to V(v) \equiv \frac{\mu^2}{2}v^2 + \frac{\lambda}{4}v^4\,, \quad \text{with} \quad v\in\mathbb{R}_0^+\,. \tag{2.17}$$

Thus, the minimisation of $V(\Phi)$ is equivalent to that of a potential $V(v)$ with a single hermitian scalar field. One must choose $\lambda > 0$ so that $V(v)$ is bounded from below. However, the sign of μ^2 is arbitrary and the shape of $V(v)$ in Fig. 2.1 must be carefully analysed.

For $\mu^2 > 0$, there is only one minimum at $v = 0$ and SU(2)$_L\otimes$ U(1)$_Y$ is unbroken, i.e. $U_{G_{\rm SM}}\langle\Phi\rangle = \langle\Phi\rangle$. This case corresponds to the so-called Wigner-Weyl realisation of the symmetry. The other possibility, $\mu^2 < 0$, corresponds to SSB, also known as the Nambu-Goldstone realisation of the symmetry. In this case $U_{G_{\rm SM}}\langle\Phi\rangle \neq \langle\Phi\rangle$ and the SU(2)$_L\otimes$ U(1)$_Y$ symmetry is broken with a minimum at

$$v = \sqrt{\frac{-\mu^2}{\lambda}}\,. \tag{2.18}$$

For the sake of completeness, one must say that for $\mu^2 = 0$ it is not sufficient to consider the classical theory. In this case, it can be proven that by adding quantum corrections to the potential the symmetry is again spontaneously broken [113].

Thus, from now on, we will consider the case $\mu^2 < 0$, for which the generators I^k and Y are spontaneously broken[4]. Namely, we have

$$I^k\langle\Phi\rangle = \frac{\tau^k}{2}\cdot\frac{1}{\sqrt{2}}\begin{pmatrix}0\\ v\end{pmatrix} \neq 0,\ k=1,2,3, \qquad Y\langle\Phi\rangle = \frac{1}{2}\cdot\frac{1}{\sqrt{2}}\begin{pmatrix}0\\ v\end{pmatrix} \neq 0\,. \tag{2.19}$$

[4]To see which symmetry groups G are unbroken one simply needs to check if the VEV of the field belongs to the kernel of the transformations defined by the group generators T, since in this case $e^{i\alpha T}\langle\phi\rangle = (1 + i\alpha T + ...)\langle\phi\rangle = \langle\phi\rangle + i\alpha T\langle\phi\rangle + ... \approx \langle\phi\rangle$.

However, there is still a combination of SU(2)$_L\otimes$ U(1)$_Y$ generators which leaves the vacuum invariant:

$$\left[\frac{Y}{2}+I^3\right]\langle\Phi\rangle=\left[\frac{1+\tau^3}{2}\right]\frac{1}{\sqrt{2}}\begin{pmatrix}0\\ v\end{pmatrix}=\frac{1}{\sqrt{2}}\begin{pmatrix}1 & 0\\ 0 & 0\end{pmatrix}\begin{pmatrix}0\\ v\end{pmatrix}=0\,. \tag{2.20}$$

To this unbroken U(1)$_Q$ symmetry we associate electric charge conservation, and the unbroken generator Q is interpreted as the electric charge operator, related to the weak isospin generator I^3 and to the hypercharge operator Y by the Gell-Mann-Nishijima relation [114]:

$$Q=\frac{Y}{2}+I^3\,. \tag{2.21}$$

Applying this operator to the Higgs doublet Φ, we get

$$Q\Phi=\begin{pmatrix}1 & 0\\ 0 & 0\end{pmatrix}\begin{pmatrix}\phi^+\\ \phi^0\end{pmatrix}=\begin{pmatrix}\phi^+\\ 0\end{pmatrix}\,, \tag{2.22}$$

showing that ϕ^+ is a singly-charged scalar field whereas ϕ^0 is a neutral scalar field.

In order to derive the physical consequences of SSB, one must quantise the theory around the classical vaccum state, i.e. write $\Phi=\langle\Phi\rangle+\Phi'$, where Φ' is a scalar field with zero VEV. At first order, the Higgs doublet can be written as

$$\Phi(x)=\begin{pmatrix}\phi^+\\ \frac{(v+H+i\varphi_z)}{\sqrt{2}}\end{pmatrix}\approx\frac{1}{\sqrt{2}}\exp\left(i\xi^jL^j\right)\begin{pmatrix}0\\ v+H\end{pmatrix}\,,\quad j=1,2,3\,, \tag{2.23}$$

with $\phi^+\approx\frac{\xi^2+i\xi^1}{\sqrt{2}}$ and $\varphi_z\approx-\xi^3$. The L^j are the three broken generators I^1, I^2 and $I^3-Y/2$, and H is a real scalar field, the physical Higgs boson obtained by excitations of the neutral Higgs field above the vacuum. The fields ξ^1, ξ^2 and ξ^3 would be the massless pseudoscalar Goldstone bosons if we had been dealing with a global symmetry [115, 116]. In a gauge theory, these unphysical fields can be *gauged away* from the physical spectrum by the following gauge transformation

$$\Phi\to\exp\left(-i\xi^jL^j\right)\Phi=\frac{1}{\sqrt{2}}\begin{pmatrix}0\\ v+H\end{pmatrix}\,, \tag{2.24}$$

which defines the so-called unitary gauge, where only physical degrees of freedom remain. Rewritting the Higgs Lagrangian (2.15) in the unitary gauge, we then obtain

$$\begin{aligned}\mathcal{L}_{\text{Higgs}}&=\frac{1}{2}\left(\partial_\mu H\right)\left(\partial^\mu H\right)-\mu^2H^2\\ &+\frac{1}{2}\left(1+\frac{H}{v}\right)^2\left\{\frac{v^2}{4}g^2\left(A^1_\mu A^{1\mu}+A^2_\mu A^{2\mu}\right)+\begin{pmatrix}A^3_\mu\\ B_\mu\end{pmatrix}^T\begin{pmatrix}g^2 & -gg'\\ -gg' & g'^2\end{pmatrix}\begin{pmatrix}A^3_\mu\\ B_\mu\end{pmatrix}\right\}\\ &+\text{nonbilinear terms}\,.\end{aligned} \tag{2.25}$$

Diagonalising the mass (squared) matrix

$$M^2 = \frac{1}{4}v^2 \begin{pmatrix} g^2 & -gg' \\ -gg' & g'^2 \end{pmatrix} , \tag{2.26}$$

we get two mass eigenstates A_μ and Z_μ with eigenvalues 0 and $\frac{v^2}{4}(g^2 + g'^2)$, respectively:

$$\begin{cases} A_\mu = \sin\theta_W A^3_\mu + \cos\theta_W B_\mu \\ Z_\mu = \cos\theta_W A^3_\mu - \sin\theta_W B_\mu \end{cases} , \qquad \tan\theta_W \equiv \frac{g'}{g} , \tag{2.27}$$

where θ_W is the weak mixing angle [41, 43]. Defining the fields W_μ and $W^\dagger_\mu$ through the relations

$$W_\mu = \frac{A^1_\mu + iA^2_\mu}{\sqrt{2}} , \qquad W^\dagger_\mu = \frac{A^1_\mu - iA^2_\mu}{\sqrt{2}} , \tag{2.28}$$

we can finally rewrite the Higgs Lagrangian (2.26) in terms of the new massive fields W_μ, Z_μ and A_μ as

$$\begin{aligned} \mathcal{L}_{\text{Higgs}} = &\frac{1}{2}(\partial_\mu H)(\partial^\mu H) - \mu^2 H^2 + \frac{1}{4}\left(1 + \frac{H}{v}\right)^2 \left\{ \frac{v^2}{2} g^2 \left(W^\dagger_\mu W^\mu\right) + \frac{v^2}{4}(g^2 + g'^2) Z_\mu Z^\mu \right\} \\ &+ \text{nonbilinear terms} . \end{aligned} \tag{2.29}$$

From (2.29), it is clear that we have succeded in our quest to generate three massive vector bosons (Z and W's) while keeping one vector boson massless (the photon A_μ). This mass generation can be thought as resulting from constant interactions of the W and Z bosons with the condensate of scalar fields. In the unitary gauge, each *gauged away* Goldstone boson has reemerged as the longitudinal polarisation of a massive vector boson, which is confirmed by counting degrees of freedom (twelve, before and after SSB). This is the essence of the Higgs mechanism. At tree level, the SM prediction is

$$M_W = \left|\frac{gv}{2}\right| , \qquad M_Z = \sqrt{\frac{g^2 + g'^2}{4}} = \frac{M_W}{\cos\theta_W} , \qquad M_A = 0 . \tag{2.30}$$

and experiments yield the values $M_Z = 91.1876 \pm 0.0021$ GeV and $M_W = 80.385 \pm 0.015$ GeV [66]. Thus, in the SM one expects the below defined ρ parameter to be unit at tree level:

$$\rho = \frac{M_W^2}{M_Z^2 \cos\theta_W^2} = 1 . \tag{2.31}$$

If we extend the Higgs sector of the SM to include several Higgs multiplets Φ_k, there is a deviation from (2.31), since the new VEVs v_k will give additional contributions to the masses of gauge bosons [117]:

$$\rho = \frac{\sum_k \left[I_k(I_k + 1) - (I^3_k)^2\right] v_k^2}{2\sum_k (I^3_k)^2 v_k^2} , \tag{2.32}$$

where I_k is the weak isospin of the Higgs multiplet Φ_k and I^3_k is the third isospin component of the component of Φ_k which acquires a VEV. From Eq. (2.32), we see that $\rho = 1$ for any number of Higgs doublets ($I_k = 1/2$), whereas additional isospin multiplets are severely constrained by the experimental value $\rho_{\text{exp.}} = 1.0004^{+0.0003}_{-0.0004}$ [66]. On the other hand, from (2.30), one can also observe that in the limit

$g' \to 0$ one has $M_W = M_Z$. This is because the global O(4) symmetry of (2.16) is broken to O(3) ∼ SU(2) by SSB and this global symmetry is respected by the gauge interactions in (2.15) for $g' = 0$. In this limit the W's and the Z form a triplet of an unbroken symmetry, and that is why in this limit their masses is the same. It is this *custodial symmetry* [118], an accidental approximate symmetry of the SM, what 'protects' the ρ parameter from acquiring large radiative corrections in the SM.

Finally, the second term in the Lagrangian (2.29) represents a (tree level) mass

$$M_H = \sqrt{-2\mu^2} = v\sqrt{2\lambda} \tag{2.33}$$

for the Higgs boson, which experimentally has the value $M_H = 125.7 \pm 0.4$ GeV [66].

2.3 Fermion masses

Until now, we have described how the W and Z bosons become massive after SSB but, with no further considerations, the fermions of the theory remain massless. However, by introducing the Higgs doublet (2.14) with hypercharge $y = +1$, one can couple it to fermions through the Yukawa Lagrangian

$$\mathcal{L}_{\text{Yuk.}} = -\left(\mathbf{Y}^{\ell}_{\alpha\beta}\overline{L_{\alpha L}}\Phi\ell_{\beta R} + \text{h.c.}\right) - \left(\mathbf{Y}^{u}_{\alpha\beta}\overline{Q_{\alpha L}}\widetilde{\Phi}u_{\beta R} + \text{h.c.}\right) - \left(\mathbf{Y}^{d}_{\alpha\beta}\overline{Q_{\alpha L}}\Phi d_{\beta R} + \text{h.c.}\right) \ , \tag{2.34}$$

where $\widetilde{\Phi} \equiv i\tau_2\Phi^*$ [5]. The matrices $Y^{\ell,\,d,\,u}$ of Yukawa couplings are completely arbitrary $n_g \times n_g$ matrices. They introduce most of the free parameters and break almost every U(n_g) family symmetry of the SM. As we will see, this implies that the masses of charged leptons cannot be predicted by the SM.

Fermion masses arise from the Yukawa interactions after electroweak spontaneous symmetry breaking (EWSB). To be explicit, after EWSB the Yukawa Lagrangian (2.34) becomes

$$\begin{aligned}
\mathcal{L}_{\text{Yuk.}} &= -\left(\frac{v+H}{\sqrt{2}}\right)\left(\mathbf{Y}^{\ell}_{\alpha\beta}\overline{\ell_{\alpha L}}\ell_{\beta R} + \mathbf{Y}^{u}_{\alpha\beta}\overline{u_{\alpha L}}u_{\beta R} + \mathbf{Y}^{d}_{\alpha\beta}\overline{d_{\alpha L}}d_{\beta R}\right) + \text{h.c.} \\
&= -\left(\mathbf{M}^{\ell}_{\alpha\beta}\overline{\ell_{\alpha L}}\ell_{\beta R} + \mathbf{M}^{u}_{\alpha\beta}\overline{u_{\alpha L}}u_{\beta R} + \mathbf{M}^{d}_{\alpha\beta}\overline{d_{\alpha L}}d_{\beta R}\right) + \mathcal{L}^{H}_{\text{Yuk.}} \ ,
\end{aligned} \tag{2.35}$$

where $\mathbf{M}^{\psi} \equiv v\mathbf{Y}^{\psi}/\sqrt{2}$ is the mass matrix for the fermion fields ψ and $\mathcal{L}^{H}_{\text{Yuk.}}$ contains the trilinear couplings $H\overline{\psi_L}\psi_R$. However, since $\mathbf{Y}^{\psi}$ are in general non-diagonal matrices, the weak eigenstate fields do not have definite masses. In order to identify the physical particle content it is mandatory to diagonalise the mass matrices $\mathbf{M}^{\ell,\,d,\,u}$. This can be achieved throught the following biunitary transformations [3]:

$$\begin{aligned}
{V^{\ell}_L}^{\dagger}\mathbf{M}^{\ell}V^{\ell}_R &= \text{diag}(m_e,\, m_\mu,\, m_\tau) \equiv \mathbf{D}^{\ell} \ , \\
{V^{u}_L}^{\dagger}\mathbf{M}^{u}V^{u}_R &= \text{diag}(m_u,\, m_c,\, m_t) \equiv \mathbf{D}^{u} \ , \\
{V^{d}_L}^{\dagger}\mathbf{M}^{d}V^{d}_R &= \text{diag}(m_d,\, m_s,\, m_b) \equiv \mathbf{D}^{d} \ ,
\end{aligned} \tag{2.36}$$

where $V^{l,u,d}_{L,R}$ are appropriate $n_g \times n_g$ unitary matrices and m_j are real and positive masses. A more

[5]The invariance of the second term in the Yukawa Lagrangian (2.34) is ensured by the field $\widetilde{\Phi}$, which transforms as $(\mathbf{1}, \mathbf{2}, -1)$. That is because the 2^* representation of SU(2) is equivalent to the 2, i.e. there is a unitary matrix U such that $-I^{k*}_2 = UI^k_2U^{\dagger}$. In fact, with $U = \tau^2$ we have $I^{k*}_2 = -\frac{\tau^{k*}}{2} = \tau^2\frac{\tau^k}{2}\tau^2$.

interesting way of interpreting the bi-diagonalisation defined by (3.3) is to say that one must 'rotate' the weak eigenfields to bring them to a physical basis where fermions have a definite mass:

$$
\begin{aligned}
\ell_{\alpha L} &\to \left(V_L^\ell\right)_{\alpha\beta} \ell_{\beta L} \,, & \ell_{\alpha R} &\to \left(V_R^\ell\right)_{\alpha\beta} \ell_{\beta R} \,, \\
u_{\alpha L} &\to \left(V_L^u\right)_{\alpha\beta} u_{\beta L} \,, & u_{\alpha R} &\to \left(V_R^u\right)_{\alpha\beta} u_{\beta R} \,, \\
d_{\alpha L} &\to \left(V_L^d\right)_{\alpha\beta} d_{\beta L} \,, & d_{\alpha R} &\to \left(V_R^d\right)_{\alpha\beta} d_{\beta R} \,.
\end{aligned} \tag{2.37}
$$

Thus, one sees that the EWSB mechanism allowed not only the generation of masses for vector bosons but also of Dirac masses for SM fermions. On the other hand, since neutrino fields are left-handed in the SM, the appearance in the SM Lagrangian of a Dirac mass term for them upon EWSB, as in the case of other fermion fields, is not possible. Hence,

neutrinos are strictly massless particles in the SM.

2.4 Electroweak currents and fermion mixing

We are now in position to derive the interactions between the fermion fields ψ and the physical vector bosons W's, Z and A. The first step is to rewrite the covariant derivative (2.5) in terms of the physical vector bosons defined through Eqs. (2.27) and (2.28):

$$
D_\mu\psi = \left[\partial_\mu - i\frac{g}{\sqrt{2}}W_\mu^\dagger\tau^+ - i\frac{g}{\sqrt{2}}W_\mu\tau^- - ig\sin\theta_W QA_\mu - i\frac{gZ_\mu}{\cos\theta_W}\left(\frac{\tau_3}{2} - \sin^2\theta_W Q\right)\right]\psi \,, \tag{2.38}
$$

where we have used the usual definitions $\tau^+ \equiv (\tau^1 + i\tau^2)/2$ and $\tau^- \equiv (\tau^1 - i\tau^2)/2$. The interaction terms in the fermions Lagrangian (2.11) can then be written as

$$
\mathcal{L}_{\rm f}^{\rm int.} = \underbrace{\left[g\sin\theta_W J_{\rm EM}^\mu A_\mu + \frac{g}{\cos\theta_W}J_Z^\mu Z_\mu\right]}_{\text{Neutral currents}} + \underbrace{\frac{g}{\sqrt{2}}\left(J_W^\mu W_\mu + \text{h.c.}\right)}_{\text{Charged currents}} \,, \tag{2.39}
$$

where $J_{\rm EM}^\mu$, J_Z^μ and J_W^μ represent the electromagnetic (EM) vector current, weak neutral currents (NC) and the weak charged currents (CC), respectively. In a flavour basis, their definitions are:

$$
J_{\rm EM}^\mu = \sum_f Q_f\overline{\psi_f}\gamma^\mu\psi_f = \frac{2}{3}\overline{u_\alpha}\gamma^\mu u_\alpha - \frac{1}{3}\overline{d_\alpha}\gamma^\mu d_\alpha - \overline{\ell_\alpha}\gamma^\mu\ell_\alpha \,, \tag{2.40}
$$

$$
J_Z^\mu = \sum_f \overline{\psi_f}\gamma^\mu\left[I_f^3 P_L - Q_f\sin^2\theta_W\right]\psi_f = \sum_f I_f^3\overline{\psi_{fL}}\gamma^\mu\psi_{fL} - \sin^2\theta_W J_{EM}^\mu \,, \tag{2.41}
$$

$$
J_W^\mu = \sum_f \overline{\ell_{\alpha L}}\gamma^\mu\nu_{\alpha L} + \overline{d_{\alpha L}}\gamma^\mu u_{\alpha L} \,, \tag{2.42}
$$

where the sums $\sum_f$ extend over fermion fields and I_f^3 is the third isospin component for the fermion field f ($+1/2$ for the up-fields, $-1/2$ for the down-fields and 0 for SU(2)$_L$ singlets).

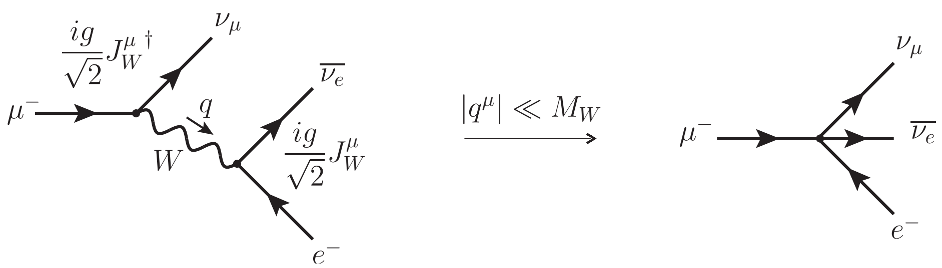

Figure 2.2: Tree-level diagram for muon decay (left) and its low-energy approximation (right).

If we want the first term in the interaction Lagrangian (2.39) to be the usual EM vector current in QED, $eJ^\mu_{\text{EM}}A_\mu$, then the positron electric charge e must be identified with

$$e = g\sin\theta_W = g'\cos\theta_W \quad \Longrightarrow \quad g^2 + g'^2 = e^2 \,, \tag{2.43}$$

which gives us an important relation among the coupling constants g and g' and the electric charge e. As expected, neutrinos do not couple to the photon since they are neutral particles. The EM currents only mix fields of the same charge and chirality. This means that the EM current is family universal, flavour diagonal and C (charge), P (parity) and CP invariant. An immediate consequence is that, upon the rotations (2.37) to the mass eigenstates basis, the electromagnetic current is not changed.

On the other hand, the weak neutral currents J^μ_Z in Eq. (2.41) have a $V-A$ component and a purely vector one proportional to the EM current. Therefore, these currents violate C and P symmetries, though not maximally. Similarly to the electromagnetic current, J^μ_Z is flavour diagonal and as such takes the same form in the flavour and mass eigenstate bases. This phenomenon is the so-called GIM mechanism [55], which forbids flavour-changing neutral currents (FCNC). The absence of such transitions can be used to constrain extensions of the SM involving exotic fermions [119].

Finally, the CC in Eq. (2.42) have a $V-A$ structure and thus violate C and P maximally. An important result that can be extracted in the flavour basis is the amplitude T for a t-channel 4-fermion interaction, such as the muon decay $\mu^- \to e^-\nu_\mu\overline{\nu_e}$ represented in Fig. 2.2. In the unitary gauge, we have

$$-iT = \left(\frac{ig}{\sqrt{2}}\right)^2 \left[\overline{u}_{\nu_e}(p_{\nu_e})\gamma^\mu\left(\frac{1-\gamma^5}{2}\right)v_e(p_e)\right] \frac{-i\left(g_{\mu\nu} - \frac{q_\mu q_\nu}{M_W^2}\right)}{q^2 - M_W^2} \left[\overline{u}_{\nu_\mu}(p_{\nu_\mu})\gamma^\nu\left(\frac{1-\gamma^5}{2}\right)u_\mu(p_\mu)\right] \,, \tag{2.44}$$

which, for a small momentum transfer, $|q^\mu| \ll M_W$, leads to the Fermi effective Lagrangian (1.1):

$$\mathcal{L}_{\text{eff.}} \xrightarrow{|q^\mu|\ll M_W} -\frac{G_F}{\sqrt{2}} J^\dagger_{W\mu} J^\mu_W \,, \qquad \frac{G_F}{\sqrt{2}} = \frac{g^2}{8M_W^2} = \frac{1}{2v^2} \,. \tag{2.45}$$

We can therefore extract the Fermi constant $G_F = 1.166367(5)\times 10^{-5}\,\text{GeV}^{-2}$ [66] from the muon decay $\mu^- \to e^-\nu_\mu\overline{\nu_e}$ and provide an estimated value for the electroweak scale v:

$$v = 2M_W/g \approx (\sqrt{2}G_F)^{-1/2} \approx 246\,\text{GeV} \,. \tag{2.46}$$

Matrix type	# Parameters	# Moduli	# Phases
$n \times m$ General	$2nm$	nm	nm
$n \times n$ Symmetric	$n(n+1)$	$n(n+1)/2$	
$n \times n$ Unitary	n^2	$n(n-1)/2$	$n(n+1)/2$
$n \times n$ Hermitian	n^2	$n(n+1)/2$	$n(n-1)/2$

Table 2.4: Number of parameters for the various types of matrices considered in this thesis.

Contrary to what happens with the EM and neutral currents, charged currents do not take the same form in the weak and mass eigenstate bases. More specifically, upon the rotations (2.37) the CC read

$$\begin{aligned} J_W^\mu &= \overline{\ell_{\beta L}} \gamma^\mu \left(V_L^{\ell\dagger}\right)_{\beta\alpha} \nu_{\alpha L} + \overline{d_{\beta L}} \gamma^\mu \left(V_L^{d\dagger}\right)_{\beta\alpha} (V_L^u)_{\alpha\rho}\, u_{\rho L} \\ &= \overline{\ell_{\beta L}} \gamma^\mu \left(V_L^{\ell\dagger}\right)_{\beta\alpha} \nu_{\alpha L} + \overline{d_{\alpha L}} \gamma^\mu \left(V_{\text{CKM}}^\dagger\right)_{\alpha\beta} u_{\beta L} \,, \end{aligned} \tag{2.47}$$

where the $n_g \times n_g$ unitary matrix V_{CKM} is known as the Cabibbo-Kobayashi-Maskawa matrix [120, 121] or quark mixing matrix. It describes the mismatch between the unitary rotations (2.37) for the up and down-type quarks and can be interpreted by saying that in the CC each massive up-type quark interacts with a linear combination $d'_{\alpha L} = (V_{\text{CKM}})_{\alpha\beta}\, d_{\beta L}$ of massive down-type quarks.

The unitarity condition on V_{CKM} imposes n_g^2 constraints on its elements, $\left(V_{\text{CKM}}^\dagger V_{\text{CKM}}\right)_{mn} = \delta_{mn}$, and so it can be described by n_g^2 parameters, $n_g(n_g-1)/2$ of which are rotation angles (the number of angles in an O(n_g) rotation) and $n_g(n_g+1)/2$ are phases. This result is summarised in Table 2.4 along with its generalisation to other types of matrices. However, not all of the parameters in V_{CKM} are observable, since some phases can be removed through a rephasing of quark fields. In fact, apart from the CC interactions, the SM Lagrangian possesses a U(1)^{2n_g} symmetry corresponding to its invariance under global phase transformations of quark fields:

$$u_{\alpha\, L,R} \to e^{i\varphi_\alpha^u} u_{\alpha\, L,R} \,, \qquad d_{\alpha\, L,R} \to e^{i\varphi_\alpha^d} d_{\alpha\, L,R} \,. \tag{2.48}$$

This property can be used to eliminate the phases from one line and one column in the CKM matrix, i.e. $2n_g - 1$ phases can be eliminated. The reason why there are just $2n_g - 1$ unphysical phases instead of $2n_g$ is that a common global rephasing of the quark fields leaves the SM Lagrangian invariant. This U(1)$_B$ symmetry is related, through Noether's theorem, to baryon number conservation. For the case of interest, $n_g = 3$, the CKM matrix thus depends on three mixing angles θ_{12}, θ_{13}, $\theta_{23} \in [0, \pi/2]$ and one physical phase $\delta \in [0, 2\pi]$, with its standard parametrisation given by [122]

$$V_{\text{CKM}} = \begin{pmatrix} c_{12}c_{13} & s_{12}c_{13} & s_{13}e^{-i\delta} \\ -s_{12}c_{23} - c_{12}s_{23}s_{13}e^{i\delta} & c_{12}c_{23} - s_{12}s_{23}s_{13}e^{i\delta} & s_{23}c_{13} \\ s_{12}s_{23} - c_{12}c_{23}s_{13}e^{i\delta} & -s_{23}c_{12} - s_{12}c_{23}s_{13}e^{i\delta} & c_{23}c_{13} \end{pmatrix} , \tag{2.49}$$

where $c_{ab} \equiv \cos\theta_{ab}$ and $s_{ab} \equiv \sin\theta_{ab}$. There are other useful parametrisations of V_{CKM}, such as the Wolfenstein parametrisation [123], but the standard one is the most advantageous to our future discussion. The physical phase δ is responsible for CP violation in the SM quark sector, whose strength can be

	L_e	L_μ	L_τ		L_e	L_μ	L_τ
(ν_e, e^-)	+1	0	0	$(\overline{\nu}_e, e^+)$	-1	0	0
(ν_μ, μ^-)	0	+1	0	$(\overline{\nu}_\mu, \mu^+)$	0	-1	0
$(\nu_\tau, \tau -)$	0	0	+1	$(\overline{\nu}_e, \tau^+)$	0	0	-1

Table 2.5: Assignment of flavour lepton numbers to particles (left) and antiparticles (right).

quantified in a rephasing invariant way in terms of the Jarlskog invariant [124]:

$$\mathrm{Im}[V_{\alpha\beta}V_{\gamma\eta}V^*_{\alpha\eta}V^*_{\gamma\beta}] = J_{\text{CKM}} \sum_{m,n=e,\mu,\tau} \epsilon_{\alpha\gamma m}\epsilon_{\beta\eta n}, \qquad J_{\text{CKM}} = c_{12}s_{12}c_{13}^2 s_{13}c_{13}s_{23}\sin\delta \,. \tag{2.50}$$

The study of CP violation in the quark sector is an extremely challenging and very wide subject but we shall not pursuit it on this thesis. A detailed treatment can be found in Ref. [125].

Let us now analyse the lepton CC, i.e. the first term in Eq. (2.47). Since neutrinos are strictly massless particles in the SM, performing a rotation of the neutrino fields in flavour space leaves the Lagrangian of the SM invariant, apart from the CC term. In fact, the EM and neutral currents are flavour diagonal and, in what concerns $\mathcal{L}_{\text{Yuk.}}$, there is no neutrino mass term to spoil, i.e. neutrinos have zero mass in all bases. Therefore, we can freely rotate the neutrino fields and in particular cancel the effects of the charged lepton mixing matrix V_L^ℓ in Eq. (2.47). By performing the rotation

$$\nu_{\alpha L} \to \left(V_L^\ell\right)_{\alpha\beta} \nu_{\beta L} \,, \tag{2.51}$$

it is then evident that the leptonic CC $J^\mu_{W,L}$ takes the same form in the weak and mass eigenstate bases:

$$J^\mu_{W,L} = \overline{\nu_{\alpha L}}\gamma^\mu \ell_{\alpha L} \,. \tag{2.52}$$

Thus, one concludes that there is no mixing in the leptonic sector of the SM and that the existence of neutrino masses is a necessary condition for leptonic mixing.

In general, one defines flavour neutrino fields $\nu_{e,\mu,\tau}$ as the neutrino field combinations which couple with the corresponding charged lepton e, μ, τ in the CC (2.52). As a consequence of the absence of leptonic mixing, the SM Lagrangian exhibits a global U(1)^{n_g} symmetry associated with the rephasings

$$\nu_{\alpha L} \to e^{i\varphi_\alpha}\nu_{\alpha L} \,, \qquad \ell_{\alpha L} \to e^{i\varphi_\alpha}\ell_{\alpha L} \,, \qquad \ell_{\alpha R} \to e^{i\varphi_\alpha}\ell_{\alpha R} \,, \tag{2.53}$$

ans Noether's theorem requires the existence of n_g conserved charges, the flavour lepton numbers

$$L_\alpha = \int d^3x \left(\nu^\dagger_\alpha \nu_\alpha + \ell^\dagger_\alpha \ell_\alpha\right) \,, \tag{2.54}$$

as assigned in Table 2.5. A trivial consequence is that the total lepton number $L = L_e + L_\mu + L_\tau$ is also conserved. As we will see, the nonconservation of the flavour (or family) lepton numbers L_α plays a crucial role in neutrino physics beyond the SM.

2.5 Summary of the SM

One is finally in position to write the full Lagrangian of the SM[6]:

$$\mathcal{L}_{\text{SM}} = \mathcal{L}_{\text{gauge}} + \mathcal{L}_{\text{Higgs}} + \mathcal{L}_{\text{f}} + \mathcal{L}_{\text{Yuk.}} \,. \tag{2.55}$$

In addition to the gauge and Poincaré symmetries, the SM possesses a miscellaneous of accidental symmetries and associated conservation laws, summarised in Table 2.6. In particular, processes like $\ell_\alpha \to \ell_\beta \gamma$ are forbidden since they violate flavour lepton number conservation. There are very strong bounds on the rates of these processes [127] but, as we will see, lepton number violating processes are closely related to the problem of neutrino masses. As such, the study of SM extensions with lepton number violation is a fundamental step on our path towards the understanding of neutrino masses.

Symmetry	**Lie Group**	**Symmetry type**	**Conserved Charges**
Poincaré	ISO(1,3)	Global, Exact	Energy, Momentum, Angular Momentum
Gauge	$\text{SU}(3)_c \otimes \text{SU}(2)_L \otimes \text{U}(1)_Y$	Local, Broken	Color/Electric charge
Quarks rephasing	$\text{U}(1)_B$	Global, Accidental	Baryon number
Electron rephasing	$\text{U}(1)_{L_e}$	Global, Accidental	Electron number L_e
Muon rephasing	$\text{U}(1)_{L_\mu}$	Global, Accidental	Muon number L_μ
Tau rephasing	$\text{U}(1)_{L_\tau}$	Global, Accidental	Tau number L_τ

Table 2.6: Symmetries of the Standard Model.

The electroweak sector of the SM depends on seventeen parameters. However, the SM offers no prediction for the values of fermion masses and gives no definite explanation to why there are three generations of fermions. Nevertheless, some valid clues may be hidden in the closeness of V_{CKM} to the identity matrix as well as in the presence of mass hierarchies between generations (see Table 2.1).

Other shortcomings of the SM are the absence of a description of gravity and of dark matter. There is also the (weak) hierarchy problem, related to the fine-tuning of parameters required to give M_H a value near the electroweak scale ($v \sim 10^2$ GeV) if the SM is to be valid up to the Planck scale (10^{19} GeV). Another concern is the absence of a CP-violating term in the strong sector of the SM despite there being no symmetry which forbids it. Additionally, the SM cannot achieve exact unification of its gauge coupling constants at high-energies, unlike what happens in supersymmetric models or GUTs.

All these issues support the idea that the SM is an effective low-energy theory of a more fundamental one. Although some of these problems can be classified as theoretical prejudice, undeniable evidence for physics beyond the Standard Model arises when one considers the experimental evidence for neutrino oscillations [128]: neutrinos have small but nonzero masses. In the next chapter, simple extensions of the SM will be considered in order to generate naturally small neutrino masses.

[6]In addition to these terms, the quantisation of the theory requires the presence of gauge-fixing and Faddeev-Popov terms in the Lagrangian of the SM. For a detailed introduction to the quantisation of the SM see, for instance, [112, 126]. A short outline is given in Appendix A.1.

3 Neutrino masses and seesaw-type models

" Even though it is perhaps not yet possible to ask experiments to decide between the new theory and a simple extension of the Dirac equations to neutral particles, one should keep in mind that the new theory introduces a smaller number of hypothetical entities, in this yet unexplored field. "

– E. Majorana in [129]

The absence of electric charge for neutrinos allows their masses to have a Majorana nature (lepton number violating) rather than a Dirac one (lepton number conserving). But the nature and origin of small neutrino masses remains a mystery. Their tiny values suggest that neutrino masses are a low-energy manifestation of new physics beyond the SM with a high-energy scale $\Lambda_{\rm NP}$. It is therefore expected that the SM predictions, in particular (zero) neutrino masses, are affected by small effects proportional to powers of $v^2/\Lambda_{\rm NP}$. The most popular high-energy models consider the existence of heavy fields with masses of order $\Lambda_{\rm NP}$. Among all possible scenarios, the seesaw mechanism is perhaps the best known example of how neutrino mass suppression can be achieved.

In this chapter, we discuss how to describe a massive neutrino in the general Dirac-Majorana case and the resulting leptonic mixing and observables. Finally, we study ultraviolet completions of the SM in which the seesaw mechanism can be implemented through tree-level exchange of heavy fermion singlets (type I), scalar triplets (type II) or fermionic triplets (type III).

3.1 The Dirac-Majorana mass term

It is possible to define a Dirac mass term for neutrinos consistently with the gauge symmetries of the SM by adding three right-handed neutrino fields $\nu_{\alpha R}$ ($\alpha = e, \mu, \tau$) to its particle content. These extra fields are weak isospin singlets with null hypercharge, $y = 0$. Therefore, right-handed neutrino fields do not participate in electroweak interactions and, as such, are called *sterile*. On the other hand, the usual left-handed neutrino fields $\nu_{\alpha L}$ that participate in weak interactions are called *active*.

To the SM Yukawa Lagrangian (2.34), we must therefore add a lepton term similar to the one which generates the masses of up-type quarks. This extra Lagrangian term reads, before and after EWSB:

$$\mathcal{L}^{\nu}_{\rm Yuk.} = -\left(\mathbf{Y}^{\nu}_{\alpha\beta}\overline{L_{\alpha_L}}\widetilde{\Phi}\nu_{\beta_R} + \text{h.c.}\right) \xrightarrow{\text{EWSB}} -\left(\mathbf{M}^{\nu}_{\alpha\beta}\overline{\nu_{\alpha_L}}\nu_{\beta_R} + \text{h.c.}\right), \qquad \mathbf{M}^{\nu}_{\alpha\beta} = \frac{v}{\sqrt{2}}\mathbf{Y}^{\nu}_{\alpha\beta}\,. \tag{3.1}$$

The neutrino mass matrix $\mathbf{M}^{\nu}_{\alpha\beta}$ can be bi-diagonalised by rotating flavour neutrino fields into the basis of massive states $\nu_{1,2,3}$,

$$\nu_{\alpha L} \to (V_L^{\nu})_{\alpha j}\, \nu_{jL} \;, \qquad \nu_{\alpha R} \to (V_R^{\nu})_{\alpha j}\, \nu_{jR} \;, \tag{3.2}$$

resulting in a diagonal neutrino mass matrix:

$$(V_L^{\nu})^{\dagger}\, \mathbf{M}^{\nu} V_R^{\nu} = \text{diag}(m_{\nu_1},\, m_{\nu_2},\, m_{\nu_3}) \equiv \mathbf{M}^{\nu}_{\text{diag.}} \;. \tag{3.3}$$

As a consequence of (3.2), there will be lepton mixing in the CC in an analogous way to the quark case (2.47), with a mixing matrix parametrised as V_{CKM}. Therefore, flavour lepton numbers [Eq. (2.54)] are not conserved but it is easy to see that total lepton number $L = L_e + L_\mu + L_\tau$ is conserved. However, a fundamental problem arises if we take a quick glance at Table 2.1. One immediately sees that the couplings $\mathbf{Y}^{\nu}$ should be much smaller than $\mathbf{Y}^{\ell,u,d}$, which poses a naturalness problem. As a matter of fact, a Dirac mass term for neutrinos is not natural according to the 't Hooft criterium [130],

> *"at any energy scale μ, a physical parameter or a set of parameters $\alpha_i(\mu)$ is allowed to be very small only if the replacement $\alpha_i(\mu) = 0$ would increase the symmetry of the system."*, (Z1)

because in the $\mathbf{Y}^{\nu} \to 0$ limit the theory does not exhibit any new symmetry. This signals the presence of an alternative description for naturally small neutrino Yukawa couplings $\mathbf{Y}^{\nu}$.

In fact, it is possible to build a Majorana mass term for neutrinos. Such a construction is related with the possibility of describing a massless fermion by a chiral field (two-component theory). The first thing to note is that the Dirac equation for a fermion is equivalent to two coupled equations:

$$(i\gamma^\mu \partial_\mu - m)\,\psi = 0 \qquad \Leftrightarrow \qquad \begin{cases} i\gamma^\mu \partial_\mu \psi_L & = m\psi_R \\ i\gamma^\mu \partial_\mu \psi_R & = m\psi_L \end{cases} . \tag{3.4}$$

If the fermion ψ is massless, then the two previous equations are decoupled into two *Weyl equations*:

$$i\gamma^\mu \partial_\mu \psi_L = 0 \qquad \text{and} \qquad i\gamma^\mu \partial_\mu \psi_R = 0 \;, \tag{3.5}$$

which proves our claim that a massless fermion can be described by a single chiral field. In a similar manner, also a massive fermion can be described by a two-component spinor [129]. This is achieved assuming that the chiral components ψ_R and ψ_L are not independent, which means that the two coupled Eqs. (3.4) must be two ways of writing the same equation for one independent chiral field. Indeed, after some manipulation of the second coupled equation in (3.4) we arrive at

$$i\gamma^\mu \partial_\mu \mathcal{C}\overline{\psi_R}^T = m\mathcal{C}\overline{\psi_L}^T \;, \tag{3.6}$$

where $\mathcal{C}$ is the charge conjugation matrix. This is just the first equation in (3.4) if we set

$$\psi_R = \mathcal{C}\overline{\psi_L}^T \;, \tag{3.7}$$

where $\mathcal{C}\overline{\psi_L}^T$ has right-handed chirality and transforms as a spinor under Lorentz transformations.

The Majorana condition for the field ψ then reads

$$\psi = \psi_L + \psi_R = \psi_L + \mathcal{C}\overline{\psi_L}^T \Leftrightarrow \psi = \mathcal{C}\overline{\psi}^T = \psi_L + \psi_L^c = \psi^c \,, \tag{3.8}$$

with ψ^c being the charge-conjugated field of ψ. The Majorana condition implies the equality of particle and antiparticle. Hence, only neutral fermions, as neutrinos, can be described by a Majorana field.

For the case of neutrinos, taking $\psi = \nu_\alpha$ in Eq. (3.7), one can build a Majorana Lagrangian:

$$\mathcal{L}^M = \overline{\nu}_{\alpha L} i\partial\!\!\!/ \nu_{\alpha L} - \frac{1}{2}\left(\mathbf{M}^\nu_{\alpha\beta}\overline{\nu^c_{\alpha L}}\,\nu_{\beta L} + \text{h.c.}\right) = \frac{1}{2}\overline{\nu_\alpha}\left(i\partial\!\!\!/ \delta_{\alpha\beta} - \mathbf{M}^\nu_{\alpha\beta}\right)\nu_\beta \,, \tag{3.9}$$

where $\mathbf{M}^\nu$ is a symmetric neutrino mass matrix. The factor $1/2$ distinguishes a Majorana from a Dirac Lagrangian and is needed in order to avoid double counting of the dependent fields ν_L^c and $\overline{\nu_L}$ when obtaining the equation of motion for Majorana neutrinos [3]. We should also remark that the Majorana mass term (3.9) is nonzero due to the anticommutation property of fermion fields because for commuting fields $\nu_L^T \mathcal{C}^\dagger \nu_L = -\nu_L^T \mathcal{C}^\dagger \nu_L$, and the mass term vanishes identically.

There is, nonetheless, a symmetry clearly broken by the Majorana Lagrangian (3.9). This becomes clear if we notice that it is not invariant under a global U(1) gauge transformation:

$$\nu_{\alpha L} \to e^{i\varphi}\nu_{\alpha L} \qquad \Longrightarrow \qquad \mathcal{L}^M \to \overline{\nu_{\alpha L}} i\partial\!\!\!/ \nu_{\alpha L} - \frac{1}{2}\left(e^{2i\varphi}\mathbf{M}^\nu_{\alpha\beta}\overline{\nu^c_{\alpha L}}\,\nu_{\beta L} + \text{h.c.}\right) . \tag{3.10}$$

Therefore, total lepton number is not conserved. We could have considered the transformation $\nu_\alpha \to e^{i\varphi}\nu_\alpha$ for the Majorana fields, which leaves invariant the Lagrangian (3.9). However, such a transformation is not compatible with the Majorana constraint (3.8), since we would have $\nu_\alpha^c \to e^{-i\varphi}\nu_\alpha^c$. Therefore, taking the limit $\mathbf{M}^\nu \to \mathbf{0}$, we recover lepton number conservation and small Majorana masses are thus natural according to 't Hooft.

Let us now analyse the general case when active and sterile neutrinos are both present. To be exact, we consider the existence of n_g left-handed neutrino fields $\nu_{\alpha L}$ and n' right-handed neutrino fields ν_{sR}. We define the column vector N_L with $n = n_g + n'$ left-handed fields:

$$N_L \equiv \begin{pmatrix} \nu_L \\ \nu_R^c \end{pmatrix}, \qquad \text{where} \qquad \nu_L = \begin{pmatrix} \nu_{eL} \\ \nu_{\mu L} \\ \nu_{\tau L} \end{pmatrix} \qquad \text{and} \qquad \nu_R^c = \begin{pmatrix} \nu^c_{s_1 R} \\ \vdots \\ \nu^c_{s_{n'} R} \end{pmatrix} . \tag{3.11}$$

Then, in general it is possible to have the Dirac-Majorana mass term

$$\mathcal{L}^{\text{D+M}}_{\text{mass}} = -\frac{1}{2}\overline{N_L^C}\,\mathbf{M}^{\text{D+M}}\,N_L + \text{h.c.} \,, \qquad \mathbf{M}^{\text{D+M}} \equiv \begin{pmatrix} \mathbf{M}_L & \mathbf{M}_D^T \\ \mathbf{M}_D & \mathbf{M}_R \end{pmatrix} , \tag{3.12}$$

where $\mathbf{M}_D$ is a $n' \times n_g$ mass matrix, and $\mathbf{M}_L$ and $\mathbf{M}_R$ are $n_g \times n_g$ and $n' \times n'$ symmetric mass matrices, respectively. The symmetric mass matrix $\mathbf{M}^{\text{D+M}}$ can be diagonalised with the transformation [3]:

$$\left(V_L^\nu\right)^T \mathbf{M}^{\text{D+M}} V_L^\nu \equiv \mathbf{M}^{\text{diag}} = \text{diag}(m_1, ..., m_n) \,, \tag{3.13}$$

with V_L^ν a $n \times n$ unitary matrix and m_k real and positive masses. This diagonalisation can be achieved by writing the flavour fields N_L as a unitary rotation of n mass eigenfields ν_{kL} (roman indices):

$$N_L = V_L^\nu n_L \qquad \text{with} \qquad n_L = (\nu_{1L}, \dots, \nu_{nL})^T \quad . \tag{3.14}$$

Defining the Majorana fields $\nu_k = \nu_{kL} + \nu_{kL}^c$, we can finally write the free Lagrangian for neutrinos:

$$\mathcal{L}^{\text{D+M}} = \frac{1}{2}\overline{\nu_k}\left(i\partial\!\!\!/ - \mathbf{M}_{kk}^{\text{diag}}\right)\nu_k \ , \tag{3.15}$$

which shows that, in the most general Dirac-Majorana case, massive neutrinos are Majorana particles.

3.2 Lepton mixing and observables

The mixing of sterile and active neutrinos, defined in Eq. (3.14), has important consequences for weak interactions. In the mass basis (3.14), the leptonic weak currents involving neutrinos are

$$J_W^\mu \ = 2\,\overline{L_L}\gamma^\mu U n_L \ , \qquad J_{Z,\nu}^\mu = 2\,\overline{n_L}\gamma^\mu U^\dagger U n_L \ , \tag{3.16}$$

where U is a $3 \times n$ non-unitary mixing matrix defined by:

$$U_{\alpha k} = \sum_{\beta=e,\mu,\tau} (V_L^{\ell^\dagger})_{\alpha\beta}(V_L^\nu)_{\beta k} \ . \tag{3.17}$$

The non-unitarity of U implies that the GIM mechanism does not work, which means that in the general Dirac-Majorana case there are flavour-changing neutral currents among different massive neutrinos.

In the rest of this section, we will consider the special case $n = n_g = 3$, with no sterile neutrinos, in which the 3×3 mixing matrix is called the Pontecorvo-Maki-Nakagawa-Sakata mixing matrix [70, 74], $U_{\text{PMNS}} = V_L^{\ell^\dagger} V_L^\nu$. A general $n_g \times n_g$ unitary matrix can be parametrised in terms of $n_g(n_g-1)/2 = 3$ mixing angles θ_{12}, θ_{13}, θ_{23} and of $n_g(n_g+1)/2 = 6$ phases (see Table 2.4). However a convenient rephasing of the charged lepton fields allows us to eliminate $n_g = 3$ phases from U_{PMNS}, as is evident from Eq. (3.16). The same does not apply to the neutrino fields n_L due to the lepton number violating nature of the Majorana mass term (3.9). Therefore, U_{PMNS} can be parametrised in terms of three mixing angles and $n_g(n_g-1)/2 = 3$ physical phases, one Dirac phase δ and two Majorana phases α_1 and α_2 [66]:

$$U_{\text{PMNS}} = \begin{pmatrix} c_{12}c_{13} & s_{12}c_{13} & s_{13}e^{-i\delta} \\ -s_{12}c_{23} - c_{12}s_{23}s_{13}e^{i\delta} & c_{12}c_{23} - s_{12}s_{23}s_{13}e^{i\delta} & s_{23}c_{13} \\ s_{12}s_{23} - c_{12}c_{23}s_{13}e^{i\delta} & -s_{23}c_{12} - s_{12}c_{23}s_{13}e^{i\delta} & c_{23}c_{13} \end{pmatrix} \begin{pmatrix} 1 & 0 & 0 \\ 0 & e^{i\alpha_1} & 0 \\ 0 & 0 & e^{i\alpha_2} \end{pmatrix} , \tag{3.18}$$

where $c_{ij} \equiv \cos\theta_{ij}$ and $s_{ij} \equiv \sin\theta_{ij}$. In particular, CP violation due to the Dirac phase δ can be quantified in terms of the Jarlskog invariant (2.50) and the two Majorana phases are CP-violating phases. One should remark that this same parametrisation also applies to the case of Dirac neutrinos, with $\alpha_{1,2} = 0$.

As a consequence of lepton mixing, a neutrino beam with a specific flavour can change along their trajectory into another flavour. Remember that we define flavour neutrino fields $\nu_{e,\mu,\tau}$ (greek indices) as the field combinations which couple to the corresponding charged lepton in the CC (3.16), i.e. as

$$\nu_L = U n_L = V_L^{\ell\dagger} N_L, \qquad \text{with} \qquad \nu_L = \left(\nu_{eL}\,, \quad \nu_{\mu L}\,, \quad \nu_{\tau L}\right)^T . \tag{3.19}$$

In a plane-wave approximation, the transition probability from a flavour neutrino $|\nu_\alpha\rangle$ produced at the source $(0,0)$ with energy E to a neutrino $|\nu_\beta\rangle$ at the detector (t,L) is easily seen to be given by [3]

$$P_{\nu_\alpha\to\nu_\beta}(L,E) = |\langle\nu_\beta\,|\,\nu_\alpha(t,L)\rangle|^2 = \sum_{j,k} U^*_{\alpha k}U_{\beta k}U_{\alpha j}U^*_{\beta j}\exp\left(-i\frac{\Delta m^2_{kj}L}{2E}\right), \qquad \Delta m^2_{kj} \equiv m_k^2 - m_j^2\ . \tag{3.20}$$

This shows that neutrino oscillations are only sensitive to mass-squared differences Δm^2_{kj}, providing no information on the absolute neutrino mass scale. As expected, it also proves that the Majorana phases $\alpha_{1,2}$ do not appear in the transition probability because neutrino oscillations are lepton number conserving. Therefore, oscillation experiments are not sensitive to the nature of massive neutrinos. Depending on the experimental settings, the oscillations will be governed by different mixing angles and mass-squared differences. From this fact, a common notation emerged such that $\Delta m^2_{12} \equiv \Delta m^2_{\text{sol}}$, $\Delta m^2_{31} \equiv \Delta m^2_{\text{atm}}$, $\theta_{12} \equiv \theta_{\text{sol}}$ (solar), $\theta_{23} \equiv \theta_{\text{atm}}$ (atmospheric) and θ_{13} is called the reactor mixing angle. The ordering of neutrino masses is unknown because experiments are only sensitive to $|\Delta m_{kj}|^2$. We assume that ν_1 and ν_2 are the neutrinos involved in solar neutrino oscillations, with $m_1 < m_2$. Since experiments dictate that $|\Delta m^2_{31}| \gg \Delta m^2_{21}$, there is room for two possible orderings:

Normal neutrino mass Spectrum (NS): $\quad m_1 < m_2 \ll m_3\,;$

Inverted neutrino mass Spectrum (IS): $\quad m_3 \ll m_1 < m_2\,.$

The latest global fit results to oscillation data are the ones in Refs. [131–133]. We consider the global fit of Ref. [131], with results shown in Table 3.1. The mass-squared differences are well determined as well as the value of θ_{12}. The reactor experiments Double Chooz, Daya Bay and RENO also impressively confirmed that the reactor mixing angle is non-zero, $\theta_{13} \approx 9^{\text{o}}$. The global fit values for the atmospheric mixing angle θ_{23} indicate a deviation from maximal mixing $\sin^2\theta_{23} = 1/2$. However, it is still not clear in which octant θ_{23} lies. Finally, the Dirac phase δ is still completely undetermined at 3σ.

As discussed, neutrino oscillations are not sensitive to the absolute neutrino mass scale. The most direct way to determine this scale is through the investigation of the β-decay endpoint of tritium, ${}^3\text{H} \rightarrow{}^3$ He $+\, e^- + \overline{\nu}_e$. The obtained bounds are those for an effective electron antineutrino mass $m_\beta = \sqrt{\sum_k |U_{ek}|^2 m_k^2}$ which, in the regime $m_\beta \gg \sqrt{|\Delta m^2_{31}|}$, is equivalent to the absolute neutrino mass scale. Using this technique, the Mainz [134] and Troitsk [135] experiments obtained the most stringent upper bounds at 95% level $m_\beta < 2.3$ eV and $m_\beta < 2.05$ eV, respectively. An improved experiment, KATRIN, is going to start in 2016, planning to reach a sensitivity of about 0.2 eV . Furthermore, oscillation experiments do not distinguish Dirac from Majorana neutrinos [136]. Thus, CP and T violation effects

Parameter	Best fit	1σ range	2σ range	3σ range
$\Delta m^2_{21}/10^{-5}$ eV^2 (NS or IS)	7.54	7.32 – 7.80	7.15 – 8.00	6.99 – 8.18
$\sin^2\theta_{12}/10^{-1}$ (NS or IS)	3.08	2.91 – 3.25	2.75 – 3.42	2.59 – 3.59
$\Delta m^2/10^{-3}$ eV^2 (NS)	2.44	2.38 – 2.52	2.30 – 2.59	2.22 – 2.66
$\Delta m^2/10^{-3}$ eV^2 (IS)	2.40	2.33 – 2.47	2.25 – 2.54	2.17 – 2.61
$\sin^2\theta_{13}/10^{-2}$ (NS)	2.34	2.16 – 2.56	1.97 – 2.76	1.77 – 2.97
$\sin^2\theta_{13}/10^{-2}$ (IS)	2.39	2.18 – 2.60	1.98 – 2.80	1.78 – 3.00
$\sin^2\theta_{23}/10^{-1}$ (NS)	4.25	3.98 – 4.54	3.76 – 5.06	3.57 – 6.41
$\sin^2\theta_{23}/10^{-1}$ (IS)	4.37	4.08 – 4.96 $\oplus$ 5.31 – 6.10	3.84 – 6.37	3.63 – 6.59
δ/π (NS)	1.39	1.12 – 1.72	0 – 0.11 $\oplus$ 0.88 – 2.00	—
δ/π (IS)	1.35	0.96 – 1.59	0 – 0.04 $\oplus$ 0.65 – 2.00	—

Table 3.1: Results taken from [131] of a global 3ν oscillation analysis, in terms of best-fit values and allowed ranges for the 3ν mass-mixing parameters. Δm^2 is defined as $m_3^2 - (m_1^2 + m_2^2)/2$, with $+\Delta m^2$ for NS and $-\Delta m^2$ for IS. The overall χ^2 difference between IS and NS is insignificant ($\Delta\chi^2_{\mathrm{I-N}} = +0.3$).

measurable by neutrino oscillations depend solely on the Dirac phase δ, whose experimental value is sensitive to both the ordering of the neutrino masses and to the value of the reactor angle θ_{13} [137]. The determination of Majorana phases is possible through lepton-number violating processes such as the neutrinoless double-β-decay [138, 139]. In fact, the decay amplitude is proportional to an effective neutrino mass $m_{\beta\beta}$,

$$A(0\nu 2\beta) \propto m_{\beta\beta} \equiv \left|\sum_{i=k}^{3} U_{ek}^2 m_k\right| = \left|(m_1 c_{12}^2 + m_2 s_{12}^2 e^{2i\alpha_1})c_{13}^2 + m_3 s_{13}^2 e^{2i(\alpha_2-\delta)}\right| \,, \tag{3.21}$$

and we immediately notice that Majorana phases of the neutrinos are important. A recent upper limit on $m_{\beta\beta}$ was determined by the GERDA collaboration to be $m_{\beta\beta} \lesssim 0.2 - 0.4$ eV [140]. An additional (indirect) constraint on the absolute neutrino masses scale comes from cosmological considerations, which limit the sum of neutrino masses $m_{\text{total}} = \sum_\nu m_\nu$. The recent bound obtained by the Planck Collaboration [141] is $\sum_\nu m_\nu < 0.66$ eV, at 95% CL. However, there is still no consensus on the value of the cosmological neutrino mass limit. For example, considering baryon acoustic oscillation data, the Planck Collaboration obtained $\sum_\nu m_\nu < 0.23$ eV (95% CL) [142].

3.3 Seesaw mechanism(s)

Despite its theoretical appeal, the Majorana neutrino mass term (3.9) is forbidden in the SM since it has weak isospin $I = 1$ and hypercharge $y = -2$. Therefore, in order to write a renormalisable Lagrangian which generates Majorana neutrino masses, we would need an isospin scalar triplet ($I = 1$) with $y = 2$, which the SM does not contain. This fact suggests that the SM is a low energy effective theory resulting from a more complete theory at a high-energy scale Λ.

At low energies, an analysis independent of the high energy theory can be performed in terms of an effective theory description, in which the impact of the high-energy theory is parametrised by means of an effective Lagrangian valid at energies less than Λ. This amounts to adding a set of non-renormalisable higher-dimension operators to the gauge-invariant SM Lagrangian:

$$\mathcal{L}_{\text{eff.}} = \mathcal{L}_{\text{SM}} + \delta\mathcal{L}^{d=5} + \delta\mathcal{L}^{d=6} + \dots \, , \tag{3.22}$$

where each operator is suppressed by inverse powers of the high-energy scale Λ. More specifically, we have $\delta\mathcal{L}^{d>4} \sim \mathcal{O}\left(1/\Lambda^{d-4}\right)$. The effective Lagrangian can be calculated in the path integral formalism by integrating out the heavy fields N. The effective action $S_{\text{eff.}}$ is then obtained from the full action S by separating the terms S_N involving the heavy fields N from those involving only the SM fields, S_{SM}, i.e.

$$e^{iS_{\text{eff.}}} \equiv \int \mathcal{D}N\mathcal{D}\overline{N} e^{iS} = e^{iS_{\text{SM}}} \int \mathcal{D}N\mathcal{D}\overline{N} e^{iS_N[N]} \, , \tag{3.23}$$

where $\mathcal{D}N$ is the integration measure. Expanding the action $S_N[N]$ around the stationary (classical) configuration N_0, one gets

$$e^{iS_N^{\text{eff.}}} = \int \mathcal{D}N\mathcal{D}\overline{N} e^{i(S_N[N_0] + \delta S_N[N_0] + \delta^2 S_N[N_0] + \dots)} \approx e^{iS_N[N_0]} \, , \tag{3.24}$$

where the first order variation $\delta S_N[N_0]$ is zero by definition of stationarity, and the higher-order terms can be perturbatively neglected. The effective action is thus

$$S_{\text{eff.}} = S_{\text{SM}} + S_N[N_0] = \int d^4x \left[\mathcal{L}_{\text{SM}} + \mathcal{L}_N(N_0) \right] \, , \tag{3.25}$$

with the stationary fields defined through:

$$\left.\frac{\delta S}{\delta N_i}\right|_{N_{0i}} = 0 \, , \qquad \left.\frac{\delta S}{\delta \overline{N}_i}\right|_{\overline{N_{0i}}} = 0 \, . \tag{3.26}$$

Inserting these fields to $S_N[N_0]$, we finally obtain the effective Lagrangian [compare with Eq. (3.22)]:

$$\mathcal{L}_{\text{eff.}} = \mathcal{L}_{\text{SM}} + \mathcal{L}_N(N_0) = \mathcal{L}_{\text{SM}} + \delta\mathcal{L}^{d=5} + \delta\mathcal{L}^{d=6} + \dots \tag{3.27}$$

For $d = 5$, there is just one possible operator made out of SM fields, the Weinberg operator [83]:

$$\delta\mathcal{L}^{d=5} = \frac{1}{2}\boldsymbol{c}_{\alpha\beta}^{d=5}\left(\overline{L_{\alpha_L}^c}\widetilde{\Phi}^*\right)\left(\widetilde{\Phi}^\dagger L_{\beta_L}\right) + \text{h.c.} = -\frac{1}{2}\boldsymbol{c}_{\alpha\beta}^{d=5}\left(\widetilde{\Phi}^\dagger L_{\alpha_L}\right)^T C^\dagger\left(\widetilde{\Phi}^\dagger L_{\beta_L}\right) + \text{h.c.}\ , \tag{3.28}$$

where $\boldsymbol{c}_{\alpha\beta}^{d=5} \sim \mathcal{O}(1/\Lambda)$ are complex matrix coefficients. This operator is not invariant under $B - L$ symmetry. As a matter of fact, after EWSB this operator induces naturally small Majorana neutrino masses provided that the scale Λ is high enough. More specifically,

$$\delta\mathcal{L}^{d=5} \xrightarrow{\text{EWSB}} \left(-\frac{1}{2}\mathbf{M}_{\alpha\beta}^{d=5}\overline{\nu_{\alpha_L}^c}\nu_{\beta_L} + \text{h.c.}\right) + \ldots\ , \quad \mathbf{M}_{\alpha\beta}^{d=5} = -\frac{v^2}{2}c_{\alpha\beta}^{d=5}\ . \tag{3.29}$$

This suggests that neutrino masses are the lowest-order effect of high-energy physics beyond the SM. However, there are several $d = 6$ operators which may arise from different high-energy models [143]. Their identification is thus crucial to get some hints on the origin of neutrino masses. An important scenario is that in which the suppresion of the $d = 6$ operators is not as strong as that of the $d = 5$ operator, leading to potentially observable low-energy effects. This becomes clear from the point of view of the 't Hooft naturalness criterium (Z1). In fact, it may be natural to consider large coefficients for the $B - L$ conserving $d = 6$ operators while having small coefficients for the $B - L$ odd operator $\delta\mathcal{L}^{d=5}$. We will see that this requires a value of Λ not far from the electroweak scale.

Effective operators modify the SM parameters. In addition to fermion masses, there are four parameters relevant to our discussion, namely the coupling constants g and g', the Higgs VEV v and the Higgs quartic self-coupling λ . In our analysis, the first three parameters will be constrained using as input parameters the well-determined experimental values of the fine structure constant α, the Fermi constant G_F (as extracted from the muon decay rate by the removal of SM process-dependent radiative corrections) and the very precise measurement of M_Z [66].

In the following, we analyse seesaw extensions of the SM, in which the Weinberg operator (3.28) arises after integrating out heavy fields, with masses $M \sim \Lambda$. Thus, at low energy, such interactions reduce to a four-point interaction of the form $\Phi\Phi L_L L_L$, which produces Majorana neutrino masses after electroweak symmetry breaking (EWSB). In order to generate such an effective interaction, the high-energy theory Lagrangian must respect the SM gauge symmetry and the heavy fields χ must have interaction terms of the form $\chi\Phi L_L$ or both $\chi\Phi\Phi$ and $\chi L_L L_L$. In order to fathom the possibilities of building those couplings, we need to consider the possible invariants built from two SU(2)$_L$ doublets. For the case of $\chi\Phi L_L$ couplings, the bilinear terms formed with Φ and L_L after integrating out χ must have the form $\widetilde{\Phi}^\dagger L_L$. Looking at the tensor product

$$\left(\widetilde{\Phi}\right)^* \otimes L_L \sim \mathbf{2} \otimes \mathbf{2} = \mathbf{1} \oplus \mathbf{3}\ , \tag{3.30}$$

it is then clear that the heavy fields χ must have $y = 0$, and that either transform as an SU(2)$_L$ singlet (type I seesaw) or as an SU(2)$_L$ triplet (type III seesaw). Additionally, invariance under the Poincaré group requires these χ to be spin 1/2 fields. On the other hand, for both $\chi\Phi\Phi$ and $\chi L_L L_L$ interaction terms, it is evident that χ must be a scalar field. The bilinears formed from the doublets L_L after

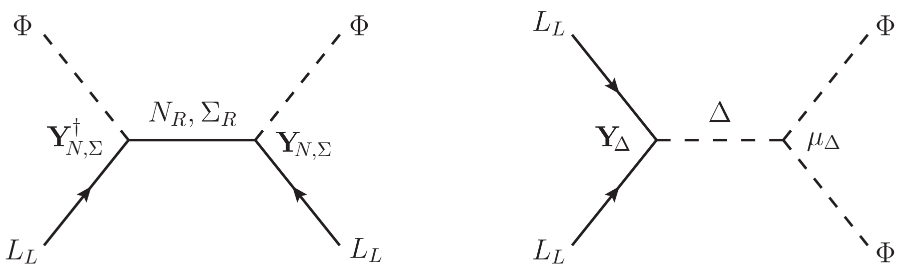

Figure 3.1: Tree-level exchange interactions which in the low-energy effective description generate the Weinberg operator (3.28). These interactions correspond to the exchange of: fermionic singlets N (type I seesaw) or triplets Σ (type III seesaw) on the left; scalar triplet Δ (type II seesaw) on the right.

integrating out the heavy field χ must have the structure $\overline{L^c_L} L_L$. Looking at the tensor product

$$(L^c_L)^* \otimes L_L \sim \mathbf{2} \otimes \mathbf{2} = \mathbf{1} \oplus \mathbf{3}\,, \tag{3.31}$$

we see that one needs a scalar field χ with hypercharge $y = +2$, which transforms either as a singlet or as a triplet of SU(2)$_L$. The Yukawa coupling with an SU(2)$_L$ singlet χ would be given by

$$\overline{L^c_{\alpha L}} \varepsilon L_{\beta L} \chi + \text{h.c.}\,, \qquad \varepsilon \equiv i\tau_2\,, \tag{3.32}$$

and SU(2)$_L$-invariance follows from

$$U^T \varepsilon U = (\det U)\, \varepsilon = \varepsilon\,, \qquad \text{with} \qquad U \in \text{SU(2)}_L\,. \tag{3.33}$$

However, such a singlet would have an electric charge $Q_\chi = +1$ and any VEV of χ would break U(1)$_{\text{EM}}$, being therefore forbidden. Consequently, such Yukawa coupling cannot generate tree-level neutrino masses and one is left with the scalar triplet option, corresponding to the type II seesaw mechanism. Each one of these standard realisations of the seesaw mechanism is graphically represented in Fig. 3.1.

In the following, we describe the high-energy theory and deduce the low-energy effective Lagrangian and its consequences at order $\mathcal{O}(M^{-2})$ for the above realisations of the seesaw mechanism. It is expected that the conclusions obtained here will hold for their generalisations or embeddings in larger theories.

3.3.1 Type I seesaw mechanism

We begin our analysis with the study of the type I seesaw model [82, 144, 145], in which n' sterile neutrino fields $N_{sR} \sim (\mathbf{1}, \mathbf{1}, 0)$ are added to the SM. Aside from the Yukawa term (3.1), one can add to the Lagrangian a Majorana mass term for the sterile fields N_{sR}. The type I seesaw Lagrangian is then

$$\mathcal{L}_{\text{type I}} = \mathcal{L}_{\text{SM}} + i\overline{N_R}\,\partial\!\!\!/\, N_R - \left(\overline{L_L}\,\tilde{\Phi}\,\mathbf{Y}^\dagger_N\, N_R + \frac{1}{2}\overline{N_R}\,\mathbf{M}_N\, N^c_R + \text{h.c.}\right)\,, \tag{3.34}$$

where $\mathbf{Y}_N$ is an $n' \times n_g$ matrix of Yukawa couplings and $\mathbf{M}_N$ is an $n' \times n'$ symmetric mass matrix. We will work in a basis where both $\mathbf{M}_N$ and $\mathbf{M}_\ell$ are real and diagonal, which is always possible by a convenient rotation of the neutrino fields N_{sR} of the type (3.14) and of the charged-lepton fields as done in the SM [remember Eqs. (2.38) and (2.51)]. The necessary unitary rotations can be absorbed by redefining of the (fully general) Yukawa matrix $\mathbf{Y}_N$ and, therefore, we can always start with the type I seesaw Lagrangian (3.34) written in this basis. Notice also the use of a compact notation in (3.34), in which indices in generation space are omitted but implicitly summed.

The type I seesaw Lagrangian (3.34) then reads

$$\mathcal{L}_{\text{type I}} = \mathcal{L}_{\text{SM}} + i\overline{N_R}\,\partial\!\!\!/\, N_R - \left[\overline{\nu_L}\,\phi^0\,\mathbf{Y}_N^\dagger\,N_R - \overline{\ell_L}\,\phi^-\,\mathbf{Y}_N^\dagger\,N_R + \frac{1}{2}\overline{N_R}\,\mathbf{M}_N\,N_R^c + \text{h.c.}\right] , \tag{3.35}$$

and we immediately see that a Dirac-Majorana mass term emerges for neutral leptons:

$$\mathcal{L}^{\text{mass}}_{\text{type I}} = -\frac{1}{2}\overline{n_L^c}\begin{pmatrix} 0 & \frac{v\mathbf{Y}_N^T}{\sqrt{2}} \\ \frac{v\mathbf{Y}_N}{\sqrt{2}} & \mathbf{M}_N \end{pmatrix} n_L + \text{h.c.} \equiv -\frac{1}{2}\overline{n_L^c}\begin{pmatrix} \mathbf{M}_L & \mathbf{M}_D^T \\ \mathbf{M}_D & \mathbf{M}_N \end{pmatrix} n_L + \text{h.c.}\,, \qquad n_L \equiv \begin{pmatrix} \nu_L \\ N_L \end{pmatrix} , \tag{3.36}$$

where $N_L \equiv N_R^c$. Since N_{sR} are sterile, the elements of the mass matrix $\mathbf{M}_N$ are allowed to be much larger than the electroweak scale. More precisely, for a mass matrix $\mathbf{M}_X$ we define its scale m_X to be of the order of magnitude of the eigenvalues of $\sqrt{\mathbf{M}_X^\dagger \mathbf{M}_X}$. In seesaw-type models, we assume $\mathbf{M}_N$ to be non-singular[1] and that all the matrix elements of $\mathbf{M}_L$ and $\mathbf{M}_D$ are much smaller than the scale m_N:

$$(\mathbf{M}_L)_{\alpha\beta}\,,\ (\mathbf{M}_D)_{s\alpha} \ll m_N\,. \tag{3.37}$$

This should be understood in the sense that the eigenvalues of $\sqrt{\mathbf{M}_N^\dagger \mathbf{M}_N}$, though not necessarily all of the same order of magnitude, are all much larger than the matrix elements of $\mathbf{M}_L$ and $\mathbf{M}_D$. Under these assumptions, there are in the theory n' heavy neutrinos with masses of order m_N, and n_g light neutrinos with masses which, in the case $\mathbf{M}_L = 0$, are suppressed by inverse powers of m_N.

The diagonalisation of the $(n_g + n') \times (n_g + n')$ Dirac-Majorana mass matrix $\mathbf{M}^{\text{D+M}}$ can be accomplished by starting with a block-diagonalisation of $\mathbf{M}^{\text{D+M}}$, following the procedure developed in Ref. [148]. This allows to simply decouple the high mass scale from the low one, up to any order in m_N^{-1}. Such decoupling is done by performing a unitary rotation of the neutrino fields n_L by means of an $(n_g + n') \times (n_g + n')$ unitary matrix U_L^n,

$$n_L \longrightarrow U_L^n\, n_L\,, \qquad U_L^n = \begin{pmatrix} V & S \\ R & T \end{pmatrix} , \tag{3.38}$$

and by demanding from this unitary rotation that it block-diagonalises $\mathbf{M}^{\text{D+M}}$:

$$(U_L^n)^T \begin{pmatrix} \mathbf{M}_L & \mathbf{M}_D^T \\ \mathbf{M}_D & \mathbf{M}_N \end{pmatrix} U_L^n = \begin{pmatrix} \mathbf{M}_{\text{light}} & 0 \\ 0 & \mathbf{M}_{\text{heavy}} \end{pmatrix} , \tag{3.39}$$

where $\mathbf{M}_{\text{light}}$ and $\mathbf{M}_{\text{heavy}}$ are, respectively, $n_g \times n_g$ and $n' \times n'$ symmetric mass matrices.

[1] In the framework of the *singular seesaw mechanism* [146, 147], $\mathbf{M}_N$ can even be singular, with n_0 eigenvalues of $\sqrt{\mathbf{M}_N^\dagger \mathbf{M}_N}$ equal to 0. However, going into a basis where $\mathbf{M}_N$ is diagonal, we realise that this case is mathematically contained in the usual seesaw model with $n_g' = n_g + n_0$ left-handed doublets and $n_s' = n' - n_0$ right-handed singlets.

Eq. (3.39) can be solved using the following *ansatz* for the unitary transformation U_L^n:

$$U_L^n = \begin{pmatrix} \sqrt{1-BB^\dagger} & B \\ -B^\dagger & \sqrt{1-B^\dagger B} \end{pmatrix} , \tag{3.40}$$

where the square-root of matrices should be understood in the sense of a Taylor expansion. Inserting the transformation (3.40) into Eq. (3.39), yields the following results at first order in m_N^{-1}:

$$\begin{cases} V &= \sqrt{1-BB^\dagger} & \approx \mathbb{1} - \frac{1}{2}\mathbf{M}_D^\dagger \left(\mathbf{M}_N^*\right)^{-1} \mathbf{M}_N^{-1}\mathbf{M}_D \, , \\ S &= B & \approx \mathbf{M}_D^\dagger \left(\mathbf{M}_N^*\right)^{-1} \, , \\ R &= -S^\dagger & \approx -\mathbf{M}_N^{-1}\mathbf{M}_D \, , \\ T &= \sqrt{1-B^\dagger B} & \approx \mathbb{1} - \frac{1}{2}\mathbf{M}_N^{-1}\mathbf{M}_D\mathbf{M}_D^\dagger \left(\mathbf{M}_N^*\right)^{-1} \, . \end{cases} \tag{3.41}$$

For $\mathbf{M}_L = 0$, the mass matrices for the light and heavy neutrinos are then, at lowest order:

$$\mathbf{M}_{\text{light}} = \left(V^T\mathbf{M}_L + R^T\mathbf{M}_D\right)\left(V - ST^{-1}R\right) \approx -S^*\mathbf{M}_N S^\dagger \approx -\mathbf{M}_D^T\mathbf{M}_N^{-1}\mathbf{M}_D \, , \tag{3.42}$$

$$\mathbf{M}_{\text{heavy}} = \left(S^T\mathbf{M}_L + T^T\mathbf{M}_D\right)\left(S - VR^{-1}T\right) \approx -\mathbf{M}_D R^{-1} \approx \mathbf{M}_N \, . \tag{3.43}$$

We thus see that $\mathbf{M}_{\text{light}}$ is suppressed with respect to the Dirac mass matrix $\mathbf{M}_D$ by the small factor ${\mathbf{M}_D}^T\mathbf{M}_N^{-1}$. Therefore, if the scale m_N is high enough, we are able to get naturally small neutrino masses.

The next step is the diagonalisation of the mass matrices $\mathbf{M}_{\text{light}}$ and $\mathbf{M}_{\text{heavy}}$. This is achieved through a unitary rotation of the neutrino fields ν_L and N_L:

$$\nu_L \to \left(U_L^\nu\right)\nu_L \, , \qquad N_L \to \left(U_L^N\right) N_L \, , \tag{3.44}$$

where $U_L^N \approx \mathbb{1}$ at first order in m_N^{-1} since $\mathbf{M}_N$ is already diagonal. Defining the Majorana fields

$$\nu = \nu_L + \nu_L^c \, , \qquad N = N_L + N_L^c \, , \tag{3.45}$$

we obtain for the charged and neutral interactions involving only the light Majorana neutrinos ν_i:

$$\mathcal{L}_{\text{CC}}^\nu = \frac{g}{\sqrt{2}}\,\overline{\ell_\alpha}\gamma^\mu\left(VU_L^\nu\right)_{\alpha i} P_L\,\nu_i\,W_\mu^- + \text{h.c.} \, , \tag{3.46}$$

$$\mathcal{L}_{\text{NC}}^\nu = \frac{g}{2\cos^2\theta_W}\overline{\nu_i}\gamma^\mu\left[\left(VU_L^\nu\right)^\dagger\left(VU_L^\nu\right)\right]_{ij} P_L\,\nu_j\,Z_\mu \, , \tag{3.47}$$

where $\alpha = e, \mu, \tau$ as usual and $i, j = 1, \ldots, n_g$. From the charged-current expression (3.46), it is straightforward to see that the usual PMNS unitary mixing matrix (3.18) is now replaced by a nonunitary matrix,

$$U_{\text{PMNS}} \longrightarrow VU_L^\nu \approx \left(\mathbb{1} - \frac{1}{2}\mathbf{M}_D^\dagger\left(\mathbf{M}_N^*\right)^{-1}\mathbf{M}_N^{-1}\mathbf{M}_D\right)U_L^\nu \equiv \boldsymbol{N} \, , \tag{3.48}$$

whose deviation from unitarity is characterised by the suppressed matrix

$$\boldsymbol{\epsilon}^N \equiv \mathbf{M}_D^\dagger\left(\mathbf{M}_N^*\right)^{-1}\mathbf{M}_N^{-1}\mathbf{M}_D = \left(SU_L^N\right)\left(SU_L^N\right)^\dagger \, . \tag{3.49}$$

The elements of U_{PMNS} are extracted from neutrino oscillation experiments which study the oscillation of flavour neutrinos $\nu_{\alpha L} = (VU_L^\nu)_{\alpha i}\,\nu_{iL}$ at relatively low energies. In these experiments, the heavy Majorana neutrino states N_j are not present in the superpositions representing the initial flavour neutrino states. This is what leads to deviations from unitarity of the PMNS matrix.

On the other hand, the CC and NC involving the heavy fields N_k are, up to first order in m_N^{-1}:

$$\mathcal{L}_{\text{CC}}^N = \frac{g}{\sqrt{2}}\,\overline{\ell_\alpha}\gamma^\mu\left(SU_L^N\right)_{\alpha k} P_L\, N_k\, W_\mu^- + \text{h.c.}\,, \tag{3.50}$$

$$\mathcal{L}_{\text{NC}}^N = \frac{g\,Z_\mu}{2\cos^2\theta_W}\left\{\overline{\nu_i}\gamma^\mu\left[(VU_L^\nu)^\dagger(SU_L^N)\right]_{ik} N_{kL} + \text{h.c.}\right\} + \frac{g\,Z_\mu}{2\cos^2\theta_W}\overline{N_k}\gamma^\mu\left[(SU_L^N)^\dagger(SU_L^N)\right]_{kk'} N_{k'L}\,. \tag{3.51}$$

We thus see that the matrix elements of the matrix SU_L^N appearing in Eq. (3.49) determine the strength of the CC and NC involving the heavy Majorana neutrinos N_k. It is this matrix (or $\boldsymbol{\epsilon}^N$) that, as a consequence of the unobservable signal from heavy Majorana neutrinos, shall be constrained.

The main aspects of the high-energy theory are thus revised. Let us now focus on its effective description [149]. Following the procedure outlined in Eqs. (3.23)-(3.27), the stationary fields N_0 are given by the equations of motion (3.26) for the Majorana fields $N \equiv N_R + N_R^c$, namely

$$(i\partial\!\!\!/ - \mathbf{M}_N)N_0 = \left(\mathbf{Y}_N\widetilde{\Phi}^\dagger L_L + \mathbf{Y}_N^*\widetilde{\Phi}^T L_L^c\right), \tag{3.52}$$

and the effective Lagrangian for the type I seesaw scenario is:

$$\mathcal{L}_{\text{type I}}^{\text{eff.}} = \mathcal{L}_{\text{SM}} + \mathcal{L}_N[N_0] = \mathcal{L}_{\text{SM}} - \frac{1}{2}\left[\overline{L_L}\widetilde{\Phi}\mathbf{Y}_N^\dagger + \overline{L_L^c}\widetilde{\Phi}^*\mathbf{Y}_N^T\right] N_0\,. \tag{3.53}$$

All effective operators can then be obtained by expanding the heavy neutrino propagator in Eq. (3.52) and inserting such expansion in the effective Lagrangian (3.53). The first new term in the expansion of Eq. (3.53) corresponds to an effective operator of dimension $d=5$, the Weinberg operator (3.28), with coefficients given by the following expression:

$$\boldsymbol{c}_{\alpha\beta}^{d=5} = \left(\mathbf{Y}_N^T\,\mathbf{M}_N^{-1}\,\mathbf{Y}_N\right)_{\alpha\beta}\,. \tag{3.54}$$

After EWSB, this operator generates a Majorana mass matrix for the light left-handed neutrinos,

$$\mathbf{M}_\nu \equiv -\frac{v^2}{2}\boldsymbol{c}^{d=5} = -\frac{v^2}{2}\left(\mathbf{Y}_N^T\,\mathbf{M}_N^{-1}\,\mathbf{Y}_N\right), \tag{3.55}$$

which is precisely the same result as the one of Eq. (3.42), obtained for $\mathbf{M}_{\text{light}}$ in the high-energy description. On the other hand, the second contribution gives rise to an effective dimension $d=6$ operator,

$$\delta\mathcal{L}^{d=6} = \boldsymbol{c}_{\alpha\beta}^{d=6}\left(\overline{L_{\alpha L}}\,\widetilde{\Phi}\right) i\partial\!\!\!/\left(\widetilde{\Phi}^\dagger\, L_{\beta L}\right), \tag{3.56}$$

with coefficients expressed in terms of the full high-energy theory parameters by

$$\frac{v^2}{2}\boldsymbol{c}^{d=6} = \boldsymbol{\epsilon}^N = \frac{v^2}{2}\mathbf{Y}_N^\dagger\left(\mathbf{M}_N^*\right)^{-1}\mathbf{M}_N^{-1}\mathbf{Y}_N\,. \tag{3.57}$$

As the $d = 5$ coefficients $\boldsymbol{c}^{d=5}$, these parameters are also quadratic in the Yukawa couplings, but are suppresed by m_N^{-2}. From (3.57), we also see that the $d = 6$ coefficients encode deviations from unitarity of the neutrino mixing matrix.

After EWSB and disregarding couplings with the Higgs and Goldstone bosons, the type I neutrino effective Lagrangian up to dimension $d = 6$ operators is thus given by:

$$\mathcal{L}_\nu^{d\leq 6} = i\overline{\nu}_L \not{\partial} \left(\mathbb{1} + \boldsymbol{\epsilon}^N\right) \nu_L - \frac{1}{2}\left(\overline{\nu_L^c}\, \mathbf{M}_\nu\, \nu_L + \text{h.c.}\right) \ , \tag{3.58}$$

from which we see that the immediate effect of the $d = 6$ operator (3.56) is to rescale the neutrino kinetic energy. The neutrino kinetic-terms can be brought back to canonical form through the field redefinitions

$$\nu_L \to \left(\mathbb{1} + \boldsymbol{\epsilon}^N\right)^{-\frac{1}{2}} \nu_L \ . \tag{3.59}$$

Rotating ν_L with a unitary matrix U_L^ν which diagonalises the mass matrix $\mathbf{M}_\nu$, we obtain an effective Lagrangian for the type I seesaw which, at order m_N^{-2}, is given by:

$$\mathcal{L}_{\text{leptons}}^{d\leq 6} = \frac{1}{2}\overline{\nu_j}\left(i\not{\partial} - \mathbf{M}_{\nu j}^{\text{diag}}\right)\nu_j + \overline{\ell_\alpha}(i\not{\partial} - \mathbf{M}_{\ell\alpha}^{\text{diag.}})\ell_\alpha + \mathcal{L}_{\text{CC}} + \mathcal{L}_{\text{NC}} + \mathcal{L}_{\text{EM}} \ , \tag{3.60}$$

where $\nu_j = \nu_{Lj} + \nu_{Lj}^c$ $(j = 1, 2, 3)$ are Majorana mass eigenfields, and $\mathbf{M}_\ell^{\text{diag.}}$ is the diagonal mass matrix for the SM charged leptons ($\alpha = e, \mu, \tau$). In this mass basis, the weak currents are then given by:

$$\mathcal{L}_{\text{CC}} = \frac{g}{\sqrt{2}}\overline{\ell_L}\not{W}^- \boldsymbol{N}\nu_L + \text{h.c.} \ , \tag{3.61}$$

$$\mathcal{L}_{\text{NC}} = \frac{gZ_\mu}{2\cos^2\theta_W}\left[\overline{\nu_L}\gamma^\mu\left(\boldsymbol{N}^\dagger\boldsymbol{N}\right)\nu_L - \overline{\ell_L}\gamma^\mu\ell_L - 2\sin^2\theta_W J_{\text{EM}}^\mu\right] . \tag{3.62}$$

As expected, we arrive at the same result as the one obtained in the high-energy description, namely that the usual PMNS mixing matrix (3.18) is replaced by a nonunitary matrix,

$$U_{\text{PMNS}} \longrightarrow \boldsymbol{N} \equiv \left(\mathbb{1} - \frac{\boldsymbol{\epsilon}^N}{2}\right) U_L^\nu \ , \tag{3.63}$$

and that there are FCNCs involving neutrinos, with mixing matrix $\boldsymbol{N}^\dagger\boldsymbol{N}$. The translation from the high-energy theory to its effective description is thus simply made with the prescription $(VU_L^\nu) \to \boldsymbol{N}$, and neglecting all interactions involving the heavy fields N_k.

An immediate phenomenological consequence of the above result is that the experimentally measured Fermi constant, G_F, cannot be identified anymore with its SM tree-level value G_F^{SM} in Eq. (2.45). For example, the Fermi constant G_F extracted from muon decay, $\mu \to \nu_\mu e\overline{\nu_e}$, is now given by

$$G_F = G_F^{\text{SM}}\sqrt{(\boldsymbol{N}\boldsymbol{N}^\dagger)_{ee}(\boldsymbol{N}\boldsymbol{N}^\dagger)_{\mu\mu}} \, , \tag{3.64}$$

since $\boldsymbol{N}\boldsymbol{N}^\dagger = (1 - \boldsymbol{\epsilon}^N)$ and neutrino flavour eigenfields [remember the definition (3.19)] are given by $\nu_\alpha \approx (\mathbb{1} - \frac{\boldsymbol{\epsilon}^N}{2})_{\alpha j}\nu_j \approx \sqrt{(\boldsymbol{N}\boldsymbol{N}^\dagger)_{\alpha j}}\,\nu_j$, at order m_N^{-2}. The remaining parameters in the Lagrangian match

Matrix	Full theory		Effective Description	
	Modules	Phases	Modules	Phases
$\mathbf{Y}_\ell$	n_g^2	n_g^2	n_g^2	n_g^2
$\mathbf{Y}_N$ / $\mathbf{c}^{d=5}$	$n_g n'$	$n_g n'$	$n_g(n_g+1)/2$	$n_g(n_g+1)/2$
$\mathbf{M}_N$ / $\mathbf{c}^{d=6}$	$n'(n'+1)/2$	$n'(n'+1)/2$	$n_g(n_g+1)/2$	$n_g(n_g-1)/2$
$\boldsymbol{V}_L^\ell$	$n_g(n_g-1)/2$	$n_g(n_g+1)/2$	$n_g(n_g-1)/2$	$n_g(n_g+1)/2$
$\boldsymbol{V}_R^\ell$	$n_g(n_g-1)/2$	$n_g(n_g+1)/2$	$n_g(n_g-1)/2$	$n_g(n_g+1)/2$
$\boldsymbol{V}^N$	$n'(n'-1)/2$	$n'(n'+1)/2$	-	-
N_{physical}	$n_g+n'+n_g n'$	$n_g(n'-1)$	$n_g(n_g+2)$	$n_g(n_g-1)$

Table 3.2: Number of parameters in the type I seesaw scenario, in both the full and effective theories.

the SM ones. It is also interesting to notice that, as predicted, deviations from unitarity can be directly related with the matrix coefficients $\boldsymbol{c}^{d=6}$:

$$|\boldsymbol{N}\boldsymbol{N}^\dagger - \mathbf{1}| = |\boldsymbol{\epsilon}^N| = \frac{v^2}{2}|\boldsymbol{c}^{d=6}| = \frac{v^2}{2}\left|\mathbf{Y}_N^\dagger \frac{1}{\mathbf{M}_N^\dagger \mathbf{M}_N}\mathbf{Y}_N\right| . \tag{3.65}$$

The non-unitarity of $\boldsymbol{N}$ also generates a "zero-distance" effect in oscillation experiments, i.e. a flavour transition at the source before oscillations can even take place. Althoug interesting, we shall not pursue this subject in the present thesis. For more details, the reader is addressed to Ref. [150].

Finally, let us analyse the number of parameters in the leptonic sector of both the full theory and its low-energy description. For that, we follow the method developed in Ref. [151]. Let $\mathbf{Y}_\ell$ be the charged lepton Yukawas of Eq. (2.34). If $\mathbf{Y}_\ell = \mathbf{Y}_N = \mathbf{M}_N = 0$, the Lagrangian (3.34) is invariant under

$$L_L \to V_L^\ell L_L\,, \qquad \ell_R \to V_R^\ell \ell_R\,, \qquad N_R \to V^N N_R\,, \tag{3.66}$$

where V^N is a unitary $n' \times n'$ matrix in flavour space and $V_{L,R}^\ell$ are $n_g \times n_g$ unitary matrices. The Lagrangian (3.34) is then invariant under the symmetry group $G = \mathrm{U}(n_g)_{\ell_L} \times \mathrm{U}(n_g)_{\ell_R} \times \mathrm{U}(n')_N$, with $N_G = 2n_g^2 + n'^2$ generators. Both the Yukawa coupling and Majorana mass matrices explicitly break that symmetry group into $G' \subset G$ with $N_{G'}$ generators. The $N_G - N_{G'}$ broken generators can be used to absorve parameters of $\mathbf{Y}_\ell$, $\mathbf{Y}_N$ and $\mathbf{M}_N$. The number of physical parameters is then

$$N_{\text{physical}} = N_{Y,M} - (N_G - N_G') \ , \tag{3.67}$$

where $N_{Y,M}$ is the number of parameters in $\mathbf{Y}_\ell$, $\mathbf{Y}_N$ and $\mathbf{M}_N$. On the other hand, in the effective theory with dimension $d \leq 6$ operators, the symmetry group is $G = \mathrm{U}(n)_{\ell_L} \times \mathrm{U}(n)_{\ell_R}$, which is explicitly broken by the $d = 5$ operator. As in both descriptions the symmetry groups are completely broken, $N_{G'} = 0$, we obtain the counting of physical parameters shown in Table 3.2. These results show that for $n' = n_g$ (or $n' < n_g$) the number of parameters is the same in both theories, thus proving that all the parameters of the full theory appear in the effective theory through the dimension $d \leq 6$ operators. On the other hand, if $n' > n_g$, the number of parameters in the full theory is larger than in the effective theory and we would need to consider operators of dimension $d > 6$, in order to account for the remaining parameters.

3.3.2 Type II seesaw mechanism

In the minimal type II seesaw [145, 152–154] we extend the SM with a scalar triplet $\vec{\Delta} = (\Delta_1, \Delta_2, \Delta_3)^T$ with $y = 2$. This flavour isospin triplet pertains to the adjoint representation of SU(2)$_L$ with generators

$$I_1 = \begin{pmatrix} 0 & 0 & 0 \\ 0 & 0 & -i \\ 0 & i & 0 \end{pmatrix}, \qquad I_2 = \begin{pmatrix} 0 & 0 & i \\ 0 & 0 & 0 \\ -i & 0 & 0 \end{pmatrix}, \qquad I_3 = \begin{pmatrix} 0 & -i & 0 \\ i & 0 & 0 \\ 0 & 0 & 0 \end{pmatrix}. \tag{3.68}$$

In order to work with charge eigenfields, we must diagonalise the charge operator $Q = (Y + I_3)/2$. This is done through a change of SU(2)$_L$ basis by a unitary change of basis matrix B which relates the new charge eigenfields and SU(2)$_L$ generators I'_k with the old ones by

$$I'_k = B^\dagger I_k B\,, \qquad \begin{pmatrix} -\Delta^{++} \\ \Delta^{+} \\ \Delta^{0} \end{pmatrix} \equiv B^\dagger \vec{\Delta} = \begin{pmatrix} \frac{(-\Delta^1 + i\Delta^2)}{\sqrt{2}} \\ \Delta^3 \\ \frac{\Delta^1 + i\Delta^2}{\sqrt{2}} \end{pmatrix}, \qquad B = \frac{1}{\sqrt{2}} \begin{pmatrix} -1 & 0 & 1 \\ -i & 0 & -i \\ 0 & \sqrt{2} & 0 \end{pmatrix}. \tag{3.69}$$

The flavour isospin triplet $\vec{\Delta}$ matches exactly the field we need to build a renormalisable Lagrangian for Majorana neutrino mass generation. The coupling between two doublets L_L and the triplet $\vec{\Delta}$ can be obtained by analysing the Kronecker product of two doublets and one triplet of SU(2)$_L$ [155]:

$$\mathbf{2} \otimes \mathbf{2} \otimes \mathbf{3} = (\mathbf{1} \otimes \mathbf{3}) \otimes \mathbf{3} = \mathbf{3} \oplus (\mathbf{3} \otimes \mathbf{3}) = \mathbf{3} \oplus (\mathbf{1} \oplus \mathbf{3} \oplus \mathbf{5})\,. \tag{3.70}$$

From this decomposition, one notices that a singlet representation ($\mathbf{1}$) is extracted from the product of two triplet representations ($\mathbf{3} \otimes \mathbf{3}$), one of which should be obtained from the product of two doublets ($\mathbf{2} \otimes \mathbf{2}$). Looking at the Clebsch-Gordan coefficients for SU(2), one sees that for two doublets $L_{\alpha L} = (\nu_{\alpha L}, \ell_{\alpha L})$ and $L_{\beta L} = (\nu_{\beta L}, \ell_{\beta L})$, the Lorentz-invariant combination transforming as a triplet is

$$\begin{pmatrix} \nu_{\alpha L}^T C^\dagger \nu_{\beta L} \\ \left(\nu_{\alpha L}^T C^\dagger \ell_{\beta L} + \nu_{\beta L}^T C^\dagger \ell_{\alpha L}\right)/\sqrt{2} \\ \ell_{\alpha L}^T C^\dagger \ell_{\beta L} \end{pmatrix} = - \begin{pmatrix} \overline{\nu_{\alpha L}^c} \nu_{\beta L} \\ \left(\overline{\nu_{\alpha L}^c} \ell_{\beta L} + \overline{\ell_{\alpha L}^c} \nu_{\beta L}\right)/\sqrt{2} \\ \overline{\ell_{\alpha L}^c} \ell_{\beta L} \end{pmatrix}. \tag{3.71}$$

Using now the Clebsch-Gordan coefficients for the product of two SU(2)$_L$ triplets, the above one and $\vec{\Delta}$, we are allowed to write the Yukawa couplings:

$$\begin{aligned} \mathcal{L}_{\text{Yukawa, }\Delta} &= -\sqrt{2}\,(\mathbf{Y}_\Delta)_{\alpha\beta} \left[\overline{\nu_{\alpha L}^c} \nu_{\beta L} \Delta^0 - \frac{\left(\overline{\nu_{\alpha L}^c} \ell_{\beta L} + \overline{\ell_{\alpha L}^c} \nu_{\beta L}\right)}{\sqrt{2}} \Delta^+ + \overline{\ell_{\alpha L}^c} \ell_{\beta L} (-\Delta^{++})\right] + \text{h.c.}\,. \\ &= -\overline{L_L^c}\, \mathbf{Y}_\Delta \underbrace{[i\tau_2(\vec{\tau} \cdot \vec{\Delta})]}_{\equiv \Delta} L_L + \text{h.c.}\,, \end{aligned} \tag{3.72}$$

where $\mathbf{Y}_\Delta$ is a $n_g \times n_g$ symmetric matrix since $\left(\overline{L_L^c} \mathbf{Y}_\Delta [i\tau_2(\vec{\tau} \cdot \vec{\Delta})] L_L\right)^T = \overline{L_L^c} \mathbf{Y}_\Delta^T [i\tau_2(\vec{\tau} \cdot \vec{\Delta})] L_L$. We define the matrix Δ of charge eigenfields by $\Delta \equiv i\tau_2(\tau \cdot \vec{\Delta})$. Under an SU(2)$_L \otimes$ U(1)$_Y$ transformation (2.3), we see from (3.72) that Δ transforms as $\Delta \to U_g^*\, \Delta\, U_g^\dagger$.

Following the same reasoning, it is also possible to couple the scalar triplet to the Higgs doublet as:

$$-\mu_\Delta \widetilde{\Phi}^T i\tau_2(\vec{\tau}\cdot\vec{\Delta})\widetilde{\Phi} + \text{h.c.} = -\mu_\Delta \widetilde{\Phi}^T \Delta\, \widetilde{\Phi} + \text{h.c.}\,. \tag{3.73}$$

We can then write the type II seesaw Lagrangian in the charge eigenfield basis:

$$\begin{aligned}\mathcal{L}_{\text{type II}} = \mathcal{L}_{\text{SM}} &+ \frac{1}{2}\text{Tr}\left[(D_\mu\Delta)^\dagger(D^\mu\Delta)\right] - \frac{1}{2}M_\Delta^2\text{Tr}\left(\Delta^\dagger\Delta\right) - \left[\overline{L_L^c}\mathbf{Y}_\Delta\Delta\, L_L + \mu_\Delta\widetilde{\Phi}^T\Delta\,\widetilde{\Phi} + \text{h.c.}\right] \\ &- \left\{\chi_1\text{Tr}\left[(\Delta^\dagger\Delta)\right]^2 + \chi_2\Phi^\dagger\Phi\text{Tr}\left(\Delta^\dagger\Delta\right) + \chi_3\text{Tr}\left(\Delta^\dagger\Delta\,\Delta^\dagger\Delta\right) + \chi_4\Phi^\dagger\Delta^\dagger\Delta\Phi\right\}\,,\end{aligned} \tag{3.74}$$

where, as in the type I seesaw scenario, we work in the mass basis for charged leptons. For future purposes, it is convenient to write this Lagrangian in the flavour basis defined by (3.68) as

$$\begin{aligned}\mathcal{L}_{\text{type II}} = \mathcal{L}_{\text{SM}} &+ (D_\mu\vec{\Delta})^\dagger\cdot(D^\mu\vec{\Delta}) - \vec{\Delta}^\dagger\mathbf{M}_\Delta^2\vec{\Delta} + \left[\overline{\widetilde{L_L}}\mathbf{Y}_\Delta(\vec{\tau}\cdot\vec{\Delta})L_L - \mu_\Delta\Phi^\dagger(\vec{\tau}\cdot\vec{\Delta})\widetilde{\Phi} + \text{h.c.}\right] \\ &- \left\{\frac{\lambda_1}{2}\left(\vec{\Delta}^\dagger\vec{\Delta}\right)^2 + \lambda_2\Phi^\dagger\Phi\left(\vec{\Delta}^\dagger\vec{\Delta}\right) + \frac{\lambda_3}{2}\left(\vec{\Delta}^\dagger I_i\vec{\Delta}\right)^2 + \lambda_4\left(\vec{\Delta}^\dagger I^i\vec{\Delta}\right)\left(\Phi^\dagger\tau_i\Phi\right)\right\}\,,\end{aligned} \tag{3.75}$$

where $\mathbf{M}_\Delta = M_\Delta\text{diag}(1,1,1)$ is the mass matrix for the triplet $\vec{\Delta}$, $\widetilde{L_L} \equiv i\tau_2\left(L_L^c\right)$ and λ_i are real coefficients. The translation from the first Lagrangian (3.74) to this second form is given by the prescriptions:

$$\left\{\begin{array}{rcl} 2\left(\vec{\Delta}^\dagger\vec{\Delta}\right) &=& \text{Tr}\left(\Delta^\dagger\Delta\right) \\ 4\left(\vec{\Delta}^\dagger I_i\vec{\Delta}\right)^2 &=& 2\text{Tr}\left(\Delta^\dagger\Delta\,\Delta^\dagger\Delta\right) - \left[\text{Tr}\left(\Delta^\dagger\Delta\right)\right]^2 \\ \left(\vec{\Delta}^\dagger I^i\vec{\Delta}\right)\left(\Phi^\dagger\tau_i\Phi\right) &=& -\Phi^\dagger\Delta^\dagger\Delta\Phi + \frac{1}{2}\Phi^\dagger\Phi\text{Tr}\left(\Delta^\dagger\Delta\right)\end{array}\right. \longrightarrow \left\{\begin{array}{rcl}\lambda_1 &=& 8\chi_1 + 4\chi_3 \\ \lambda_2 &=& 2\chi_2 + \chi_4 \\ \lambda_3 &=& 4\chi_3 \\ \lambda_4 &=& -\chi_4\end{array}\right.. \tag{3.76}$$

For the triplet mass matrix $\mathbf{M}_\Delta$, we must have $\mathbf{M}_\Delta = M_\Delta\,\text{diag}(1,1,1)$ in order to obtain an invariant mass term, i.e. $U_g^\dagger\,\mathbf{M}_\Delta^2\,U_g = \mathbf{M}_\Delta^2$ under an SU(2)$_L\otimes$U(1)$_Y$ transformation U_g.

The essence of the type II seesaw mechanism consists in the suppression of the triplet VEV v_Δ compared to the Higgs VEV v. In fact, v_Δ is severely constrained by the experimental value of the ρ parameter, $\rho_{\text{exp.}} = 1.0004^{+0.0003}_{-0.0004}$ [66]. Considering Eq. (2.32) with an additional scalar triplet, we have

$$\rho_{\text{type II}} = \frac{1 + 2\,v_\Delta^2/v^2}{1 + 4\,v_\Delta^2/v^2}\,, \tag{3.77}$$

and we see that v_Δ is constrained by electroweak precision data to be of magnitude $v_\Delta \leq 1 - 10$ GeV [66]. We assume that the VEVs have the form

$$\langle 0|\Delta|0\rangle = \begin{pmatrix}\sqrt{2}\,\langle\Delta^0\rangle & -\langle\Delta^+\rangle \\ -\langle\Delta^+\rangle & -\sqrt{2}\,\langle\Delta^{++}\rangle\end{pmatrix} = \begin{pmatrix} v_\Delta & 0 \\ 0 & 0\end{pmatrix}, \qquad \langle 0|\Phi|0\rangle = \frac{1}{\sqrt{2}}\begin{pmatrix}0\\ v\end{pmatrix}, \qquad \left|\frac{v_\Delta}{v}\right| \ll 1\,. \tag{3.78}$$

Minimising the scalar potential, the Higgs VEV remains unchanged, while in the limit $M_\Delta^2 \gg (\lambda_2+\lambda_4)v^2$ the triplet VEV is given by

$$v_\Delta = -\frac{v^2\mu_\Delta^*}{M_\Delta^2 + (\lambda_2+\lambda_4)v^2/2} \approx -\frac{v^2\mu_\Delta^*}{M_\Delta^2}\,, \tag{3.79}$$

Therefore, we see that the triplet VEV is small, $v_\Delta \ll v$, if $M_\Delta^2 \gg v\mu_\Delta$. Note at this point that the physical singly-charged mass eigenstate H^+ practically coincides with Δ^+, with an admixture of the Higgs doublet component ϕ^+ suppressed by a factor v_Δ/v. In general, singly- and doubly- harged scalars fields Δ^{++} and Δ^+ have different masses [156]. In this thesis, however, we will always use the approximation $M_\Delta^+ \approx M_\Delta^{++} \equiv M_\Delta$, unless stated otherwise. After EWSB, the Yukawa interactions (3.72) then generate a naturally small Majorana neutrino mass matrix:

$$\mathcal{L}_{\text{Yukawa, }\Delta} \xrightarrow{\text{EWSB}} -\frac{1}{2}\overline{\nu_L^c}\,\mathbf{M}_\nu\,\nu_L\,, \qquad \mathbf{M}_\nu = 2v_\Delta \mathbf{Y}_\Delta \approx -\frac{2v^2\mu_\Delta^*}{M_\Delta^2}\mathbf{Y}_\Delta\,. \tag{3.80}$$

Notice that for Yukawa couplings of $\mathcal{O}(10^{-9})$ or higher, the most stringent constraint on v_Δ does not come from EW precision measurements but from the absolute scale of neutrino masses. The neutrino mass matrix turns out to be proportional to both $\mathbf{Y}_\Delta$ and μ_Δ^*. This was already expected from the Lagrangian (3.75), in which the breaking of lepton number L results precisely from the simultaneous presence of the Yukawa and μ_Δ couplings.

As usual, the diagonalisation of the mass matrix (3.80) is achieved through the unitary rotation

$$\nu_L \to U_L^\nu \nu_L \quad \Longrightarrow \quad 2v_\Delta\left(U_L^{\nu T}\mathbf{Y}_\Delta U_L^\nu\right) = \mathbf{M}_\nu^{\text{diag.}} = \text{diag}(m_{\nu_1}, m_{\nu_2}, \ldots, m_{\nu_{n_g}})\,. \tag{3.81}$$

The weak currents involving neutrinos are then affected in the standard way described in Section 3.2.

The triplet Yukawa interaction (3.72) also generates couplings between the triplet-component fields and the charged leptons. The relevant terms for our discussion are:

$$\mathcal{L}_{\Delta\ell\ell} = \sqrt{2}\,(\overline{\ell_L^c}\mathbf{Y}_\Delta\ell_L)\Delta^{++} + \sqrt{2}\,(\overline{\ell_L}\mathbf{Y}_\Delta^\dagger\ell_L^c)\Delta^{--}\,, \tag{3.82}$$

$$\mathcal{L}_{\Delta\ell\nu} = 2\,\left[\overline{\ell_L^c}\,(\mathbf{Y}_\Delta U_L^\nu)\,\nu_L\right]\Delta^+ + 2\left[\overline{\nu_L}\,(\mathbf{Y}_\Delta U_L^\nu)^\dagger\,\ell_L^c\right]\Delta^-\,, \tag{3.83}$$

where the obvious definitions $\Delta^{--} = (\Delta^{++})^\dagger$ and $\Delta^- = (\Delta^+)^\dagger$ apply.

Also relevant to our analysis are the gauge interactions of the charged triplet components, which are obtained from the kinetic term of the triplet in the Lagrangian (3.75):

$$\mathcal{L}_{W,\Delta^\pm} = igW_\mu^\dagger\left[(\partial^\mu\Delta^{--})\,\Delta^+ - \Delta^{--}\,(\partial^\mu\Delta^+)\right] + \text{h.c.}\,, \tag{3.84}$$

$$\mathcal{L}_{Z,\Delta} = \frac{ig}{c_W}\left\{(1-2s_W^2)\left[\Delta^{--}\,(\partial^\mu\Delta^{++})\right] + \frac{s_W^2}{c_W}\left[\Delta^+\,(\partial^\mu\Delta^-)\right]\right\}Z_\mu + \text{h.c.}\,, \tag{3.85}$$

$$\mathcal{L}_{\gamma,\Delta} = 2ie\left[\Delta^{--}\,(\partial^\mu\Delta^{++})\right]A_\mu + ie\left[\Delta^-\,(\partial^\mu\Delta^+)\right]A_\mu + \text{h.c.}\,. \tag{3.86}$$

where we have defined $s_W \equiv \sin\theta_W$ and $c_W \equiv \cos\theta_W$.

Let us now discuss the low-energy effective description of the type II seesaw model [105]. In the flavour basis, the equations of motion for the triplet components Δ^α are

$$\Delta_\alpha = \left[(D_\mu)^2 + \lambda_4 T^i\Phi^\dagger\tau^i\Phi + M_\Delta^2 + \lambda_2\Phi^\dagger\Phi + \lambda_1\vec{\Delta}^\dagger\vec{\Delta} + \lambda_3 T^i(\vec{\Delta}^\dagger T^i\vec{\Delta})\right]^{-1}_{\alpha\beta}\left[\overline{L_L}\mathbf{Y}_\Delta^\dagger\tau^\beta\widetilde{L_L} - \mu_\Delta^*\tilde{\Phi}^\dagger\tau^\beta\Phi\right]\,, \tag{3.87}$$

where $(D_\mu)^2 \equiv D_\mu^\dagger D^\mu$. In order to find the dominant terms of the effective low-energy Lagrangian up to $d \leq 6$ operators, it suffices to solve the problem perturbatively in the quartic couplings of λ_2 and λ_4.

At zero order, the effective Lagrangian is then obtained expanding Eq. (3.87) in inverse powers of M_Δ^2. The first contribution to the effective Lagrangian comes from a $d = 4$ operator,

$$\delta\mathcal{L}^{d=4} = \frac{|\mu_\Delta|^2}{M_\Delta^2}\left(\widetilde{\Phi}^\dagger \tau^i \Phi\right)\left(\Phi^\dagger \tau^i \widetilde{\Phi}\right) = 2\frac{|\mu_\Delta|^2}{M_\Delta^2}\left(\Phi^\dagger\Phi\right)^2 , \tag{3.88}$$

whose effect is to correct the quartic coupling λ of the Higgs in Eq. (2.16):

$$\delta\lambda = -2\frac{|\mu_\Delta|^2}{M_\Delta^2} . \tag{3.89}$$

We also obtain the $d = 5$ Weinberg operator (3.28), with coefficients

$$c^{d=5} = 4\mathbf{Y}_\Delta \frac{\mu_\Delta^*}{M_\Delta^2} , \tag{3.90}$$

which generates a Majorana mass matrix for neutrinos

$$\mathbf{M}_\nu = -2\mathbf{Y}_\Delta v^2 \frac{\mu_\Delta^*}{M_\Delta^2} , \tag{3.91}$$

in agreement with the result (3.80) obtained in the complete theory. It must be noted that, unlike to the fermionic seesaw models, the neutrino mass matrix in the type II seesaw mechanism depends linearly on the Yukawa coupling matrix $\mathbf{Y}_\Delta$. This means that the study of the $d = 5$ operator coefficients of the low-energy theory allows us to determine the high-energy theory parameters $\mathbf{Y}_{\boldsymbol{\Delta}}$. This is possible up to an overall scale μ_Δ/M_Δ^2, whose experimental access will be analised in Chapter 4.

From the effective Lagrangian, we also obtain a set of three effective operators with dimension $d = 6$:

$$\begin{cases} \delta\mathcal{L}_{4F} = & -\frac{(\mathbf{Y}_\Delta)_{\rho\sigma}(\mathbf{Y}_\Delta)^\dagger_{\alpha\beta}}{{M_\Delta}^2}\left(\overline{L_{L\beta}}\gamma_\mu L_{L\rho}\right)\left(\overline{L_{L\alpha}}\gamma^\mu L_{L\sigma}\right) \\ \delta\mathcal{L}_{6\Phi} = & -2\left(\lambda_2+\lambda_4\right)\frac{|\mu_\Delta|^2}{M_\Delta^4}\left(\Phi^\dagger\Phi\right)^3 \\ \delta\mathcal{L}_{\Phi D} = & 4\frac{|\mu_\Delta|^2}{M_\Delta^4}\left(\Phi^\dagger\Phi\right)\left[\left(D^\mu\Phi\right)^\dagger\left(D_\mu\Phi\right)\right] + 4\frac{|\mu_\Delta|^2}{M_\Delta^4}\left[\Phi^\dagger D^\mu\Phi\right]^\dagger\left[\Phi^\dagger D_\mu\Phi\right] . \end{cases} \tag{3.92}$$

The operator $\delta\mathcal{L}_{4F}$ induces a shift to the SM value of the Fermi constant, $G_F^{\text{SM}} = 1/(\sqrt{2}v^2)$, as extracted from muon decay [see Eq. (2.44) and Fig. 2.2]:

$$G_F = G_F^{\text{SM}} + \delta G_F , \qquad \delta G_F = \frac{1}{\sqrt{2}M_\Delta^2}\left|(\mathbf{Y}_\Delta)_{e\mu}\right|^2 . \tag{3.93}$$

The value of M_Z also gets a correction from the last operator $\delta\mathcal{L}_{\Phi D}$:

$$\frac{\delta M_Z^2}{M_Z^2} = 2v^2\frac{|\mu_\Delta|^2}{M_\Delta^4} . \tag{3.94}$$

Finally, besides a correction to the Higgs quartic coupling, the Higgs potential (2.16) is also modified by the presence of the dimension $d = 6$ operator $\delta\mathcal{L}_{6\Phi}$. It now reads

$$V = \mu^2\left|\Phi\right|^2 + \tilde{\lambda}\left|\Phi\right|^4 - 2\left(\lambda_2+\lambda_4\right)\frac{|\mu_\Delta|^2}{M_\Delta^4}\left|\Phi\right|^6 , \tag{3.95}$$

where $\tilde{\lambda} = \lambda + \delta\lambda$ is the corrected value of the Higgs quartic coupling. Therefore, the combined effect of the $\delta\mathcal{L}^{d=4}$ and $\delta\mathcal{L}_{6\Phi}$ operators is to induce a shift in the VEV v of the Higgs doublet:

$$\frac{\delta v^2}{v^2} = -3v^2 \frac{|\mu_\Delta|^2}{M_\Delta^4} \frac{(\lambda_2 + \lambda_4)}{\lambda + \delta\lambda} \,. \tag{3.96}$$

Using all these parameters, we will consider in Section 4.3 the deviations from SM predictions induced to several physical observables. Also interesting is the minus sign Eq. (3.89), which could affect the stability of the Higgs potential. An analysis of this possibility can be found in Ref. [156].

Let us finally proceed to the counting of the number of parameters in the type II seesaw model. In the full theory, one introduces the triplet mass M_Δ, 5 coupling parameters λ_i and μ_Δ, and $n_g(n_g+1)$ Yukawa couplings. There are also n_g lepton masses and $n_g(n_g-1)$ parameters in the mixing matrix U_L^ν (n_g phases can be eliminated from U_L^ν with a convenient rephasing of the charged-lepton fields). Therefore, the lepton sector in the type II seesaw model contains $n_g(2n_g+1)+6 = 27$ parameters. It is easy to verify by comparison of Eq. (3.75) with Eqs. (3.88) and (3.92) that this number is larger than the number of parameters in the effective theory with dimension $d \leq 6$ operators. In order to obtain an equal number of parameters in both theories, we would need to consider all $d \leq 8$ operators [105].

3.3.3 Type III seesaw mechanism

Consider, finally, the type III seesaw scenario [157], in which the SM field content is extended with n' right-handed fermionic triplets $\vec{\Sigma}_{kR} = (\Sigma^1_{kR}, \Sigma^2_{kR}, \Sigma^3_{kR})^T$ with null hypercharge. As in the type II seesaw scenario, these flavour isospin triplets pertain to the adjoint representation of SU(2)$_L$ with generators given by Eq. (3.68). The charge eigenfields are related with the flavour eigenfields by:

$$\Sigma^{\pm} = \frac{\Sigma^1 \mp i\Sigma^2}{\sqrt{2}}, \qquad\qquad \Sigma^0 \equiv \Sigma^3 \,. \tag{3.97}$$

Following the same argument that led to Eq. (3.72) in the type II seesaw, Lorentz-invariance and SU(2)$_L$⊗U(1)$_Y$ invariance allow Yukawa couplings involving the doublets $i\tau_2 L_L^*$ and $\widetilde{\Phi}$:

$$\mathcal{L}_{\text{Yukawa, }\Sigma} = -\overline{L_L}\mathbf{Y}_\Sigma^\dagger \left[(\vec{\tau}\cdot\vec{\Sigma}_R) \right] \widetilde{\Phi} + \text{h.c.} = -\overline{\vec{\Sigma}_R}\cdot\mathbf{Y}_\Sigma(\widetilde{\Phi}^\dagger\vec{\tau}L_L) + \text{h.c.}\,, \tag{3.98}$$

with $\mathbf{Y}_\Sigma$ a $n' \times n$ matrix. Allowing lepton number violation, it is also possible to build a Majorana mass term for the triplet:

$$\mathcal{L}^{\text{Maj.}}_{\text{type III}} = -\frac{1}{2}\left[\overline{\Sigma^+_R}\mathbf{M}_\Sigma(\vec{\Sigma}^-_R)^c + \overline{\Sigma^0_R}\mathbf{M}_\Sigma(\vec{\Sigma}^0_R)^c + \overline{\Sigma^-_R}\mathbf{M}_\Sigma(\vec{\Sigma}^+_R)^c \right] + \text{h.c.} = -\frac{1}{2}\overline{\vec{\Sigma}_R}\mathbf{M}_\Sigma\vec{\Sigma}^c_R + \text{h.c.}\,, \tag{3.99}$$

where $\mathbf{M}_\Sigma$ is a $n' \times n'$ symmetric mass matrix. The type III seesaw Lagrangian is then

$$\mathcal{L}_{\text{type III}} = \mathcal{L}_{\text{SM}} + i\,\overline{\vec{\Sigma}_R}\ \overleftrightarrow{\not{D}}\ \vec{\Sigma}_R - \left[\frac{1}{2}\overline{\vec{\Sigma}_R}\mathbf{M}_\Sigma\vec{\Sigma}^c_R + \overline{\vec{\Sigma}_R}\cdot\mathbf{Y}_\Sigma(\widetilde{\Phi}^\dagger\vec{\tau}L_L) + \text{h.c.} \right] . \tag{3.100}$$

As done in the type I seesaw scenario, we work in the basis where both the charged-lepton and triplet mass matrices $\mathbf{M}_\ell$ and $\mathbf{M}_\Sigma$ are diagonal, with $m_\Sigma \gg v$.

The physical particles are neutral Majorana fermions and charged fermions. The flavour fields are defined as:

$$E \equiv \Sigma_R^- + \left(\Sigma_R^+\right)^c \;, \qquad N \equiv \Sigma_R^0 + \left(\Sigma_R^0\right)^c \;, \qquad \nu \equiv \nu_L + \left(\nu_L\right)^c \;. \tag{3.101}$$

After EWSB, the type III Lagrangian (3.100) leads to a neutrino Dirac-Majorana mass matrix

$$\mathcal{L}^{\nu,\,\text{mass}}_{\text{type III}} = -\frac{1}{2}\begin{pmatrix}\overline{\nu_R} & \overline{N_R}\end{pmatrix}\begin{pmatrix}0 & \mathbf{M}_D^T \\ \mathbf{M}_D & \mathbf{M}_\Sigma\end{pmatrix}\begin{pmatrix}\nu_L \\ N_L\end{pmatrix} + \text{h.c.}\,, \qquad \mathbf{M}_D \equiv \frac{v}{\sqrt{2}}\mathbf{Y}_\Sigma\,, \tag{3.102}$$

which is similar to (3.34) in the type I seesaw model. On the other hand, the type III Lagrangian also leads to a mass matrix for charged leptons:

$$\mathcal{L}^{\ell,\,\text{mass}}_{\text{type III}} = -\begin{pmatrix}\overline{\ell_R} & \overline{E_R}\end{pmatrix}\begin{pmatrix}\mathbf{M}_\ell^\dagger & 0 \\ \sqrt{2}\mathbf{M}_D & \mathbf{M}_\Sigma\end{pmatrix}\begin{pmatrix}\ell_L \\ E_L\end{pmatrix} + \text{h.c.}\,, \qquad \mathbf{M}_\ell \equiv \frac{v}{\sqrt{2}}\mathbf{Y}_\ell\,. \tag{3.103}$$

As in the type I seesaw, we assume that $\mathbf{M}_\Sigma$ is non-singular and that all the matrix elements of $\mathbf{M}_\ell$ and $\mathbf{M}_D$ are much smaller than the scale m_Σ:

$$\left(\mathbf{M}_\ell\right)_{\alpha\beta}\,,\; \left(\mathbf{M}_D\right)_{k\alpha} \ll m_\Sigma\,. \tag{3.104}$$

Under these assumptions, there will be n' heavy neutrinos and charged fermions with masses of order m_Σ, n_g light neutrinos with masses suppresed by inverse powers of m_Σ and also n_g charged fermions with mass matrix approximately given by $\mathbf{M}_\ell$.

The diagonalisation of the mass matrices in Eq. (3.102) and Eq. (3.103) can be accomplished similarly to the type I seesaw, i.e. we start by performing the following unitary rotations of fermion fields:

$$\begin{pmatrix}\nu_L \\ N_L\end{pmatrix} \to U_0\begin{pmatrix}\nu_L \\ N_L\end{pmatrix}\,, \qquad \begin{pmatrix}\ell_{L,R} \\ E_{L,R}\end{pmatrix} \to U^\ell_{L,R}\begin{pmatrix}\ell_{L,R} \\ E_{L,R}\end{pmatrix}\,, \tag{3.105}$$

where we define the unitary rotations U_0 and $U_{L,R}$ by blocks as

$$U_0 = \begin{pmatrix}U_{0\nu\nu} & U_{0\nu N} \\ U_{0N\nu} & U_{0NN}\end{pmatrix}\,, \qquad U_L = \begin{pmatrix}U_{L\ell\ell} & U_{L\ell E} \\ U_{LE\ell} & U_{LEE}\end{pmatrix}\,, \qquad U_R = \begin{pmatrix}U_{R\ell\ell} & U_{R\ell E} \\ U_{RE\ell} & U_{REE}\end{pmatrix}\,. \tag{3.106}$$

Applying the procedure in Ref. [148], we then get the following results up to order $\mathcal{O}\left[(m_D, m_\ell)^2/m_\Sigma^2\right]$:

$$\begin{array}{llll}
U_{L\ell\ell} = \mathbb{1} - \boldsymbol{\epsilon}^\Sigma & U_{L\ell E} = \sqrt{2}\mathbf{M}_D^\dagger\mathbf{M}_\Sigma^{-1} & U_{LE\ell} = -\sqrt{2}\mathbf{M}_\Sigma^{-1}\mathbf{M}_D & U_{LEE} = \mathbb{1} - \boldsymbol{\epsilon}'^\Sigma \\
U_{R\ell\ell} = \mathbb{1} & U_{R\ell E} = \sqrt{2}\mathbf{M}_\ell\mathbf{M}_D^\dagger\mathbf{M}_\Sigma^{-2} & U_{RE\ell} = -\sqrt{2}\mathbf{M}_\Sigma^{-2}\mathbf{M}_D\mathbf{M}_\ell & U_{REE} = \mathbb{1} \\
U_{0\nu\nu} = (\mathbb{1} - \frac{\boldsymbol{\epsilon}^\Sigma}{2}) & U_{0\nu N} = \mathbf{M}_D^\dagger\mathbf{M}_\Sigma^{-1} & U_{0N\nu} = -\mathbf{M}_\Sigma^{-1}M_D & U_{0NN} = (\mathbb{1} - \frac{\boldsymbol{\epsilon}'^\Sigma}{2})
\end{array}\,, \tag{3.107}$$

where the following definitions have been used:

$$\boldsymbol{\epsilon}^{\Sigma} \equiv \mathbf{M}_D^\dagger \left(\mathbf{M}_\Sigma^*\right)^{-1} \mathbf{M}_\Sigma \mathbf{M}_D \,, \qquad \boldsymbol{\epsilon}'^{\Sigma} \equiv \mathbf{M}_\Sigma^{-1} \mathbf{M}_D \mathbf{M}_D^\dagger \left(\mathbf{M}_\Sigma^*\right)^{-1} \,. \tag{3.108}$$

At lowest order, the mass matrices for the light and heavy fields are then given by:

$$\mathbf{M}^\nu_{\text{light}} = \left(U^T_{0\nu\nu}\mathbf{M}_L + U^T_{0N\nu}\mathbf{M}_D\right)\left(U_{0\nu\nu} - U_{0\nu N}U^{-1}_{0NN}U_{0N\nu}\right) \approx -\mathbf{M}_D^T\mathbf{M}_\Sigma^{-1}\mathbf{M}_D \,, \tag{3.109}$$

$$\mathbf{M}^\nu_{\text{heavy}} = \left(U^T_{0\nu N}\mathbf{M}_L + U^T_{0NN}\mathbf{M}_D\right)\left(U_{0\nu N} - U_{0\nu\nu}U^{-1}_{0N\nu}U_{0NN}\right) \approx \mathbf{M}_\Sigma \,, \tag{3.110}$$

$$\mathbf{M}^\ell_{\text{light}} = (U^\dagger_{R\ell\ell}\mathbf{M}^\dagger_\ell + \sqrt{2}U^\dagger_{RE\ell}\mathbf{M}_D)U_{L\ell\ell} + U^\dagger_{RE\ell}\mathbf{M}_\Sigma U_{LE\ell} \approx \mathbf{M}_\ell \,, \tag{3.111}$$

$$\mathbf{M}^\ell_{\text{heavy}} = (U^\dagger_{R\ell E}\mathbf{M}^\dagger_\ell + \sqrt{2}U^\dagger_{REE}\mathbf{M}_D)U_{L\ell E} + U^\dagger_{REE}\mathbf{M}_\Sigma U_{LEE} \approx \mathbf{M}_\Sigma \,. \tag{3.112}$$

We see that the mixing between flavour fields is small and its only relevant effect is, as happened in the type I seesaw scenario, the generation of a light neutrino mass matrix $\mathbf{M}^\nu_{\text{light}}$ suppressed as ${\mathbf{M}_D}^T\mathbf{M}_\Sigma^{-1}$ with respect to the Dirac mass matrix $\mathbf{M}_D$ by the small factor ${\mathbf{M}_D}^T\mathbf{M}_\Sigma^{-1}$. The final step is the diagonalisation of the mass matrices $\mathbf{M}^{\nu,\ell}_{\text{light}}$ and $\mathbf{M}^{\nu,\ell}_{\text{heavy}}$. This is achieved through the unitary rotations

$$\nu_L \to \left(U^\nu_L\right)\nu_L \,, \qquad N_L \to \left(U^N_L\right)N_L \,, \qquad \ell_L \to \left(U^\ell_L\right)\ell_L \,, \qquad E_L \to \left(U^E_L\right)E_L \,, \tag{3.113}$$

where $U^{N,\ell,E}_L \approx \mathbb{1}$ at first order in m_Σ^{-1} because $\mathbf{M}_\Sigma$ and $\mathbf{M}_\ell$ are already diagonal mass matrices.

Having completely diagonalised the mass matrices in Eq. (3.102) and Eq. (3.103), the charged and neutral interactions involving only the light fields ν_i and ℓ_α are then:

$$\mathcal{L}^{\nu,\ell}_{\text{CC}} \approx \frac{g}{\sqrt{2}}\,\overline{\ell}\gamma^\mu\left[\left(\mathbb{1} + \frac{1}{2}\boldsymbol{\epsilon}^\Sigma\right)U^\nu_L\right]P_L\,\nu\,W_\mu + \text{h.c.}\,, \tag{3.114}$$

$$\mathcal{L}^{\nu,\ell}_{\text{NC}} \approx \frac{g}{2\cos^2\theta_W}\left[\overline{\nu}\gamma^\mu\left(U^\nu_L\right)^\dagger\left(\mathbb{1} - \boldsymbol{\epsilon}^\Sigma\right)U^\nu_L P_L\,\nu - \overline{\ell}\gamma^\mu\left(\mathbb{1} + 2\boldsymbol{\epsilon}^\Sigma\right)P_L\,\ell - 2\sin\theta^2_W J^\mu_{\text{EM}}\right]Z_\mu \,, \tag{3.115}$$

where J^μ_{EM} is the usual SM electromagnetic current [Eq. (2.39)]. From Eq. (3.114), it is clear that, as happened in the type I seesaw scenario, the usual PMNS unitary mixing matrix (3.18) is now replaced by a nonunitary matrix,

$$U_{\text{PMNS}} \longrightarrow \boldsymbol{N} \equiv \left(\mathbb{1} + \frac{1}{2}\boldsymbol{\epsilon}^\Sigma\right)U^\nu_L \,, \tag{3.116}$$

whose deviation from unitarity is characterised by the small hermitian matrix $\boldsymbol{\epsilon}^\Sigma$. Also noticeable is the presence of FCNCs for both neutral and charged fermions.

Determining the remaining Lagrangian terms, we obtain the Lagrangian for the leptonic sector:

$$\mathcal{L} = \mathcal{L}_{\text{Kin}} + \mathcal{L}_{\text{CC}} + \mathcal{L}_{\text{NC}} + \mathcal{L}_{H,\eta} + \mathcal{L}_{\phi^-} \,, \tag{3.117}$$

where the relevant interactions for our future discussion are the following:

$$\mathcal{L}_{\rm CC} = \frac{g}{\sqrt{2}} \begin{pmatrix} \overline{\ell} & \overline{E} \end{pmatrix} \gamma^\mu W_\mu \left(P_L g_L^{\rm CC} + P_R g_R^{\rm CC}\sqrt{2}\right) \begin{pmatrix} \nu \\ N \end{pmatrix} + \text{h.c.}\,, \tag{3.118}$$

$$\mathcal{L}_{\rm NC} = \frac{g}{\cos\theta_W} \begin{pmatrix} \overline{\ell} & \overline{E} \end{pmatrix} \gamma^\mu Z_\mu \left(P_L g_L^{\rm NC} + P_R g_R^{\rm NC}\right) \begin{pmatrix} \ell \\ E \end{pmatrix} \tag{3.119}$$

$$+ \frac{g}{\cos\theta_W} \begin{pmatrix} \overline{\nu} & \overline{N} \end{pmatrix} \gamma^\mu Z_\mu \left(P_L g_{L_\nu}^{\rm NC} + P_R g_{R_\nu}^{\rm NC}\right) \begin{pmatrix} \nu \\ N \end{pmatrix}, \tag{3.120}$$

$$\mathcal{L}_{H,\eta}^{\ell,E} = \frac{g}{2M_W} \begin{pmatrix} \overline{\ell} & \overline{E} \end{pmatrix} H \left(P_L g_L^H + P_R g_R^H\right) \begin{pmatrix} \ell \\ E \end{pmatrix}$$

$$+ i\frac{g}{2M_W} \begin{pmatrix} \overline{\ell} & \overline{E} \end{pmatrix} \eta \left(P_L g_L^\eta + P_R g_R^\eta\right) \begin{pmatrix} \ell \\ E \end{pmatrix}, \tag{3.121}$$

$$\mathcal{L}_{\phi^-}^{\ell} = -\phi^- \overline{\ell} \frac{g}{\sqrt{2}M_W} \left[\left(P_L g_{L_\nu}^{\phi^-} + P_R g_{R_\nu}^{\phi^-}\right)\nu + \left(P_L g_{L_N}^{\phi^-} + P_R g_{R_N}^{\phi^-}\right) N\right] + \text{h.c.}\,, \tag{3.122}$$

with

$$g_L^{\rm CC} = \left(\begin{array}{c|c} \left(\mathbb{1} + \frac{\boldsymbol{\epsilon}^\Sigma}{2}\right) U_L^\nu & -\mathbf{M}_D^\dagger \mathbf{M}_\Sigma^{-1} \\ \hline 0 & \sqrt{2}\left(\mathbb{1} - \frac{\boldsymbol{\epsilon}'}{2}\right) \end{array}\right), \quad g_R^{\rm CC} = -\left(\begin{array}{c|c} 0 & \sqrt{2}\mathbf{M}_\ell^\dagger \mathbf{M}_D^\dagger \mathbf{M}_\Sigma^{-2} \\ \hline \mathbf{M}_\Sigma^{-1}\mathbf{M}_D^* \left(U_L^\nu\right)^* & -\left(\mathbb{1} - \frac{\boldsymbol{\epsilon}'^*}{2}\right) \end{array}\right), \tag{3.123}$$

$$g_L^{\rm NC} = \left(\begin{array}{c|c} \sin^2\theta_W - \frac{1}{2}\left(\mathbb{1} + 2\boldsymbol{\epsilon}^\Sigma\right) & \frac{1}{\sqrt{2}}\mathbf{M}_D^\dagger \mathbf{M}_\Sigma^{-1} \\ \hline \frac{1}{\sqrt{2}}\mathbf{M}_\Sigma^{-1}\mathbf{M}_D & \boldsymbol{\epsilon}' - \cos^2\theta_W \end{array}\right), \quad g_R^{\rm NC} = \left(\begin{array}{c|c} \sin^2\theta_W & \sqrt{2}\mathbf{M}_\ell^\dagger \mathbf{M}_D^\dagger \mathbf{M}_\Sigma^{-2} \\ \hline \sqrt{2}\mathbf{M}_\Sigma^{-2}\mathbf{M}_D\mathbf{M}_\ell & -\cos^2\theta_W \end{array}\right), \tag{3.124}$$

$$g_{L_\nu}^{\rm NC} = \left(\begin{array}{c|c} (U_L^\nu)^\dagger(\mathbb{1} - \boldsymbol{\epsilon}^\Sigma) U_L^\nu & (U_L^\nu)^\dagger \mathbf{M}_D^\dagger \mathbf{M}_\Sigma^{-1} \\ \hline \mathbf{M}_\Sigma^{-1}\mathbf{M}_D U_L^\nu & \boldsymbol{\epsilon}'^\Sigma \end{array}\right), \qquad g_{R_\nu}^{\rm NC} = 0\,, \tag{3.125}$$

$$g_L^H = \left(\begin{array}{c|c} \mathbf{M}_\ell^\dagger\left(3\boldsymbol{\epsilon}^\Sigma - \mathbb{1}\right) & -\sqrt{2}\mathbf{M}_\ell^\dagger \mathbf{M}_D^\dagger \mathbf{M}_\Sigma^{-1} \\ \hline -\sqrt{2}\mathbf{M}_D\left(\mathbb{1} - \boldsymbol{\epsilon}^\Sigma\right) - \sqrt{2}\mathbf{M}_\Sigma^{-2}\mathbf{M}_D\mathbf{M}_\ell\mathbf{M}_\ell^\dagger & \ldots \end{array}\right), \qquad g_R^H = \left(g_L^H\right)^\dagger, \tag{3.126}$$

$$g_L^\eta = \left(\begin{array}{c|c} \mathbf{M}_\ell^\dagger\left(\mathbb{1} + \boldsymbol{\epsilon}^\Sigma\right) & \sqrt{2}\mathbf{M}_\ell^\dagger \mathbf{M}_D^\dagger \mathbf{M}_\Sigma^{-1} \\ \hline -\sqrt{2}\mathbf{M}_D\left(\mathbb{1} - \boldsymbol{\epsilon}^\Sigma\right) + \sqrt{2}\mathbf{M}_\Sigma^{-2}\mathbf{M}_D\mathbf{M}_\ell\mathbf{M}_\ell^\dagger & \ldots \end{array}\right), \qquad g_R^\eta = -\left(g_L^\eta\right)^\dagger, \tag{3.127}$$

and

$$\begin{cases} g_{L_\nu}^{\phi^-} = \mathbf{M}_\ell^\dagger\left(\mathbb{1} - \frac{1}{2}\boldsymbol{\epsilon}^\Sigma\right) U_L^\nu \\ g_{R_\nu}^{\phi^-} = \left(\mathbb{1} - \boldsymbol{\epsilon}^\Sigma\right) U_L^\nu \mathbf{M}_\nu^{\rm diag.} \left(U_L^\nu\right)^T \end{cases}, \quad \begin{cases} g_{L_N}^{\phi^-} = \sqrt{2}\mathbf{M}_\ell^\dagger \mathbf{M}_D^\dagger \mathbf{M}_\Sigma^{-1} \\ g_{R_N}^{\phi^-} = \left(\mathbb{1} - \boldsymbol{\epsilon}^\Sigma\right)\mathbf{M}_D^\dagger\left(1 - \frac{\boldsymbol{\epsilon}'^*}{2}\right) - 2U_L^\nu \mathbf{M}_\nu^{\rm diag.}\left(U_L^\nu\right)^T \mathbf{M}_D^T \mathbf{M}_\Sigma^{-1} \end{cases}. \tag{3.128}$$

The dots in Eqs. (3.123)-(3.128) correspond to E-E interactions which do not contribute to the one-loop $\ell_1 \to \ell_2\gamma$ rates and, therefore, are irrelevant for our purposes.

We now conclude our study of the type III seesaw by analysing its effective description. Expanding the triplet propagator up to order $\mathcal{O}(1/\mathbf{M}_\Sigma^2)$, the stationary fields are given by:

$$\vec{\Sigma}_R = P_R\left[i\not{D} - \mathbf{M}_\Sigma\right]^{-1}\left[\mathbf{Y}_\Sigma^*\Phi^\dagger\vec{\tau}\widetilde{L_L} + \mathbf{Y}_\Sigma\widetilde{\Phi}^\dagger\vec{\tau}L_L\right] \approx -\mathbf{M}_\Sigma^{-1}\mathbf{Y}_\Sigma^*\Phi^\dagger\vec{\tau}\widetilde{L_L} - i\not{D}\left(\mathbf{M}_\Sigma^\dagger\right)^{-1}\mathbf{M}_\Sigma^{-1}\mathbf{Y}_\Sigma\widetilde{\Phi}^\dagger\vec{\tau}L_L\,. \tag{3.129}$$

Inserting these equations in the Lagrangian (3.100), the first effective operator that we obtain is the Weinberg operator (3.28) with coefficients given by

$$\mathbf{c}^{d=5} = \mathbf{Y}_\Sigma^T\,\mathbf{M}_\Sigma^{-1}\,\mathbf{Y}_\Sigma\,. \tag{3.130}$$

This results in a Majorana mass matrix for the light neutrinos after EWSB with an identical structure to the mass matrix in the type I scenario:

$$\mathbf{M}_\nu = -\frac{v^2}{2}\left(\mathbf{Y}_\Sigma^T\,\mathbf{M}_\Sigma^{-1}\,\mathbf{Y}_\Sigma\right)\,. \tag{3.131}$$

This result matches exactly the one obtained in the high-energy description for $\mathbf{M}_{\text{light}}$ in Eq. (3.109). From the effective Lagrangian we extract a single operator with dimension $d = 6$,

$$\delta\mathcal{L}^{d=6} = \mathbf{c}_{\alpha\beta}^{d=6}\left(\overline{L_{\alpha L}}\vec{\tau}\widetilde{\Phi}\right)i\not{D}\left(\widetilde{\Phi}^\dagger\vec{\tau}L_{\beta L}\right)\,, \qquad \frac{v^2}{2}\mathbf{c}^{d=6} = \epsilon^\Sigma = \mathbf{Y}_\Sigma^\dagger\left(\mathbf{M}_\Sigma^*\right)^{-1}\mathbf{M}_\Sigma^{-1}\,\mathbf{Y}_\Sigma\,. \tag{3.132}$$

Notice again the similarity between this operator and the corresponding one in the type I seesaw mechanism, Eqs. (3.56) and (3.57). However, the usual derivative $\not{\partial}$ appears now replaced by a covariant derivative version $\not{D}$, which leads to a richer interaction pattern.

After EWSB, the $d = 6$ operator corrects the lepton fields kinetic terms as well as their couplings with the SU(2)$_L$ gauge bosons A_μ^k. Going to a basis with kinetic terms canonically normalised at order $\mathcal{O}(1/M^2)$ and with diagonal lepton mass matrices, we get an effective Lagrangian similar to the one obtained in the type I seesaw model. Up to order $\mathcal{O}(1/M^2)$, the effective Lagrangian reads

$$\mathcal{L}_{\text{leptões}}^{d\leq 6} = \frac{1}{2}\overline{\nu_j}\left(i\not{\partial} - \mathbf{M}_{\nu j}^{\text{diag}}\right)\nu_j + \overline{\ell_\alpha}(i\not{\partial} - \mathbf{M}_{\ell\alpha}^{\text{diag.}})\ell_\alpha + \mathcal{L}_{\text{CC}} + \mathcal{L}_{\text{NC}} + \mathcal{L}_{\text{EM}}\,, \tag{3.133}$$

where $\nu_i = \nu_{Li} + \nu_{Li}^c$ are Majorana neutrino mass eigenfields and the weak currents are given by:

$$\mathcal{L}_{\text{CC}} = \frac{g}{\sqrt{2}}\overline{\ell_L}\not{W}^-\boldsymbol{N}\nu_L + \text{h.c.}\,, \tag{3.134}$$

$$\mathcal{L}_{\text{NC}} = \frac{gZ^\mu}{2\cos\theta_W}\left\{\overline{\nu_L}\gamma_\mu\left(\boldsymbol{N}^\dagger\boldsymbol{N}\right)^{-1}\nu_L - \overline{\ell_L}\gamma_\mu\left(\boldsymbol{N}\boldsymbol{N}^\dagger\right)^2\ell_L - 2\sin\theta_W^2 J_\mu^{\text{EM}}\right\}\,, \tag{3.135}$$

which coincides with the result obtained in the high-energy description. Namely, the usual PMNS mixing matrix (3.18) is replaced by a nonunitary matrix,

$$U_{\text{PMNS}} \longrightarrow \boldsymbol{N} \equiv \left(\mathbb{1} + \frac{1}{2}\boldsymbol{\epsilon}^\Sigma\right)U_L^\nu\,, \tag{3.136}$$

and now there are FCNCs involving both neutrino and charged lepton fields. The translation from

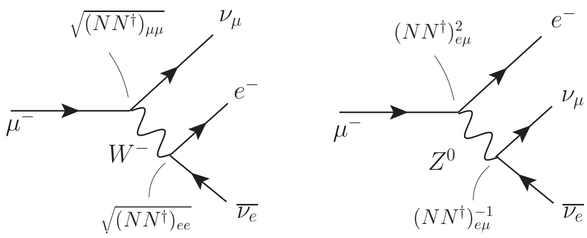

Figure 3.2: Tree-level diagrams for muon decay in the effective description of the type III seesaw model.

the high-energy to the effective theory description is thus made by simply neglecting all interactions involving the heavy fields N_k.

With the presence of FCNCs involving charged lepton fields, the Fermi constant G_F extracted from muon decay (Fig. 3.2) gets a slightly different correction than the one in the type I seesaw [see Eq. (3.64)],

$$G_F = G_F^{\rm SM}\sqrt{(\boldsymbol{N}\boldsymbol{N}^\dagger)_{ee}(\boldsymbol{N}\boldsymbol{N}^\dagger)_{\mu\mu} + \frac{3}{4}(\boldsymbol{N}\boldsymbol{N}^\dagger)^2_{e\mu}} \approx G_F^{\rm SM}\sqrt{(\boldsymbol{N}\boldsymbol{N}^\dagger)_{ee}(\boldsymbol{N}\boldsymbol{N}^\dagger)_{\mu\mu}}\,. \tag{3.137}$$

Finally, the deviations from unitarity of the mixing matrix $\boldsymbol{N}$ can once more be directly related with the dimension $d = 6$ operator coefficients:

$$|\boldsymbol{N}\boldsymbol{N}^\dagger - \mathbf{1}| = \frac{v^2}{2}|\boldsymbol{c}^{d=6}| = \frac{v^2}{2}\left|\mathbf{Y}_N^\dagger \frac{1}{\mathbf{M}_N^\dagger \mathbf{M}_N}\mathbf{Y}_N\right|\,. \tag{3.138}$$

The counting of the number of parameters in both the full theory and its low-energy effective description is identical to the type I seesaw one, shown in Table 3.2. The translation from the former case to the latter is done with the trivial replacement $N \to \Sigma$. Again, the effective theory with dimension $d \leq 6$ effective operators allows us to determine all the full theory parameters if the number of triplets n' equals (or is less than) the number of generations n_g in the SM.

As a summary of this section, we have gathered in Table 3.3 the effective operators with mass dimension $d \leq 6$ for the three types of seesaw mechanism.

Seesaw	Effective Lagrangian $\mathcal{L}_{\rm eff.} = c_i\mathcal{O}_i$			
	$c^{d=4}\mathcal{O}^{d=4}$	$c^{d=5}$	$c_i^{d=6}$	$\mathcal{O}_i^{d=6}$
Type I	-	$Y_N^T\frac{1}{\mathbf{M}_N}\mathbf{Y}_N$	$\left[\mathbf{Y}_N^\dagger\left(\mathbf{M}_N^\dagger\right)^{-1}\mathbf{M}_N^{-1}\mathbf{Y}_N\right]_{\alpha\beta}$	$\left(\overline{L_{L\alpha}}\widetilde{\Phi}\right) i\partial\!\!\!/\left(\widetilde{\Phi}^\dagger L_{L\beta}\right)$
Type II	$2\frac{\lvert\mu_\Delta\rvert^2}{M_\Delta^2}\left(\Phi^\dagger\Phi\right)^2$	$4Y_\Delta\frac{\mu_\Delta}{M_\Delta^2}$	$-\frac{(\mathbf{Y}_\Delta)_{\rho\sigma}(\mathbf{Y}_\Delta)^\dagger_{\alpha\beta}}{M_\Delta{}^2}$	$\left(\overline{L_{L\beta}}\gamma_\mu L_{L\rho}\right)\left(\overline{L_{L\alpha}}\gamma^\mu L_{L\sigma}\right)$
			$\frac{\lvert\mu_\Delta\rvert^2}{M_\Delta^4}$	$\left(\Phi^\dagger\vec{\tau}\widetilde{\Phi}\right)\left(\overleftarrow{D_\mu}\overrightarrow{D^\mu}\right)\left(\widetilde{\Phi}^\dagger\vec{\tau}\Phi\right)$
			$-2\left(\lambda_2+\lambda_4\right)\frac{\lvert\mu_\Delta\rvert^2}{M_\Delta^4}$	$\left(\Phi^\dagger\Phi\right)^3$
Type III	-	$\mathbf{Y}_\Sigma^T\mathbf{M}_\Sigma^{-1}\mathbf{Y}_\Sigma$	$\left[\mathbf{Y}_\Sigma^\dagger\left(\mathbf{M}_\Sigma^\dagger\right)^{-1}\mathbf{M}_\Sigma^{-1}\mathbf{Y}_\Sigma\right]_{\alpha\beta}$	$\left(\overline{\ell_{L\alpha}}\vec{\tau}\widetilde{\Phi}\right) iD\!\!\!\!/\left(\widetilde{\Phi}^\dagger\vec{\tau}\ell_{L\beta}\right)$

Table 3.3: Coefficients $\mathbf{c}_i$ and effective operators $\mathbf{c}_i\mathcal{O}_i$ obtained for the three seesaw scenarios.

3.4 Low scale seesaw, $M \sim \mathcal{O}(\mathrm{TeV})$

3.4.1 Electroweak hierarchy problem

An unsatisfactory aspect of the seesaw-type models pertains to a potential worsening of the electroweak hierarchy problem [158]. More specifically, if the above seesaw models are regarded as theories valid at energies below a high-energy scale Λ, the bare Higgs mass M_H^0 receives quadratically-divergent, finite and logarithmic quantum corrections. In fact, using a cutoff regularisation procedure and an on-shell renormalisation scheme, the one-loop correction to the Higgs mass in the type I seesaw is

$$\delta M_H^2 = -\sum_{i=1}^{n'} \frac{\left(\mathbf{Y}_N \mathbf{Y}_N^\dagger\right)_{ii}}{16\pi^2} \left[2\Lambda^2 + 2\left(\mathbf{M}_N^2\right)_{ii} \ln \frac{\left(\mathbf{M}_N^2\right)_{ii}}{\Lambda^2}\right] , \tag{3.139}$$

while for the fermionic-triplet model (type III seesaw):

$$\delta {M_H}^2 = -3\sum_{i=1}^{n'} \frac{\left(\mathbf{Y}_\Sigma \mathbf{Y}_\Sigma^\dagger\right)_{ii}}{16\pi^2} \left[2\Lambda^2 + 2\left(\mathbf{M}_\Sigma^2\right)_{ii} \ln \frac{\left(\mathbf{M}_\Sigma^2\right)_{ii}}{\Lambda^2}\right] . \tag{3.140}$$

Finally, in the type II seesaw one has:

$$\delta M_H^2 = \frac{3}{16\pi^2} \left[\lambda_2 \left(\Lambda^2 - M_\Delta^2 \ln \frac{\Lambda^2}{M_\Delta^2}\right) - 4|\mu_\Delta|^2 \log \frac{\Lambda^2}{M_\Delta^2}\right] . \tag{3.141}$$

Notice that in this last expression there is no dependence on the quartic coupling λ_4 of the Lagrangian (3.75). The reason for this is that the λ_4 interactions involving the charged scalar fields Δ^{++} (Δ^{--}) cancel with those involving Δ^0. This occurs because the Higgs fields in the λ_4 term are combined as a triplet of SU(2)$_L$. Note also that in these equations the aproximations $m_\nu \ll M \ll \Lambda$ have been used.

These results show that, even if the quadratically-divergent contributions of the SM cancel the ones in Eqs. (3.139)-(3.141), there are other troubling logarithmic contributions which do not cancel. Thus, if any of the new scales Λ or M is much larger than the electroweak scale v, large fine-tunings would be necessary to cancel all these contributions and accommodate a value $M_H \approx 125$ GeV for the Higgs mass. These cancellations would however be artificial and depend on the adopted renormalisation scheme.

For instance, working in the $\overline{\mathrm{MS}}$ scheme, the demand of no fine-tuning ($\delta M_H^2 \sim M_H^2$) requires for the type I and type III seesaw mass matrices:

$$m_{N,\Sigma} \lesssim 10^7 \mathrm{GeV} \left(\frac{M_H}{125\,\mathrm{GeV}}\right)^{2/3} \left(\frac{m_\nu}{10^{-9}\,\mathrm{GeV}}\right)^{-1/3} \left[\ln \frac{\Lambda^2}{m_{N,\Sigma}^2} + 1\right]^{-1/3} , \tag{3.142}$$

which leads to $m_{N,\Sigma} \lesssim 10^7$GeV. However, this result is only satisfied with Yukawa couplings of order $Y_N = \sqrt{2} m_\nu^{1/2} m_{N,\Sigma}^{1/2}/v \lesssim 10^{-4}$ [remember Eq. (3.55)], which spoils the naturalness of the seesaw mechanism to explain the smallness of m_ν. This problem could be obviously soften if it is possible to choose the high-energy scale M of the seesaw scenario close to the electroweak scale, rather than to the Grand-Unified scale. It is precisely this possibility that we briefly comment in the following.

3.4.2 *Direct lepton violation*

We now assume that the seesaw scale $M = m_N, m_\Delta, m_\Sigma$ is large but not too far from the TeV scale. From the point of view of the effective theory, the issue now is whether it is possible to accomodate tiny neutrino masses while keeping the $d = 6$ operators (suppressed as $1/M^2$) close to observability without fine-tunings or cancellations in the heavy mass matrices or Yukawa couplings.[2]

According to the 't Hooft naturalness criterium (Z1), such decoupling of the lepton-number odd $d = 5$ operator responsible for neutrino masses from the lepton-number preserving $d = 6$ operators may be a natural possibility. In fact, lepton-number symmetry may be broken by a small parameter whose value cannot be destabilised by other large scales of the theory through radiative corrections since, by nature, it can only be multiplicatively renormalised. On the other hand, other beyond-the-SM effects of the high-energy theory are lepton-number preserving and, as such, do not need to be strongly suppressed. Therefore, this reasoning suggests the *ansatz*[105]:

when lepton-number symmetry is broken in the full theory through a small mass parameter μ, $\mu \ll M$, the coefficients of the $d = 5$ operator are naturally suppressed in powers of μ/M, while the fermionic $d = 6$ operators keep their unsuppressed (by the small mass parameter μ) $1/M^2$ dependence. (Z2)

Such decoupling pattern for minimal seesaw models has the qualitative structure:

$$c^{d=5} = f(Y)\frac{\mu}{M^2}\,, \qquad\qquad c^{d=6} = g(Y)\,\frac{1}{|M|^2}\,, \tag{3.143}$$

where f and g are functions of the Yukawa couplings scale Y. From the $d = 5$ operator, we thus get a neutrino mass matrix proportional to the small parameter μ while the effects of the μ-independent $d = 6$ operator may be sizable, even of $\mathcal{O}(1)$, for generic Yukawa couplings. Notice that such a feature has already been found in the type II seesaw model, in Eqs. (3.90)-(3.92), thus suggesting that $\mu_\Delta \ll M_\Delta$ and $Y_\Delta \sim \mathcal{O}(1)$. In accordance to Ref. [105], we call this pattern *direct lepton violation* (DLV), since neutrino masses are proportional to the odd lepton-number parameter μ.

Low-scale models of light neutrino masses with large Yukawa couplings

There are models in the literature which illustrate and support the general ansatz (Z2). An interesting example is the *inverse seesaw model* [159]. Considering, for simplicity, only one left-handed neutrino and two singlet fermions, (ν_L, N_1, N_2), this model assumes the following structure for the full mass matrix:

$$\begin{pmatrix} 0 & m_{D_1} & 0 \\ m_{D_1} & 0 & M_{N_1} \\ 0 & M_{N_1} & \mu \end{pmatrix}, \tag{3.144}$$

where μ is a small mass parameter, $\mu \ll M_{N_1}$. Notice that μ is a Majorana mass while all the other are of Dirac nature. In fact, with lepton number assignements $L = 1, -1, 1$ to $\nu_l, N_1 N_2$, respectively, L is

[2] We can safely restrain the analysis to the $d \le 6$ operators without significant changes to the main physical aspects, as long as the heavy scale M keeps being larger than $\mathcal{O}(v)$.

conserved if $\mu = 0$. Expanding the eigenvalues of Eq. (3.144) in powers of the ratio $\mu/M_{N_1} \ll 1$, we obtain one light and two heavy neutrinos with masses:

$$m_\nu \approx \frac{\mu}{M_{N_1}} \frac{m_{D_1}^2}{M_{N_1}} \frac{M_{N_1}^2}{M_{N_1}^2 + m_{D_1}^2}, \qquad m_{\text{heavy}}^{\pm} \approx \sqrt{m_{D_1}^2 + M_{N_1}^2} \pm \frac{M_{N_1}^3}{2\left(m_{D_1}^2 + M_{N_1}^2\right)} \frac{\mu}{M_{N_1}}. \tag{3.145}$$

As m_{D_1} is a typical Dirac mass term, $m_{D_1} \sim Y_1\, v/\sqrt{2}$, Eq. (3.145) shows that m_ν is suppressed by an extra factor μ/M_{N_1} with respect to the result for the minimal type I seesaw model [Eq. (3.42)], exactly as expected from the general argument leading to Eq. (3.143). Therefore, we see that in the inverse seesaw model it is possible to avoid fine-tuning ($M_{N_1} \sim 1\,\text{TeV}$) while having Yukawa couplings of order $\mathcal{O}(1)$ as long as $\mu/M_{N_1} \sim 10^{-11}$. On the other hand, the lepton-number conserving $d = 6$ operators are independent of μ. Thus, low-energy effects associated to it could be discovered in the near future.

The above results generalise to the case with a non-zero 22 element in the mass matrix [160]:

$$\begin{pmatrix} 0 & m_{D_1} & 0 \\ m_{D_1} & M_{N_2} & M_{N_1} \\ 0 & M_{N_1} & \mu \end{pmatrix}. \tag{3.146}$$

The interesting feature about this case is that M_{N_2} acts as a strong source of lepton number violation without inducing by itself neutrino masses: for $\mu = 0$ the determinant still vanishes leading to massless neutrinos [3]. However, regarding the decoupling and suppresion of the $d = 5$ operators relative to $d = 6$ operators, we arrive at no new conclusions. For an extension of the above argument to the 3 left-handed plus 3 right-handed neutrico case, see, for instance, Ref. [105]. A generalisation to the type III inverse seesaw scenario as well as to a quintuplet version can be found in Ref. [161, 162].

The conclusion of the above discussion is that, irrespective of the specific model, having large effects from $d = 6$ operators requires lowering the scale M towards the TeV range and decoupling the $d = 5$ and $d = 6$ coefficients along the pattern discussed above and summarised in Eq. (3.143). This allows to account for the experimental values of neutrino masses without neither fine-tuning the Yukawa couplings nor assuming cancellations in combinations of them. For a seesaw scale of $\mathcal{O}(\text{TeV})$, observable effects are then possible. The next chapter, which deals with the phenomenological aspects of seesaw models including bounds for any value of M, will focus on those effects.

Note that the canonical seesaw models analysed in this chapter correspond only to a small portion of all possible SM extensions with naturally small neutrino masses. In fact, the inverse-seesaw models just discussed are viable tree-level alternatives [105, 159, 161]. Another option is to invoke loop processes, as in the case of the Zee-Babu model [163, 164], with two additional charged $\text{SU}(2)_L$ scalar singlets and Majorana neutrino masses generated via a two-loop diagram. Other exotic possibilities include the breaking of R-parity without inducing proton decay in SUSY models, as well as theories with extra dimensions or expanded gauge symmetries (see Ref. [165] and references therein).

[3] Since the 22 matrix element breaks lepton number, extra interaction couplings to N_i could induce neutrino masses. Such contribution would be suppressed by loop factors, couplings of the extra interactions, as well as the masses of the new states, but would not be necessarily negligible with respect to the contribution in Eq. (3.145).

4 Phenomenology of seesaw models

The discovery of neutrino oscillations and, consequently, of neutrino masses, has shown that lepton flavour is violated. This automatically leads to rare charged-lepton flavour violating (CLFV) processes, such as $\ell_\alpha \to \ell_\beta\gamma$, $\ell \to 3\ell$ or $\mu - e$ conversion in atomic nuclei. These processes have been subject of intense experimental investigation for decades and current experimental sensitivities on the various rates are expected to improve by several orders of magnitude [127] (see Table 4.1). For $\mu - e$ transitions, in particular for the $\mu \to 3e$ decay [166, 167] and $\mu - e$ conversion in atomic nuclei [168], an improvement by as much as four to six orders of magnitude could be expected. An important improvement of one order of magnitude is also foreseen for the $\ell_\alpha \to \ell_\beta\gamma$ decays [169–171].

Process	Present Limit	Future Sensitivity
$\mu \to e\gamma$	5.7×10^{-13} (MEG)	5×10^{-14} (MEG II)
$\tau \to e\gamma$	3.3×10^{-8} (Belle)	10^{-9} (Super B)
$\tau \to \mu\gamma$	4.4×10^{-8} (Belle)	$10^{-8,-9}$ (Belle II, Super B)
$\mu^- \to e^+e^-e^-$	1.0×10^{-12} (SIN/SINDRUM)	$10^{-16,-16,-17}$ (Mu3e, MUSIC, Project X)
$\tau^- \to e^+e^-e^-$	2.7×10^{-8} (Belle,BaBar)	10^{-10} (Super B)
$\tau^- \to \mu^+\mu^-e^-$	2.7×10^{-8} (Belle,BaBar)	10^{-10} (Super B)
$\tau^- \to e^+\mu^-\mu^-$	1.7×10^{-8} (Belle,BaBar)	10^{-10} (Super B)
$\tau^- \to e^+e^-\mu^-$	1.8×10^{-8} (Belle,BaBar)	10^{-10} (Super B)
$\tau^- \to \mu^+e^-e^-$	1.5×10^{-8} (Belle,BaBar)	10^{-10} (Super B)
$\tau^- \to \mu^+\mu^-\mu^-$	2.1×10^{-8} (Belle,BaBar)	10^{-10} (Belle II, Super B)
$\mu^-\mathrm{Ti} \to e^-\mathrm{Ti}$	4.3×10^{-12} (SINDRUM II)	$10^{-17,-17,-18,-19}$ (COMET, Mu2e, PRISM/PRIME, Project X)
$\mu^-\mathrm{Au} \to e^-\mathrm{Au}$	7.0×10^{-13} (SINDRUM II)	$10^{-17,-17,-18,-19}$ (COMET, Mu2e, PRISM/PRIME, Project X)
$\mu^-\mathrm{Pb} \to e^-\mathrm{Pb}$	4.6×10^{-11} (SINDRUM II)	$10^{-17,-17,-18,-19}$ (COMET, Mu2e, PRISM/PRIME, Project X)
$\mu^-\mathrm{Al} \to e^-\mathrm{Al}$		10^{-16} (COMET, Mu2e, PRISM/PRIME, Project X)

Table 4.1: Present experimental bounds on the branching ratios of charged lepton flavour violating processes considered in our analysis and corresponding future sensitivities. [66, 127].

In the framework of the SM extended with light neutrino masses, CLFV rates are expected to be far below expected sensitivities. In fact, assuming Dirac massive neutrinos, the $\mu \to e\gamma$ rate is

$$\mathrm{BR}(\mu \to e\gamma) = \frac{3\alpha}{32\pi} \frac{\left|\left(\mathbf{M}_\nu \mathbf{M}_\nu^\dagger\right)_{e\mu}\right|^2}{M_W^4} \sim \frac{3\alpha}{32\pi} \left(\frac{m_v^2}{M_W^4}\right) \sim 10^{-52} \,, \tag{4.1}$$

where we have assumed $m_\nu \sim 0.1$ eV for the neutrino mass scale. However, for the Majorana case, the existence of additional states can potentially induce CLFV transitions not suppressed by neutrino masses and, therefore, at the reach of future experiments. As we have seen in Section 3.4.2, this is the case if neutrino masses are generated through *direct lepton violation*, in which neutrino masses turn out to be directly proportional to a small lepton number violating parameter. From Eq. (3.145), such setup predicts a quasi-degenerate mass spectrum for heavy neutrinos. This fact will play an important role below. In fact, for a quasi-degenerate mass spectrum of right-handed neutrinos, the ratio of two $\mu - e$ transition processes depends only on the right-handed mass scale $m_{N,\Sigma}$. As such, predicted ratios constitute a precious model-discriminating tool. Finally, by analysing those ratios, we can also determine the range of Yukawa couplings and right-handed neutrino masses that future experiments can reach.

Experimental bounds on those CLFV decays can also be used to constrain combinations of Yukawa couplings $(\mathbf{Y}_\Delta)_{ij}$ in the type II seesaw scenario, while in the type I and type III seesaw models these bounds constrain the off-diagonal elements of the matrix $\boldsymbol{N}\boldsymbol{N}^\dagger$, characterising deviations from unitarity of the leptonic mixing matrix $\boldsymbol{N}$ [see Eq. (3.65)]. On the other hand, the diagonal elements of $\boldsymbol{N}\boldsymbol{N}^\dagger$ can be constrained by a combined analysis of well-known lepton flavour conserving processes: W decays, Z decays and universality tests listed in Tables 4.2 and 4.3.

Process/Quantity	Experimental Value
$\Gamma(W \to e\overline{\nu_e})$	$224.1375 \pm 0.0053\,\mathrm{MeV}$
$\Gamma(W \to \mu\overline{\nu_\mu})$	$220.385 \pm 0.051\,\mathrm{MeV}$
$\Gamma(W \to \tau\overline{\nu_\tau})$	$234.563 \pm 0.056\,\mathrm{MeV}$
$\Gamma(Z \to \text{invisible})$	$499.0 \pm 1.5\,\mathrm{MeV}$
$\mathrm{BR}(Z \to \sum_\alpha \ell_\alpha \overline{\ell_\alpha})$	$3.3658 \pm 0.0023\,\%$

Table 4.2: Low-energy gauge boson decays. Data taken from [66].

Process/Quantity	Experimental Value
$\mathrm{BR}(\tau \to \pi\overline{\nu_\tau})$	$10.83 \pm 0.06\,\%$
$\mathrm{BR}(\pi \to e\overline{\nu_e})$	$(1.230 \pm 0.004) \times 10^{-4}$
$\mathrm{BR}(\pi \to \mu\overline{\nu_\mu})$	$99.98770 \pm 0.00004\,\%$
$\mathrm{BR}(\tau \to \nu_\tau e\overline{\nu_e})$	$17.83 \pm 0.04\,\%$
$\mathrm{BR}(\tau \to K\overline{\nu_\tau})$	$(7.00 \pm 0.10) \times 10^{-3}$
$\mathrm{BR}(\tau \to \nu_\tau \mu\overline{\nu_\mu})$	$17.41 \pm 0.06\,\%$
$\mathrm{BR}(K \to e\overline{\nu_e})$	$(1.581 \pm 0.008) \times 10^{-5}$
$\mathrm{BR}(\mu \to \nu_\mu e\overline{\nu_e})$	$\approx 100\,\%$
$\mathrm{BR}(K \to \mu\overline{\nu_\mu})$	$63.55 \pm 0.11\,\%$

Table 4.3: Low-energy decays of leptons, pions and kaons. Data taken from [66].

Process	Constraint On	Upper Bound	Future Sensitivity on $\lvert(\boldsymbol{NN}^\dagger)_{\alpha\beta}\rvert$
$\mu \to e\gamma$	$\lvert(\boldsymbol{NN}^\dagger)_{e\mu}\rvert$	2.6×10^{-5}	7.6×10^{-6}
$\tau \to e\gamma$	$\lvert(\boldsymbol{NN}^\dagger)_{\tau e}\rvert$	1.5×10^{-2}	2.5×10^{-3}
$\tau \to \mu\gamma$	$\lvert(\boldsymbol{NN}^\dagger)_{\tau\mu}\rvert$	1.7×10^{-2}	2.5×10^{-3}

Table 4.4: Bounds on the coefficients $(\boldsymbol{NN}^\dagger)_{\alpha\beta}$ resulting from $\ell_\alpha \to \ell_\beta\gamma$ decays in the type I seesaw.

4.1 Type I seesaw model

4.1.1 Charged-lepton flavour violating processes

We begin our phenomenological study with the analysis of $\ell_\alpha \to \ell_\beta\gamma$, $\ell \to 3\ell$ and $\mu - e$ conversion in nuclei in the type I seesaw. All these processes are induced at one-loop level. The contribution to μ -e conversion in nuclei and $\ell \to 3\ell$ decays can be divided in penguin diagrams, mediated by either a photon or a Z boson, and box diagrams mediated by two W bosons. The corresponding form factors are calculated in Appendix C, resulting in the effective Lagrangians for Z-penguin and box diagrams:

$$\mathcal{L}^{(Z)}_{\text{eff.}} = \frac{G_F^{\text{SM}} g^2 e}{4\sqrt{2}\pi^2} F_Z^{\alpha\beta} \left[\overline{\psi}\gamma_\mu \left(I_\psi^3 P_L - Q_\psi s_W^2\right)\psi\right] \left[\overline{\ell_\beta}\gamma^\mu P_L \ell_\alpha\right] + \text{h.c.}\,, \tag{4.2}$$

$$\mathcal{L}^{(\text{Box})}_{\text{eff.}} = \frac{G_F^{\text{SM}} g^2 e}{8\sqrt{2}\pi^2 M_W^2} F_{\text{Box}}^{\alpha\beta\psi\psi} \left[\overline{\psi}\gamma_\mu P_L \psi\right] \left[\overline{\ell_\beta}\gamma^\mu P_L \ell_\alpha\right] + \text{h.c.}\,, \tag{4.3}$$

where Q_ψ is electric charge of ψ, which is a quark (for $\mu - e$ conversion) or a lepton (for $\ell \to 3\ell$ decays). On the other hand, the effective Lagrangian for the photon-penguin diagram is

$$\mathcal{L}^{(\gamma)}_{\text{eff.}} = \frac{G_F^{\text{SM}} e}{4\sqrt{2}\pi^2} \left[(eQ_\psi)\, F_\gamma^{\alpha\beta} \left(\overline{\psi}\gamma_\mu\psi\right) \left(\overline{\ell_\beta}\gamma^\mu P_L \ell_\alpha\right) + \frac{G_\gamma^{\alpha\beta}}{2} \left[\overline{\ell_\beta}\sigma_{\mu\rho}(m_\alpha P_R + m_\beta P_L)\ell_\alpha\right] F^{\mu\rho} \right] + \text{h.c.}\,, \tag{4.4}$$

where $F^{\mu\rho}$ is the EM field tensor. Unlike for Z-penguin and box diagrams, the photon contribution contains a non-local term in $G_\gamma^{\mu e}$, which is the only one contributing for an on-shell photon and, therefore, to $\ell_\alpha \to \ell_\beta\gamma$ decays. In these expressions, the form factors $F_\gamma^{\alpha\beta}$, $G_\gamma^{\alpha\beta}$, $F_Z^{\alpha\beta}$ and $F_{\text{Box}}^{\alpha\beta\psi\psi}$ are given in Appendix C in terms of the full $(n' + n_g) \times (n' + n_g)$ neutrino mixing matrix U defined in Eq. (C.11).

Using the non-local contribution in the effective Lagrangian (4.4) and Eq. (3.49), we obtain a simple expression for the branching ratio of $\ell_\alpha \to \ell_\beta\gamma$ decays:

$$\frac{\text{BR}\left(\ell_\alpha \to \ell_\beta\gamma\right)}{\text{BR}(\ell_\alpha \to \nu_\alpha e \overline{\nu_e})} = \frac{3\alpha}{2\pi |U^\dagger_{\alpha\alpha} U_{\beta\beta}|^2} \left| \sum_{j=1}^{n_g+n'} U_{\alpha j} U^*_{\beta j} G_\gamma(\lambda_j) \right|^2 \xrightarrow{m_N \gg M_W} \frac{3\alpha}{8\pi} \frac{\left|(\boldsymbol{NN}^\dagger)_{\alpha\beta}\right|^2}{(\boldsymbol{NN}^\dagger)_{\alpha\alpha}(\boldsymbol{NN}^\dagger)_{\beta\beta}}\,, \tag{4.5}$$

in agreement with Refs. [172, 173]. The last approximation is valid in the large mass regime $m_N \gg M_W$ since the form factor $G_\gamma(\lambda_j)$ obeys $G_\gamma(\lambda_j \gg 1) \approx 1/2$ and $G_\gamma(\lambda_j \ll 1) \approx \lambda_j/4$, with $\lambda_j \equiv m_j^2/M_W^2$ and m_j the neutrino masses. Eq. (4.5) allows to constrain the off-diagonal elements $\left(\boldsymbol{NN}^\dagger\right)_{\alpha\beta}$[1]. In fact, using the present experimental bounds on $\ell_\alpha \to \ell_\beta\gamma$ (Table 4.1), we obtain the upper bounds on $\boldsymbol{NN}^\dagger$ listed in Table 4.4. We see that the most stringent upper bound of $|(\boldsymbol{NN}^\dagger)_{e\mu}| < 2.6 \times 10^{-5}$ comes from $\mu \to e\gamma$, while the remaining off-diagonal elements are constrained to be less than a few percent.

[1]We have neglected the elements $(\boldsymbol{NN}^\dagger)_{\beta\beta}$ in expression (4.5) since corrections are suppressed at $\sim \mathcal{O}(m_N^{-2})$.

${}^{A}_{Z}$Nucleus	$Z_{\text{eff.}}$	$F(-m_\mu^2)$	$D\, m_\mu^{-5/2}$	$V^{(p)}\, m_\mu^{-5/2}$	$V^{(n)}\, m_\mu^{-5/2}$	Γ_{cap} ($\times 10^{-18}$ GeV)
${}^{27}_{13}$Al	11.5	0.64	0.0362	0.0161	0.0173	0.464
${}^{48}_{22}$Ti	17.6	0.54	0.0864	0.0396	0.0468	1.70
${}^{196}_{79}$Au	33.5	0.16	0.189	0.0974	0.146	8.60
${}^{207}_{82}$Pb	34.0	0.15	0.161	0.0834	0.128	8.85

Table 4.5: Nuclear parameters related to $\mu - e$ conversion in nuclei (values taken from Ref. [174]).

As for $\mu - e$ conversion in nuclei, we study it in the effective way described in Ref. [174], using the couplings (4.2)-(4.4). The nuclear information is encoded in the form factors D, $V^{(p)}$ and $V^{(n)}$, as well as in the muon capture rate $\Gamma_{\text{capt.}}$, with values reported in Table 4.5 for the analysed nuclei, namely ^{27}Al, ^{48}Ti, ^{196}Au and ^{207}Pb. The expression for the conversion rate reads

$$\frac{\text{CR}\,(\mu\mathcal{N}\to e\mathcal{N})}{\text{BR}(\mu\to\nu_\mu e\overline{\nu_e})} = \frac{3g^4}{2\pi}\cdot\frac{\Gamma_\mu}{\Gamma_{\text{capt.}}}\left|4V^{(p)}\left(2F_u^{\mu e}+F_d^{\mu e}\right)+4V^{(n)}\left(F_u^{\mu e}+2F_d^{\mu e}\right)+s_W^2 G_\gamma^{\mu e}\frac{D}{2e}\right|^2\frac{1}{|U^\dagger_{\alpha\alpha}U_{\beta\beta}|^2}\,, \tag{4.6}$$

in conformity with Ref. [172]. In this expression, $\Gamma_\mu \approx 2.996\times 10^{-19}$ GeV is the muon decay width [66] and the form factors $F_q^{\mu e}$ $(q=u,d)$ are given in terms of the functions $F_\gamma^{\alpha\beta}$, $F_Z^{\alpha\beta}$ and $F_{\text{Box}}^{\alpha\beta\psi\psi}$ by

$$F_q^{\mu e} = Q_q s_W^2 F_\gamma^{\mu e} + F_Z^{\mu e}\left(\frac{I_q^3}{2}-Q_q s_W^2\right)+\frac{1}{4}F_{\text{Box}}^{\mu e q q}\,, \qquad \text{with} \qquad I_u^3 = -I_d^3 = \frac{1}{2}\,. \tag{4.7}$$

Finally, we will also be interested in $\ell_\alpha^- \to \ell_\beta^+\ell_\beta^-\ell_\beta^-$ decays. Following Ref. [175], we get:

$$\begin{aligned}\frac{\text{BR}(\ell_\alpha\to 3\ell_\beta)}{\text{BR}(\ell_\alpha\to\nu_\alpha e\overline{\nu_e})} = \frac{g^2}{1024\pi^4}\times\Bigg\{&32 s_W^4\left|G_\gamma^{\alpha\beta}\right|^2\left(\ln\frac{m_\alpha^2}{m_\beta^2}-\frac{11}{4}\right)-48 s_W^4\,\text{Re}\left[\left(F_Z^{\alpha\beta}-F_\gamma^{\alpha\beta}\right)G_\gamma^{\alpha\beta *}\right]\\ &+4s_W^4\left|F_Z^{\alpha\beta}-F_\gamma^{\alpha\beta}\right|^2+16 s_W^2\,\text{Re}\left[\left(F_Z^{\alpha\beta}+\frac{1}{2}F_{\text{Box}}^{\alpha\beta\beta\beta}\right)G_\gamma^{\alpha\beta *}\right]\\ &+2\left|\frac{1}{2}F_{\text{Box}}^{\alpha\beta\beta\beta}+F_Z^{\alpha\beta}-2s_W^2\left(F_Z^{\alpha\beta}-F_\gamma^{\alpha\beta}\right)\right|^2\Bigg\}\frac{1}{|U^\dagger_{\alpha\alpha}U_{\beta\beta}|^2}\,.\end{aligned} \tag{4.8}$$

Thus, $\mu - e$ conversion in nuclei and $\mu \to e\gamma$ are sensitive to different combinations of form factors. Moreover, the rates for $\mu - e$ conversion in nuclei and $\ell \to 3\ell$ decays exhibit a non-vanishing logarithmic dependence on heavy neutrino masses [172]. Therefore, a simple expression as Eq. (4.5) is not possible to obtain. However, models that lead naturally to observable CLFV rates imply a quasi-degenerate mass spectrum $m_{N_1} \approx m_{N_2} \approx \ldots \equiv m_N$ [see Eq. (3.145)]. As a result, in such scenario, the dependence on the mixing matrix factorises out, leaving only a dependence on the mass scale m_N ($\lambda_N = m_N^2/M_W^2$):

$$\frac{\text{BR}\,(\ell_\alpha\to\ell_\beta\gamma)}{\text{BR}(\ell_\alpha\to\nu_\alpha e\overline{\nu_e})} = \frac{3\alpha}{2\pi}\left|G_\gamma(\lambda_N)\right|^2\times\frac{\left|\sum_{N_j}U_{\alpha j}U_{\beta j}^*\right|^2}{|U^\dagger_{\alpha\alpha}U_{\beta\beta}|^2}\,, \tag{4.9}$$

$$\frac{\text{CR}\,(\mu\mathcal{N}\to e\mathcal{N})}{\text{BR}(\mu\to\nu_\mu e\overline{\nu_e})} = \frac{3g^4}{2\pi}\cdot\left(\frac{\Gamma_\mu}{\Gamma_{\text{capt.}}}\right)\left|C_{\mu e}(\lambda_N)\right|^2\times\frac{\left|\sum_{N_j}U_{\alpha j}U_{\beta j}^*\right|^2}{|U^\dagger_{\alpha\alpha}U_{\beta\beta}|^2}\,, \tag{4.10}$$

$$\frac{\text{BR}(\ell_\alpha\to 3\ell_\beta)}{\text{BR}(\ell_\alpha\to\nu_\alpha e\overline{\nu_e})} = \frac{g^4}{1024\pi^4}\left|C_{\alpha 3\beta}(\lambda_N)\right|^2\times\frac{\left|\sum_{N_j}U_{\alpha j}U_{\beta j}^*\right|^2}{|U^\dagger_{\alpha\alpha}U_{\beta\beta}|^2}\,. \tag{4.11}$$

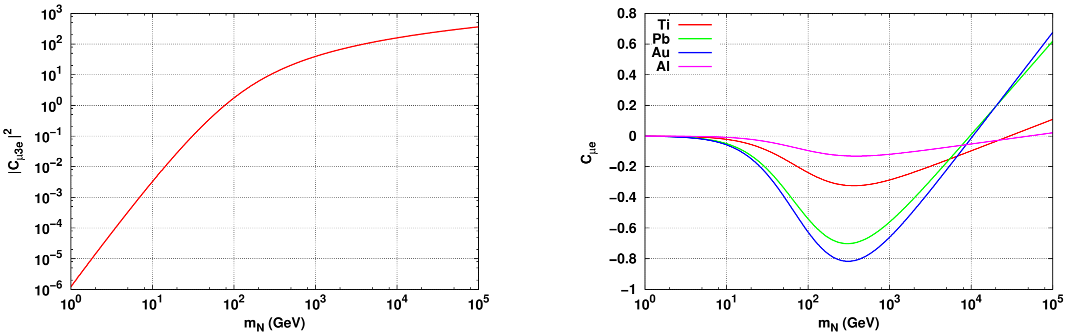

Figure 4.1: Loop factors $|C_{\mu 3e}|^2$ and $C_{\mu e}$ as functions of the seesaw scale m_N in the type I seesaw. Note that we only stop at 1 GeV for plot-aesthetic reasons.

The loop factors $C_{\mu e}$ and $C_{\mu 3e}$ in Eqs. (4.10) and (4.11) are functions of the mass scale m_N, given by

$$C_{\mu e} = \left| 4V^{(p)}\left(2F_u + F_d\right) + 4V^{(n)}\left(F_u + 2F_d\right) + s_W^2 G_\gamma \frac{D}{2e} \right|^2 , \tag{4.12}$$

$$\begin{aligned} |C_{\alpha 3\beta}|^2 = {} & 32 s_W^4 |G_\gamma|^2 \left(\ln \frac{m_\alpha^2}{m_\beta^2} - \frac{11}{4} \right) - 48 s_W^4 \left(\widetilde{F}_Z - F_\gamma \right) G_\gamma{}^* + 4 s_W^4 \left| \widetilde{F}_Z - F_\gamma \right|^2 \\ & + 16 s_W^2 \left(\widetilde{F}_Z - \widetilde{F}_{\mathrm{d\,Box}} \right) G_\gamma^* + 2 \left| - \widetilde{F}_{\mathrm{d\,Box}} + \widetilde{F}_Z - 2 s_W^2 (\widetilde{F}_Z - F_\gamma) \right|^2 . \end{aligned} \tag{4.13}$$

where G_γ, F_γ, G_Z, $\widetilde{F}_Z$ and $\widetilde{F}_{\mathrm{q\,Box}}$ $(q = u, d)$ are functions only of $\lambda_N \equiv m_N^2/M_W^2$ given in Appendix C, while the form factor F_q inherits the structure of definition (4.7) for $F_q^{\mu e}$:

$$F_q = Q_q s_W^2 F_\gamma + \widetilde{F}_Z \left(\frac{I_q^3}{2} - Q_q s_W^2 \right) + \frac{1}{4} \widetilde{F}_{q\mathrm{Box}} . \tag{4.14}$$

As LFV μ processes are presently the most constrained ones, we limit our analysis of CLFV processes to $\mu - e$ conversion in nuclei, $\mu \to e\gamma$ and $\mu \to 3e$. The dependence of the loop factor $|C_{\mu 3e}|^2$ on the seesaw mass scale m_N is represented in Fig. 4.1. At $m_N = 100\,(1000)$ GeV, we have: $|C_{\mu e}|^2 \approx 1.75\,(38.73)$ and, therefore, the $\mu \to 3e$ branching ratio increases by a factor of ~ 22 when m_N goes from 100 GeV to 1000 GeV. Using the experimental upper bounds on BR($\mu \to 3e$), we obtain the following constraint:

$$|\left(\boldsymbol{N}\boldsymbol{N}^\dagger\right)_{\mu e}| \lesssim 5.8 \times 10^{-4}\,(1.2 \times 10^{-4}) \qquad \text{for} \qquad m_N = 100\,(1000)\ \text{GeV} , \tag{4.15}$$

which is around one order of magnitude less stringent than that obtained from BR($\mu \to e\gamma$) (in Table 4.4). On the other hand, the loop factor $C_{\mu e}$ for the nuclei of interest is represented in Fig. 4.1 as a function of m_N. The first feature to notice is that $|C_{\mu e}|$ has maxima at $m_N \approx 360,\ 350, 310\,,\ 310$ GeV for ^{27}Al, ^{48}Ti, ^{196}Au and ^{207}Pb, respectively. In other words, the conversion rates suffer the strongest enhancement at approximately the same mass $m_N \leq 1000$ GeV. Besides the maxima, $|C_{\mu e}|$ vanishes for mass values in the $10 - 50$ TeV range, respectively 51, 30, 11 and 9.7 TeV for ^{27}Al, ^{48}Ti, ^{196}Au and ^{207}Pb. This feature was already noticed in Ref. [172] and is due to opposite up- and down-quark contributions in Eq. (4.6).

As a result of the factorisation of the dependence on the mixing matrix in Eqs. (4.9)-(4.11), the ratio of two same-flavour-transition rates offer several possibilities to test the seesaw model.

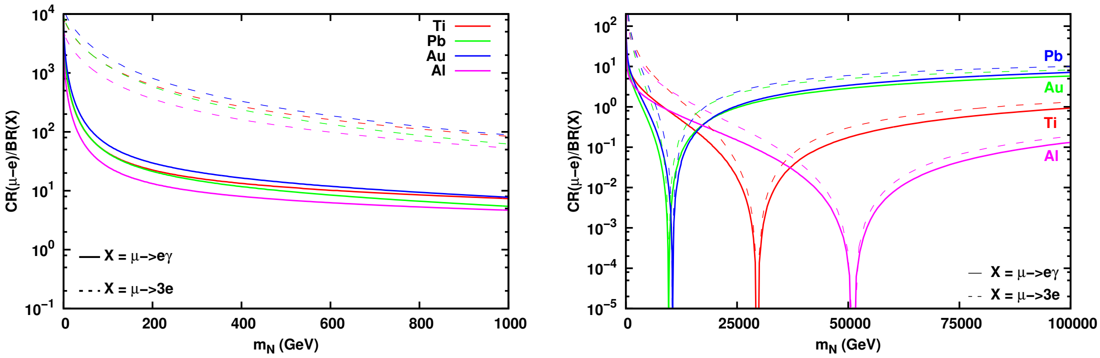

Figure 4.2: Ratios of the $\mu - e$ conversion rate for several nuclei and BR($\mu \to e\gamma$) (solid lines) or BR($\mu \to 3e$) (dashed lines), as functions of the seesaw scale m_N in the type I seesaw.

In Fig. 4.2, we show the ratios of conversion rates in nuclei to the $\mu\to e\gamma$ and $\mu \to 3e$ decay branching ratios. For $m_N \leq 1000$ GeV, the observation of monotonous functions means that the measurement of this ratio would allow for a determination of m_N. In fact the observation of a single rate that, together with the experimental upper bound on another one, leads to a ratio incompatible with the expectations of Fig. 4.2, can be sufficient to exclude the model. Additionally, in the large mass regime $m_N \gg M_W$, we see that, as expected, both ratios vanish at a value of m_N dependent on the nucleus. This shows how important the search for $\mu \to e$ conversion in several nuclei could be in testing the model.

Finally, present bounds and future sensitivities to Yukawa couplings resulting from CLFV processes are shown in Fig. 4.3. The results clearly suggest that μ–e conversion experiments will become dominant in the study of flavour physics, allowing to probe Yukawa couplings as small as 10^{-2}, 10^{-3} or even 10^{-4} for $m_N = 10$ TeV, 1 TeV and 100 GeV, respectively. By requiring $\mathbf{Y}_N \sim \mathcal{O}(1)$, we can rephrase the bounds of Fig. 4.3 as upper bounds on m_N. The most stringent bound comes from $\mu - e$ conversion in ^{48}Ti:

$$m_N \lesssim 2000\ \text{TeV} \cdot \left(\frac{10^{-18}}{\text{CR}^{\text{Ti}}_{\mu\to e}}\right)^{\frac{1}{4}} |\sum_{N_j} (\mathbf{Y}_N)_{je}\, (\mathbf{Y}_N)^\dagger_{j\mu}|^{1/2}\,, \tag{4.16}$$

showing that future experiments may probe the type I seesaw scenario beyond the ~ 1000 TeV scale.

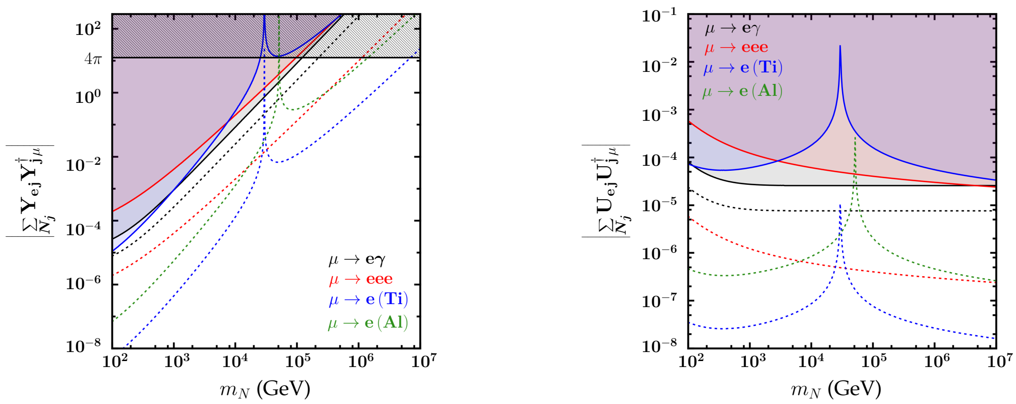

Figure 4.3: Bounds on $\left|\sum_{N_j} \mathbf{Y}_{e\,j}\mathbf{Y}^\dagger_{j\,\mu}\right|$ and $\left|\sum_{N_j} U_{e\,j}U^\dagger_{j\,\mu}\right|$ for a type I seesaw scenario with a single heavy mass scale m_N. The present experimental upper bounds are represented by solid lines and excluded regions by shaded areas, while dashed lines correspond to expected experimental sensitivities. Our analysis is valid below $\left|\sum_{N_j} \mathbf{Y}_{e\,j}\mathbf{Y}^\dagger_{j\,\mu}\right| = 4\pi$, i.e. in the non-perturbative regime $\mathbf{Y}_N \geq \sqrt{4\pi}$.

4.1.2 Unitarity of the lepton mixing matrix

In the previous section, we discussed the possibility of having observable CLFV processes unsuppressed by neutrino masses, i.e. large effects from $d = 6$ operators with small neutrino masses. Directly related to the $d = 6$ operators is the possibility of having a non-unitary lepton mixing matrix $\boldsymbol{N}$, leading to non-standard effects in neutrino propagation [176]. As such, in this section we aim at obtaining bounds on non-unitarity which are independent of the heavy masses and applicable to any type I seesaw theory. For that, we will work in the large mass regime $m_N \gg M_W$ ($m_N \sim \mathcal{O}(\mathrm{TeV})$ for example) in which the bounds in Table 4.4 resulting from $\ell_\alpha \to \ell_\beta \gamma$ decays can be used. These bounds constrain the off-diagonal elements of $\boldsymbol{N}\boldsymbol{N}^\dagger$. On the other hand, in order to set bounds on the diagonal elements $\left(\boldsymbol{N}\boldsymbol{N}^\dagger\right)_{\alpha\alpha}$ an additional analysis of (tree-level) W and Z decays as well as of constraints on the universality of weak interactions will be pursued.

$\boldsymbol{W}$ decays

With a non-unitary mixing matrix $\boldsymbol{N}$ in the leptonic CC defined in Eq. (3.114), we obtain for the $W \to \ell_\alpha \nu_\alpha$ decay width the following expression:

$$\Gamma(W \to \ell_\alpha \nu_\alpha) = \frac{G_F^{\mathrm{SM}} M_W^3}{6\sqrt{2}\pi} (\boldsymbol{N}\boldsymbol{N}^\dagger)_{\alpha\alpha} \Longrightarrow \frac{(\boldsymbol{N}\boldsymbol{N}^\dagger)_{\alpha\alpha}}{\sqrt{(\boldsymbol{N}\boldsymbol{N}^\dagger)_{ee}(\boldsymbol{N}\boldsymbol{N}^\dagger)_{\mu\mu}}} = f_\alpha \,. \tag{4.17}$$

Using the experimental values of the W decay widths and mass from Ref. [66] and the value of the Fermi constant as extracted from muon decay [see Eq. (3.64)], $G_F = (1.16637 \pm 0.00001) \times 10^{-5}$ [66], the parameters f_α in the above expression are:

$$f_\alpha \equiv \frac{\Gamma(W \to \ell_\alpha \nu_\alpha)\, 6\sqrt{2}\pi}{G_F M_W^3} = \begin{cases} 0.983 \pm 0.023\,, & \text{for } \alpha = e \\ 0.975 \pm 0.024\,, & \text{for } \alpha = \mu \\ 1.044 \pm 0.023\,, & \text{for } \alpha = \tau\,. \end{cases} \tag{4.18}$$

Inserting these values in Eq. (4.17), allows to obtain the constraints shown in Table 4.6, from where we immediately see that, as expected, the elements $\left(\boldsymbol{N}\boldsymbol{N}^\dagger\right)_{\alpha\alpha}$ are equal up to a few percent.

Invisible $\boldsymbol{Z}$ decay

Additional constraints come from the analysis of invisible Z decay. In fact, for a non-unitary leptonic mixing matrix $\boldsymbol{N}$, the neutral weak couplings in Eqs. (3.47) or (3.62) result in the decay width:

$$\Gamma(Z \to \text{invisible}) = \sum_{i,j} \Gamma(Z \to \bar{\nu}_i \nu_j) = \frac{G_F^{\mathrm{SM}} M_Z^3}{12\sqrt{2}\pi}\,(1+\rho_t) \sum_{i,j} |(\boldsymbol{N}^\dagger \boldsymbol{N})_{ij}|^2\,, \tag{4.19}$$

where $\rho_t \approx 0.008$ [66] accounts for (non-negligible) radiative corrections, mainly involving the top quark. As these corrections do not involve leptons, the dependence on the mixing matrix in Eq. (4.19) remains exact beyond tree level. Converting the summation in Eq. (4.19) to a summation over flavour eigenstates, through the relation $\sum_{i,j} |(\boldsymbol{N}^\dagger \boldsymbol{N})_{ij}|^2 = \sum_{\alpha\beta} |(\boldsymbol{N}^\dagger \boldsymbol{N})_{\alpha\beta}|^2$, and writing the decay width in

Process	Constraint On	Bound
$\frac{\Gamma(W\to\mu\bar{\nu}_\mu)}{\Gamma(W\to e\bar{\nu}_e)}$	$\frac{(\boldsymbol{N}\boldsymbol{N}^\dagger)_{\mu\mu}}{(\boldsymbol{N}\boldsymbol{N}^\dagger)_{ee}}$	0.9925 ± 0.0338
$\frac{\Gamma(W\to\tau\bar{\nu}_\tau)}{\Gamma(W\to e\bar{\nu}_e)}$	$\frac{(\boldsymbol{N}\boldsymbol{N}^\dagger)_{\tau\tau}}{(\boldsymbol{N}\boldsymbol{N}^\dagger)_{ee}}$	1.0626 ± 0.0022
$\frac{\Gamma(\tau\to\nu_\tau\mu\bar{\nu}_\mu)}{\Gamma(\tau\to\nu_\tau e\bar{\nu}_e)}$	$\frac{(\boldsymbol{N}\boldsymbol{N}^\dagger)_{\mu\mu}}{(\boldsymbol{N}\boldsymbol{N}^\dagger)_{ee}}$	0.9764 ± 0.0040
$\frac{\Gamma(\tau\to\nu_\tau e\bar{\nu}_e)}{\Gamma(\mu\to\nu_\mu e\bar{\nu}_e)}$	$\frac{(\boldsymbol{N}\boldsymbol{N}^\dagger)_{\tau\tau}}{(\boldsymbol{N}\boldsymbol{N}^\dagger)_{\mu\mu}}$	1.0006 ± 0.0021
$\frac{\Gamma(\tau\to\nu_\tau\mu\bar{\nu}_\mu)}{\Gamma(\mu\to\nu_\mu e\bar{\nu}_e)}$	$\frac{(\boldsymbol{N}\boldsymbol{N}^\dagger)_{\tau\tau}}{(\boldsymbol{N}\boldsymbol{N}^\dagger)_{ee}}$	1.0004 ± 0.0021
$\frac{\Gamma(\pi\to\mu\bar{\nu}_\mu)}{\Gamma(\pi\to e\bar{\nu}_e)}$	$\frac{(\boldsymbol{N}\boldsymbol{N}^\dagger)_{\mu\mu}}{(\boldsymbol{N}\boldsymbol{N}^\dagger)_{ee}}$	1.0021 ± 0.0016
$\frac{\Gamma(\tau\to\pi\bar{\nu}_\tau)}{\Gamma(\pi\to\mu\bar{\nu}_\mu)}$	$\frac{(\boldsymbol{N}\boldsymbol{N}^\dagger)_{\tau\tau}}{(\boldsymbol{N}\boldsymbol{N}^\dagger)_{\mu\mu}}$	0.9956 ± 0.0031
$\frac{\Gamma(\tau\to K\bar{\nu}_\tau)}{\Gamma(K\to\mu\bar{\nu}_\mu)}$	$\frac{(\boldsymbol{N}\boldsymbol{N}^\dagger)_{\mu\mu}}{(\boldsymbol{N}\boldsymbol{N}^\dagger)_{ee}}$	0.9852 ± 0.0072
$\frac{\Gamma(\tau\to\pi\bar{\nu}_\tau)}{\Gamma(K\to e\bar{\nu}_e)}$	$\frac{(\boldsymbol{N}\boldsymbol{N}^\dagger)_{\tau\tau}}{(\boldsymbol{N}\boldsymbol{N}^\dagger)_{\mu\mu}}$	1.0180 ± 0.0420

Table 4.6: Constraints on $(\boldsymbol{N}\boldsymbol{N}^\dagger)_{\alpha\alpha}$ from a selection of processes.

terms of the Fermi constant as measured in muon decay [see Eq. (3.64)], we obtain the constraint [66]

$$\frac{\sum_{\alpha,\beta}|(\boldsymbol{N}\boldsymbol{N}^\dagger)_{\alpha\beta}|^2}{\sqrt{(\boldsymbol{N}\boldsymbol{N}^\dagger)_{ee}(\boldsymbol{N}\boldsymbol{N}^\dagger)_{\mu\mu}}} = \frac{12\sqrt{2}\pi\,\Gamma(Z\to\text{invisible})}{G_F M_Z^3(1+\rho_t)} = 2.984 \pm 0.009\,. \tag{4.20}$$

Notice that this quantity corresponds to the number of active neutrinos at LEP. Its departure from 3 could signal the presence of new physics but the 2σ deviation is not (yet) statistically significant.

Universality tests

Finally, constraints on the universality of weak interactions, as ratios of lepton, W and π decays, can also be translated into bounds on $\left(\boldsymbol{N}\boldsymbol{N}^\dagger\right)_{\alpha\alpha}$. The results of our analysis are displayed in Table 4.6. When analysing leptonic decays $\ell_\alpha \to \nu_\alpha\ell_\beta$, we used the following expression for the decay width:

$$\Gamma(\ell_\alpha \to \nu_\alpha\ell_\beta\bar{\nu}_\beta) = \frac{{G_F^{\text{SM}}}^2 m_\alpha^5}{192\pi^3}(\boldsymbol{N}\boldsymbol{N}^\dagger)_{\alpha\alpha}(\boldsymbol{N}\boldsymbol{N}^\dagger)_{\beta\beta}\,. \tag{4.21}$$

Note that in Table 4.6 we have also considered low-energy leptonic decays involving pions (π) and kaons (K), whose bounds were taken from Ref. [176].

Combination of all constraints

Finally, from all constraints resulting from electroweak decays, in Tables 4.6 and 4.4 as well as in Eq. (4.66), a global fit leads to the following elements of $\boldsymbol{N}\boldsymbol{N}^\dagger$ at 90% CL:

$$|\boldsymbol{N}\boldsymbol{N}^\dagger| \approx \begin{pmatrix} 0.996\pm0.003 & <2.6\cdot10^{-5} & <1.5\cdot10^{-2} \\ <2.6\cdot10^{-5} & 0.994\pm0.003 & <1.7\cdot10^{-2} \\ <1.5\cdot10^{-2} & <1.7\cdot10^{-2} & 1.001\pm0.004 \end{pmatrix}. \tag{4.22}$$

The constraints on the off-diagonal elements $\left(\boldsymbol{N}\boldsymbol{N}^\dagger\right)_{\alpha\beta}$ result mainly from experimental bounds existing on $\ell_\alpha \to \ell_\beta\gamma$ while the diagonal ones come from the combined analysis of all other processes mentioned above, although a small interference between both constraints appears through Eq. (4.21). However, in view of the present upper bounds in Table 4.4 for the off-diagonal elements, their (quadratic) contributions are negligible small and, as such, were neglected in the analysis. From these results, we conclude that there is a 2σ departure from unity of the diagonal elements in Eq. (4.67), which can be interpreted as resulting from a similar discrepancy in the invisible width of the Z boson, Eq. (4.20). As we remarked there, this 2σ deviation is not significant enough to be interpreted as a signal of physics beyond the SM.

Let us finally remark that, as discussed in the beginning of this section, the bounds above are valid for any values of the heavy-field masses, provided they satisfy $m_{N_j} \gg M_W$. Notice also that these bounds apply to any type I seesaw theory. In particular, they apply to the inverse seesaw model (Section 3.4.2), characterised by a quasi-degenerate heavy mass spectrum with a scale m_N possibly near the TeV scale, while maintaining large Yukawa couplings and signals possibly at the edge of experimental limits.

4.2 Type II seesaw model

4.2.1 Charged lepton flavour violating processes

As we saw above, in the type I seesaw all CLFV processes can only be induced at loop level. The type II-model introduces a novelty, with tree-level $\ell \to 3\ell$ decays. As a result, we expect $\ell \to 3\ell$ rates to be the largest ones. Another important difference with respect to the type I seesaw case is that from the ratio of two same flavour transition rates we do not always get a function of the mass scale m_Δ.

In the mass-eigenstate basis, the effective charged lepton flavour changing $\overline{\ell_\beta}\ell_\alpha\gamma$ vertex arises at one-loop order from the exchange of singly- and doubly-charged scalar fields $\Delta^\pm$ and $\Delta^{\pm\pm}$, respectively. The form factors are calculated in detail in Appendix D and the resulting effective Lagrangian, corresponding to Eqs. (D.22) and (D.23), can be written as [177–179]:

$$\mathcal{L}_{\text{eff.}}^{(\gamma)} = -4\frac{G_F^{\text{SM}}}{\sqrt{2}}\left(m_\alpha A_R \overline{\ell_\beta}\sigma^{\rho\sigma}P_R\ell_\alpha F_{\rho\sigma} + \text{h.c.}\right) - \frac{G_F^{\text{SM}}}{\sqrt{2}}\left[A_L(q^2)\overline{\ell_\beta}\gamma^\rho P_L \ell_\alpha \sum_{\psi=u,d} Q_\psi\overline{\psi}\gamma_\rho\psi + \text{h.c.}\right] , \quad (4.23)$$

with

$$A_R = -\frac{e}{4\sqrt{2}G_F^{\text{SM}}}\frac{\left(\mathbf{Y}_\Delta\mathbf{Y}_\Delta^\dagger\right)_{\alpha\beta}}{6\pi^2}\left(\frac{1}{8M_{\Delta^+}} + \frac{1}{M_{\Delta^{++}}}\right) , \quad (4.24)$$

$$A_L(q^2) = -\frac{\sqrt{2}e^2}{G_F^{\text{SM}}}\frac{\mathbf{Y}^*_{\Delta\beta j}\mathbf{Y}_{\Delta\alpha j}}{6\pi^2}\left[\frac{1}{12M_{\Delta^+}^2} + \frac{1}{M_{\Delta^{++}}^2} f\left(\frac{-q^2}{M_{\Delta^{++}}}, \frac{m_{\ell_\sigma}^2}{M_{\Delta^{++}}}\right)\right] , \quad (4.25)$$

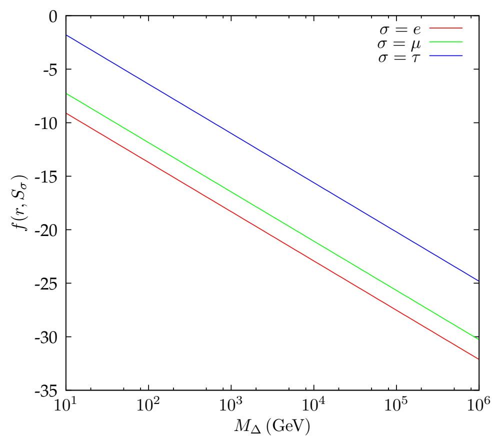

Figure 4.4: Plot of $f(r, S_\sigma)$ in Eq. (4.26), as a function of the type II seesaw mass scale M_Δ.

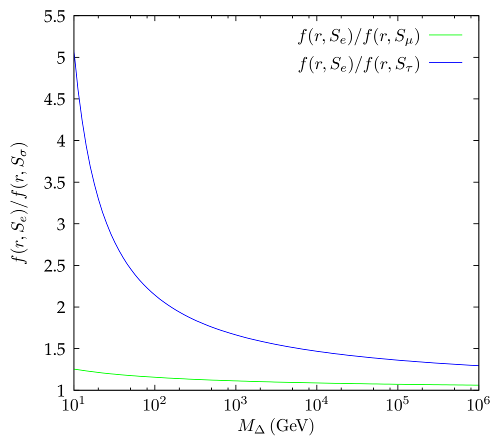

Figure 4.5: Ratios $f(r, S_e)/f(r, S_\sigma)$ as a function of the type II seesaw mass scale M_Δ.

and where q is the momentum carried by the photon. The loop function $f(r,S_\sigma)$ is given by:

$$f(r,S_\sigma)=\frac{4S_\sigma}{r}+\ln S_\sigma+\left(1-\frac{2S_\sigma}{r}\right)\sqrt{1+\frac{4S_\sigma}{r}}\,\ln\left|\frac{\sqrt{r+4S_\sigma}+\sqrt{r}}{\sqrt{r+4S_\sigma}-\sqrt{r}}\right|\,,\qquad r\equiv\frac{-q^2}{M_{\Delta^{++}}}\,,\quad S_\sigma\equiv\frac{m^2_{\ell_\sigma}}{M_{\Delta^{++}}}\,. \tag{4.26}$$

Notice that $f(r, S_\sigma)$ is a monotonically decreasing function of $M_{\Delta^{++}}$ (see Fig. 4.4) and that, for $\sigma = e$, $f(r, S_e) \approx \ln r$ to a very good approximation. Moreover, the ratios $f(r, S_e)/f(r, S_\sigma)$ do not change significantly when $M_{\Delta^{++}}$ increases from 100 GeV to 1000 GeV (Fig. 4.5). At $M_{\Delta^{++}} = 100\,(1000)$ GeV, $f(r, S_e)/f(r, S_\mu) \approx 1.2\,(1.1)$ and $f(r, S_e)/f(r, S_\sigma) \approx 2.1\,(1.7)$.

$\ell_\alpha \to \ell_\beta\gamma$ decays

The first term in the Lagrangian (4.23), with form factor A_R, generates the on-shell $\ell_\alpha \to \ell_\beta\gamma$ decay amplitude; it comes from the contribution of one-loop diagrams with virtual neutrino and Δ^+ and with virtual charged lepton and Δ^{++}. A trivial calculation based on Eq. (4.23) leads to the result:

$$\begin{aligned}\mathrm{BR}(\ell_\alpha\to\ell_\beta\gamma)&=384\pi^2(4\pi\alpha)\,|A_R|^2\,\mathrm{BR}(\ell_\alpha\to e\nu_\alpha\overline{\nu_e})\\&=\frac{\alpha}{48\pi}\frac{\left|\left(\mathbf{Y}_\Delta\mathbf{Y}_\Delta^\dagger\right)_{\alpha\beta}\right|^2}{(G_F^{\rm SM})^2}\left(\frac{1}{M^2_{\Delta^+}}+\frac{8}{M^2_{\Delta^{++}}}\right)^2\mathrm{BR}(\ell_\alpha\to e\nu_\alpha\overline{\nu_e})\\&\approx\frac{27\alpha}{16\pi}\frac{\left|\left(\mathbf{Y}_\Delta\mathbf{Y}_\Delta^\dagger\right)_{\alpha\beta}\right|^2}{(G_F^{\rm SM})^2M_\Delta^4}\mathrm{BR}(\ell_\alpha\to e\nu_\alpha\overline{\nu_e})\,,\end{aligned} \tag{4.27}$$

in agreement with Refs. [177, 178]. Note that in the last step above we have used $M_{\Delta^+} \approx M_{\Delta^{++}} \equiv M_\Delta$ [2]. The upper limits on $\mathrm{BR}(\ell_\alpha \to \ell_\beta\gamma)$ reported in Table 4.1 then imply the upper bounds on $|(\mathbf{Y}_\Delta\mathbf{Y}_\Delta^\dagger)_{\alpha\beta}|$ given in Table 4.7. From this last table, we see that the most stringent bound comes from $\mu \to e\gamma$ and that for an $\mathcal{O}(\mathrm{TeV})$ seesaw scale M_Δ, the Yukawa couplings are allowed to be of $\mathcal{O}(10^{-1})$, while they

[2] We have also neglected the phase space factor $\approx 1 - 8m_\beta^2/m_\alpha^2$ in the decay width $\Gamma(\ell_\alpha \to \ell_\beta\nu_\alpha\overline{\nu_\beta})$. However, even for $\tau \to \mu\gamma$ decays, it corresponds only to a correction smaller than 3%.

Process	Constraint On	Upper Bound $\left(\times\left(\frac{M_\Delta}{1\,\text{TeV}}\right)^2\right)$	Future Sens. $\left(\times\left(\frac{M_\Delta}{1\,\text{TeV}}\right)^2\right)$
$\mu\to e\gamma$	$\lvert(\mathbf{Y}_\Delta\mathbf{Y}_\Delta^\dagger)_{\mu e}\rvert$	1.4×10^{-4}	4.5×10^{-5}
$\tau\to e\gamma$	$\lvert(\mathbf{Y}_\Delta\mathbf{Y}_\Delta^\dagger)_{\tau e}\rvert$	8.0×10^{-2}	1.4×10^{-2}
$\tau\to \mu\gamma$	$\lvert(\mathbf{Y}_\Delta\mathbf{Y}_\Delta^\dagger)_{\tau \mu}\rvert$	9.4×10^{-2}	1.4×10^{-2}

Table 4.7: Bounds on combinations of Yukawa couplings resulting from $\ell_\alpha\to\ell_\beta\gamma$ in the type II seesaw.

should be sizeably smaller by up to 3 orders of magnitude for specific flavours.

The upper bounds in Table 4.7 can be used to extract lower bounds on the vacuum expectation value v_Δ of the triplet [180]. In fact, from Eq. (3.81), we obtain

$$\left|\left(\mathbf{Y}_\Delta\mathbf{Y}_\Delta^\dagger\right)_{\alpha\beta}\right| = \frac{1}{4v_\Delta^2}\left|(U_L^\nu)_{\beta 2}\,(U_L^\nu)^\dagger_{2\alpha}\,\Delta m_{21}^2 + (U_L^\nu)_{\beta 3}\,(U_L^\nu)^\dagger_{3\alpha}\,\Delta m_{31}^2\right|\,, \tag{4.28}$$

where we have used the unitarity of U_L^ν. It follows from Eq. (4.28) that the prediction for $|(\mathbf{Y}_\Delta\mathbf{Y}_\Delta^\dagger)_{\alpha\beta}|$ and, thus, for $\text{BR}(\ell_\alpha\to\ell_\beta\gamma)$, depends on the Dirac phase δ of the mixing matrix U_L^ν [see Eq. (3.18)]. For the best-fit values of the oscillation parameters listed in Table 3.1, the term $\propto\Delta m_{21}^2$ in Eq. (4.28) is approximately one order of magnitude smaller than the term $\propto\Delta m_{31}^2$. It is easy to check that this implies a relatively weak dependence of $\text{BR}(\ell_\alpha\to\ell_\beta\gamma)$ on the Dirac phase and on the neutrino mass spectrum. Thus, neglecting the term $\propto\Delta m_{21}^2$, we obtain from Eq. (4.28) and Table 4.7:

$$v_\Delta > 42.2\,|s_{13}s_{23}c_{13}\Delta m_{31}^2|^{1/2}\cdot\left(\frac{1\,\text{TeV}}{M_\Delta}\right)\approx 0.71\text{ eV}\cdot\left(\frac{1\,\text{TeV}}{M_\Delta}\right)\,, \tag{4.29}$$

$$v_\Delta > 1.77\,|s_{13}c_{23}c_{13}\Delta m_{31}^2|^{1/2}\cdot\left(\frac{1\,\text{TeV}}{M_\Delta}\right)\approx 0.029\text{ eV}\cdot\left(\frac{1\,\text{TeV}}{M_\Delta}\right)\,, \tag{4.30}$$

$$v_\Delta > 1.63\,|s_{23}c_{23}c_{13}^2\Delta m_{31}^2|^{1/2}\cdot\left(\frac{1\,\text{TeV}}{M_\Delta}\right)\approx 0.056\text{ eV}\cdot\left(\frac{1\,\text{TeV}}{M_\Delta}\right)\,. \tag{4.31}$$

As expected, the contribution from $\mu\to e\gamma$ sets the highest lower bound on v_Δ [see Eq. (4.27)]. We therefore see that for $M_\Delta\sim\mathcal{O}(\text{TeV})$ seesaw mass we get $v_\Delta\gtrsim 1$ eV. We can therefore rewrite $\text{BR}(\ell_\alpha\to\ell_\beta\gamma)$ for the most stringent process $\mu\to e\gamma$ as

$$\text{BR}(\mu\to e\gamma)\approx 1.4\times10^{-13}\left(\frac{1\,\text{eV}}{v_\Delta}\right)^4\cdot\left(\frac{1\,\text{TeV}}{M_\Delta}\right)^4\,. \tag{4.32}$$

from which follows that, for the values of v_Δ and M_Δ of interest, $\text{BR}(\mu\to e\gamma)$ may reach values within the projected sensitivity of the MEG II experiment [169].

$\mu - e$ conversion in nuclei

Together with the on-shell contribution in the effective Lagrangian (4.23), the off-shell contribution - involving the form factor A_L - generates the $\mu - e$ conversion amplitude. In the type II seesaw scenario,

Process	Constraint On	Upper Bound $\left(\times\left(\frac{M_\Delta}{1\,\mathrm{TeV}}\right)^2\right)$	Future Sens. $\left(\times\left(\frac{M_\Delta}{1\,\mathrm{TeV}}\right)^2\right)$
$\mu\,\mathrm{Ti} \to e\,\mathrm{Ti}$	$\lvert C_{\mu e}^{(\mathrm{II})}\rvert$	3.1×10^{-3}	4.7×10^{-6}
$\mu\,\mathrm{Al} \to e\,\mathrm{Al}$	$\lvert C_{\mu e}^{(\mathrm{II})}\rvert$	-	2.0×10^{-5}

Table 4.8: Bounds on $|C_{\mu e}^{(\mathrm{II})}|$ [see Eq. (4.38)] resulting from $\mu - e$ conversion in the type II seesaw model.[3]

$\mu - e$ conversion in nuclei thus arises only from photon-exchange contributions. In the same way that was done in Section 4.3.1, we obtain the conversion rate following the effective theory approach developed in [174]. Therefore, from the effective Lagrangian (4.23), we get the following conversion rate in the type II seesaw scenario:

$$\mathrm{CR}\,(\mu\mathcal{N}\to e\mathcal{N}) \approx (4\pi\alpha)^2\,\frac{2\left(G_F^{\mathrm{SM}}\right)^2}{\Gamma_{\mathrm{capt.}}}\left|A_R^*\frac{D}{\sqrt{4\pi\alpha}} + (2Q_u+Q_d)\,A_L(q^2)V^{(p)}\right|^2 , \tag{4.33}$$

with an energy scale $q^2 \approx -m_\mu^2$ for this process. Using the light nuclei ($Z \le 30$) approximation

$$V^{(p)} = m_\mu^{5/2}\alpha^{3/2}Z_{\mathrm{eff.}}^2 Z^{1/2}F(q^2)/4\pi\ , \qquad\qquad D \approx 8eV^{(p)}\ , \tag{4.34}$$

we arrive at the relevant expression for the conversion rate:

$$\mathrm{CR}\,(\mu\mathcal{N}\to e\mathcal{N}) \approx \frac{\alpha^5}{9\pi^4}\frac{m_\mu^5}{\Gamma_{\mathrm{capt.}}}Z_{\mathrm{eff.}}^4 ZF^2(-m_\mu^2) \tag{4.35}$$

$$\times\left|\left(\mathbf{Y}_\Delta\mathbf{Y}_\Delta^\dagger\right)_{e\mu}\left(\frac{5}{24M_{\Delta^+}^2}+\frac{1}{M_{\Delta^{++}}^2}\right)+\frac{1}{M_{\Delta^{++}}^2}\sum_{\rho=e,\mu,\tau}\mathbf{Y}_{\Delta e\rho}^\dagger f(r,S_\rho)\mathbf{Y}_{\Delta\rho\mu}\right|^2 \tag{4.36}$$

$$\approx \frac{\alpha^5}{9\pi^4}\frac{m_\mu^5}{\Gamma_{\mathrm{capt.}}}Z_{\mathrm{eff.}}^4 ZF^2(-m_\mu^2)\left|C_{\mu e}^{(\mathrm{II})}\right|^2 , \tag{4.37}$$

where we have used the approximation $M_{\Delta^+} \approx M_{\Delta^{++}} = M_\Delta$. The quantity $C_{\mu e}^{(\mathrm{II})}$ is defined by

$$C_{\mu e}^{(\mathrm{II})} \equiv \frac{1}{M_\Delta^2}\left[\frac{29}{24}\left(\mathbf{Y}_\Delta\mathbf{Y}_\Delta^\dagger\right)_{e\mu}+\sum_{\rho=e,\mu,\tau}\mathbf{Y}_{\Delta e\rho}^\dagger f(r,S_\rho)\mathbf{Y}_{\Delta\rho\mu}\right] . \tag{4.38}$$

Using the upper bounds on the $\mu - e$ conversion rates of Table 4.1, as well as the values for the effective atomic number $Z_{\mathrm{eff.}}$, the nuclear form factors $F^2(-m_\mu^2)$ and the muon capture rate $\Gamma_{\mathrm{capt.}}$ given in Table 4.5, we are then able to get the upper limits for $|C_{\mu e}^{(\mathrm{II})}|$ collected in Table 4.8. From this table, we see that $\mu - e$ conversion in ^{48}Ti sets an upper bound $|C_{\mu e}^{(\mathrm{II})}| < 3.1\times10^{-3}\,(M_\Delta/1\,\mathrm{TeV})^2$. On the other hand, using the (less optimistic) future sensitivities to $\mu - e$ conversion rates in Table 4.1, we are also able to set lower bounds on the value of $|C_{\mu e}^{(\mathrm{II})}|$ that future experiments can probe. From Table 4.8, we then conclude that future experiments with ^{48}Ti will be sensitive to $|C_{\mu e}^{(\mathrm{II})}| \gtrsim 4.7\times10^{-6}(M_\Delta/1\,\mathrm{TeV})^2$.

[3]Only the $^{48}_{22}$Ti and $^{27}_{13}$Al nuclei are considered due to the light nuclei approximation used in Eq. (4.37). Notice that for $^{27}_{13}$Al there is no present upper bound.

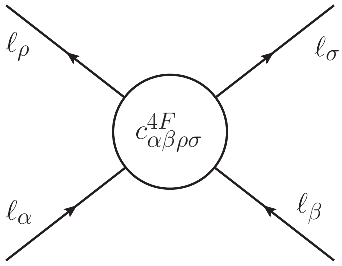

Figure 4.6: $\ell \to 3\ell$ in the type II the effective theory.

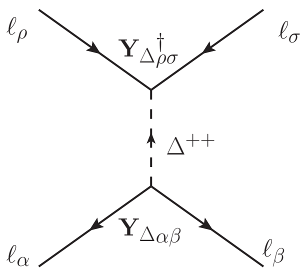

Figure 4.7: $\ell \to 3\ell$ in the type II full theory.

$\ell \to 3\ell$ decays

Contrary to what happens with the other CLFV decays, the leading contribution to the $\ell \to 3\ell$ decays in the scalar triplet model is due to tree-level exchange of a doubly-charged scalar Δ^{++} [177, 181]. From the point of view of the effective theory, these processes are generated by the $d = 6$ effective operator $\delta\mathcal{L}_{4F}$ [105, 182]. The comparison between these two approaches can be illustrated as sketched in Figs. 4.6 and 4.7. In terms of the coefficients $c^{4\text{F}}_{\alpha\beta\rho\sigma}$ of the $d = 6$ operator $\delta\mathcal{L}_{4\text{F}}$ in Eq. (3.92),

$$c^{4\text{F}}_{\alpha\beta\rho\sigma} \equiv \frac{1}{M_\Delta^2}\mathbf{Y}_{\Delta_{\alpha\beta}}\mathbf{Y}^\dagger_{\Delta_{\rho\sigma}}\,, \tag{4.39}$$

we obtain for the $\ell^-_\alpha \to \ell^+_\beta\ell^-_\sigma\ell^-_\sigma$ decay branching ratio for any β, σ:

$$\text{BR}(\ell^-_\alpha \to \ell^+_\beta\ell^-_\sigma\ell^-_\sigma) = \frac{4\left|c^{4\text{F}}_{\alpha\beta\rho\sigma}\right|^2}{\left(G_F^{\text{SM}}\right)^2}\text{BR}(\ell^-_\alpha \to e^-\nu_\alpha\overline{\nu}_e) = \frac{4\,|\mathbf{Y}_{\Delta_{\alpha\beta}}|^2|\mathbf{Y}_{\Delta_{\rho\rho}}|^2}{M_\Delta^4\left(G_F^{\text{SM}}\right)^2}\text{BR}(\ell^-_\alpha \to e^-\nu_\alpha\overline{\nu}_e)\,. \tag{4.40}$$

Similarly, for $\ell^-_\alpha \to \ell^+_\beta\ell^-_\sigma\ell^-_\rho$ decays with $\sigma \neq \rho$, we obtain the expression:

$$\text{BR}(\ell^-_\alpha \to l^+_\beta l^-_\sigma l^-_\rho) = \frac{8}{M_\Delta^4\left(G_F^{\text{SM}}\right)^2}|\mathbf{Y}_{\Delta_{\alpha\beta}}|^2|\mathbf{Y}_{\Delta_{\rho\sigma}}|^2\text{BR}(\ell^-_\alpha \to e^-\nu_\alpha\overline{\nu}_e)\,, \tag{4.41}$$

which is in agreement with the results of [177, 181]. Instead, it is off by a factor of 4 from that of Ref. [105], probably because the authors of this work have not included a factor of 2 in the derivation of the Feynman rules with two identical fields.

From the present experimental upper limits on branching ratios given in Table 4.1, we obtain the upper bounds on the Yukawa couplings listed in Table 4.9. From the latter table, we see that the most stringent upper bound comes from the process $\mu^- \to e^+e^-e^-$, namely $|\mathbf{Y}_{\Delta\mu e}||\mathbf{Y}_{\Delta ee}| \lesssim 5.8\times10^{-6}\times(M_\Delta/1\,\text{TeV})^2$. For Yukawa couplings of order unity, we also see that the present non-observation of $\mu^- \to e^+e^-e^-$ implies a lower bound on the seesaw scale

$$M_\Delta \geq 414\,\text{TeV}\,, \qquad \text{for} \quad \mathbf{Y}_\Delta \sim \mathcal{O}(1)\,. \tag{4.42}$$

On the other hand, the (less optimistic) future sensitivities given in Table 4.9 indicate that future experiments will be able to probe values of Yukawa couplings combinations one of magnitude below the present bounds (or one order of magnitude above for the masses M_Δ).

Process	Constraint On	Upper Bound	Future Sens. on $\lvert\mathbf{Y}_{\Delta_{\alpha\beta}}\rvert\lvert\mathbf{Y}_{\Delta_{\rho\sigma}}\rvert$
$\mu^- \to e^+e^-e^-$	$\lvert\mathbf{Y}_{\Delta\mu e}\rvert\lvert\mathbf{Y}_{\Delta ee}\rvert$	5.8×10^{-6}	5.8×10^{-8}
$\tau^- \to e^+e^-e^-$	$\lvert\mathbf{Y}_{\Delta\tau e}\rvert\lvert\mathbf{Y}_{\Delta ee}\rvert$	2.3×10^{-3}	1.4×10^{-4}
$\tau^- \to \mu^+\mu^-\mu^-$	$\lvert\mathbf{Y}_{\Delta\tau\mu}\rvert\lvert\mathbf{Y}_{\Delta\mu\mu}\rvert$	1.4×10^{-3}	9.8×10^{-5}
$\tau^- \to \mu^+e^-e^-$	$\lvert\mathbf{Y}_{\Delta\tau\mu}\rvert\lvert\mathbf{Y}_{\Delta ee}\rvert$	1.2×10^{-3}	9.8×10^{-5}
$\tau^- \to e^+\mu^-\mu^-$	$\lvert\mathbf{Y}_{\Delta\tau e}\rvert\lvert\mathbf{Y}_{\Delta\mu\mu}\rvert$	1.3×10^{-3}	9.8×10^{-5}
$\tau^- \to \mu^+\mu^-e^-$	$\lvert\mathbf{Y}_{\Delta\tau\mu}\rvert\lvert\mathbf{Y}_{\Delta\mu e}\rvert$	1.6×10^{-3}	9.8×10^{-5}
$\tau^- \to e^+e^-\mu^-$	$\lvert\mathbf{Y}_{\Delta\tau e}\rvert\lvert\mathbf{Y}_{\Delta\mu e}\rvert$	1.3×10^{-3}	9.8×10^{-5}

Table 4.9: Bounds on $\mathbf{Y}_{\Delta ij}\left[\times\left(\frac{M_\Delta}{1\,\text{TeV}}\right)^2\right]$ from tree level $\ell \to 3\ell$ decays in the type II seesaw scenario.

4.2.2 M_W and the ρ parameter

The μ_Δ parameter in the Lagrangian (3.75) can also be constrained by the well-determined observables ρ and M_W [105]. In fact, the operator $\mathcal{L}_{\phi D}$ in Eq. (3.92) corrects the value of both. Considering Eq. (2.31), if the ρ parameter is extracted from data using only hadronic transitions (which do not depend on the leptonic Yukawa couplings) its value is shifted from the SM prediction by:

$$\delta\rho_{\text{had}} = -\frac{|\mu_\Delta|^2}{M_\Delta^4}\frac{\sqrt{2}}{G_F^{\text{SM}}}\,. \tag{4.43}$$

As an estimate, using the average experimental value of ρ ($\rho_{\text{exp.}} = 1.0004^{+0.0003}_{-0.0004}$) as if it were indeed dominated by the hadronic contributions, we are able to obtain the following constraint on μ_Δ/M_Δ^2:

$$v^2\frac{|\mu_\Delta|^2}{M_\Delta^4} \lesssim 0.0002^{+0.0001}_{-0.0002} \quad \Longrightarrow \quad |\mu_\Delta| \lesssim 5.7\times 10^{-2}\left(\frac{M_\Delta^2}{1\,\text{TeV}}\right)\,. \tag{4.44}$$

Using the relation $M_W^2 \approx 8\rho G_F/\sqrt{2}g$, the W boson mass is also shifted,

$$\begin{aligned}\delta M_W^2 &= -\frac{M_W^2}{2{M_W}^2 - M_Z^2}\left[\delta\rho_{\text{had}}\,M_W^2 - \frac{\delta G_F}{G_F}(M_W^2 - M_Z^2)\right] \\ &= -\frac{M_W^2}{2{M_W}^2 - M_Z^2}\left[\frac{|\mu_\Delta|^2}{M_\Delta^4}\frac{M_W^2}{G_F\sqrt{2}} - \frac{M_W^2 - M_Z^2}{\sqrt{2}G_F M_\Delta^2}\mathbf{Y}_{\Delta e\mu}{\mathbf{Y}_\Delta}^\dagger{}_{e\mu}\right]\,,\end{aligned} \tag{4.45}$$

where M_W is the SM value for the W-boson mass as predicted in the ($\overline{\text{MS}}$) scheme at the Z-pole (Z-scheme), $M_W^{\text{SM}} = 80.4887 \pm 0.0515$ GeV, and G_F is extracted from muon decay, see Eq. (3.93). Barring extreme cancellations between both terms in Eq. (4.45), the precise experimental value of M_W allows to set stringent bounds on both the Yukawa couplings and on the μ_Δ parameter:

$$|\mathbf{Y}_{\Delta\mu e}|^4 = (0.00023 \pm 0.00109)\left(\frac{M_\Delta}{1\text{ TeV}}\right)^{-4}\,, \qquad |\mu_\Delta| \lesssim 8.7\times 10^{-2}\left(\frac{M_\Delta^2}{1\,\text{TeV}}\right)\,. \tag{4.46}$$

Notice that the ratio $v^2|\mu_\Delta|/M_\Delta^2$ is directly related to neutrino masses via Eq. (3.80). For example, $m_\nu \sim 1$ eV and $\mathbf{Y}_\Delta \sim \mathcal{O}(1)$, require a ratio $\mu_\Delta/M_\Delta^2 \sim 10^{-11}$ TeV^{-1} below the bound in Eq. (4.46).

4.2.3 Experimental signatures of scalar triplets

Another difference of the scalar triplet model compared to the type I seesaw scenario is that the ratio of two rates with the same flavour transition exhibit a different dependence on the masses M_{Δ^+} and $M_{\Delta^{++}}$. An analysis based on these ratios, as performed in the type I seesaw, is therefore not possible except in very particular cases. For instance, in the limit $M_{\Delta^{++}} \gg M_{\Delta^+}$ (where the dominant contribution to the $\mu - e$ conversion is given by the exchange of the singly-charged scalar Δ^+), we have $|C_{\mu e}^{(\mathrm{II})}| \propto (\mathbf{Y}_\Delta \mathbf{Y}_\Delta^\dagger)_{\mu e}$ and an analysis based on the ratio of the $\mu \to e\gamma$ and $\mu - e$ conversion rates is possible [173]. The measurement of any of these ratios can give us the value of M_Δ if these CLFV transitions are due to scalar triplet interactions. Future facilities open up the possibility of observing such new signals of the type II seesaw scenario. For instance, expected sensitivities on M_Δ are:

$$M_\Delta \lesssim 200\,\mathrm{TeV} \cdot |(\mathbf{Y}_\Delta \mathbf{Y}_\Delta^\dagger)_{\mu e}|^{1/2} \cdot \left[\frac{10^{-14}}{\mathrm{BR}(\mu \to e\gamma)}\right]^{1/4} , \tag{4.47}$$

$$M_\Delta \lesssim 400\,\mathrm{TeV} \cdot |C_{\mu e}^{(\mathrm{II})}|^{1/2} \cdot \left[\frac{10^{-18}}{\mathrm{CR}(\mu\mathrm{Ti} \to e\mathrm{Ti})}\right]^{1/4} , \tag{4.48}$$

$$M_\Delta \lesssim 2400\,\mathrm{TeV} \cdot \sqrt{|\mathbf{Y}_{\Delta\mu e}||\mathbf{Y}_{\Delta ee}|} \cdot \left[\frac{10^{-16}}{\mathrm{BR}(\mu \to eee)}\right]^{1/4} , \tag{4.49}$$

which shows that for $Y_\Delta \sim \mathcal{O}(1)$ future CLFV decay experiments may in principle probe the type II seesaw model beyond $\sim 1000\,\mathrm{TeV}$.

Assuming that M_Δ could be as low as $\mathcal{O}(\mathrm{TeV})$, a striking signal of the type II seesaw mechanism would be the production of the doubly-charged scalars Δ^{++} and Δ^{--} at the LHC, and their subsequent decay into pairs of leptons with equal charge [183]. However, even with a detection of a boson with such behavior, the identification of a type II seesaw mechanism would still require the measurement of at least three CLFV processes in order to determine the Yukawa couplings in Tables 4.7 and 4.9.

Other interesting signals of the type II seesaw mechanism would be the observation of the processes: $\Delta^{++} \to W^+W^+$, $W^+W^+ \to \Delta^{++}$, $Z^0 \to \Delta^+W^-$, or $\Delta^+ \to ZW^+$. For example, the Δ^{++} and Δ^{--} produced by a Drell-Yann process ($\bar{q}q \to \Delta^{--}\Delta^{++}$) [183], could decay into pairs of W bosons ($\Delta^{\pm\pm} \to W^\pm W^\pm$). However, for such a decay, the decay width is proportional to $v^2 \frac{M_\Delta^3}{M_W^2} \frac{|\mu_\Delta|^2}{M_\Delta^4}$ and the constraint obtained in Eq. (4.46) largely suppresses this decay. The same holds for other decays [184]. Thus, the only relevant channel will be the $\Delta^{\pm\pm} \to l^\pm l^\pm$, with a decay rate proportional to $M_\Delta |\mathbf{Y}_{\Delta ij}|^2$.

Alternative investigations involve the study of modifications to SM Higgs physics. For instance, the $\mathcal{L}_{6\phi}$ [Eq. (3.92)] and $\mathcal{L}_{\phi D}$ [Eq. (3.92)] operators induce the following new couplings with the Higgs boson: $HHWW$, $HHZZ$, H^4, HWW, HZZ and H^3. However, the strong upper limit in Eq. (4.46) precludes observable effects, except maybe from $\mathcal{L}_{6\phi}$ for very large values of λ_2 and/or λ_4. Similarly, $\mathcal{L}_{\phi D}$ also affects Higgs processes but, once more, the bound coming from the ρ parameter discussed above excludes observation in the planned future facilities such as the ILC [185].

Process	Constraint On	Upper Bound	Future Sensitivity on $\lvert\epsilon^{\Sigma}_{\beta\alpha}\rvert(\lvert\epsilon^{\Sigma}_{\beta\rho}\rvert)$
$\mu \to e\gamma$	$\lvert\epsilon^{\Sigma}_{e\mu}\rvert$	2.3×10^{-5}	6.5×10^{-6}
$\tau \to e\gamma$	$\lvert\epsilon^{\Sigma}_{e\tau}\rvert$	1.3×10^{-2}	2.3×10^{-3}
$\tau \to \mu\gamma$	$\lvert\epsilon^{\Sigma}_{\mu\tau}\rvert$	1.5×10^{-2}	2.3×10^{-3}
$\mu^- \to e^+e^-e^-$	$\lvert\epsilon^{\Sigma}_{e\mu}\rvert$	1.1×10^{-6}	1.1×10^{-8}
$\tau^- \to e^+e^-e^-$	$\lvert\epsilon^{\Sigma}_{e\tau}\rvert$	4.3×10^{-4}	2.6×10^{-6}
$\tau^- \to \mu^+\mu^-\mu^-$	$\lvert\epsilon^{\Sigma}_{\mu\tau}\rvert$	3.8×10^{-4}	2.6×10^{-5}
$\tau^- \to \mu^+\mu^-e^-$	$\lvert\epsilon^{\Sigma}_{e\tau}\rvert$	3.2×10^{-4}	1.9×10^{-5}
$\tau^- \to e^+\mu^-\mu^-$	$\lvert\epsilon^{\Sigma}_{\tau\mu}\rvert\lvert\epsilon^{\Sigma}_{e\mu}\rvert$	2.2×10^{-4}	1.7×10^{-5}
$\tau^- \to e^+e^-\mu^-$	$\lvert\epsilon^{\Sigma}_{\tau\mu}\rvert$	2.6×10^{-4}	1.9×10^{-5}
$\tau^- \to \mu^+e^-e^-$	$\lvert\epsilon^{\Sigma}_{\tau e}\rvert\lvert\epsilon^{\Sigma}_{\mu e}\rvert$	2.1×10^{-4}	1.7×10^{-5}
$\mu\,\mathrm{Pb} \to e\,\mathrm{Pb}$	$\lvert\epsilon^{\Sigma}_{e\mu}\rvert$	2.5×10^{-6}	3.7×10^{-10}
$\mu\,\mathrm{Ti} \to e\,\mathrm{Ti}$	$\lvert\epsilon^{\Sigma}_{e\mu}\rvert$	5.3×10^{-7}	2.6×10^{-10}
$\mu\,\mathrm{Au} \to e\,\mathrm{Au}$	$\lvert\epsilon^{\Sigma}_{e\mu}\rvert$	1.5×10^{-7}	1.8×10^{-10}
$\mu\,\mathrm{Al} \to e\,\mathrm{Al}$	$\lvert\epsilon^{\Sigma}_{e\mu}\rvert$		2.1×10^{-9}

Table 4.10: Bounds on the coefficients $\epsilon^{\Sigma}_{\beta\alpha}$ resulting from CLFV decays in the type III seesaw scenario.

4.3 Type III seesaw model

A crucial difference between the type I and type III seesaws is that in the latter there is charged-lepton flavour mixing in neutral currents [see Eq. (3.135)]. As a result, in the type III seesaw, $\ell \to 3\ell$ and $\mu - e$ conversion are tree-level processes. Only $\ell_\alpha \to \ell_\beta\gamma$ decays still have to proceed at one-loop level since the QED coupling (2.40) remains flavour diagonal.

4.3.1 Charged lepton flavour violating processes

$\ell_\alpha \to \ell_\beta\gamma$ decays

Following the detailed computation in Appendix E, we have for $m_\Sigma \gg M_W$ [186]:

$$\mathrm{BR}(\ell_\alpha \to \ell_\beta\gamma) \approx \frac{3\alpha}{32\pi}\left|\left(\frac{13}{3}+C\right)(\epsilon^{\Sigma})_{\beta\alpha} - \sum_j w_{\nu_j}(U_L^{\nu})_{\beta j}\left(U_L^{\nu\dagger}\right)_{j\alpha} + \mathcal{O}\left(\frac{m_\Sigma}{M_W}\right)^3\right|^2 \mathrm{BR}(\ell_\alpha \to \ell_\beta\overline{\nu_\beta}\nu_\alpha)\,, \quad (4.50)$$

where $w_{\nu_j} \equiv m^2_{\nu_j}/M^2_W$ and $C = \frac{16}{3}\left(\cos^2\theta_W - 2\right)$. The second term in Eq. (4.50) is the usual contribution (4.1) from neutrino mixing, while the first corresponds to the explicit contribution of the triplet(s). For a given value of the seesaw scale m_Σ we would expect $\epsilon^{\Sigma} \sim m_\nu/m_\Sigma \sim 10^{-12}\,(10^2\,\mathrm{GeV}/m_\Sigma)$ and $w_\nu = m^2_\nu/M^2_W \sim 10^{-24}$ (see Table 3.1). Therefore, even for m_Σ as low as 100 GeV, we would get $\mathrm{BR}\,(\ell_\alpha \to \ell_\beta\gamma) \sim 10^{-27}\,\mathrm{BR}(\ell_\alpha \to \ell_\beta\overline{\nu_\beta}\nu_\alpha)$, which is far below the present upper limits in Table 4.1. However, as discussed in Section 3.4.2, the rates can be naturally much larger if neutrino masses are generated through *direct lepton violation*. This can be realised in the type III seesaw if, besides the high scale m_Σ, a small parameter μ responsible for lepton-number violation is also present. In this case, the ϵ^{Σ} term in Eq. (4.50) is magnified to much larger values and the second term can be safely disregarded. Therefore,

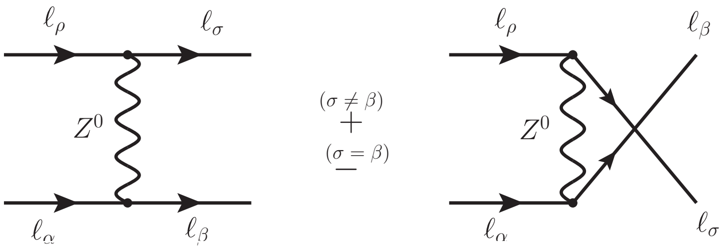

Figure 4.8: Tree-level contributions to $\ell_\alpha^- \to \ell_\rho^+ \ell_\beta^- \ell_\sigma^-$ decays in the type III seesaw scenario.

we can rewrite the branching ratio for $\ell_\alpha \to \ell_\beta \gamma$ as

$$\frac{\mathrm{BR}(\ell_\alpha \to \ell_\beta \gamma)}{\mathrm{BR}(\ell_\alpha \to \ell_\beta \overline{\nu_\beta} \nu_\alpha)} = \frac{3\alpha}{32\pi} \left| \left(\frac{13}{3} + C \right) \right|^2 \left| \epsilon_{\beta\alpha}^{\Sigma} \right|^2 \approx 1.08 \times 10^{-3} \cdot \left| \epsilon_{\beta\alpha}^{\Sigma} \right|^2 , \tag{4.51}$$

and, using present upper limits and future sensitivities in Table 4.1, we obtain the constraints on the coefficients $\epsilon_{\beta\alpha}^{\Sigma}$ listed in Table 4.10. Again, the most stringent bound comes from $\mu \to e\gamma$ and we see that present experiments preclude off-diagonal coefficients $\epsilon_{\beta\alpha}^{\Sigma}$ larger than $\sim 10^{-2}$.

$\ell \to 3\ell$ decays

On the other hand, the $\ell_\alpha \overline{\ell_\beta} Z$ coupling in the Lagrangian (3.115) provides a tree-level contribution to $\ell \to 3\ell$ decay rates, as illustrated in Fig. 4.8. For $\ell_\alpha^- \to \ell_\beta^+ \ell_\beta^- \ell_\beta^-$, the branching ratio is given by

$$\frac{\mathrm{BR}(\ell_\alpha^- \to \ell_\beta^+ \ell_\beta^- \ell_\beta^-)}{\mathrm{BR}(\ell_\alpha^- \to e^- \nu_\alpha \overline{\nu_e})} = 4 |\epsilon_{\beta\alpha}^{\Sigma}|^2 \left(3 s_W^4 - 2 s_W^2 + \frac{1}{2} \right) \approx 0.81 |\epsilon_{\beta\alpha}^{\Sigma}|^2 , \tag{4.52}$$

while for - $\ell_\alpha^- \to \ell_\rho^+ \ell_\rho^- \ell_\beta^-$ and $\ell_\alpha^- \to \ell_\rho^+ \ell_\rho^- \ell_\beta^-$, with $\rho \neq \beta$, the branching ratios are given by:

$$\frac{\mathrm{BR}(\ell_\alpha^- \to \ell_\rho^+ \ell_\rho^- \ell_\beta^-)}{\mathrm{BR}(\ell_\alpha^- \to e^- \nu_\alpha \overline{\nu_e})} = 4 |\epsilon_{\beta\alpha}^{\Sigma}|^2 \left(2 s_W^4 - s_W^2 + \frac{1}{4} \right) \approx 0.51 |\epsilon_{\beta\alpha}^{\Sigma}|^2 , \tag{4.53}$$

$$\frac{\mathrm{BR}(\ell_\alpha^- \to \ell_\rho^+ \ell_\beta^- \ell_\beta^-)}{\mathrm{BR}(\ell_\alpha^- \to e^- \nu_\alpha \overline{\nu_e})} = 2 |\epsilon_{\beta\alpha}^{\Sigma}|^2 |\epsilon_{\beta\rho}^{\Sigma}|^2 . \tag{4.54}$$

Taking into account the above expressions and the experimental upper limits reported in Table 4.1 for these processes, we then get the upper bounds on the coefficients $\epsilon_{\beta\rho}^{\Sigma}$ listed in Table 4.10. From this table, we see that the most constraining bound of $|\epsilon_{e\mu}^{\Sigma}| \lesssim 10^{-6}$ comes from $\mu \to 3e$, whereas for the remaining coefficients $|\epsilon_{\beta\alpha}^{\Sigma}| \lesssim 10^{-4}$. Notice also that the bounds obtained from $\ell_\alpha^- \to \ell_\rho^+ \ell_\beta^- \ell_\beta^-$ are not particularly stringent since they are set on the product of two coefficients, $|\epsilon_{\beta\alpha}^{\Sigma}||\epsilon_{\beta\rho}^{\Sigma}|$.

$\mu - e$ conversion in nuclei

More stringent bounds on the $\mu - e - Z$ coupling can be obtained using data from $\mu - e$ conversion in nuclei. In fact, in the fermion triplet model, $\mu - e$ conversion in atomic nuclei proceeds at tree level via the same diagram as $\mu \to 3e$ (left diagram in Fig. 4.8), with the electron line replaced by a quark line.

The $\mu-e$ conversion ratio in a generic nucleus $\mathcal{N}$ can be straightforwardly obtained from the quark-lepton effective interaction induced by Z exchange [see Eqs. (3.119) and (2.41)]:

$$\mathcal{L}^{\mu-e}_{\text{eff.}} = -\frac{2G_F}{\sqrt{2}} \left[\bar{e}\gamma^\sigma P_L \left(g_L^{\text{NC}}\right)_{e\mu} \mu\right] \times \left(\bar{u}\gamma_\sigma \left[g_{LV(u)} - \gamma_5\right] u + \bar{d}\gamma_\sigma \left[g_{LV(d)} + \gamma_5\right] d\right) , \tag{4.55}$$

where

$$g_{LV(u)} = 1 - \frac{8}{3} s_W^2 \qquad \text{and} \qquad g_{LV(d)} = -1 + \frac{4}{3} s_W^2 \,. \tag{4.56}$$

Using the general parametrisation given in [174], we then have for the $\mu-e$ conversion ratio in a nucleus $\mathcal{N}$ with N neutrons and Z protons [186]:

$$\frac{\text{CR}\,(\mu\mathcal{N} \to e\mathcal{N})}{\text{BR}(\mu \to e\gamma)} = \frac{8\left(G_F^{\text{SM}}\right)^2 \Gamma_\mu}{\Gamma_{\text{capt.}}} \left|\boldsymbol{\epsilon}^\Sigma_{\mu e}\right|^2 \left|\left(2g_{LV}(u) + g_{LV}(d)\right) V^{(p)} + \left(g_{LV}(u) + 2g_{LV}(d)\right) V^{(n)}\right|^2 , \tag{4.57}$$

with nuclear parameters $V^{(p)}$, $V^{(p)}$ and $\Gamma_{\text{capt.}}$ given in Table 4.5 for the analysed nuclei.

From the present upper limits on μ-e conversion rates, we extract the upper bounds on $|\boldsymbol{\epsilon}^\Sigma_{\mu e}|$ reported in Table 4.10. The most stringent bound comes from $^{197}_{79}$Au and present upper limits on CR$(\mu\mathcal{N} \to e\mathcal{N})$ preclude a coefficient $|\boldsymbol{\epsilon}^\Sigma_{\mu e}|$ larger than $\sim 10^{-6}$. On the other hand, if prospective experimental sensitivities to CR$(\mu\mathcal{N} \to e\mathcal{N})$ of $\sim 10^{-18}$ are reached, one will be able to probe values of $|\boldsymbol{\epsilon}^\Sigma_{\mu e}| \sim 10^{-10}$.

Comparison of CLFV decays

From the results (4.51), (4.52)-(4.53) and (4.57), we notice that all CLFV rates in the type III seesaw do not involve logarithmic terms and exhibit the general form

$$\text{BR}_{\ell_\alpha \to \ell_\beta} = g(M_W, m_\ell) \cdot \left|\boldsymbol{\epsilon}^\Sigma_{\beta\alpha}\right|^2 \,. \tag{4.58}$$

with $g(M_W, m_\ell)$ a function which depends only on M_W and m_ℓ. Therefore, the ratio of processes with the same flavour transition are predicted to a fixed value. Namely, we obtain:

$$\text{BR}(\mu \to e\gamma) = 1.3 \times 10^{-3} \cdot \text{BR}(\mu \to eee)\,, \tag{4.59}$$

$$\text{BR}(\tau \to \mu\gamma) = 1.3 \times 10^{-3} \cdot \text{BR}(\tau \to \mu\mu\mu) = 2.1 \times 10^{-3} \cdot \text{BR}(\tau^- \to e^- e^+ \mu^-)\,, \tag{4.60}$$

$$\text{BR}(\tau \to e\gamma) = 1.3 \times 10^{-3} \cdot \text{BR}(\tau \to eee) \; = 2.1 \times 10^{-3} \cdot \text{BR}(\tau^- \to \mu^- \mu^+ e^-)\,, \tag{4.61}$$

and, for ratios involving $\mu - e$ conversion in nuclei (in $^{48}_{22}$Ti for example),

$$\text{BR}(\mu \to e\gamma) = 3.1 \times 10^{-4} \cdot \text{CR}(\mu\,\text{Ti} \to e\,\text{Ti})\,, \tag{4.62}$$

$$\text{BR}(\mu \to eee) = 2.4 \times 10^{-1} \cdot \text{CR}(\mu\,\text{Ti} \to e\,\text{Ti})\,. \tag{4.63}$$

It is apparent from these results that in the type III seesaw model $\ell \to 3\ell$ and $\mu-e$ conversion rates are much larger than BR$(\mu \to e\gamma)$. Obviously, the reason for this is that $\ell_\alpha \to \ell_\beta\gamma$ is a one-loop process while $\ell \to 3\ell$ and $\mu-e$ conversion in nuclei proceeed at tree level. Notice, however, that these results hold only in the limit where $m_\Sigma \gg M_{W,Z,H}$, as they are based on Eq. (4.50). If we do not take this limit, i.e. if we use Eq. (E.30) in Appendix E, a study based on these ratios is only possible if we assume a quasi-degenerate mass spectrum of fermion triplets (as predicted by *direct lepton violation*) with scale m_Σ. In this case, the above ratios can change by up to one order of magnitude for values of m_Σ as low as ~ 100 GeV.

On the other hand, from Table 4.10 we verify that the bounds on $|\boldsymbol{\epsilon}_{\beta\alpha}|$ resulting from $\ell_\alpha \to \ell_\beta \gamma$ are not as constraining as the ones coming from $\ell \to 3\ell$ decays and that, even if the upper limits on $\ell_\alpha \to \ell_\beta \gamma$ are improved in the future by three or two orders of magnitude, respectively, the $\ell \to 3\ell$ decays will still provide more competitive bounds on $|\boldsymbol{\epsilon}_{\beta\alpha}|$. Nonetheless, the most stringent bound comes from $\mu - e$ conversion in nuclei for which the experimental sensitivity to CR($\mu\mathcal{N} \to e\mathcal{N}$) is expected to improve by several orders of magnitude. Therefore, unlike for other seesaw models, the observation of a CLFV radiative decay rate close to the present bounds, would rule out the minimal type III seesaw mechanism since it would be incompatible with bounds arising from $\ell \to 3\ell$ and $\mu - e$ conversion in nuclei.

4.3.2 Unitarity of the leptonic mixing matrix

While CLFV processes put bounds on the off-diagonal elements $\left(\boldsymbol{N}\boldsymbol{N}^\dagger\right)_{\alpha\beta} = \boldsymbol{\epsilon}^\Sigma_{\alpha\beta}$ [remember Eq. (3.116)], the additional analysis of (tree-level) W and Z decays as well as of constraints on the universality of weak interactions, already discussed in the type I seesaw scenario, allows us to set bounds on the diagonal elements $\left(\boldsymbol{N}\boldsymbol{N}^\dagger\right)_{\alpha\alpha}$. The relevant expressions concerning W decays and the universality of weak interactions are identical to the ones for the type I seesaw, namely Eqs. (4.17) and (4.21), respectively. Therefore, the bounds obtained in Table 4.6 for the type I seesaw apply as well in the type III seesaw scenario. However, a slight modification is required in the expression (4.19) for the invisible Z decay width. Indeed, in the type III seesaw model, the modified neutral weak couplings in Eq. (3.135) leads to

$$\Gamma(Z \to \text{invisible}) = \sum_{i,j} \Gamma(Z \to \bar{\nu}_i \nu_j) = \frac{G_F^{\text{SM}} M_Z^3}{12\sqrt{2}\pi}\,(1+\rho_t) \sum_{i,j} |[(\boldsymbol{N}^\dagger \boldsymbol{N})^{-1}]_{ij}|^2\,, \tag{4.64}$$

which should be compared with the expression (4.19) obtained in the type I seesaw. Here, the parameter $\rho \approx 0.008$ accounts for radiative corrections involving the top quark. Using the approximation

$$\sum_{i,j} |[(\boldsymbol{N}^\dagger \boldsymbol{N})^{-1}]_{ij}|^2 = \text{Tr}(1 - 2\,\boldsymbol{\epsilon}^\Sigma) = 9 - 2\sum_\alpha (\boldsymbol{N}\boldsymbol{N}^\dagger)_{\alpha\alpha}\,, \tag{4.65}$$

valid at first order in m_Σ^{-1}, and the data provided in Ref. [66], we then obtain the following constraint:

$$\frac{9 - 2\sum_\alpha (\boldsymbol{N}\boldsymbol{N}^\dagger)_{\alpha\alpha}}{\sqrt{(\boldsymbol{N}\boldsymbol{N}^\dagger)_{ee}(\boldsymbol{N}\boldsymbol{N}^\dagger)_{\mu\mu}}} = \frac{12\sqrt{2}\pi\,\Gamma(Z \to \text{invisible})}{G_F M_Z^3 (1+\rho_t)} = 2.984 \pm 0.009\,. \tag{4.66}$$

As pointed out in Section 4.1.2, this is the number of active neutrinos at LEP and it gives us one constraint on the diagonal elements $\left(\boldsymbol{N}\boldsymbol{N}^\dagger\right)_{\alpha\alpha}$. It is the difference between this constraint and the one in Eq. (4.20) for the type I seesaw that makes the unitarity analysis for the type III seesaw any different.

Combination of all constraints

From all constraints reported in Table 4.6 and in Eq. (4.66), we have performed a global fit of the diagonal elements to the experimental data. Using the lower upper bounds for the off-diagonal elements in Table 4.10, we can then write for the $\boldsymbol{N}\boldsymbol{N}^\dagger$ elements, at the 90% CL:

$$|\boldsymbol{N}\boldsymbol{N}^\dagger| \approx \begin{pmatrix} 1.004 \pm 0.011 & < 1.5 \cdot 10^{-7} & < 3.2 \cdot 10^{-4} \\ < 1.5 \cdot 10^{-7} & 0.993 \pm 0.011 & < 2.6 \cdot 10^{-4} \\ < 3.2 \cdot 10^{-4} & < 2.6 \cdot 10^{-4} & 1.014 \pm 0.012 \end{pmatrix} . \tag{4.67}$$

As in the type I seesaw scenario, small deviations from unity in the diagonal elements are not significant enough to be interpreted as a signal of new physics. Note also that, due to the fact that CLFV processes are now allowed at tree level, the bounds on off-diagonal elements are stronger than those obtained in the type I seesaw model.

Concerning the direct production and detection of fermionic triplets, the type III seesaw model is less promising than the scalar triplet model. In fact, in the type III seesaw, only particles with electric charge ± 1 exist, resulting in less clean experimental signals. For a detailed discussion on searches for type III seesaw at the LHC see, for example, Refs. [154, 187]. Recall, however, that in the type III seesaw scenario the observation of a single CLFV radiative decay close to the present bounds would provide an important (indirect) possibility to exclude this model as the unique low-energy source of lepton flavour violation.

5 Summary and conclusions

In the present thesis, we have investigated seesaw extensions of the SM, which naturally accomodate tiny neutrino masses via tree-level exchange of heavy particles: fermion singlets (triplets) in the type I (III) seesaw and a scalar triplet in the type II seesaw. From a low-energy effective viewpoint, neutrino masses are generated by a dimension-five operator, common to all theories with Majorana neutrinos. However, a plethora of dimension-six operators exists and, therefore, they are a crucial tool to discriminate among various models. In a nutshell, for the fermionic seesaw models the effective operators induce non-unitary lepton mixing matrices in the weak currents, while in the scalar triplet model mixing matrices remain unitary but dimension-six operators induce exotic four-fermion couplings and modifications to gauge and Higgs potential parameters.

We have also discussed the possible values of the heavy mass scale M from a theoretical perspective. An unsatisfatory aspect of seesaw models pertains to a worsening of the electroweak hierarchy problem, which could be soften if M is close to the TeV scale. Such scenario is indeed possible if neutrino masses are generated through *direct lepton violation*, in which neutrino masses are directly proportional to a small lepton number violating parameter μ. Such a pattern is already included in the minimal type II seesaw and also in fermionic seesaw models, such as the inverse seesaw. Within the DLV framework, small neutrino masses can be accomodated while keeping the effects of $d = 6$ operators close to observability without fine-tunings or cancellations in the heavy neutrino mass matrices or Yukawa couplings.

Finally, in Chapter 4, we have analysed CLFV processes such as $\ell_\alpha \to \ell_\beta \gamma$, $\ell \to 3\ell$ and $\mu - e$ conversion in nuclei for the three canonical seesaw models discussed in Chapter 3. In the type I seesaw, our results show that $\mu \to e\gamma$ and $\mu \to 3e$ decays as well as $\mu \to e$ conversion in nuclei have predicted rates within the sensitivities of the next-generation experiments. Still, the rates of $\mu \to e$ conversion in nuclei could vanish at a value of the heavy mass scale of $m_N \sim 10$ TeV. Constraints on the dimension-six operator coming from a combined analysis of other lepton flavour conserving processes also predict a 2σ departure from unitarity of the mixing matrix. In the type II scenario, we have set bounds and analysed future sensitivities for Yukawa couplings combinations. The results show that $\mathcal{O}(1)$ Yukawa couplings are allowed by present bounds for a seesaw scale of $\mathcal{O}(\text{TeV})$ and that, for a value of the triplet VEV $v_\Delta \sim 1$ eV, CLFV rates could be within projected sensitivities. Finally, in the type III seesaw scenario, the ratio of two same-flavour transition processes is a constant. Combined with the presence of tree-level FCNCs and, therefore, large $\mu \to 3e$ and $\mu \to e$ conversion rates, this offers a clear possibility of tests.

In summary, the work presented in this thesis clearly illustrates how important the exploration of synergies among the intensity and energy frontiers of particle physics will be to improve our knowledge on the fundamental laws of Nature.

labor omnia vincit

Bibliography

[1] S. Bilenky, Eur.Phys.J. **H38**, 345–404 (2013).

[2] M. Zralek, Acta Phys.Polon. **B41**, 2563–2582 (2011).

[3] C. Giunti and C. Kim, *Fundamentals of Neutrino Physics and Astrophysics* (Oxford University Press, 2007).

[4] W. Pauli, "Pauli letter to Lise Meitner", Typed copy and english translation.

[5] C. D. Ellis and W. A. Wooster, Royal Society of London Proceedings Series A **117**, 109–123 (1927).

[6] L. Meitner and W. Orthmann, German, Zeitschrift für Physik **60**, 143–155 (1930).

[7] J. Chadwick, Proc. R. Soc. London A **136**, 692–708 (1932).

[8] W. Heisenberg, Z.Phys. **77**, 1–11 (1932).

[9] E. Majorana, Zeitschrift fur Physik **82**, 137–145 (1933).

[10] D. Ivanenko, Nature **129**, 798 (1932).

[11] E. Fermi, Ricerca Scientifica **2**, 12 (1933).

[12] J. Chadwick, Comptes Rendues Academie des Sciences **197**, 1625–1627 (1933).

[13] E. Fermi, Z.Phys. **88**, 161–177 (1934).

[14] G. Gamow and E. Teller, Phys.Rev. **51**, 289–289 (1937).

[15] H. A. Bethe, Phys. Rev. **72**, 339–341 (1947).

[16] S. Tomonaga, Progress of Theoretical Physics **1**, 27–42 (1946).

[17] F. J. Dyson, Phys. Rev. **75**, 486–502 (1949).

[18] R. P. Feynman, Phys. Rev. **80**, 440–457 (1950).

[19] J. C. Street and E. C. Stevenson, Phys. Rev. **52**, 1003–1004 (1937).

[20] S. H. Neddermeyer and C. D. Anderson, Phys. Rev. **51**, 884–886 (1937).

[21] B. Pontecorvo, Phys. Rev. **72**, 246–247 (1947).

[22] G. Puppi, Italian, Il Nuovo Cimento **5**, 587–588 (1948).

[23] O. Klein, Nature **161**, 897–899 (1948).

[24] J. A. Wheeler, Rev. Mod. Phys. **21**, 133–143 (1949).

[25] T. D. Lee, M. Rosenbluth, and C. N. Yang, Phys. Rev. **75**, 905–905 (1949).

[26] J. Davis, Raymond, Phys.Rev. **97**, 766–769 (1955).

[27] F. Reines and C. Cowan, Phys.Rev. **92**, 830–831 (1953).

[28] C. Cowan, F. Reines, F. Harrison, H. Kruse, and A. McGuire, Science **124**, 103–104 (1956).

[29] R. Dalitz, Phil.Mag. **44**, 1068–1080 (1953).

[30] T. Lee and C.-N. Yang, Phys.Rev. **104**, 254–258 (1956).

[31] C. Wu, E. Ambler, R. Hayward, D. Hoppes, and R. Hudson, Phys.Rev. **105**, 1413–1414 (1957).

[32] A. Salam, Nuovo Cim. **5**, 299–301 (1957).

[33] L. Landau, Nucl.Phys. **3**, 127–131 (1957).

[34] T. D. Lee and C. N. Yang, Phys. Rev. **105**, 1671–1675 (1957).

[35] M. Goldhaber, L. Grodzins, and A. W. Sunyar, Phys. Rev. **109**, 1015–1017 (1958).

[36] R. P. Feynman and M. Gell-Mann, Phys. Rev. **109**, 193–198 (1958).

[37] E. C. G. Sudarshan and R. E. Marshak, Phys. Rev. **109**, 1860–1862 (1958).

[38] J. Sakurai, English, Il Nuovo Cimento **7**, 649–660 (1958).

[39] B. Pontecorvo, Sov.Phys.JETP **10**, 1236–1240 (1960).

[40] G. Danby et al., Phys. Rev. Lett. **9**, 36–44 (1962).

[41] S. Weinberg, Phys. Rev. Lett. **19**, 1264–1266 (1967).

[42] A. Salam, Conf.Proc. **C680519**, 367–377 (1968).

[43] S. L. Glashow, Nuclear Physics **22**, 579 –588 (1961).

[44] P. W. Anderson, Phys. Rev. **130**, 439–442 (1963).

[45] F. Englert and R. Brout, Phys. Rev. Lett. **13**, 321–323 (1964).

[46] G. S. Guralnik, C. R. Hagen, and T. W. B. Kibble, Phys. Rev. Lett. **13**, 585–587 (1964).

[47] P. W. Higgs, Phys. Rev. Lett. **13**, 508–509 (1964).

[48] T. W. B. Kibble, Phys. Rev. **155**, 1554–1561 (1967).

[49] G. Hooft, Nuclear Physics B **35**, 167 –188 (1971).

[50] G. 't Hooft and M. Veltman, Nuclear Physics B **44**, 189 –213 (1972).

[51] F. Hasert et al., Gargamelle Neutrino Collaboration, Phys.Lett. **B46**, 138–140 (1973).

[52] F. Hasert et al., Gargamelle Neutrino Collaboration, Nucl.Phys. **B73**, 1–22 (1974).

[53] J. J. Aubert et al., Phys. Rev. Lett. **33**, 1404–1406 (1974).

[54] J. Augustin et al., Phys. Rev. Lett. **33**, 1406–1408 (1974).

[55] S. L. Glashow, J. Iliopoulos, and L. Maiani, Phys. Rev. D **2**, 1285–1292 (1970).

[56] M. Banner et al., Physics Letters B **122**, 476 –485 (1983).

[57] G. Arnison et al., Physics Letters B **122**, 103 –116 (1983).

[58] G. Arnison et al., Physics Letters B **126**, 398 –410 (1983).

[59] P. Bagnaia et al., Physics Letters B **129**, 130 –140 (1983).

[60] J. Augustin et al., Phys. Rev. Lett. **33**, 1406–1408 (1974).

[61] S. Herb et al., Phys. Rev. Lett. **39**, 252–255 (1977).

[62] D. DeCamp et al., Physics Letters B **231**, 519 –529 (1989).

[63] M. Kobayashi and T. Maskawa, Prog.Theor.Phys. **49**, 652–657 (1973).

[64] S. Abachi et al., D0 Collaboration, Phys. Rev. Lett. **74**, 2632–2637 (1995).

[65] F. Abe et al., CDF Collaboration, Phys. Rev. Lett. **74**, 2626–2631 (1995).

[66] K. Olive et al., Particle Data Group, Chin. Phys. C **38**, 090001 (2014).

[67] G. Aad et al., ATLAS Collaboration, Phys.Lett. **B716**, 1–29 (2012).

[68] S. Chatrchyan et al., CMS Collaboration, Phys.Lett. **B716**, 30–61 (2012).

[69] D. R. Hamilton, W. P. Alford, and L. Gross, Phys. Rev. **92**, 1521–1525 (1953).

[70] B. Pontecorvo, Sov.Phys.JETP **6**, 429 (1957).

[71] M. Gell-Mann and A. Pais, Phys. Rev. **97**, 1387–1389 (1955).

[72] B. Pontecorvo, Sov.Phys.JETP **7**, 172–173 (1958).

[73] R. Davis, Phys. Rev. **97**, 766–769 (1955).

[74] Z. Maki, M. Nakagawa, and S. Sakata, Progress of Theoretical Physics **28**, 870–880 (1962).

[75] B. Pontecorvo, Sov.Phys.JETP **26**, 984–988 (1968).

[76] R. Davis, Phys. Rev. Lett. **12**, 303–305 (1964).

[77] S. Eliezer and A. R. Swift, Nuclear Physics B **105**, 45 –51 (1976).

[78] H. Fritsch and P. Minkowski, Physics Letters B **62**, 72 –76 (1976).

[79] S. Bilenky and B. Pontecorvo, English, Lettere Al Nuovo Cimento Series 2 **17**, 569–574 (1976).

[80] J. C. Pati and A. Salam, Phys. Rev. Lett. **31**, 661–664 (1973).

[81] H. Georgi and S. L. Glashow, Phys. Rev. Lett. **32**, 438–441 (1974).

[82] M. Gell-Mann, P. Ramond, and R. Slansky, Conf.Proc. **C790927**, 315–321 (1979).

[83] S. Weinberg, Phys. Rev. Lett. **43**, 1566–1570 (1979).

[84] K. S. Hirata et al., Phys. Rev. Lett. **63**, 16–19 (1989).

[85] P Anselmann et al., Physics Letters B **327**, 377 –385 (1994).

[86] J. Abdurashitov et al., Physics Letters B **328**, 234 –248 (1994).

[87] Y. Fukuda et al., Phys. Rev. Lett. **81**, 1158–1162 (1998).

[88] Q. R. Ahmad et al., **89**, 011301 (2002).

[89] S. Mikheev and A. Y. Smirnov, Sov.J.Nucl.Phys. **42**, 913–917 (1985).

[90] S. Mikheyev and A. Smirnov, English, Il Nuovo Cimento C **9**, 17–26 (1986).

[91] L. Wolfenstein, Phys. Rev. D **17**, 2369–2374 (1978).

[92] J. N. Bahcall, A. M. Serenelli, and S. Basu, Astrophys.J.Suppl. **165**, 400–431 (2006).

[93] F. Reines et al., Phys. Rev. Lett. **15**, 429–433 (1965).

[94] C. V. Achar et al., Phys. Lett. **19**, 78–80 (1965).

[95] M. Aglietta et al., NUSEX Collaboration, Europhys.Lett. **8**, 611–614 (1989).

[96] K. Daum et al., English, Zeitschrift für Physik C Particles and Fields **66**, 417–428 (1995).

[97] M. H. Ahn et al., Phys. Rev. Lett. **90**, 041801 (2003).

[98] D. G. Michael et al., MINOS Collaboration, Phys. Rev. Lett. **97**, 191801 (2006).

[99] T. Araki et al., KamLAND Collaboration, Phys. Rev. Lett. **94**, 081801 (2005).

[100] K. Abe et al., Phys.Rev.Lett. **107**, 041801 (2011).

[101] P. Adamson et al., Phys.Rev.Lett. **107**, 181802 (2011).

[102] Y. Abe et al., Phys.Rev.Lett. **108**, 131801 (2012).

[103] F. An et al., Phys.Rev.Lett. **108**, 171803 (2012).

[104] J. Ahn et al., Phys.Rev.Lett. **108**, 191802 (2012).

[105] A. Abada, C. Biggio, F. Bonnet, M. Gavela, and T. Hambye, JHEP **0712**, 061 (2007).

[106] D. Dinh, A. Ibarra, E. Molinaro, and S. Petcov, JHEP **1208**, 125 (2012).

[107] H. Georgi and S. L. Glashow, Phys. Rev. D **6**, 429–431 (1972).

[108] P. Langacker, *The Standard Model and Beyond* (2010).

[109] K. Brading and E. Castellani, (2003).

[110] S. Weinberg, *The Quantum Theory of Fields. Vol. 2.* (Cambridge University Press, 2005).

[111] J. M. Cornwall, D. N. Levin, and G. Tiktopoulos, Phys. Rev. Lett. **30**, 1268–1270 (1973).

[112] C. Itzykson and J. B. Zuber, *Quantum Field Theory* (McGraw-Hill, New York, 1980).

[113] S. Coleman and E. Weinberg, Phys. Rev. D **7**, 1888–1910 (1973).

[114] T. Nakano and K. Nishijima, Progress of Theoretical Physics **10**, 581–582 (1953).

[115] J. Goldstone, English, Il Nuovo Cimento **19**, 154–164 (1961).

[116] J. Goldstone, A. Salam, and S. Weinberg, Phys. Rev. **127**, 965–970 (1962).

[117] P. Langacker, Physics Reports **72**, 185 –385 (1981).

[118] P. Sikivie, L. Susskind, M. Voloshin, and V. Zakharov, Nuclear Physics B **173**, 189 –207 (1980).

[119] P. Langacker and D. London, Phys. Rev. D **38**, 886–906 (1988).

[120] N. Cabibbo, Phys. Rev. Lett. **10**, 531–533 (1963).

[121] M. Kobayashi and T. Maskawa, Progress of Theoretical Physics **49**, 652–657 (1973).

[122] L.-L. Chau and W.-Y. Keung, Phys. Rev. Lett. **53**, 1802–1805 (1984).

[123] L. Wolfenstein, Phys. Rev. Lett. **51**, 1945–1947 (1983).

[124] C. Jarlskog, Phys. Rev. Lett. **55**, 1039–1042 (1985).

[125] G. C. Branco, L. Lavoura, and J. P. Silva, *CP Violation*, Vol. 103 (1999), pp. 1–536.

[126] J. C. Romão, *Advanced Quantum Field Theory* (2012).

[127] R. H. Bernstein and P. S. Cooper, Phys.Rept. **532**, 27–64 (2013).

[128] Y. Fukuda et al., Phys. Rev. Lett. **81**, 1562–1567 (1998).

[129] E. Majorana, Nuovo Cim. **14**, 171–184 (1937).

[130] G. 't Hooft, NATO Sci.Ser.B **59**, 135 (1980).

[131] F. Capozzi et al., Phys.Rev. **D89**, 093018 (2014).

[132] M. González-Garcia, M. Maltoni, J. Salvado, and T. Schwetz, JHEP **1212**, 123 (2012).

[133] D. Forero, M. Tortola, and J. Valle, Phys.Rev. **D86**, 073012 (2012).

[134] C. Kraus et al., Eur.Phys.J. **C40**, 447–468 (2005).

[135] V. Lobashev et al., Phys.Lett. **B460**, 227–235 (1999).

[136] S. M. Bilenky, J. Hosek, and S. Petcov, Phys.Lett. **B94**, 495 (1980).

[137] G. Branco, R. G. Felipe, and F. Joaquim, Rev.Mod.Phys. **84**, 515–565 (2012).

[138] W. Furry, Phys.Rev. **56**, 1184–1193 (1939).

[139] S. Bilenky and C. Giunti, Mod.Phys.Lett. **A27**, 1230015 (2012).

[140] M. Agostini et al., Phys.Rev.Lett. **111**, 122503 (2013).

[141] P. Ade et al., A&A **571**, A1 (2014).

[142] P. Ade et al., Astron.Astrophys. **571**, A16 (2014).

[143] W. Buchmuller and D. Wyler, Nucl.Phys. **B268**, 621–653 (1986).

[144] T. Yanagida, Conf.Proc. **C7902131**, 95–99 (1979).

[145] R. N. Mohapatra and G. Senjanovic, Phys.Rev.Lett. **44**, 912 (1980).

[146] S. L. Glashow, Phys.Lett. **B256**, 255–257 (1991).

[147] M. Fukugita and T. Yanagida, Phys.Rev.Lett. **66**, 2705–2707 (1991).

[148] W. Grimus and L. Lavoura, JHEP **0011**, 042 (2000).

[149] A. Broncano, M. Gavela, and E. E. Jenkins, Phys.Lett. **B552**, 177–184 (2003).

[150] P. Langacker and D. London, Phys. Rev. D **38**, 907–916 (1988).

[151] A. Santamaria, Phys.Lett. **B305**, 90–97 (1993).

[152] J. Schechter and J. W. F. Valle, Phys. Rev. D **22**, 2227–2235 (1980).

[153] G. Lazarides, Q. Shafi, and C. Wetterich, Nucl.Phys. **B181**, 287–300 (1981).

[154] F. del Aguila and J. Aguilar-Saavedra, Nucl.Phys. **B813**, 22–90 (2009).

[155] J. Penedo, *Neutrinos, symmetries and the origin of matter*, M.Sc. Thesis (Técnico Lisboa, 2013).

[156] A. Arhrib et al., Phys.Rev. **D84**, 095005 (2011).

[157] R. Foot, H. Lew, X. He, and G. C. Joshi, Z.Phys. **C44**, 441 (1989).

[158] J. Casas, J. Espinosa, and I. Hidalgo, JHEP **0411**, 057 (2004).

[159] M. González-Garcia and J. Valle, Phys.Lett. **B216**, 360 (1989).

[160] E. Dudas and C. A. Savoy, Acta Phys.Polon. **B33**, 2547–2558 (2002).

[161] S. S. Law and K. L. McDonald, Phys.Rev. **D87**, 113003 (2013).

[162] F. del Aguila and J. Aguilar-Saavedra, Phys.Lett. **B672**, 158–165 (2009).

[163] A. Zee, Nucl.Phys. **B264**, 99 (1986).

[164] K. Babu, Phys.Lett. **B203**, 132 (1988).

[165] M.-C. Chen and J. Huang, Mod.Phys.Lett. **A26**, 1147–1167 (2011).

[166] U. Bellgardt et al., Nuclear Physics B **299**, 1 –6 (1988).

[167] N. Berger, Nuclear Physics B - Proceedings Supplements **248–250**, 35 –40 (2014).

[168] R. J. Abrams et al., *Mu2e Conceptual Design Report*, tech. rep. (2012).

[169] A. Baldini, F. Cei, C. Cerri, S. Dussoni, L. Galli, et al., (2013).

[170] T. Abe et al., *Belle II Technical Design Report*, tech. rep. (2010).

[171] T. Aushev et al., *Physics at Super B Factory*, tech. rep. (2010).

[172] R. Alonso, M. Dhen, M. Gavela, and T. Hambye, JHEP **1301**, 118 (2013).

[173] T. Hambye, Nucl.Phys.Proc.Suppl. **248-250**, 13–19 (2014).

[174] R. Kitano, M. Koike, and Y. Okada, Phys.Rev. **D66**, 096002 (2002).

[175] A. Ilakovac and A. Pilaftsis, Nucl.Phys. **B437**, 491 (1995).

[176] S. Antusch and O. Fischer, JHEP **1410**, 94 (2014).

[177] A. Akeroyd, M. Aoki, and H. Sugiyama, Phys.Rev. **D79**, 113010 (2009).

[178] E. Ma, M. Raidal, and U. Sarkar, Nucl.Phys. **B615**, 313–330 (2001).

[179] A. Pich, A. Santamaría, and J. Bernabéu, Physics Letters B **148**, 229 –233 (1984).

[180] J. Chakrabortty, P. Ghosh, and W. Rodejohann, Phys.Rev. **D86**, 075020 (2012).

[181] D. Dinh and S. Petcov, JHEP **1309**, 086 (2013).

[182] V. Cirigliano and B. Grinstein, Nucl.Phys. **B752**, 18–39 (2006).

[183] A. Akeroyd and M. Aoki, Phys.Rev. **D72**, 035011 (2005).

[184] K. Huitu, J. Maalampi, A. Pietila, and M. Raidal, Nucl.Phys. **B487**, 27–42 (1997).

[185] S. Kanemura, D. Nomura, and K. Tsumura, Phys.Rev. **D74**, 076007 (2006).

[186] A. Abada, C. Biggio, F. Bonnet, M. Gavela, and T. Hambye, Phys.Rev. **D78**, 033007 (2008).

[187] J. Aguilar-Saavedra, P. Boavida, and F. Joaquim, Phys.Rev. **D88**, 113008 (2013).

[188] D. A. Owen, Singapore: World Scientific, 341–347 (1998).

[189] J. C. Romão and J. P. Silva, International Journal of Modern Physics A **27**, 1230025 (2012).

[190] R. Mertig, M. Bohm, and A. Denner, Comput.Phys.Commun. **64**, 345–359 (1991).

[191] A. Denner, H. Eck, O. Hahn, and J. Kublbeck, Nucl.Phys. **B387**, 467–484 (1992).

[192] K.-i. Aoki et al., Progress of Theoretical Physics Supplement **73**, 1–226 (1982).

[193] L. Lavoura, Eur.Phys.J. **C29**, 191–195 (2003).

A One-loop calculations

A.1 Beyond the unitary gauge: R_ξ gauges

The unitary gauge introduced in Eq. (2.24) is not convenient when calculating loop corrections to some process. In fact, the propagator for massive vector bosons V in this gauge is given by

$$D_V^{\mu\nu}(k) = \frac{-i}{q^2 - M_V^2 + i\epsilon}\left[g^{\mu\nu} - \frac{q^\mu q^\nu}{M_V^2}\right] , \tag{A.1}$$

and its $q^\mu q^\nu$ term does not vanish as $q \to \infty$. Therefore, it induces harsh ultraviolet divergences in higher order calculations and very delicate cancellations between diagrams must be satisfied [188].

More convenient is to work in the so-called R_ξ gauges. In this class of gauges the Higgs doublet is written in its full form (2.23), and *gauge fixing* terms are added to the SM Lagrangian:

$$\mathcal{L}_{\text{GF}} = \frac{-1}{\xi_W}(\partial^\mu W_\mu^\dagger - i\xi_W M_W \phi^+)(\partial^\nu W_\nu + i\xi_W M_W \phi^-) - \frac{1}{\xi_Z}(\partial^\mu Z_\mu - i\xi_Z M_Z \phi_Z)^2 - \frac{1}{\xi_A}(\partial^\mu A_\mu)^2 , \tag{A.2}$$

where $\xi_{A,W,Z}$ are free parameters corresponding to different choices of renormalisable gauges. $\mathcal{L}_{\text{GF}}$ is demanded by a correct quantisation procedure of the theory [112, 126] and allows us to define vector boson propagators, as it removes ambiguous terms in the gauge part of the Higgs Lagrangian. In addition, the quantisation of the theory requires the introduction in the theory of nonphysical anticommutative scalar fields, the *Faddeev-Popov ghosts*, along with their Lagrangian $\mathcal{L}_{\text{FP}}$. However, since these fields do not couple with matter fields, their contribution to one-loop corrections of physical processes involving fermions in external lines is zero. As such, we will not concern ourselves with ghost fields.

In a general R_ξ gauge, the propagators of gauge and Goldstone bosons are collected in Fig. A.1. In order to avoid cumbersome calculations, we will use the 't Hooft-Feynman gauge ($\xi_{A,Z,W} = 1$) in one-loop calculations and the unitary gauge ($\xi_{Z,W} \to \infty$, $\xi_A \to 1$) in tree-level calculations. For a review of the SM Feynman rules in the R_ξ gauge ($\xi_{A,Z,W} = \xi$) with convention-independent notation, see [189].

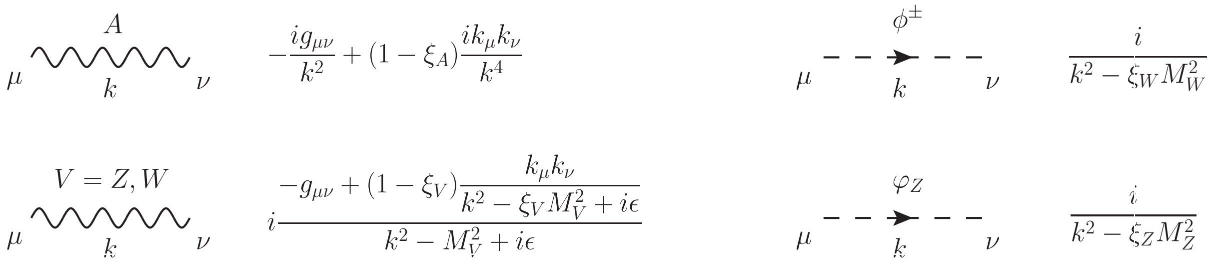

Figure A.1: Propagators of gauge and Goldstone bosons in R_ξ gauges.

A.2 Regularisation procedure

For an arbitrary 1-loop diagram with n internal lines, the most general integrals in Minkowski 4-dimensional space that we need to calculate have the following form:

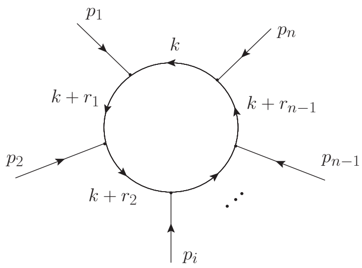

$$\hat{T}_n^{\mu_1,\ldots,\mu_\rho} = \int \frac{d^4k}{(2\pi)^4} \frac{k^{\mu_1}...k^{\mu_\rho}}{D_1 D_2 ... D_n}\,, \tag{A.3}$$

where $D_j = (k+r_j)^2 - m_j^2 + i\varepsilon$ is the propagator denominator of the virtual particle i (with $\varepsilon > 0$ an infinitesimal parameter) and

$$r_j = \sum_{i=1}^{j} p_i, \qquad r_n = \sum_{i=1}^{n} p_i = 0, \qquad j = 1, ..., n-1\,. \tag{A.4}$$

The external momenta are p_i and the virtual particle j carries a 4-momentum $(k + r_j)$ and a mass m_j.

These integrals are often divergent but the amplitude for a physical process must be finite. As such, we need a procedure to make sense of these divergences. In this thesis we adopt the *dimensional regularisation* method [50], where calculations are extended to d-dimensional space-time. In such space-time, the Lagrangian has mass dimension d, and it is easy to verify that the coupling constant g (or g') should have dimension $[g] = 2 - d/2$. As it is more convenient to work with adimensional couplings, we introduce a mass parameter μ and make the substitution

$$g \to g\mu^{\epsilon/2}\,, \qquad \epsilon \equiv 4 - d\,. \tag{A.5}$$

With this, the 1-loop integrals have the general form

$$T_n^{\mu_1,\ldots,\mu_\rho} = \int \frac{d^dk}{(2\pi)^d} \frac{k^{\mu_1}...k^{\mu_\rho}}{D_1 D_1, ... D_n}\,. \tag{A.6}$$

The first step is to combine the products of denominators D_i in Eq. (A.6) in just one common denominator. This is achieved by the Feynman parametrisation technique:

$$\frac{1}{a_1...a_n} = \Gamma(n)\int_0^1 dx_1 \int_0^1 dx_2 \ldots \int_0^1 dx_{n-1} \frac{x_1^{n-2} \ldots x_{n-2}}{[a_1(1-x_1) + a_2 x_1(1-x_2) + \ldots + a_n x_1 \ldots x_{n-1}]^n}\,,\; n \geq 2\,. \tag{A.7}$$

The loop structure of 1-loop diagrams with n propagators can then be rewritten as:

$$D^{(n)}(k, r_i, m_i) = \frac{1}{D_1 \ldots D_n} = \Gamma(n) \int_0^1 dx_1 \ldots \int_0^1 dx_{n-1} \frac{x_1^{n-2} \ldots x_{n-2}}{[(k+P_n)^2 - \Delta_n + i\varepsilon]^n}\,, \tag{A.8}$$

with the generalised 1-loop momentum and mass squared defined by

$$\begin{cases} P_n \equiv r_1(1-x_1) + \ldots + r_n x_1 \ldots x_{n-1} \,, \\ \Delta_n \equiv -x_1(1-x_1)A_n^2 + (1-x_1)m_1^2 + B_n x_1 \,, \end{cases} \tag{A.9}$$

where A_n and B_n are coefficients defined by

$$\begin{cases} A_n \equiv \sum_{i=2}^{n-1} r_i(1-x_i)\Pi_{j=2}^{i-1}x_j + r_n\left(\Pi_{j=2}^{n-1}x_j\right) - r_1 \,, \\ B_n \equiv -\sum_{i=2}^{n-1}(1-x_i)\left(r_i^2 - m_i^2\right)\Pi_{j=2}^{i-1}x_j + \left(\sum_{i=2}^{n-1} r_i(1-x_i)\Pi_{j=2}^{i-1}x_j\right)^2 \\ \qquad + 2r_n\left(\Pi_{s=2}^{n-1}x_s\right)\sum_{i=2}^{n-1} r_i(1-x_i)\left(\Pi_{j=2}^{i-1}x_j\right) + \left(\Pi_{s=2}^{n-1}x_s\right)\left(r_n^2\left(\Pi_{j=2}^{n-1}x_j - 1\right) + m_n^2\right) \,. \end{cases}$$

Applying a change of variables $k \to k + P_n$, we then get the k-even function:

$$D^{(n)}(k + P_n, r_i, m_i) = \Gamma(n)\int_0^1 dx_1 \ldots \int_0^1 dx_{n-1}\frac{x_1^{n-2}\ldots x_{n-2}}{[k^2 - \Delta_n + i\varepsilon]^n} \,, \tag{A.10}$$

From this calculation, it is obvious that all scalar integrals T_n can be reduced to the family of integrals

$$I_{r,n} = \int \frac{d^dk}{(2\pi)^d}\frac{k^{2r}}{[k^2 - \Delta_n + i\varepsilon]^n} \,. \tag{A.11}$$

The same is also true for tensor integrals [126], among which:

$$\begin{aligned} \int \frac{d^dk}{(2\pi)^d}\frac{k^\mu}{[k^2 - \Delta_n + i\varepsilon]^m} &= 0 \,, \\ \int \frac{d^dk}{(2\pi)^d}\frac{k^\mu k^\nu}{[k^2 - \Delta_n + i\varepsilon]^m} &= \frac{1}{d}g^{\mu\nu}\int \frac{d^dk}{(2\pi)^d}\frac{k^2}{[k^2 - \Delta_n + i\varepsilon]^m} \,. \end{aligned} \tag{A.12}$$

The integration of the 1-loop integrals $I_{r,n}$ is done in the complex plane of k^0, yielding the result

$$I_{r,n} = \frac{i(-1)^{r-n}}{(4\pi)^2}\left(\frac{4\pi}{\Delta_n}\right)^{\epsilon/2}\Delta_n^{2+r-n}\frac{\Gamma\left(2+r-\epsilon/2\right)}{\Gamma(2-\epsilon/2)}\frac{\Gamma\left(n-r-2+\epsilon/2\right)}{\Gamma(n)} \,, \tag{A.13}$$

which is valid for all values of d, except for those where the gamma function $\Gamma(n-r-d/2)$ has poles.

The divergences in the integrals are separated from finite terms analysing the limit $\epsilon \to 0$ (usual 4D Minkowski space). The $\Gamma(z)$ function has poles for $z = 0, -1, -2, \ldots$ and close to $z = -m$ we have

$$\Gamma(z) = \frac{(-1)^m}{m!}\frac{1}{m+z} + \frac{(-1)^m}{m!}\psi(m+1) + \mathcal{O}(z+m) \,, \qquad \psi(z) \equiv \frac{d}{dz}\ln\Gamma(z) \,. \tag{A.14}$$

Thus, when $\epsilon \to 0$, we get

$$\Gamma\left(\epsilon/2\right) = \frac{2}{\epsilon} + \psi(1) + \mathcal{O}(\epsilon/2) \,, \tag{A.15}$$

$$\Gamma\left(-n+\epsilon\right) = \frac{(-1)^n}{n!}\left[\frac{1}{\epsilon}\psi(n+1)\right] + \mathcal{O}(\epsilon) \,, \tag{A.16}$$

$$\Gamma\left(1+\epsilon\right) = 1 - \epsilon\gamma + \left(\gamma^2 + \pi^2/6\right)\frac{\epsilon^2}{2} + \ldots \,, \tag{A.17}$$

where $\gamma = -\psi(1) = 0.5772156649015329$ is the Euler-Mascheroni constant. Using the above result, the expansion in powers of ϵ of the relevant integrals $I_{r,n}$ for this work are listed in Eqs. (A.18) to (A.25). For future convenience, these integrals are multiplied by appropriate factors μ^m.

$$\mu^{3\epsilon/2} I_{0,2} = \frac{i}{16\pi^2}\left[\Delta_\epsilon - \ln\frac{\Delta_n}{\mu^3}\right] + \mathcal{O}(\epsilon)\,, \tag{A.18}$$

$$\mu^{3\epsilon/2} I_{1,2} = \frac{i}{16\pi^2}\Delta_n\left[2\Delta_\epsilon + 1 - 2\ln\frac{\Delta_n}{\mu^3}\right] + \mathcal{O}(\epsilon)\,, \tag{A.19}$$

$$\mu^{3\epsilon/2} I_{0,3} = -\frac{i}{32\pi^2\Delta_n^2} + \mathcal{O}(\epsilon)\,, \tag{A.20}$$

$$\mu^{\epsilon} I_{1,3} = \frac{i}{16\pi^2}\Delta_n\left[2\Delta_\epsilon - 1 - 2\ln\frac{\Delta_n}{\mu^3}\right] + \mathcal{O}(\epsilon)\,, \tag{A.21}$$

$$\mu^{2\epsilon} I_{0,4} = \frac{i}{96\pi^2\Delta_n^2} + \mathcal{O}(\epsilon)\,, \tag{A.22}$$

$$\mu^{2\epsilon} I_{1,4} = -\frac{i}{48\pi^2\Delta_n} + \mathcal{O}(\epsilon)\,, \tag{A.23}$$

$$\mu^{2\epsilon} I_{2,4} = \frac{i}{96\pi^2}\left[6\Delta_\epsilon - 5 - 6\ln\frac{\Delta_n}{\mu^4}\right] + \mathcal{O}(\epsilon)\,, \tag{A.24}$$

$$\Delta_\epsilon \equiv \frac{2}{\epsilon} - \gamma + \ln 4\pi\,. \tag{A.25}$$

It should be remarked that in our calculations we do not include explicitly the regularisation factors μ^m because their presence in the power expansions of ϵ is inconsequential as long as all divergences cancel at the end of the calculation. The argument of the logarithms $\ln\Delta_n$ will then be kept dimensionless by an appropriate (mass) normalisation of Δ_n. After expressing our 1-loop amplitudes in terms of the $I_{r,n}$ integrals above, the last step in our calculations is then to perform the integrations over Feynman parameters x_1, ... x_n and the simplification of the final result. (Almost) all calculations were performed in Mathematica, with the help of FeynCalc [190].

For a more complete and gentle summary of the techniques used for 1-loop calculations, see [126].

B Feynman rules with Majorana fermions

We give here the Feynman rules used in our one-loop calculations. In all processes computed, we followed the method reported in Ref. [191], which allows us to use the standard propagators and avoid the explicit appearance of the charge conjugation matrix C. With these prescriptions, the rules for propagators are the usual ones and external legs are taken following the flow defined in the fermion lines. The rules for the SM vertex and propagators are taken from [189], with the sign conventions $\eta_e = -\eta_Z = \eta = -1$. In all Feynman rules considered, the momenta follow the direction of the corresponding arrow and the compact notation $s_W \equiv \sin\theta_W$ and $c_W \equiv \cos\theta_W$ is used.

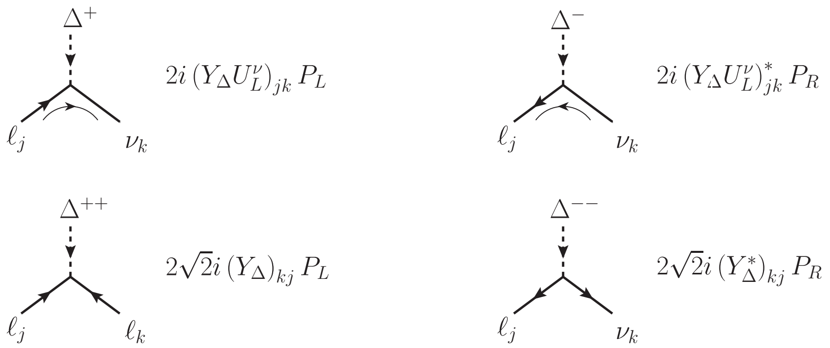

Figure B.1: Feynman rules for Yukawa interactions between the heavy scalar triplet and leptons in the type II seesaw model.

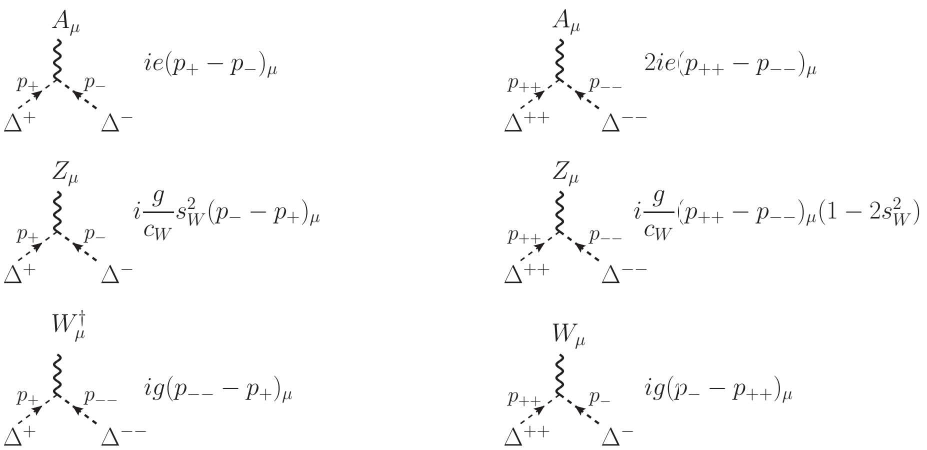

Figure B.2: Feynman rules for heavy scalar triplet gauge interactions in the type II seesaw model.

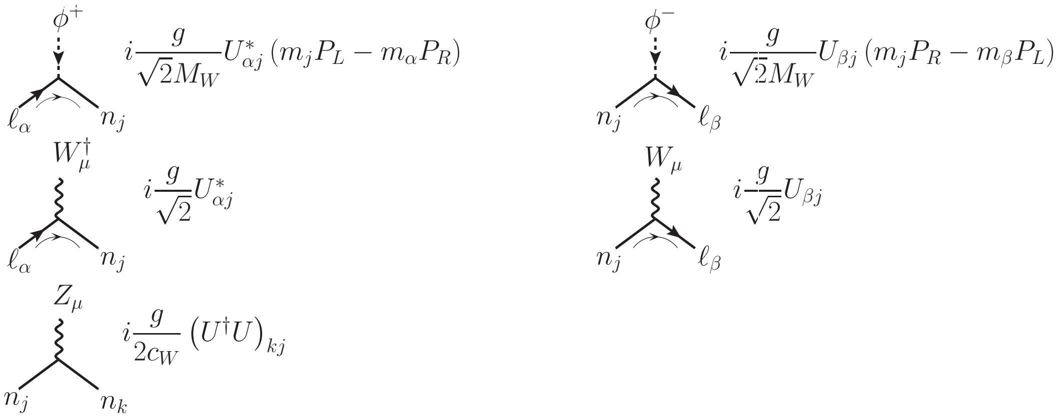

$$i\frac{g}{\sqrt{2}M_W}U^*_{\alpha j}\left(m_j P_L - m_\alpha P_R\right) \qquad i\frac{g}{\sqrt{2}M_W}U_{\beta j}\left(m_j P_R - m_\beta P_L\right)$$

$$i\frac{g}{\sqrt{2}}U^*_{\alpha j} \qquad i\frac{g}{\sqrt{2}}U_{\beta j}$$

$$i\frac{g}{2c_W}\left(U^\dagger U\right)_{kj}$$

Figure B.3: Relevant Feynman rules in the type I seesaw scenario. We use the short notation n_j to denote neutral fermions, either ν_j or N_j [see Eq. (3.45)].

Finally, for the type III seesaw model, we present the relevant Feynman rules using the compact notation defined in Eqs. (3.118)-(3.128).

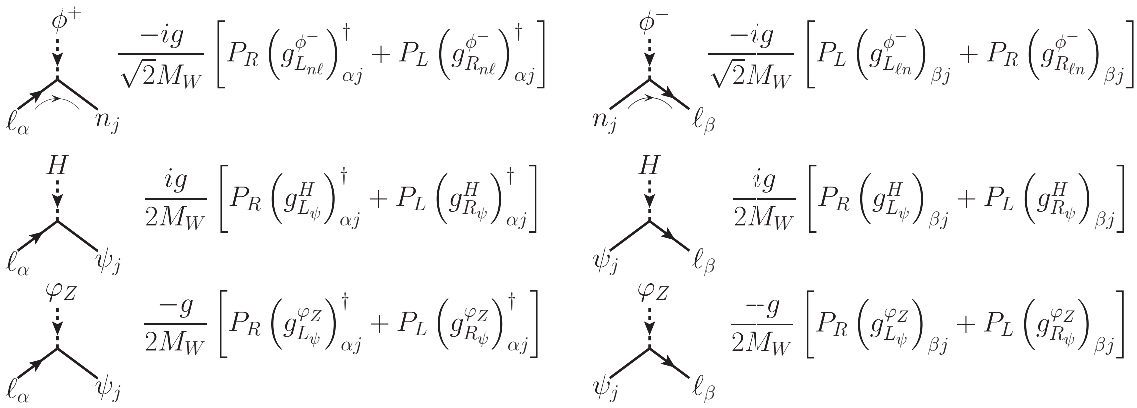

$$\frac{-ig}{\sqrt{2}M_W}\left[P_R\left(g^{\phi^-}_{L_{n\ell}}\right)^\dagger_{\alpha j} + P_L\left(g^{\phi^-}_{R_{n\ell}}\right)^\dagger_{\alpha j}\right] \qquad \frac{-ig}{\sqrt{2}M_W}\left[P_L\left(g^{\phi^-}_{L_{\ell n}}\right)_{\beta j} + P_R\left(g^{\phi^-}_{R_{\ell n}}\right)_{\beta j}\right]$$

$$\frac{ig}{2M_W}\left[P_R\left(g^{H}_{L_\psi}\right)^\dagger_{\alpha j} + P_L\left(g^{H}_{R_\psi}\right)^\dagger_{\alpha j}\right] \qquad \frac{ig}{2M_W}\left[P_R\left(g^{H}_{L_\psi}\right)_{\beta j} + P_L\left(g^{H}_{R_\psi}\right)_{\beta j}\right]$$

$$\frac{-g}{2M_W}\left[P_R\left(g^{\varphi_Z}_{L_\psi}\right)^\dagger_{\alpha j} + P_L\left(g^{\varphi_Z}_{R_\psi}\right)^\dagger_{\alpha j}\right] \qquad \frac{-g}{2M_W}\left[P_R\left(g^{\varphi_Z}_{L_\psi}\right)_{\beta j} + P_L\left(g^{\varphi_Z}_{R_\psi}\right)_{\beta j}\right]$$

Figure B.4: Feynman rules for interactions between fermions and scalars in the type III seesaw model. In our notation, $n_j = \nu_j, N_j$ are neutral fermions and $\psi_j = \ell_j, E_j$ are the charged ones.

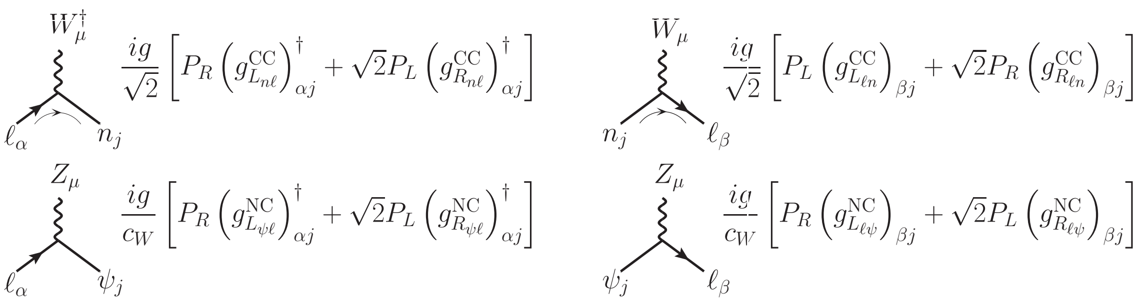

$$\frac{ig}{\sqrt{2}}\left[P_R\left(g^{\rm CC}_{L_{n\ell}}\right)^\dagger_{\alpha j} + \sqrt{2}P_L\left(g^{\rm CC}_{R_{n\ell}}\right)^\dagger_{\alpha j}\right] \qquad \frac{ig}{\sqrt{2}}\left[P_L\left(g^{\rm CC}_{L_{\ell n}}\right)_{\beta j} + \sqrt{2}P_R\left(g^{\rm CC}_{R_{\ell n}}\right)_{\beta j}\right]$$

$$\frac{ig}{c_W}\left[P_R\left(g^{\rm NC}_{L_{\psi\ell}}\right)^\dagger_{\alpha j} + \sqrt{2}P_L\left(g^{\rm NC}_{R_{\psi\ell}}\right)^\dagger_{\alpha j}\right] \qquad \frac{ig}{c_W}\left[P_R\left(g^{\rm NC}_{L_{\ell\psi}}\right)_{\beta j} + \sqrt{2}P_L\left(g^{\rm NC}_{R_{\ell\psi}}\right)_{\beta j}\right]$$

Figure B.5: Feynman rules for gauge interactions with SM fermions, in the type III seesaw model. In our notation, $n_j = \nu_j, N_j$ are neutral fermions and $\psi_j = \ell_j, E_j$ are the charged ones.

C Type I seesaw form factors

In this appendix, we calculate the form factors corresponding to the diagrams which contribute to the LFV processes $\ell_\alpha \to \ell_\beta\gamma$, $\mu \to 3e$ and $\mu - e$ conversion in nuclei, in the type I seesaw model. We use the Feynman rules given in Appendix B and notation reported in [192], namely:

$$D_3(x,y) = (1-y)m_j^2 + y\left[M_W^2 - q^2x(1-x)\right] - y(1-y)\overline{p}^2\,, \tag{C.1}$$

$$D_{3F}(x,y) = (1-y)M_W^2 + y\left\{\overline{m}^2 - q^2x(1-x)\right\} - y(1-y)\overline{p}^2\,, \tag{C.2}$$

$$D_{2\alpha}(x) = M_W^2(1-x) + m_j^2x - p_1^2x(1-x)\,, \tag{C.3}$$

$$D_{2\beta}(x) = M_W^2(1-x) + m_j^2x - p_2^2x(1-x)\,, \tag{C.4}$$

$$D_4(x,y,z) = (1-z)M_W^2 + z\left\{(1-y)m_j^2 + ym_i^2\right\} + \ldots\,, \tag{C.5}$$

$$\overline{p} = (1-x)p_1 + xp_2\,, \qquad \overline{m}^2 = (1-x)m_j^2 + xm_i^2\,, \qquad q = p_1 - p_2\,, \tag{C.6}$$

$$S_\sigma = \frac{m_\sigma^2}{M_W^2}, \qquad \lambda_j = \frac{m_j^2}{M^2}\,, \qquad r = \frac{q^2}{M_W^2}\,, \tag{C.7}$$

where m_σ is the mass of the charged lepton ℓ_σ ($\sigma = e, \mu, \tau$); $j = 1, \ldots, n_g + n'$ runs over neutrinos and m_j is the mass of the Majorana neutrino ν_j or N_j (or quark q_j); finally, p_1 and p_2 are the momenta of external leptons ℓ_α and ℓ_β, respectively.

The calculations were performed following the procedure outlined in Appendix A in the t′ Hooft-Feynman gauge ($\xi_{W,Z,A} = 1$). We also define new useful notation for integrals:

$$\text{Int}\left[f(x)\right] \equiv \int_0^1 dx\, f(x)\,, \tag{C.8}$$

$$\text{Int}\left[f(x,y)\right] \equiv \int_0^1 dx \int_0^1 dy\, f(x,y)\,, \tag{C.9}$$

$$\text{Int}\left[f(x,y,z)\right] \equiv \int_0^1 dx \int_0^1 dy \int_0^1 dz\, f(x,y,z)\,. \tag{C.10}$$

Finally, note that the matrix U in the type I seesaw corresponds to the full neutrino mixing matrix, namely the combined result of the rotations in Eqs. (3.38) and (3.44):

$$U \equiv \begin{pmatrix} V & S \\ R & T \end{pmatrix} \begin{pmatrix} U_L^\nu & 0 \\ 0 & U_L^N \end{pmatrix} = \begin{pmatrix} VU_L^\nu & SU_L^N \\ RU_L^\nu & TU_L^N \end{pmatrix}\,. \tag{C.11}$$

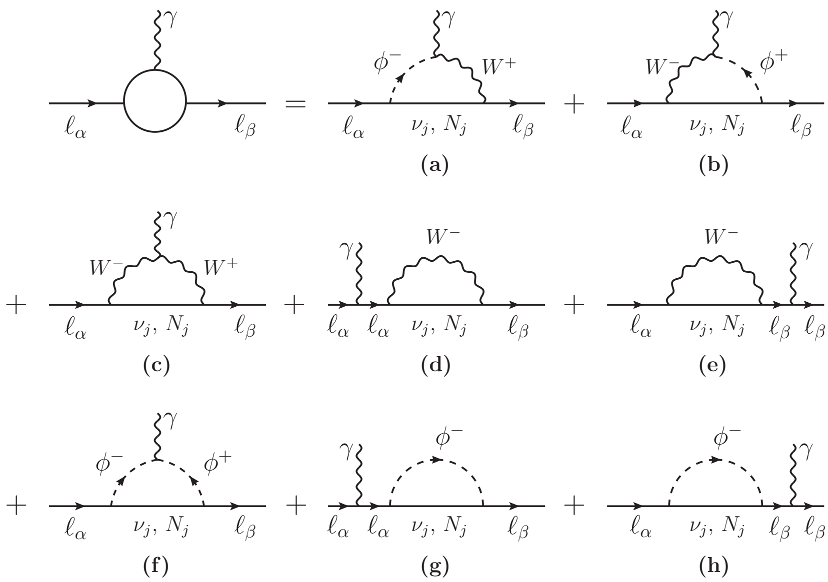

Figure C.1: One-loop contributions to the effective vertex $\overline{\ell_\beta}\ell_\alpha\gamma$ ($\ell_\alpha \neq \ell_\beta$) in the Type I Seesaw scenario.

C.1 Photon-exchange diagrams

The diagrams which, at one-loop order, contribute to the effective vertex $\overline{\ell_\beta}\ell_\alpha\gamma$ ($\ell_\alpha \neq \ell_\beta$) are shown in Fig. C.1. We assume that ℓ_α and ℓ_β are on-shell but the photon is allowed to be off-shell. Using the Feynman rules in Appendix B, and defining the effective vertex $\overline{\ell_\beta}\ell_\alpha\gamma$ as

$$ie\Lambda^\gamma_\mu \;=\; ie\sum_{m=a}^{h}\Lambda^{(r)}_\mu\,, \tag{C.12}$$

the expressions for $\Lambda^{(r)}_\mu$ are [omitting the external spinors $\overline{u}(p_2,m_\beta)$ and $u(p_1,m_\alpha)$]:

$$i\Lambda^{(a)}_\mu = \frac{g^2}{2}U_{\beta j}U^*_{\alpha j}\int\frac{d^dk}{(2\pi)^d}\frac{(\gamma_\mu P_L)\left(\not{k}+\not{p}_1+m_j\right)(m_jP_L-m_\alpha P_R)}{\left[(k+p_1)^2-m_j^2\right][(k+p_1-p_2)^2-M_W^2]\,[k^2-M_W^2]}\;; \tag{C.13}$$

$$i\Lambda^{(b)}_\mu = \frac{g^2}{2}U_{\beta j}U^*_{\alpha j}\int\frac{d^dk}{(2\pi)^d}\frac{(m_jP_R-m_\beta P_L)\left(\not{k}+\not{p}_1+m_j\right)(\gamma_\mu P_L)}{\left[(k+p_1)^2-m_j^2\right][k^2-M_W^2]\,[(k+p_1-p_2)^2-M_W^2]}\;; \tag{C.14}$$

$$\begin{aligned} i\Lambda^{(c)}_\mu &= -\frac{g^2}{2}U_{\beta j}U^*_{\alpha j}\int\frac{d^dk}{(2\pi)^d}\frac{(\gamma_\rho P_L)\left(\not{k}+\not{p}_1+m_j\right)(\gamma_\sigma P_L)\,\Gamma^{\sigma\rho}_\mu(-k,k+q,-q)}{\left[(k+p_1)^2-m_j^2\right][k^2-M_W^2]\,[(k+p_1-p_2)^2-M_W^2]}\,,\\ &\text{with}\qquad \Gamma^{\sigma\rho}_\mu(p_-,p_+,q)\equiv g^{\sigma\rho}(p_--p_+)_\mu+g^{\rho\mu}(p_+-q)_\sigma+g^{\mu\sigma}(q-p_-)_\rho\;; \end{aligned} \tag{C.15}$$

$$i\Lambda^{(d)}_\mu = -\frac{g^2}{2}U_{\beta j}U^*_{\alpha j}\int\frac{d^dk}{(2\pi)^d}\frac{(\gamma_\rho P_L)\left(\not{k}+\not{p}_2+m_j\right)(\gamma^\rho P_L)\left(\not{p}_2+m_\alpha\right)\gamma_\mu}{\left[(k+p_2)^2-m_j^2\right][k^2-M_W^2]\left[m_\beta^2-m_\alpha^2\right]}\;; \tag{C.16}$$

$$i\Lambda^{(e)}_\mu = -\frac{g^2}{2}U_{\beta j}U^*_{\alpha j}\int\frac{d^dk}{(2\pi)^d}\frac{\gamma_\mu\left(\not{p}_1+m_\beta\right)(\gamma_\rho P_L)\left(\not{k}+\not{p}_1+m_j\right)(\gamma^\rho P_L)}{\left[(k+p_1)^2-m_j^2\right][k^2-M_W^2]\left[m_\alpha^2-m_\beta^2\right]}\;; \tag{C.17}$$

$$i\Lambda_\mu^{(f)} = -\frac{g^2}{2}U_{\beta j}U^*_{\alpha j}\int\frac{d^dk}{(2\pi)^d}\frac{(m_jP_R - m_\beta P_L)\left(\not{p}_1 + \not{k} + m_\beta\right)(m_jP_L - m_\alpha P_R)(2k+q)_\mu}{\left[(k+p_1)^2 - m_j^2\right][k^2 - M_W^2][(k+q)^2 - M_W^2]}\ ; \tag{C.18}$$

$$i\Lambda_\mu^{(g)} = \frac{g^2}{2}U_{\beta j}U^*_{\alpha j}\int\frac{d^dk}{(2\pi)^d}\frac{(m_jP_R - m_\beta P_L)\left(\not{k} + \not{p}_2 + m_j\right)(m_jP_L - m_\alpha P_R)\left(\not{p}_2 + m_\alpha\right)\gamma_\mu}{\left[(k+p_2)^2 - m_j^2\right][k^2 - M_W^2]\left[m_\beta^2 - m_\alpha^2\right]}\ ; \tag{C.19}$$

$$i\Lambda_\mu^{(h)} = \frac{g^2}{2}U_{\beta j}U^*_{\alpha j}\int\frac{d^dk}{(2\pi)^d}\frac{\gamma_\mu\left(\not{p}_1 + m_\beta\right)(m_jP_R - m_\beta P_L)\left(\not{k} + \not{p}_1 + m_j\right)(m_jP_L - m_\alpha P_R)}{\left[(k+p_1)^2 - m_j^2\right][k^2 - M_W^2]\left[m_\alpha^2 - m_\beta^2\right]}\ . \tag{C.20}$$

Applying the procedure outlined in Appendix A, we then obtain the intermediate expressions:

$$\Lambda_\mu^{(a)} = -\frac{g^2}{32\pi^2}U^*_{\alpha j}U^*_{l'j}\left[-m_j^2P_R\gamma_\mu\int_0^1\frac{dx\,dy\,y}{D_3(x,y)} + m_\alpha P_R\gamma_\mu\int_0^1\frac{dx\,dy}{D_3(x,y)}y^2\overline{\not{p}}\right]\ ; \tag{C.21}$$

$$\Lambda_\mu^{(b)} = -\frac{g^2}{32\pi^2}U^*_{\alpha j}U^*_{l'j}\left[-m_j^2P_R\gamma_\mu\int_0^1\frac{dx\,dy\,y}{D_3(x,y)} + m_\beta\int_0^1\frac{dx\,dy}{D_3(x,y)}y^2\overline{\not{p}}P_R\gamma_\mu\right]\ ; \tag{C.22}$$

$$\begin{aligned}\Lambda_\mu^{(c)} = &-\frac{g^2}{32\pi^2}U^*_{\alpha j}U^*_{l'j}\left[-\gamma_\mu P_L\left\{3\Delta_\epsilon - 2 - 6\int_0^1 dx\,dy\,y\ln\left[\frac{D_3(x,y)}{M_W^2}\right]\right\}\right.\\ &\left.+ P_R\int_0^1\frac{dx\,dy\,y^2}{D_3(x,y)}\left\{\left(\not{p}_2 - 2\not{p}_1 + y\overline{\not{p}}\right)\overline{\not{p}}\gamma_\mu - 2(p_1+p_2-2y\overline{p})_\mu\overline{\not{p}} + \gamma_\mu\overline{\not{p}}(\not{p}_1 - 2\not{p}_2 + y\overline{\not{p}})\right\}\right]\ ;\end{aligned} \tag{C.23}$$

$$\begin{aligned}\Lambda_\mu^{(d)} = &\ \frac{g^2}{32\pi^2}U_{\alpha j}U^*_{\beta j}\left[m_j^2\left(m_\alpha P_R + m_\beta P_L\right)\left\{\Delta_\epsilon - \int_0^1 dx\ln\left[\frac{D_{2\beta}(x)}{M_W^2}\right]\right\}\right.\\ &\left.-\frac{\not{p}_2}{2}\left(m_j^2P_R + m_\alpha m_\beta P_L\right)\left(\Delta_\epsilon - 2\int_0^1 dx(1-x)\ln\left[\frac{D_{2\beta}(x)}{M_W^2}\right]\right)\right]\frac{\not{p}_2 + m_\alpha}{m_\beta^2 - m_\alpha^2}\gamma_\mu\ ;\end{aligned} \tag{C.24}$$

$$\begin{aligned}\Lambda_\mu^{(e)} = &\ \frac{g^2}{32\pi^2}U_{\alpha j}U^*_{\beta j}\gamma_\mu\frac{\not{p}_1 + m_\beta}{m_\alpha^2 - m_\beta^2}\left[m_j^2\left(m_\alpha P_R + m_\beta P_L\right)\left\{\Delta_\epsilon - \int_0^1 dx\ln\left[D_{2\alpha}(x)\right]\right\}\right.\\ &\left.\frac{\not{p}_1}{2}\left(m_j^2P_R + m_\alpha m_\beta P_L\right)\left(\Delta_\epsilon - 2\int_0^1 dx(1-x)\ln\left[\frac{D_{2\alpha}(x)}{M_W^2}\right]\right)\right]\ ;\end{aligned} \tag{C.25}$$

$$\begin{aligned}\Lambda_\mu^{(f)} = &-\frac{g^2}{32\pi^2M_W^2}U_{\alpha j}U^*_{\beta j}\left[m_j^2\left(m_\alpha P_R + m_\beta P_L\right)\int_0^1\frac{dx\,dy\,y}{D_3(x,y)}(p_1+p_2-2y\overline{p})_\mu\right.\\ &-\frac{1}{2}\left(m_j^2P_R + m_\alpha m_\beta P_L\right)\gamma_\mu\left(\Delta_\epsilon - 2\int_0^1 dx\,dy\,y\ln\left[\frac{D_3(x,y)}{M_W^2}\right]\right)\\ &\left.-\left(m_j^2P_R + m_\alpha m_\beta P_L\right)\int_0^1\frac{dx\,dy\,y^2}{D_3(x,y)}(p_1+p_2-2y\overline{p})_\mu\overline{\not{p}}\right]\ ;\end{aligned} \tag{C.26}$$

$$\Lambda_\mu^{(g)} = -\frac{g^2}{32\pi^2} U^*_{\alpha j} U^*_{l'j} \left[\Delta_\epsilon - 2\int_0^1 dx(1-x) \ln \left[\frac{D_{2\beta}(x)}{M_W^2} \right] \right] \not{p}_2 P_L \frac{\not{p}_2 + m_\alpha}{m_\beta^2 - m_\alpha^2} \gamma_\mu \; ; \tag{C.27}$$

$$\Lambda_\mu^{(h)} = -\frac{g^2}{32\pi^2} U^*_{\alpha j} U^*_{l'j} \left[\Delta_\epsilon - 2\int_0^1 dx(1-x) \ln \left[\frac{D_{2\alpha}(x)}{M_W^2} \right] \right] \gamma_\mu \frac{\not{p}_1 + m_\beta}{m_\alpha^2 - m_\beta^2} \not{p}_1 P_L \; . \tag{C.28}$$

It is easy to check that these results are in accordance with the ones reported in Appendix B of Ref. [192]. From the above results, one can see that divergences appear in $\Lambda_\mu^{(i)}$ for $i = c, ..., h$. The divergences in diagrams (c), (d) and (e) vanish explicitly due to the unitarity of the (full) neutrino mixing matrix, $\sum_{j=1}^{3+N_s} U_{\mu j} U_{\beta j} = 0 \, (\mu \neq \beta)$, while the ones in $\Lambda_\mu^{(f)}$, $\Lambda_\mu^{(g)}$ and $\Lambda_\mu^{(h)}$ cancel each other.

Carrying out integrations keeping only the leading order terms, we arrive at

$$\Lambda_\mu^\gamma(\lambda) = \sum_{k=a}^{h} \Lambda_\mu^{(k)}(\lambda) = \frac{g^2}{16\pi^2} U_{\alpha j} U^*_{\beta j} P_R \left[F_\gamma(\lambda_j) \left\{ -\frac{q^2}{M_W^2}\gamma_\mu + \frac{\not{q} q_\mu}{M_W^2} \right\} \right. \tag{C.29}$$

$$\left. + \; G_\gamma(\lambda_j) \left\{ \frac{(\not{p}_1 + \not{p}_2)(p_1+p_2)_\mu}{M_W^2} - (S_\alpha + S_\beta)\gamma_\mu - 2\frac{\not{p}_2 \gamma_\mu \not{p}_1}{M_W^2} \right\} \right] \; , \tag{C.30}$$

where the $F_\gamma(x)$ and $G_\gamma(x)$ are functions defined by:

$$F_\gamma(x) = -\frac{x(12 + x - 7x^2)}{12(1-x)^3} - \frac{x^2(12 - 10x + x^2)}{6(1-x)^4} \ln x \; , \tag{C.31}$$

$$G_\gamma(x) = \frac{x(1 - 5x - 2x^2)}{4(1-x)^3} - \frac{3x^3}{2(1-x)^4} \ln x \; . \tag{C.32}$$

Finally, using the Gordon-decomposition identities in the form

$$\overline{u}(p_2) \left[\not{p}_1 (p_1+p_2)_\mu - m_\alpha^2 - \not{p}_2 \gamma_\mu \not{p}_1 \right] u(p_1) \; = m_\alpha \overline{u}(p_2) \, i\sigma_{\mu\rho} q^\rho u(p_1) \; , \tag{C.33}$$

$$\overline{u}(p_2) \left[\not{p}_2 (p_1+p_2)_\mu - m_\beta^2 - \not{p}_2 \gamma_\mu \not{p}_1 \right] u(p_1) \; = m_\beta \overline{u}(p_2) \, i\sigma_{\mu\rho} q^\rho u(p_1) \; , \tag{C.34}$$

we can rewrite the effective coupling in a gauge-covariant way as:

$$\begin{aligned} ie\,\overline{u}(p_2)\, \Lambda_\mu^\gamma(\lambda)\, u(p_1) = i\frac{g^2 e}{32\pi^2 M_W^2} \overline{u}(p_2) \left[F_\gamma^{\alpha\beta} \left(q^2 \gamma_\mu - \not{q} q_\mu \right) P_L \right. \\ \left. - \; i\sigma_{\mu\rho} q^\rho G_\gamma^{\alpha\beta} \left(m_\beta P_L + m_\alpha P_R \right) \right] u(p_1) \; . \end{aligned} \tag{C.35}$$

where $F_\gamma^{\alpha\beta}$ and $G_\gamma^{\alpha\beta}$ are functions of $\lambda_j = m_j^2/M_W^2$ and the mixing matrix U defined by:

$$F_\gamma^{\alpha\beta} \equiv \sum_{j=1}^{n_g+n_s} U_{\alpha j} U^*_{\beta j} F_\gamma(\lambda_j) \; , \tag{C.36}$$

$$G_\gamma^{\alpha\beta} \equiv \sum_{j=1}^{n_g+n_s} U_{\alpha j} U^*_{\beta j} G_\gamma(\lambda_j) \; . \tag{C.37}$$

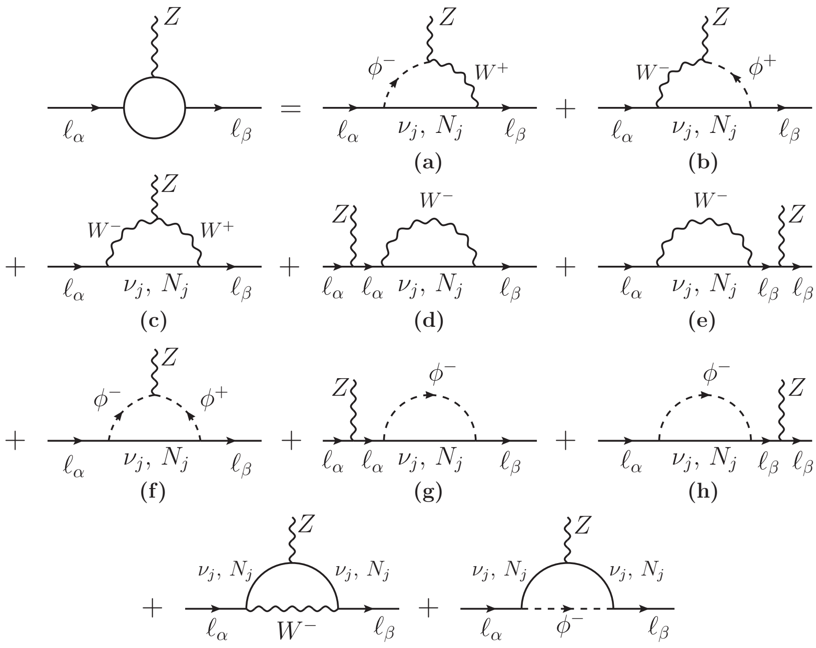

Figure C.2: One-loop contributions to the effective vertex $\overline{\ell_\beta}\ell_\alpha Z$ ($\ell_\beta \neq \ell_\alpha$) in the type I Seesaw scenario.

C.2 Z-boson exchange diagrams

In the type I Seesaw Model, the diagrams which give one-loop corrections to the effective vertex $\overline{\ell_\beta}\ell_\alpha Z$ ($\ell_\beta \neq \ell_\alpha$) are listed in Fig. C.2. The effective vertex of interest to us is defined as

$$i\frac{g}{4\cos\theta_W}\Lambda_\mu^Z = i\frac{g}{4\cos\theta_W}\sum_{m=a}^{k}\Lambda_\mu^{(m)}\,. \tag{C.38}$$

Using the same steps as in the previous case, the contribution of each diagram in Fig. C.2 is:

$$i\Lambda_\mu^{(a)} = -\,2g^2 s_W^2 U_{\beta j}U_{\alpha j}^* \int \frac{d^dk}{(2\pi)^d}\frac{(\gamma_\mu P_L)\left(\not k+\not p_1+m_j\right)(m_jP_L - m_\alpha P_R)}{\left[(k+p_1)^2-m_j^2\right]\left[(k+p_1-p_2)^2-M_W^2\right]\left[k^2-M_W^2\right]}\,; \tag{C.39}$$

$$i\Lambda_\mu^{(b)} = -\,2g^2 s_W^2 U_{\beta j}U_{\alpha j}^* \int \frac{d^dk}{(2\pi)^d}\frac{(m_jP_R - m_\beta P_L)\left(\not k+\not p_1+m_j\right)(\gamma_\mu P_L)}{\left[(k+p_1)^2-m_j^2\right]\left[k^2-M_W^2\right]\left[(k+p_1-p_2)^2-M_W^2\right]}\,; \tag{C.40}$$

$$i\Lambda_\mu^{(c)} = -\,2g^2 c_W^2 U_{\beta j}U_{\alpha j}^* \int \frac{d^dk}{(2\pi)^d}\frac{(\gamma_\rho P_L)\left(\not k+\not p_1+m_j\right)(\gamma_\sigma P_L)\,\Gamma_\mu^{\sigma\rho}(-k,k+q,-q)}{\left[(k+p_1)^2-m_j^2\right]\left[k^2-M_W^2\right]\left[(k+p_1-p_2)^2-M_W^2\right]}\,; \tag{C.41}$$

$$i\Lambda_\mu^{(d)} = -\,g^2 U_{\beta j}U_{\alpha j}^* \int \frac{d^dk}{(2\pi)^d}\frac{(\gamma_\rho P_L)\left(\not k+\not p_2+m_j\right)(\gamma^\rho P_L)\left(\not p_2+m_\alpha\right)\gamma_\mu\left(P_L-2s_W^2\right)}{\left[(k+p_2)^2-m_j^2\right]\left[k^2-M_W^2\right]\left[m_\beta^2-m_\alpha^2\right]}\,; \tag{C.42}$$

$$i\Lambda_\mu^{(e)} = -\,g^2 U_{\beta j}U_{\alpha j}^* \int \frac{d^dk}{(2\pi)^d}\frac{\gamma_\mu\left(P_L-2s_W^2\right)\left(\not p_1+m_\beta\right)(\gamma_\rho P_L)\left(\not k+\not p_1+m_j\right)(\gamma^\rho P_L)}{\left[(k+p_1)^2-m_j^2\right]\left[k^2-M_W^2\right]\left[m_\alpha^2-m_\beta^2\right]}\,; \tag{C.43}$$

$$i\Lambda_\mu^{(f)} = g^2(1-2\,s_W^2)U_{\beta j}U_{\alpha j}^* \int \frac{d^dk}{(2\pi)^d}\frac{(m_jP_R-m_\beta P_L)\left(\not p_1+\not k+m_\beta\right)(m_jP_L-m_\alpha P_R)\,(2k+q)_\mu}{\left[(k+p_1)^2-m_j^2\right]\left[k^2-M_W^2\right]\left[(k+q)^2-M_W^2\right]}\,; \tag{C.44}$$

$$i\Lambda_\mu^{(g)} = g^2 U_{\beta j} U^*_{\alpha j} \int \frac{d^d k}{(2\pi)^d} \frac{(m_j P_R - m_\beta P_L)\left(\not{k} + \not{p}_2 + m_j\right)(m_j P_L - m_\alpha P_R)\left(\not{p}_2 + m_\alpha\right)\gamma_\mu \left(P_L - 2 s_W^2\right)}{\left[(k+p_2)^2 - m_j^2\right]\left[k^2 - M_W^2\right]\left[m_\beta^2 - m_\alpha^2\right]} \; ; \quad \text{(C.45)}$$

$$i\Lambda_\mu^{(h)} = g^2 U_{\beta j} U^*_{\alpha j} \int \frac{d^d k}{(2\pi)^d} \frac{\gamma_\mu \left(P_L - 2 s_W^2\right)\left(\not{p}_1 + m_\beta\right)(m_j P_R - m_\beta P_L)\left(\not{k} + \not{p}_1 + m_j\right)(m_j P_L - m_\alpha P_R)}{\left[(k+p_1)^2 - m_j^2\right]\left[k^2 - M_W^2\right]\left[m_\alpha^2 - m_\beta^2\right]} \; ; \quad \text{(C.46)}$$

$$i\Lambda_\mu^{(k)} = g^2 U_{\beta i} U^*_{\alpha j} C_{ij} \int \frac{d^d k}{(2\pi)^d} \frac{(\gamma_\rho P_L)\left(\not{k} + \not{p}_2 + m_j\right)\gamma_\mu \left(\not{k} + \not{p}_1 + m_i\right)(\gamma^\rho P_L)}{\left[(k+p_2)^2 - m_j^2\right]\left[(k+p_1)^2 - m_i^2\right]\left[k^2 - M_W^2\right]} \; ; \quad \text{(C.47)}$$

$$i\Lambda_\mu^{(l)} = - g^2 U_{\beta i} U^*_{\alpha j} C_{ij} \int \frac{d^d k}{(2\pi)^d} \frac{(m_j P_R - m_\beta P_L)\left(\not{k} + \not{p}_2 + m_j\right)\gamma_\mu \left(\not{k} + \not{p}_1 + m_i\right)(m_i P_L - m_\alpha P_R)}{\left[(k+p_2)^2 - m_j^2\right]\left[(k+p_1)^2 - m_i^2\right]\left[k^2 - M_W^2\right]} \; ; \quad \text{(C.48)}$$

where $\Gamma_\mu^{\rho\sigma}$ is the WWZ vertex defined in Eq. (C.15).

Expressing the above results in terms of integrals $I_{r,n}$, using the results (A.18) to (A.21) and defining $C_{ji} = \sum_{\rho = e,\mu,\tau} U^*_{\rho j} U_{\rho i}$, we are able to obtain the following intermediate expressions for the amplitudes:

$$\Lambda_\mu^{(a)} = -\frac{g^2 s_W^2}{8\pi^2} U^*_{\alpha j} U^*_{l' j} \left[-m_j^2 P_R \gamma_\mu \int_0^1 \frac{dx\, dy\, y}{D_3(x,y)} + m_\alpha P_R \gamma_\mu \int_0^1 \frac{dx\, dy}{D_3(x,y)} y^2 \not{\overline{p}} \right] , \quad \text{(C.49)}$$

$$\Lambda_\mu^{(b)} = -\frac{g^2 s_W^2}{8\pi^2} U^*_{\alpha j} U^*_{l' j} \left[-m_j^2 P_R \gamma_\mu \int_0^1 \frac{dx\, dy\, y}{D_3(x,y)} + m_\beta \int_0^1 \frac{dx\, dy}{D_3(x,y)} y^2 \not{\overline{p}} P_R \gamma_\mu \right] , \quad \text{(C.50)}$$

$$\begin{aligned}\Lambda_\mu^{(c)} = &\frac{g^2 c_W^2}{8\pi^2} U^*_{\alpha j} U^*_{l' j} \left\{ -\gamma_\mu P_L \left(3\Delta_\epsilon - 2 - 6 \int_0^1 dx\, dy\, y \ln\left[\frac{D_3(x,y)}{M_W^2}\right] \right) \right. \\ &\left. + P_R \int_0^1 \frac{dx\, dy\, y^2}{D_3(x,y)} \left[\left(\not{p}_2 - 2\not{p}_1 + y\not{\overline{p}}\right)\not{\overline{p}}\gamma_\mu - 2(p_1 + p_2 - 2y\overline{p})_\mu \not{\overline{p}} + \gamma_\mu \not{\overline{p}}(\not{p}_1 - 2\not{p}_2 + y\not{\overline{p}}) \right] \right\} , \end{aligned} \quad \text{(C.51)}$$

$$\begin{aligned}\Lambda_\mu^{(d)} = &- \frac{g^2}{16\pi^2} U_{\alpha j} U^*_{\beta j} \left\{ -\frac{\not{p}_2}{2}\left(m_j^2 P_R + m_\alpha m_\beta P_L\right)\left(\Delta_\epsilon - \int_0^1 dx (1-x) \ln\left[\frac{D_{2\beta}(x)}{M_W^2}\right]\right) \right. \\ &\left. + m_j^2 \left(m_\alpha P_R + m_\beta P_L\right)\left(\Delta_\epsilon - \int_0^1 dx \ln\left[\frac{D_{2\beta}(x)}{M_W^2}\right]\right) \right\} \frac{\not{p}_2 + m_\alpha}{m_\beta^2 - m_\alpha^2} \gamma_\mu \left(P_L - 2\sin^2\theta_W\right) , \end{aligned} \quad \text{(C.52)}$$

$$\begin{aligned}\Lambda_\mu^{(e)} = &-\frac{g^2 U_{\alpha j} U^*_{\beta j}}{16\pi^2} \gamma_\mu \left(P_L - 2 s_W^2\right) \frac{\not{p}_1 + m_\beta}{m_\alpha^2 - m_\beta^2} \left\{ m_j^2 \left(m_\alpha P_R + m_\beta P_L\right) \times \left(\Delta_\epsilon - \int_0^1 dx \ln\left[\frac{D_{2\alpha}(x)}{M_W^2}\right]\right) \right. \\ &\left. -\frac{\not{p}_1}{2}\left(m_j^2 P_R + m_\alpha m_\beta P_L\right) \times \left(\Delta_\epsilon - 2\int_0^1 dx (1-x) \ln\left[\frac{D_{2\alpha}(x)}{M_W^2}\right]\right) \right\} , \end{aligned} \quad \text{(C.53)}$$

$$\begin{aligned}\Lambda_\mu^{(f)} = &\frac{g^2}{16\pi^2 M_W^2} U_{\alpha j} U^*_{\beta j} \left(1 - 2 s_W^2\right) \left\{ m_j^2 \left(m_\alpha P_R + m_\beta P_L\right) \int_0^1 \frac{dx\, dy\, y}{D_3(x,y)} (p_1 + p_2 - 2y\overline{p})_\mu \right. \\ &\left. - \frac{1}{2}\left(m_j^2 P_R + m_\alpha m_\beta P_L\right)\gamma_\mu \left(\Delta_\epsilon - 2\int_0^1 dx\, dy\, y \ln\left[\frac{D_3(x,y)}{M_W^2}\right]\right) + 2\int_0^1 \frac{dx\, dy\, y^2}{D_3(x,y)} (p_1 + p_2 - 2y\overline{p})_\mu \not{\overline{p}} \right\} , \end{aligned} \quad \text{(C.54)}$$

$$\Lambda_\mu^{(g)} = \frac{g^2}{16\pi^2} U^*_{\alpha j} U^*_{l' j} \left\{ \Delta_\epsilon - 2\int_0^1 dx (1-x) \ln\left[\frac{D_{2\beta}(x)}{M_W^2}\right] \right\} \not{p}_2 P_L \frac{\not{p}_2 + m_\alpha}{m_\beta^2 - m_\alpha^2} \gamma_\mu \left(P_L - 2 s_W^2\right) , \quad \text{(C.55)}$$

$$\Lambda_\mu^{(h)} = \frac{g^2}{16\pi^2} U^*_{\alpha j} U^*_{l' j} \left\{ \Delta_\epsilon - 2\int_0^1 dx (1-x) \ln\left[\frac{D_{2\alpha}(x)}{M_W^2}\right] \right\} \gamma_\mu \left(P_L - 2\sin^2\theta_W\right) \frac{\not{p}_1 + m_\beta}{m_\alpha^2 - m_\beta^2} \not{p}_1 P_L \,, \quad \text{(C.56)}$$

$$\Lambda_\mu^{(k)} = \frac{g^2 U_{\alpha j} C_{ji} U^*_{\beta i}}{16\pi^2} P_R \left\{ \int_0^1 \frac{dx\, dy^2}{D_{3F(x,y)}} (\not{p}_1 - y\not{p})\gamma_\mu(\not{p}_2 - y\not{p}) + \gamma_\mu \left[\Delta_\epsilon - 1 - \int_0^1 dx\, dy^2 \ln D_{3F}(x,y)\right]\right\} \,, \quad \text{(C.57)}$$

$$\begin{aligned}\Lambda_\mu^{(l)} = \frac{g^2}{16\pi^2} U_{\alpha j} C_{ji} U^*_{\beta i} \Bigg\{ & -m_j^2 m_i^2 \gamma_\mu P_L \int_0^1 \frac{dx\, dy\, y}{D_{3F}(x,y)} + m_\beta m_j^2 \int_0^1 \frac{dx\, dy\, y}{D_{3F}(x,y)} (\not{p}_2 - y\not{p})\gamma_\mu P_L \\ & + m_\alpha m_j^2 \gamma_\mu P_L \int_0^1 \frac{dx\, dy\, y}{D_{3F}(x,y)} (\not{p}_1 - y\not{p}) - m_\alpha m_\beta P_L \int_0^1 \frac{dx\, dy\, y}{D_{3F}(x,y)} (\not{p}_2 - y\not{p})\gamma_\mu(\not{p}_1 - y\not{p}) \quad \text{(C.58)} \\ & - \frac{m_\alpha m_\beta \gamma_\mu P_R}{2}\left[\Delta_\epsilon - 1 - 2\int_0^1 dx\, dy\, y \ln D_{3F}(x,y)\right]\Bigg\} \,.\end{aligned}$$

Again, the above results confirm those in Appendix B of [192] and show that there are no overall divergences. Indeed, the unitarity of the neutrino mixing matrix ensures that divergences in diagrams (e), (l) and (k) vanish explicitly, while the remaining cancel each other:

$$\mathrm{Div}\left(\Lambda_\mu^{(d)}\right) + \mathrm{Div}\left(\Lambda_\mu^{(e)}\right) = 0 \,, \quad \text{(C.59)}$$

$$\mathrm{Div}\left(\Lambda_\mu^{(f)}\right) + \mathrm{Div}\left(\Lambda_\mu^{(g)}\right) + \mathrm{Div}\left(\Lambda_\mu^{(h)}\right) = 0 \,. \quad \text{(C.60)}$$

Simplifying the results and carrying out integrations at leading order, the results read:

$$\sum_{m=a}^{h} \Lambda_\mu^{(m)} = -\frac{g^2}{8\pi^2} U_{\alpha j} U^*_{\beta j} F_Z(\lambda_j)\gamma_\mu P_L \,, \qquad \Lambda_\mu^{(k)} + \Lambda_\mu^{(l)} = -\frac{g^2}{8\pi^2} U_{\alpha j} C_{ji} U^*_{\beta i} G_Z(\lambda_j)\gamma_\mu P_L \,, \quad \text{(C.61)}$$

where $F_Z(x)$ and $G_Z(x,y)$ are defined by

$$F_Z(x) = -\frac{5x}{2(1-x)} - \frac{5x^2}{2(1-x)^2} \ln x \,, \quad \text{(C.62)}$$

$$G_Z(x,y) = -\frac{1}{2(x-y)}\left[\frac{x^2(1-y)}{(1-x)} \ln x - \frac{y^2(1-x)}{(1-y)} \ln y\right] \,. \quad \text{(C.63)}$$

Combining the above results, we can finally write the effective $\overline{\ell_\beta}\ell_\alpha Z$ vertex as:

$$\frac{g}{4\cos\theta_W}\Lambda_\mu^Z = -\frac{g^3 F_Z^{\alpha\beta}}{32\pi^2\cos\theta_W}\gamma_\mu P_L \,, \qquad F_Z^{\alpha\beta} \equiv \sum_{j,i=1}^{n_g+n_s} U_{\alpha j} U^*_{\beta i}\left[\delta_{ji} F_Z(\lambda_j) + C_{ji} G_Z(\lambda_j, \lambda_i)\right] \,, \quad \text{(C.64)}$$

Finally, note that in the limit of a degenerate mass spectrum, $m_{N_1} = m_{N_2} = ... \equiv m_N$, and for $m_N \gg M_W$, the form factor $F_Z^{\alpha\beta}$ in the previous expression simplifies to

$$F_Z^{\alpha\beta} \approx \sum_{j=n_g+1}^{n_g+n_s} U_{\alpha j} U^*_{\beta j} \widetilde{F}_Z \,, \quad \text{with} \quad \widetilde{F}_Z \equiv \left[F_Z(\lambda_N) + 2G_Z(0,\lambda_N)\right] \quad \text{and} \quad \lambda_N \equiv \frac{m_N^2}{M_W^2} \,, \quad \text{(C.65)}$$

in agreement with Ref. [172].

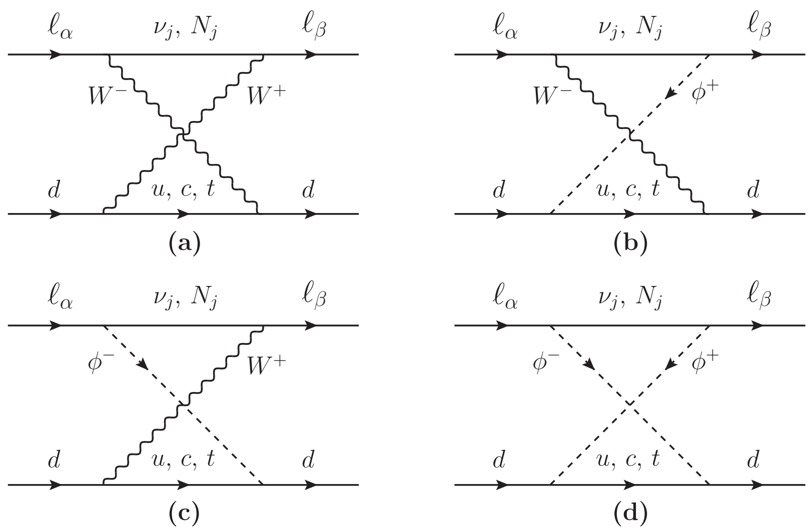

Figure C.3: d-box type diagrams that contribute at one-loop order to μ-e conversion in nuclei and to $\mu \to \ell_j^- \ell_j^- \ell_k^+$ decays, in the type I seesaw scenario.

C.3 Calculation of box diagrams

In this section we outline the calculation of the box diagrams that contribute at one-loop order to μ-e conversion in nuclei and to $\mu \to \ell_j^- \ell_j^- \ell_k^+$ in the type I Seesaw model. In u-type diagrams (Fig. C.4) participate virtual quarks (d, s, b), while the quarks taking part in d-type diagrams are (u, c, t) (Fig. C.3). It is important to remark that the final result for d-type diagrams remains valid when the d-quark is replaced by charged leptons and virtual (u, c, t) quarks by neutrinos, in which case the quark mixing matrix $V \equiv V_{\text{CKM}}$ is replaced by the leptonic mixing matrix U in Eq. (C.11).

A similar notation to Ref. [172] is used in our final results, which are in complete agreement with it.

C.3.1 d-type box diagrams

At one-loop order, the relevant d-box diagrams are the ones represented in Fig. C.3. Using the Feynman rules in Appendix B, the invariant amplitude $i\Lambda_d^{(r)}$ of each diagram is:

$$\begin{aligned} i\Lambda_d^{(a)} =& \frac{g^4}{4} U_{\alpha j}^* U_{\beta j} V_{du_i} V_{du_i}^* \int \frac{d^4k}{(2\pi)^4} \frac{\left[\overline{u}(p_2)\,(\gamma_\rho P_L)\,\left(\not{k} + \not{p}_1 + m_j\right)(\gamma_\sigma P_L)\, u(p_1)\right]}{\left[(k+p_1)^2 - m_j^2\right]\left[k^2 - M_W^2\right]} \\ & \times \frac{\left[\overline{u}(p_4)\,(\gamma^\sigma P_L)\,\left(\not{k} + \not{p}_4 + m_i\right)(\gamma^\rho P_L)\, u(p_3)\right]}{\left[(k+p_4)^2 - m_i^2\right]\left[(k+p_2-p_1)^2 - M_W^2\right]}\,; \end{aligned} \tag{C.66}$$

$$\begin{aligned} i\Lambda_d^{(b)} =& -\frac{g^4 U_{\alpha j}^* U_{\beta j} V_{du_i} V_{du_i}^*}{4} \int \frac{d^4k}{(2\pi)^4} \frac{\left[\overline{u}(p_2)\,(m_j P_R - m_\beta P_L)\,\left(\not{k} + \not{p}_1 + m_j\right)(\gamma_\rho P_L)\, u(p_1)\right]}{\left[(k+p_1)^2 - m_j^2\right]\left[k^2 - M_W^2\right]} \\ & \times \frac{\left[\overline{u}(p_4)\,(\gamma^\rho P_L)\,\left(\not{k} + \not{p}_4 + m_i\right)(m_i P_L - m_\alpha P_R)\, u(p_3)\right]}{\left[(k+p_4)^2 - m_i^2\right]\left[(k+p_2-p_1)^2 - M_W^2\right]}\,; \end{aligned} \tag{C.67}$$

$$i\Lambda_d^{(c)} = -\frac{g^4 U^*_{\alpha j} U_{\beta j} V_{du_i} V^*_{du_i}}{4} \int \frac{d^4k}{(2\pi)^4} \frac{\left[\overline{u}(p_2)\,(\gamma_\rho P_L)\,\left(\not{k} + \not{p}_1 + m_j\right)(m_j P_L - m_\alpha P_R)\, u(p_1)\right]}{\left[(k+p_1)^2 - m_j^2\right]\left[k^2 - M_W^2\right]}$$
$$\times \frac{\left[\overline{u}(p_4)\,(m_i P_R - m_\beta P_L)\left(\not{k} + \not{p}_4 + m_i\right)(\gamma_\rho P_L)\, u(p_3)\right]}{\left[(k+p_4)^2 - m_i^2\right]\left[(k+p_2-p_1)^2 - M_W^2\right]} \; ; \tag{C.68}$$

$$i\Lambda_d^{(d)} = \frac{g^4 U^*_{\alpha j} U_{\beta j} V_{du_i} V^*_{du_i}}{4} \int \frac{d^4k}{(2\pi)^4} \frac{\overline{u}(p_2)\,(m_j P_R - m_\beta P_L)\left(\not{k} + \not{p}_1 + m_j\right)(m_j P_L - m_\alpha P_R)\, u(p_1)}{\left[(k+p_1)^2 - m_j^2\right]\left[k^2 - M_W^2\right]}$$
$$\times \frac{\overline{u}(p_4)\,(m_i P_R - m_\beta P_L)\left(\not{k} + \not{p}_4 + m_i\right)(m_i P_L - m_\alpha P_R)\, u(p_3)}{\left[(k+p_4)^2 - m_i^2\right]\left[(k+p_2-p_1)^2 - M_W^2\right]} \; . \tag{C.69}$$

where m_j is the mass of Majorana neutrinos ν_j or N_j, and m_i is the mass of the virtual quark u_i.

Using dimensional regularisation and simplifying the result neglecting external masses, we are able to get the following intermediate expressions:

$$\Lambda_d^{(a)} = \frac{g^4}{32\pi^2} U_{\alpha j} U^*_{\beta j} V_{du_i} V^*_{du_i} \int_0^1 dx\, dy\, dz\, \frac{z(z-1)}{D_4(x,y,z)} \left[\overline{u}\,(p_4)\,\gamma_\rho P_L u\,(p_3)\right]\left[\overline{u}\,(p_2)\,\gamma^\rho P_L u\,(p_1)\right] \; ; \tag{C.70}$$

$$\Lambda_d^{(b,\,c)} = \frac{g^4 m_j^2 m_i^2}{64\pi^2 M_W^2} U_{\alpha j} U^*_{\beta j} V_{du_i} V^*_{du_i} \int_0^1 dx\, dy\, dz\, \frac{z(z-1)}{D_4^2(x,y,z)} \left[\overline{u}\,(p_4)\,\gamma_\rho P_L u\,(p_3)\right]\left[\overline{u}\,(p_2)\,\gamma^\rho P_L u\,(p_1)\right] \; ; \tag{C.71}$$

$$\Lambda_d^{(d)} = \frac{g^4}{128\pi^2 M_W^4} U_{\alpha j} U^*_{\beta j} V_{du_i} V^*_{du_i} \int_0^1 dx\, dy\, dz\, \frac{z(z-1)}{D_4^2(x,y,z)} \left[\overline{u}\,(p_4)\,\gamma_\rho P_L u\,(p_3)\right]\left[\overline{u}\,(p_2)\,\gamma^\rho P_L u\,(p_1)\right] \; . \tag{C.72}$$

Performing integrations and summing up the above contributions, we then arrive at the final expression for the d-type box diagrams:

$$\Lambda_d = \frac{g^4}{64\pi^2} \left[\overline{u}\,(p_4)\,\gamma_\rho P_L u\,(p_3)\right]\left[\overline{u}\,(p_2)\,\gamma^\rho P_L u\,(p_1)\right] F^{\alpha\beta dd}_{\text{dBox}} \; , \tag{C.73}$$

where the newly introduced form factor $F^{\alpha\beta dd}_{\text{dBox}}$ is defined by:

$$F^{\alpha\beta dd}_{\text{Box}} \equiv U_{\alpha j} U^*_{\beta j} V_{du_i} V^*_{du_i} F_{d\,\text{Box}}(\lambda_j, \lambda_i) \; , \tag{C.74}$$

$$F_{d\,\text{Box}}(x,y) = -\frac{1}{1-x} \left\{ \left(1 + \frac{xy}{4}\right) \left[\frac{1}{x-y} + \frac{x^2}{(1-x)^2} \ln x - \frac{1}{1-y} - \frac{y^2}{(1-y)^2} \ln y\right] \right.$$
$$\left. -\; 2xy \left[\frac{1}{x-y} + \frac{x}{(1-x)^2} \ln x - \frac{1}{1-y} - \frac{y}{(1-y)^2} \ln y\right] \right\} \; . \tag{C.75}$$

Finally, note that in the limit of a degenerate mass spectrum, $m_{N_1} = m_{N_2} = ... \equiv m_N$, and for $m_N \gg M_W$, the form factor $F^{\alpha\beta dd}_{\text{dBox}}$ in the previous expression simplifies to

$$F^{\alpha\beta dd}_{\text{Box}} \approx \sum_{j=n_g+1}^{n_g+n_s} U_{\alpha j} U^*_{\beta j} \widetilde{F}_{\text{dBox}} \; , \qquad \text{with} \qquad \widetilde{F}_{\text{dBox}} \equiv \left[F_{\text{dBox}}(\lambda_N, 0) - F_{\text{dBox}}(0,0)\right] \; . \tag{C.76}$$

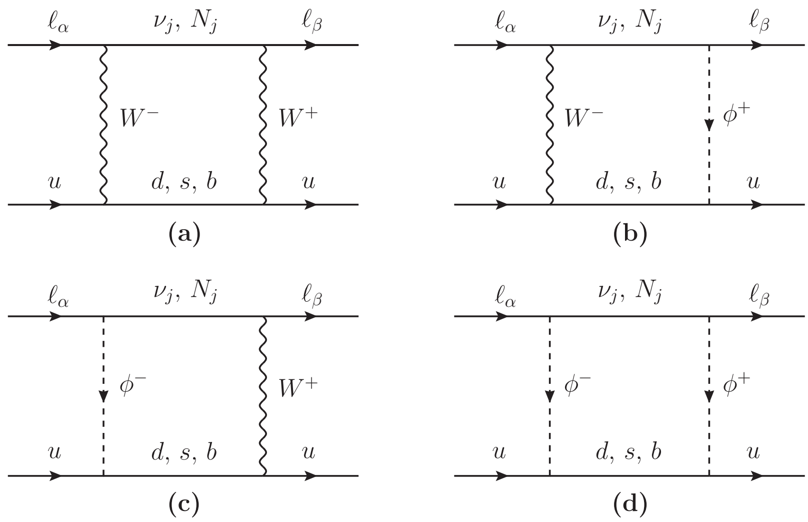

Figure C.4: u-box type diagrams that contribute at one-loop order to μ-e conversion and to $\mu \to \ell_j^- \ell_j^- \ell_k^+$, in the type I Seesaw scenario.

C.3.2 u-type box diagrams

The relevant u-box diagrams are shown in Fig. C.4. Similarly to the calculation of d-box diagrams, the invariant amplitude $i\Lambda_u^{(r)}$ of each u-box diagram is:

$$\begin{aligned} i\Lambda_u^{(a)} =& \frac{g^4}{4} U^*_{\alpha j} U_{\beta j} V_{ud_i} V^*_{ud_i} \int \frac{d^4k}{(2\pi)^4} \frac{\left[\overline{u}(p_2)\,(\gamma_\rho P_L)\,\left(\not{k} + \not{p}_1 + m_j\right)(\gamma_\sigma P_L)\,u(p_1)\right]}{\left[(k+p_1)^2 - m_j^2\right]\left[k^2 - M_W^2\right]} \\ & \times \frac{\left[\overline{u}(p_4)\,(\gamma^\rho P_L)\,\left(\not{p}_3 - \not{k} + m_i\right)(\gamma^\sigma P_L)\,u(p_3)\right]}{\left[(p_3-k)^2 - m_i^2\right]\left[(k+p_1-p_2)^2 - M_W^2\right]}\;; \end{aligned} \tag{C.77}$$

$$\begin{aligned} i\Lambda_u^{(b)} =& -\frac{g^4 U^*_{\alpha j} U_{\beta j} V_{ud_i} V^*_{ud_i}}{4} \int \frac{d^4k}{(2\pi)^4} \frac{\left[\overline{u}(p_2)\,(m_j P_R - m_\beta P_L)\,\left(\not{k} + \not{p}_1 + m_j\right)(\gamma_\rho P_L)\,u(p_1)\right]}{\left[(k+p_1)^2 - m_j^2\right]\left[k^2 - M_W^2\right]} \\ & \times \frac{\left[\overline{u}(p_4)\,(m_u P_L - m_i P_R)\,\left(\not{p}_3 - \not{k} + m_i\right)(\gamma^\rho P_L)\,u(p_3)\right]}{\left[(p_3-k)^2 - m_i^2\right]\left[(k+p_1-p_2)^2 - M_W^2\right]}\;; \end{aligned} \tag{C.78}$$

$$\begin{aligned} i\Lambda_u^{(c)} =& -\frac{g^4 U^*_{\alpha j} U_{\beta j} V_{ud_i} V^*_{ud_i}}{4} \int \frac{d^4k}{(2\pi)^4} \frac{\left[\overline{u}(p_2)\,(\gamma_\rho P_L)\,\left(\not{k} + \not{p}_1 + m_j\right)(m_j P_L - m_\alpha P_R)\,u(p_1)\right]}{\left[(k+p_1)^2 - m_j^2\right]\left[k^2 - M_W^2\right]} \\ & \times \frac{\left[\overline{u}(p_4)\,(\gamma_\rho P_L)\,\left(\not{k} + \not{p}_4 + m_i\right)(m_u P_R - m_i P_L)\,u(p_3)\right]}{\left[(k-p_3)^2 - m_i^2\right]\left[(k+p_1-p_2)^2 - M_W^2\right]}\;; \end{aligned} \tag{C.79}$$

$$\begin{aligned} i\Lambda_u^{(d)} =& \frac{g^4 U^*_{\alpha j} U_{\beta j} V_{ud_i} V^*_{ud_i}}{4} \int \frac{d^4k}{(2\pi)^4} \frac{\overline{u}(p_2)\,(m_j P_R - m_\beta P_L)\,\left(\not{k} + \not{p}_1 + m_j\right)(m_j P_L - m_\alpha P_R)\,u(p_1)}{\left[(k+p_1)^2 - m_j^2\right]\left[k^2 - M_W^2\right]} \\ & \times \frac{\overline{u}(p_4)\,(m_u P_L - m_i P_R)\,\left(\not{k} + \not{p}_4 + m_i\right)(m_u P_R - m_i P_L)\,u(p_3)}{\left[(k-p_3)^2 - m_i^2\right]\left[(k+p_1-p_2)^2 - M_W^2\right]}\;. \end{aligned} \tag{C.80}$$

where m_j is again the mass of Majorana neutrinos and m_i is the mass of virtual quarks d_i.

After applying dimensional regularisation and simplifying the result neglecting external masses, we obtain the intermediate expressions:

$$\Lambda_u^{(a)} = \frac{g^4}{8\pi^2} U_{\alpha j}^* U_{\beta j} V_{ud_i} V_{ud_i}^* \int_0^1 dx\, dy\, dz\, \frac{z(1-z)}{D_4(x,y,z)} \left[\overline{u}\,(p_4)\,\gamma_\rho P_L u\,(p_3)\right] \left[\overline{u}\,(p_2)\,\gamma^\rho P_L u\,(p_1)\right] \,, \tag{C.81}$$

$$\Lambda_u^{(b,\,c)} = \frac{g^4 m_j^2 m_i^2}{64\pi^2 M_W^2} U_{\alpha j}^* U_{\beta j} V_{ud_i} V_{ud_i}^* \int_0^1 dx\, dy\, dz\, \frac{z(1-z)}{D_4^2(x,y,z)} \left[\overline{u}\,(p_4)\,\gamma_\rho P_L u\,(p_3)\right] \left[\overline{u}\,(p_2)\,\gamma^\rho P_L u\,(p_1)\right] \,, \tag{C.82}$$

$$\Lambda_u^{(d)} = \frac{g^4}{128\pi^2 M_W^4} U_{\alpha j}^* U_{\beta j} V_{ud_i} V_{ud_i}^* \int_0^1 dx\, dy\, dz\, \frac{z(1-z)}{D_4^2(x,y,z)} \left[\overline{u}\,(p_4)\,\gamma_\rho P_L u\,(p_3)\right] \left[\overline{u}\,(p_2)\,\gamma^\rho P_L u\,(p_1)\right] \,. \tag{C.83}$$

As for d-type box diagrams, summing up the above contributions and carrying out integrations, we obtain the final expression for u-type box diagrams:

$$\Lambda_u = \frac{g^4}{64\pi^2} \left[\overline{u}\,(p_4)\,\gamma_\rho P_L u\,(p_3)\right] \left[\overline{u}\,(p_2)\,\gamma^\rho P_L u\,(p_1)\right] F_{\text{Box}}^{\alpha\beta uu} \,,$$

where $F_{\text{Box}}(x,\,y)$ is a function defined in an analogous way to Eq. (C.75):

$$F_{\text{Box}}^{\alpha\beta uu} \equiv \sum_{j=1}^{n_g+n_s} \sum_{i=d,s,b} U_{\alpha j} U_{\beta j}^* V_{ud_i} V_{ud_i}^* F_{\text{uBox}}(\lambda_j, \lambda_i) \,, \tag{C.84}$$

$$\begin{aligned} F_{\text{uBox}}(x,y) = \frac{1}{x-y} \Bigg\{ \left(4 + \frac{xy}{4}\right) \left[\frac{1}{x-y} + \frac{x^2}{(1-x)^2}\ln x - \frac{1}{1-y} - \frac{y^2}{(1-y)^2}\ln y\right] \\ - 2xy \left[\frac{1}{x-y} + \frac{x}{(1-x)^2}\ln x - \frac{1}{1-y} - \frac{y}{(1-y)^2}\ln y\right] \Bigg\} \,. \end{aligned} \tag{C.85}$$

Again, in the limit of a degenerate mass spectrum, $m_{N_1} = m_{N_2} = \ldots \equiv m_N$, and for $m_N \gg M_W$, the form factor $F_{\text{Box}}^{\alpha\beta uu}$ in the previous expression simplifies to

$$F_{\text{Box}}^{\alpha\beta uu} \approx \sum_{j=n_g+1}^{n_g+n_s} U_{\alpha j} U_{\beta j}^* \widetilde{F}_{\text{uBox}} \,, \qquad \text{with} \qquad \widetilde{F}_{\text{uBox}} \equiv \left[F_{\text{uBox}}(\lambda_N, 0) - F_{\text{uBox}}(0,0)\right] \,. \tag{C.86}$$

in agreement with the result in Ref. [172].

Finally, note that the result for d-type diagrams remains valid when the d-quark is replaced by a charged lepton ψ and the virtual (u, c, t) quarks by neutrinos. The quark mixing matrix $V \equiv V_{\text{CKM}}$ is then replaced by the leptonic mixing matrix U and, in the interesting case $\psi = \beta$, the relevant function is

$$F_{\text{Box}}^{\alpha\beta\beta\beta} \equiv \sum_{i,j=1}^{n_g+n_s} U_{\alpha j} U_{\beta j}^* U_{\beta i} U_{\beta i}^* F_{\text{dBox}}(\lambda_j, \lambda_i) \tag{C.87}$$

which, in the limit of a quasi-degenerate and large masses regime, $\lambda_j >> 1$, is simplified to:

$$F_{\text{Box}}^{\alpha\beta\beta\beta} \approx -2 \sum_{j=n_g+1}^{n_g+n_s} U_{\alpha j} U_{\beta j}^* \widetilde{F}_{\text{dBox}} \,. \tag{C.88}$$

with $\widetilde{F}_{\text{dBox}}$ defined in Eq. (C.76). This result agrees with that in Ref. [172].

D Type II seesaw form factor calculation

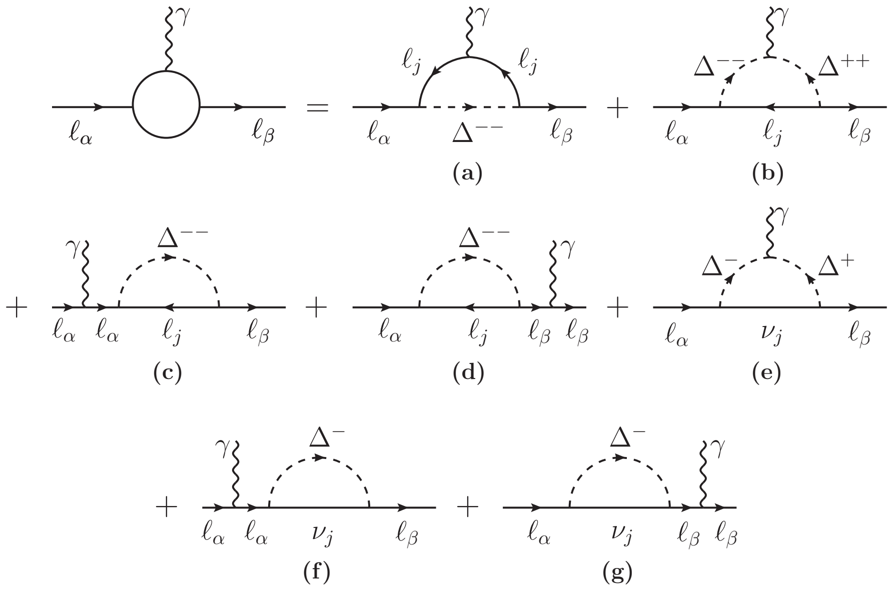

Figure D.1: Diagrams that contribute at one-loop order to the type II seesaw form factor.

In this appendix, we calculate the effective vertex $\overline{\ell_\beta}\ell_\alpha\gamma$ ($\ell_\alpha \neq \ell_\beta$) at one-loop order in the type II seesaw model. This vertex receives contributions from the diagrams shown in Fig. D.1 and, similarly to the type I seesaw scenario, the leptons ℓ_α and ℓ_β are on-shell while the photon is allowed to be off-shell. The definition of the effective vertex $\overline{\ell_\beta}\ell_\alpha\gamma$ is also the same as in the type I seesaw:

$$ie\Lambda_\mu^\gamma = ie\sum_{m=a}^{h}\Lambda_\mu^{(r)}\,. \tag{D.1}$$

Using the Feynman rules in Appendix B, the amplitudes of the diagrams can be written as follows:

$$i\Lambda_\mu^{(a)} = -8\,(Y_\Delta)^*_{\beta\sigma}\,(Y_\Delta)_{\alpha\sigma}\int\frac{d^4k}{(2\pi)^4}\frac{P_R\left(\not{k}+\not{p}_2+m_\sigma\right)\gamma_\mu\left(\not{k}+\not{p}_1+m_\sigma\right)P_L}{[(k+p_2)^2-m_\sigma^2]\,[(k+p_1)^2-m_\sigma^2]\left[k^2-M_{\Delta^{--}}^2\right]}\;; \tag{D.2}$$

$$i\Lambda_\mu^{(b)} = -16\,(Y_\Delta)^*_{\beta\sigma}\,(Y_\Delta)_{\alpha\sigma}\int\frac{d^4k}{(2\pi)^4}\frac{P_R\left(\not{k}+\not{p}_1+m_\sigma\right)P_L\,(2k+q)_\mu}{[(k+p_1)^2-m_\sigma^2]\left[(k+p_1-p_2)^2-M_{\Delta^{--}}^2\right]\left[k^2-M_{\Delta^{--}}^2\right]}\;; \tag{D.3}$$

$$i\Lambda_\mu^{(c)} = 8\,(Y_\Delta)^*_{\beta\sigma}\,(Y_\Delta)_{\alpha\sigma}\int\frac{d^4k}{(2\pi)^4}\frac{P_R\left(\not{k}+\not{p}_2+m_\sigma\right)P_L\left(\not{p}_2+m_\alpha\right)\gamma_\mu}{\left[m_\beta^2-m_\alpha^2\right][(k+p_2)^2-m_\sigma^2]\left[k^2-M_{\Delta^{--}}^2\right]}\;; \tag{D.4}$$

$$i\Lambda_\mu^{(d)} = 8\,(Y_\Delta)^*_{\beta\sigma}\,(Y_\Delta)_{\alpha\sigma}\int \frac{d^4k}{(2\pi)^4}\frac{\gamma_\mu\,(\not{p}_1+m_\beta)\,P_R\,(\not{k}+\not{p}_1+m_\sigma)\,P_L}{\left[m_\alpha^2-m_\beta^2\right]\left[(k+p_1)^2-m_\sigma^2\right]\left[k^2-M^2_{\Delta^{--}}\right]}\;; \tag{D.5}$$

$$i\Lambda_\mu^{(e)} = -4\left(U_L^{\nu T}Y_\Delta\right)_{j\alpha}\left(Y_\Delta^\dagger U_L^{\nu *}\right)_{\beta j}\int \frac{d^4k}{(2\pi)^4}\frac{P_R\left(\not{k}+\not{p}_1+m_j\right)P_L\,(2k+q)_\mu}{\left[(k+p_1)^2-m_j^2\right]\left[(k+p_1-p_2)^2-M^2_{\Delta^-}\right]\left[k^2-M^2_{\Delta^-}\right]}\;; \tag{D.6}$$

$$i\Lambda_\mu^{(f)} = 4\left(U_L^{\nu T}Y_\Delta\right)_{j\alpha}\left(Y_\Delta^\dagger U_L^{\nu *}\right)_{\beta j}\int \frac{d^4k}{(2\pi)^4}\frac{P_R\,(\not{k}+\not{p}_2+m_j)\,P_L\,(\not{p}_2+m_\alpha)\,\gamma_\mu}{\left[m_\beta^2-m_\alpha^2\right]\left[(k+p_2)^2-m_j^2\right]\left[k^2-M^2_{\Delta^-}\right]}\;; \tag{D.7}$$

$$i\Lambda_\mu^{(g)} = 4\left(U_L^{\nu T}Y_\Delta\right)_{j\alpha}\left(Y_\Delta^\dagger U_L^{\nu *}\right)_{\beta j}\int \frac{d^4k}{(2\pi)^4}\frac{\gamma_\mu\,(\not{p}_1+m_\beta)\,P_R\,(\not{k}+\not{p}_1+m_j)\,P_L}{\left[m_\alpha^2-m_\beta^2\right]\left[(k+p_1)^2-m_j^2\right]\left[k^2-M^2_{\Delta^-}\right]}\;. \tag{D.8}$$

Next, to perform the integrals, we apply dimensional regularisation and expand the resulting squared masses Δ_4 [remember Eq. (A.8)] in terms of leading and subdominant contributions. After a rather lengthy calculation, one gets to leading order (in lepton masses)

$$\begin{aligned}
\Lambda_\mu^{(a)} =& \frac{(Y_\Delta)^*_{\beta\sigma}\,(Y_\Delta)_{\alpha\sigma}\,\gamma_\mu P_L}{4\pi^2}\left\{\Delta_\epsilon+\left[\frac{1}{2}-\frac{5r}{18}-S_\sigma+\frac{S_\alpha+S_\beta}{3}+\frac{r}{3}f(r,S_\sigma)\right]\right\}\\
&+\frac{(Y_\Delta)^*_{\beta\sigma}\,(Y_\Delta)_{\alpha\sigma}\,\gamma_\mu P_R}{2\pi^2 M^2_{\Delta^{--}}}\left[-\frac{5}{36}+\frac{f(r,S_\sigma)}{6}\right](\not{p}_1\gamma_\mu\not{p}_1+\not{p}_2\gamma_\mu\not{p}_2)\\
&+\frac{(Y_\Delta)^*_{\beta\sigma}\,(Y_\Delta)_{\alpha\sigma}\,\gamma_\mu P_L}{2\pi^2 M^2_{\Delta^{--}}}\left\{\left[\frac{17}{36}-\frac{f(r,S_\sigma)}{6}\right](\not{p}_2\gamma_\mu\not{p}_1)-\left[\frac{1}{36}+\frac{f(r,S_\sigma)}{6}\right](\not{p}_1\gamma_\mu\not{p}_2)\right\}\;,
\end{aligned} \tag{D.9}$$

$$\begin{aligned}
\Lambda_\mu^{(b)} =& -\frac{(Y_\Delta)^*_{\beta\sigma}\,(Y_\Delta)_{\alpha\sigma}\,\gamma_\mu P_L}{2\pi^2}\left[\Delta_\epsilon+\left(\frac{1}{2}+\frac{4r}{18}-S_\sigma+\frac{S_\alpha+S_\beta}{6}\right)\right]\\
&-\frac{(Y_\Delta)^*_{\beta\sigma}\,(Y_\Delta)_{\alpha\sigma}\,P_R}{36\pi^2 M^2_{\Delta^{--}}}\left(\not{p}_1 p_{1\mu}+5\not{p}_1 p_{2\mu}+5\not{p}_2 p_{1\mu}+\not{p}_2 p_{2\mu}\right)\;,
\end{aligned} \tag{D.10}$$

$$\Lambda_\mu^{(c)+(d)} = \frac{(Y_\Delta)^*_{\beta\sigma}\,(Y_\Delta)_{\alpha\sigma}\,\gamma_\mu P_L}{4\pi^2}\left[\Delta_\epsilon+\left(\frac{1}{2}-S_\sigma+\frac{S_\alpha+S_\beta}{3}\right)\right]+\frac{(Y_\Delta)^*_{\beta\sigma}\,(Y_\Delta)_{\alpha\sigma}}{12\pi^2 M^2_{\Delta^{--}}}P_R(\not{p}_2\gamma_\mu\not{p}_1)\;, \tag{D.11}$$

$$\begin{aligned}
\Lambda_\mu^{(e)} =& \frac{(Y_\Delta U_L^\nu)^*_{\beta j}\,(Y_\Delta U_L^\nu)_{\alpha j}\,\gamma_\mu P_L}{8\pi^2}\left[\Delta_\epsilon+\left(\frac{3}{2}-\frac{r}{3}+\frac{S_a}{3}-\frac{S_b}{3}\right)\right]\\
&+\frac{(Y_\Delta)^*_{\beta\sigma}\,(Y_\Delta)_{\alpha\sigma}\,P_R}{12\pi^2 M^2_{\Delta^-}}\left(5\not{p}_2 p_{2\mu}-7\not{p}_2 p_{1\mu}-\not{p}_1 p_{2\mu}+3\not{p}_1 p_{1\mu}\right)\;,
\end{aligned} \tag{D.12}$$

$$\Lambda_\mu^{(f)+(g)} = -\frac{(Y_\Delta U_L^\nu)^*_{\beta j}(Y_\Delta U_L^\nu)_{\alpha j}\,\gamma_\mu P_L}{8\pi^2}\left[\Delta_\epsilon+\left(\frac{1}{2}-\lambda_j+\frac{S_\alpha+S_\beta}{3}\right)\right]-\frac{(Y_\Delta)^*_{\beta\sigma}(Y_\Delta)_{\alpha\sigma}}{24\pi^2 M^2_{\Delta^-}}P_R(\not{p}_2\gamma_\mu\not{p}_1)\;, \tag{D.13}$$

where $f(r, S_\sigma)$ is the function defined by

$$f(r, S_\sigma) = \frac{4S_\sigma}{r} + \ln S_\sigma + \left(1 - \frac{2S_\sigma}{r}\right)\sqrt{1 - \frac{4S_\sigma}{r}} \ln \frac{\sqrt{r + 4S_\sigma} + \sqrt{r}}{\sqrt{r + 4S_\sigma} - \sqrt{r}} \,. \tag{D.14}$$

It is now straightforward to obtain the contribution of the doubly-charged scalar to the effective coupling by summing up the results of the first four diagrams. We arrive at the expression

$$\Lambda_\mu^{(\Delta^{--})} = \sum_{i=a}^{d} \Lambda_\mu^{(i)} = {}^1\Lambda_\mu^{(\Delta^{--})} + {}^2\Lambda_\mu^{(\Delta^{--})} \,, \tag{D.15}$$

with

$${}^1\Lambda_\mu^{(\Delta^{--})} = -\frac{(Y_\Delta)^*_{\beta\sigma}\,(Y_\Delta)_{\alpha\sigma}}{6\pi^2 M^2_{\Delta^{--}}} f(r, S_\sigma)(q^2\gamma_\mu - q_\mu q_\nu \gamma^\nu)P_L \,, \tag{D.16}$$

$${}^2\Lambda_\mu^{(\Delta^{--})} = -\frac{(Y_\Delta)^*_{\beta\sigma}\,(Y_\Delta)_{\alpha\sigma}}{6\pi^2 M^2_{\Delta^{--}}} \left[m_\beta P_L i\sigma_{\mu\nu} q^\nu + m_\alpha P_R i\sigma_{\mu\nu} q^\nu\right] \,. \tag{D.17}$$

which is clearly gauge covariant, as expected. In the same way, it is easy to calculate the contribution of the singly-charged scalar, corresponding to diagrams (e), (f) and (g) in Fig. D.1. The result reads:

$$\Lambda_\mu^{(\Delta^{-})} = \sum_{i=e}^{g} \Lambda_\mu^{(i)} = {}^1\Lambda_\mu^{(\Delta^{-})} + {}^2\Lambda_\mu^{(\Delta^{-})} \,, \tag{D.18}$$

with

$${}^1\Lambda_\mu^{(\Delta^{-})} = -\frac{(Y_\Delta)^*_{\beta\sigma}\,(Y_\Delta)_{\alpha\sigma}}{12 \times 6\pi^2 M^2_{\Delta^{-}}} (q^2\gamma_\mu - q_\mu q_\nu \gamma^\nu)P_L \,, \tag{D.19}$$

$${}^2\Lambda_\mu^{(\Delta^{-})} = -\frac{(Y_\Delta)^*_{\beta\sigma}\,(Y_\Delta)_{\alpha\sigma}}{8 \times 6\pi^2 M^2_{\Delta^{-}}} \left[m_\beta P_L i\sigma_{\mu\nu} q^\nu + m_\alpha P_R i\sigma_{\mu\nu} q^\nu\right] \,. \tag{D.20}$$

Finally, gathering the two contributions, the one-loop form factor for the type II seesaw model is:

$$\Lambda_\mu = \sum_{i=e}^{g} \Lambda_\mu^{(i)} = {}^1\Lambda_\mu + {}^2\Lambda_\mu \,, \tag{D.21}$$

with

$${}^1\Lambda_\mu = -\frac{(Y_\Delta)^*_{\beta\sigma}\,(Y_\Delta)_{\alpha\sigma}}{6\pi^2} \left(\frac{1}{12 M^2_{\Delta^{-}}} + \frac{f(r, S_\sigma)}{M^2_{\Delta^{--}}}\right) (q^2\gamma_\mu - q_\mu q_\nu \gamma^\nu)P_L \,, \tag{D.22}$$

$${}^2\Lambda_\mu = -\frac{(Y_\Delta)^*_{\beta\sigma}\,(Y_\Delta)_{\alpha\sigma}}{6\pi^2} \left(\frac{1}{8 M^2_{\Delta^{-}}} + \frac{1}{M^2_{\Delta^{--}}}\right) \left[m_\beta P_L i\sigma_{\mu\nu} q^\nu + m_\alpha P_R i\sigma_{\mu\nu} q^\nu\right] \,. \tag{D.23}$$

This result is in complete agreement with that of Refs. [177–179].

E $\ell_\alpha \to \ell_\beta\, \gamma$ decays in the type III seesaw model

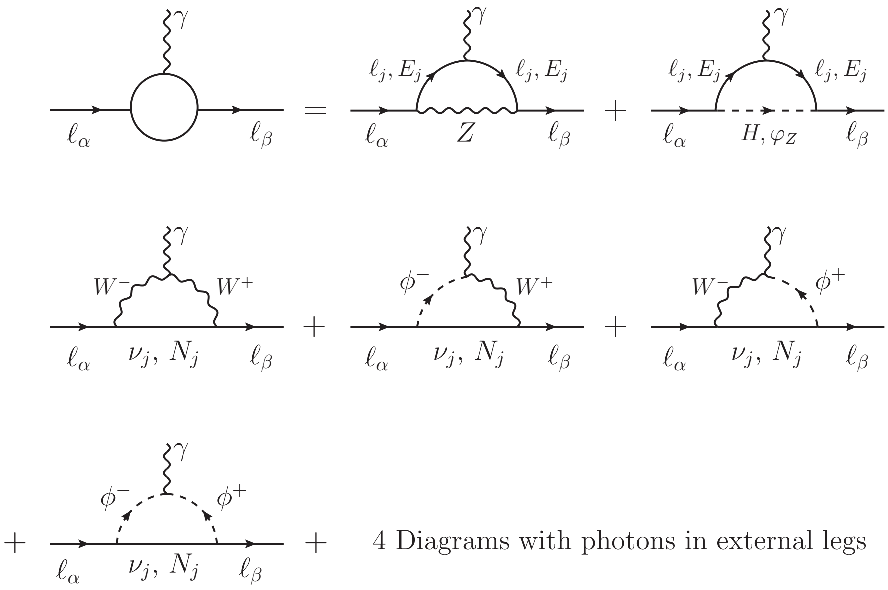

Figure E.1: One-loop diagrams contributing to $\ell_\alpha \to \ell_\beta\gamma$ in the type III seesaw model.

In this appendix we outline the essential steps followed in the one-loop calculation of the $\ell_\alpha \to \ell_\beta\gamma$ decay width in the type III seesaw. We assume that $\ell_\alpha \to \overline{\ell_\beta}\gamma$ is an on-shell transition and the calculation is done in the $m_\beta \to 0$ limit. As such, its amplitude can be written as [193]

$$iT\left(\ell_\alpha \to \overline{\ell_\beta}\gamma\right) = 2A \times \left[\overline{u_\beta}\left(p-q\right)\left[iq^\nu \varepsilon^\lambda \sigma_{\lambda\nu} P_R\right] u_\alpha\left(p\right)\right] \ , \tag{E.1}$$

where ε is the photon polarisation, p_μ is the ℓ_α lepton momentum and q_μ is the photon momentum. Using the Gordon decomposition (C.34), we can rewrite the amplitude in a more appealing way as:

$$iT\left(\ell_\alpha \to \overline{\ell_\beta}\gamma\right) = 2A \times \left[\overline{u_\beta}\left(p-q\right) P_R \left(2p\cdot\varepsilon - m_\alpha \not\varepsilon\right) u_\alpha\left(p\right)\right] \ . \tag{E.2}$$

We thus see that we only need to calculate the $p\cdot\varepsilon$ terms. The remaining terms (proportional to $\not\varepsilon$) can be recovered from the $p\cdot\varepsilon$ terms through Eq. (E.2). The decay width is thus:

$$\Gamma\left(\ell_\alpha \to \overline{\ell_\beta}\gamma\right) = \frac{m_\alpha^3}{4\pi}\left|A\right|^2 \ . \tag{E.3}$$

In a mass eigenstate basis, the diagrams that contribute to $\ell_\alpha \to \ell_\beta\gamma$ are shown in Fig. E.1.

Those with photons in external legs are omitted in Fig. E.1 since they only contribute to cancel the divergences in the remaining diagrams (similarly to what happens in the other seesaw scenarios). In fact, their invariant amplitude is proportional to $\gamma_\mu \varepsilon^\mu = \not{\varepsilon}$.

We followed a notation and a procedure similar to that of Ref. [186]. We grouped the fourteen diagrams in Fig. E.1 according to the internal fermion and the calculation was performed in the 't Hooft-Feynman gauge, up to order $\mathcal{O}\left(\frac{m_D^2}{m_\Sigma^2}\right)$, where $\mathbf{M}_D$ is the Dirac mass matrix $\mathbf{M}_D = v\mathbf{Y}_\Sigma/\sqrt{2}$ and $\mathbf{M}_\Sigma$ is the triplet mass matrix. The amplitudes for each set of diagrams are then the following:

$$\begin{aligned} T_{\nu_j}^{\phi^-,W^-} &= -\frac{G_F^{\rm SM}}{\sqrt{2}}\frac{e\,m_\alpha}{16\pi^2}\left[\overline{u_\beta}\,(p-q)\,P_R\,(2p\cdot\varepsilon - m_\alpha\not{\varepsilon})\,u_\alpha\,(p)\right]\Big[(U_{0_{\nu\nu}}U_L^\nu)_{\beta j}\,(U_{0_{\nu\nu}}U_L^\nu)^\dagger_{j\alpha}\,F_1\left(w_{\nu_j}\right) \\ &+ \left(\boldsymbol{\epsilon}^\Sigma\,U_{0_{\nu\nu}}U_L^\nu\right)_{\beta j}(U_{0_{\nu\nu}}U_L^\nu)^\dagger_{j\alpha}\,F_2\left(w_{\nu_j}\right) + (U_{0_{\nu\nu}}U_L^\nu)_{\beta j}\left(\boldsymbol{\epsilon}^\Sigma U_{0_{\nu\nu}}U_L^\nu\right)^\dagger_{j\alpha}\,F_3\left(w_{\nu_j}\right)\Big]\ , \end{aligned} \tag{E.4}$$

$$\begin{aligned} T_{N_j}^{\phi^-,W^-} &= -\frac{G_F^{\rm SM}}{\sqrt{2}}\frac{e\,m_\alpha}{16\pi^2}\left[\overline{u_\beta}\,(p-q)\,P_R\,(2p\cdot\varepsilon - m_\alpha\not{\varepsilon})\,u_\alpha\,(p)\right]\Big\{\left(\mathbf{M}_D^\dagger\mathbf{M}_\Sigma^{-1}\right)_{\beta j}\left(\mathbf{M}_\Sigma^{-1}\mathbf{M}_D\right)_{j\alpha}F_4(w_{N_j}) \\ &+ \Big[\left(\mathbf{M}_D^\dagger\mathbf{M}_\Sigma^{-1}\right)_{\beta j}\left(\mathbf{M}_\Sigma^{-1}\mathbf{M}_D\boldsymbol{\epsilon}^\Sigma\right)_{j\alpha}F_5(w_{N_j}) + \left(\boldsymbol{\epsilon}^\Sigma\mathbf{M}_D^\dagger\mathbf{M}_\Sigma^{-1}\right)_{\beta j}\left(\mathbf{M}_\Sigma^{-1}\mathbf{M}_D\right)_{j\alpha}F_6(w_{N_j})\Big]\,w_{N_j} \\ &+ \frac{1}{2M_W^2}\Big[\left(\mathbf{M}_D^\dagger\right)_{\beta j}\left(\boldsymbol{\epsilon}'^{\Sigma T}\mathbf{M}_D\right)_{j\alpha} + 4\left(\mathbf{M}_D^\dagger\right)_{\beta j}\left(\mathbf{M}_\Sigma^{-1}\mathbf{M}_D^*\,(U_L^\nu)^*\,\mathbf{M}_\nu^{\rm diag.}U_L^{\nu\dagger}\right)_{j\alpha}\Big]F_5(w_{N_j}) \\ &+ \frac{1}{2M_W^2}\Big[\left(\mathbf{M}_D^\dagger\boldsymbol{\epsilon}'^{\Sigma *}\right)_{\beta j}(\mathbf{M}_D)_{j\alpha} + 4\left(U_L^\nu\mathbf{M}_\nu^{\rm diag.}\,(U_L^\nu)^T\,\mathbf{M}_D^T\mathbf{M}_\Sigma^{-1}\right)_{\beta j}(\mathbf{M}_D)_{j\alpha}\Big]F_6(w_{N_j})\Big\}\ , \end{aligned} \tag{E.5}$$

$$\begin{aligned} T_{E_j}^{Z,H,\varphi_Z} &= -\frac{G_F^{\rm SM}}{\sqrt{2}}\frac{e\,m_\alpha}{16\pi^2}\left[\overline{u_\beta}\,(p-q)\,P_R\,(2p\cdot\varepsilon - m_\alpha\not{\varepsilon})\,u_\alpha\,(p)\right] \\ &\Big\{\left(\mathbf{M}_D^\dagger\mathbf{M}_\Sigma^{-1}\right)_{\beta j}\left(\mathbf{M}_\Sigma^{-1}\mathbf{M}_D\right)_{j\alpha}\left[F_7\left(z_{N_j}\right) + F_8\left(h_{N_j}\right)\right] \\ &- \left(\boldsymbol{\epsilon}^\Sigma\mathbf{M}_D^\dagger\mathbf{M}_\Sigma^{-1}\right)_{\beta j}\left(\mathbf{M}_\Sigma^{-1}\mathbf{M}_D\right)_{j\alpha}\left[F_8\left(z_{N_j}\right) + F_8\left(h_{N_j}\right)\right] \\ &- \left(\mathbf{M}_D^\dagger\mathbf{M}_\Sigma^{-1}\right)_{\beta j}\left(\mathbf{M}_\Sigma^{-1}\mathbf{M}_D\boldsymbol{\epsilon}^\Sigma\right)_{j\alpha}\left[F_9\left(z_{N_j}\right) + F_9\left(h_{N_j}\right)\right]\Big\}\ , \end{aligned} \tag{E.6}$$

$$T_{\ell_j}^{Z,H,\varphi_Z} = -\frac{G_F^{\rm SM}}{\sqrt{2}}\frac{e}{16\pi^2}m_\alpha\left[\overline{u_\beta}\,(p-q)\,P_R\,(2p\cdot\varepsilon - m_\alpha\not{\varepsilon})\,u_\alpha\,(p)\right]\left(\boldsymbol{\epsilon}^\Sigma\right)_{\beta\alpha}G\left(y_{l_j}, h_{\ell_j}\right)\ . \tag{E.7}$$

In the above expressions, we have defined the adimensional quantities

$$w_{\nu_j} \equiv \frac{m_{\nu_j}^2}{M_W^2}\ ,\quad w_{N_j} \equiv \frac{m_{N_j}^2}{M_W^2}\ ,\quad z_{\ell_j} \equiv \frac{m_{\ell_j}^2}{M_Z^2}\ ,\quad h_{\ell_j} \equiv \frac{m_{\ell_j}^2}{M_H^2}\ ,\quad z_{N_j} \equiv \frac{m_{N_j}^2}{M_Z^2}\ ,\quad h_{N_j} \equiv \frac{m_{N_j}^2}{M_H^2}\ , \tag{E.8}$$

along with the loop functions

$$F_1(x) = \frac{10 - 43x + 78x^2 - 49x^3 + 4x^4 + 18x^3\log(x)}{3(1-x)^4}\ , \tag{E.9}$$

$$F_2(x) = \frac{2(5 - 24x + 39x^2 - 20x^3 + 6x^2(-1+2x)\log(x))}{3(1-x)^4}\ , \tag{E.10}$$

$$F_3(x) = \frac{7 - 33x + 57x^2 - 31x^3 + 6x^2(-1+3x)\log(x)}{3(1-x)^4}\ , \tag{E.11}$$

$$F_4(x) = \frac{-38+185x-246x^2+107x^3-8x^4+18(4-3x)x^2\log(x)}{3(1-x)^4}\,, \tag{E.12}$$

$$F_5(x) = \frac{1-6x+3x^2+2x^3-6x^2\log(x)}{3(1-x)^4}\,, \tag{E.13}$$

$$F_6(x) = \frac{7-12x-3x^2+8x^3-6x(-2+3x)\log(x)}{3(1-x)^4}\,, \tag{E.14}$$

$$F_7(x) = \frac{40-46x-3x^2+2x^3+7x^4+18x(4-3x)\log(x)}{3(1-x)^4}\,, \tag{E.15}$$

$$F_8(x) = \frac{x(-16+45x-36x^2+7x^3+6(-2+3x)\log(x))}{3(1-x)^4}\,, \tag{E.16}$$

$$F_9(x) = \frac{x(2+3x-6x^2+x^3+6x\log(x))}{3(1-x)^4}\,, \tag{E.17}$$

and

$$\begin{aligned} G(z_{\ell_j}, h_{\ell_j}) = {} & \delta_{j\beta}\left(1-2\cos^2\theta_W\right)\left(F_5[z_{\ell_j})+F_6(z_{\ell_j})\right] \\ & + \delta_{j\alpha}\Big\{\left(1-2\cos^2\theta_W\right)\left[F_5(z_{\ell_j})+F_6(z_{\ell_j})\right]+8\left(1-\cos^2\theta_W\right)\left[F_6(z_{\ell_j})-F_5(z_{\ell_j})\right] \\ & \quad + \frac{1}{2}\left[F_9(z_{\ell_j})-F_8(z_{\ell_j})-3F_8(h_{\ell_j})\right]\Big\}\,. \end{aligned} \tag{E.18}$$

Since $z_{\ell_j},\ h_{\ell_j},\ w_{\nu_j} \ll 1$, as a good approximation we set the flavour conserving quantities z_{ℓ_j} and h_{ℓ_j} to zero, keeping only leading-order terms in the flavour-changing quantities w_{ν_j}, i.e.

$$F_1(w_{\nu_j}) \simeq \frac{10}{3} - w_{\nu_j}\,, \tag{E.19}$$

$$F_2(w_{\nu_j}) \simeq \frac{10}{3} - \frac{8}{3}w_{\nu_j}\,, \tag{E.20}$$

$$F_3(w_{\nu_j}) \simeq \frac{7}{3} - \frac{5}{3}w_{\nu_j}\,, \tag{E.21}$$

$$G(z_{\ell_j}, h_{\ell_j}) \approx C = \frac{32}{6}\left(\cos^2\theta_W - 2\right) \approx -6.56\,. \tag{E.22}$$

With this approximation, the final expressions can then be obtained after summing over the internal fermion states j and neglecting $\mathcal{O}\left[(m_D/m_\Sigma)^n\right]$ terms, with $n > 2$. We arrive at the expressions

$$\begin{aligned} T_\nu^{\phi^-,W^-} = \sum_j T_{\nu_j}^{\phi^-,W^-} = {} & -\frac{G_F^{\rm SM}}{\sqrt{2}}\frac{e}{16\pi^2}m_\alpha\left[\overline{u_\beta}\,(p-q)\,P_R\,(2p\cdot\varepsilon - m_\alpha\not{\varepsilon})\,u_\alpha\,(p)\right] \\ & \times\left[\frac{7}{3}\left(\boldsymbol{\epsilon}^\Sigma\right)_{\beta\alpha} - \sum_j w_{\nu_j}\,(U_L^\nu)_{\beta j}\left(U_L^{\nu\dagger}\right)_{j\alpha}\right], \end{aligned} \tag{E.23}$$

$$\begin{aligned} T_N^{\phi^-,W^-} = \sum_j T_{N_j}^{\phi^-,W^-} = {} & -\frac{G_F^{\rm SM}}{\sqrt{2}}\frac{e}{16\pi^2}m_\alpha\left[\overline{u_\beta}\,(p-q)\,P_R\,(2p\cdot\varepsilon - m_\alpha\not{\varepsilon})\,u_\alpha\,(p)\right] \\ & \times\left[-\frac{8}{3}\left(\boldsymbol{\epsilon}^\Sigma\right)_{\beta\alpha} + \sum_j\left(\mathbf{M}_D^\dagger\mathbf{M}_\Sigma^{-1}\right)_{\beta j}\left(\mathbf{M}_\Sigma^{-1}\mathbf{M}_D\right)_{j\alpha}A(w_{N_j})\right], \end{aligned} \tag{E.24}$$

$$T_{\ell}^{Z,H,\varphi_Z} = \sum_j T_{\ell_j}^{Z,H,\varphi_Z} = -\frac{G_F^{\rm SM}}{\sqrt{2}} \frac{e}{16\pi^2} m_\alpha \left[\overline{u_\beta}\,(p-q)\, P_R\,(2p\cdot\varepsilon - m_\alpha \not\varepsilon)\, u_\alpha\,(p)\right] \left(\boldsymbol{\epsilon}^{\Sigma}\right)_{\beta\alpha} \times C\,, \tag{E.25}$$

$$\begin{aligned} T_{E}^{Z,H,\varphi_Z} = \sum_j T_{E_j}^{Z,H,\varphi_Z} &= -\frac{G_F^{\rm SM}}{\sqrt{2}} \frac{e}{16\pi^2} m_\alpha \left[\overline{u_\beta}\,(p-q)\, P_R\,(2p\cdot\varepsilon - m_\alpha \not\varepsilon)\, u_\alpha\,(p)\right] \\ &\times \left\{ \frac{14}{3} \left(\boldsymbol{\epsilon}^{\Sigma}\right)_{\beta\alpha} + \sum_j \left(\mathbf{M}_D^\dagger \mathbf{M}_\Sigma^{-1}\right)_{\beta j} \left(\mathbf{M}_\Sigma^{-1}\mathbf{M}_D\right)_{j\alpha} \left[B(z_{N_j}) + C(h_{N_j})\right] \right\}, \end{aligned} \tag{E.26}$$

where the following definitions have been used:

$$A(w_{N_j}) = \frac{-30 + 153 w_{N_j} - 198 x_{N_j}^2 + 75 x_{N_j}^3 + 18(4 - 3w_{N_j}) x_{N_j}^2 \log w_{N_j}}{3(w_{N_j}-1)^4}\,, \tag{E.27}$$

$$B(z_{N_j}) = \frac{33 - 18 z_{N_j} - 45 z_{N_j}^2 + 30 z_{N_j}^3 + 18(4 - 3z_{N_j}) z_{N_j} \log z_{N_j}}{3(z_{N_j}-1)^4}\,, \tag{E.28}$$

$$C(h_{N_j}) = \frac{-7 + 12 h_{N_j} + 3 h_{N_j}^2 - 8 h_{N_j}^3 + 6(3h_{N_j} - 2) h_{N_j} \log h_{N_j}}{3(h_{N_j}-1)^4}\,. \tag{E.29}$$

The result for the total amplitude is then:

$$\begin{aligned} T\left(\ell_\alpha \to \ell_\beta \gamma\right) &= -\frac{G_F^{\rm SM}}{\sqrt{2}} \frac{e}{16\pi^2} m_\alpha \left[\overline{u_\beta}\,(p-q)\, P_R\,(2p\cdot\varepsilon - m_\alpha \not\varepsilon)\, u_\alpha\,(p)\right] \\ &\times \left\{ \left(\frac{13}{3} + C\right) \left(\boldsymbol{\epsilon}^{\Sigma}\right)_{\beta\alpha} - \sum_j w_{\nu_j} \left(U_L^\nu\right)_{\beta j} \left(U_L^{\nu\dagger}\right)_{j\alpha} + \right. \\ &\left. \sum_j \left(\mathbf{M}_D^\dagger \mathbf{M}_\Sigma^{-1}\right)_{\beta j} \left(\mathbf{M}_\Sigma^{-1}\mathbf{M}_D\right)_{j\alpha} \left[A(w_{N_j}) + B(z_{N_j}) + C(h_{N_j})\right] \right\}, \end{aligned} \tag{E.30}$$

which is valid at $\mathcal{O}\left(\frac{m_D^2}{m_\Sigma^2}\right)$. If we assume that the fields N_j are very heavy, $w_{N_j}, z_{N_j}, h_{N_j} \gg 1$, we can take the additional limit $w_{N_j}, z_{N_j}, h_{N_j} \to \infty$, which leads to the result:

$$\begin{aligned} T\left(\ell_\alpha \to \ell_\beta \gamma\right) = &-\frac{G_F^{\rm SM}}{\sqrt{2}} \frac{e}{16\pi^2} m_\alpha \left[\overline{u_\beta}\,(p-q)\, P_R\,(2p\cdot\varepsilon - m_\alpha \not\varepsilon)\, u_\alpha\,(p)\right] \\ &\times \left[\left(\frac{13}{3} + C\right) \left(\boldsymbol{\epsilon}^{\Sigma}\right)_{\beta\alpha} - \sum_j w_{\nu_j} \left(U_L^\nu\right)_{\beta j} \left(U_L^{\nu\dagger}\right)_{j\alpha} \right]. \end{aligned} \tag{E.31}$$